



This work is protected by copyright and other intellectual property rights and duplication or sale of all or part is not permitted, except that material may be duplicated by you for research, private study, criticism/review or educational purposes. Electronic or print copies are for your own personal, non-commercial use and shall not be passed to any other individual. No quotation may be published without proper acknowledgement. For any other use, or to quote extensively from the work, permission must be obtained from the copyright holder/s.



Exploring the effects of gestational diabetes on placental membrane derived stem cells

Li-Yun Chen

Ph.D. Thesis

Cell and Tissue Engineering

July 2019

Institute for Science and Technology in Medicine (ISTM)
Keele University

Abstract

The progression of regenerative medicine and advanced cell banking technology provide the hope of using perinatal tissue-derived autologous MSCs for personalised medicine. Mesenchymal stem cells (MSCs) derived from placenta, with the advantages of being non-invasive and having fewer ethical issues, are a promising source for cell therapy. The hyperglycaemic intrauterine environment in pregnancies affected by gestational diabetes mellitus (GDM) alters the development of the placenta and may have impacts on placental MSCs behaviours and functions. Therefore, we aimed to investigate the influence of the GDM on placental MSCs and further explore their therapeutic potential.

Placental MSCs were isolated from amniotic membrane (AMSCs) and chorionic membrane (CMSCs). The biological, functional, and immunological characteristics of healthy- and GDM- AMSCs/CMSCs were examined. Compared with healthy MSCs, the GDM-MSCs displayed some levels of alteration in adipogenic capacities and macrophage immunoregulatory properties while comparable immunophenotypes, osteogenesis, chondrogenesis, and T-cell regulation ability were observed in GDM-MSCs.

As the major adverse consequence of GDM is an increased risk of developing diabetes, these women may benefit from cell therapy for diabetes in the future. We developed a step-wise differentiation approach to generating functional insulin-producing cells through a short-term glucose priming period combined with a 16-day serial stimulation of compounds and growth factors, such as activin A, retinoic acid, EGF, GLP1 across different differentiation stages. This approach successfully generated insulin-producing cells from GDM- and healthy- CMSCs which displayed pancreatic beta-cell properties and functions.

Moreover, with more promising potential of CMSCs in regenerative medicine, DNA microarray was performed to examine their transcriptional profiles. Comprehensive investigation of gene expression by microarray and validation of differences between healthy- and GDM- CMSCs via real-time PCR and functional assays revealed enhanced capacities of GDM-CMSCs in wound healing and cardiogenesis compared to healthy-CMSCs. However, significantly reduced expression in detoxification enzymes belonging to the aldehyde dehydrogenase gene families (ALDH1A1/1A2, ALDH2, ALDH3) accounted for downregulation across several metabolic pathways and oxidative stress dysregulation in GDM-CMSCs.

Taken together, understanding these placental stem cell behaviours provides an insight to developing therapeutic applications of GDM-MSCs and healthy-MSCs for future autologous stem cell therapies.

Contents

ABSTRACT	I
CONTENTS	III
FIGURES.....	VIII
TABLES	IX
ABBREVIATIONS.....	X
PUBLICATIONS	XII
ACKNOWLEDGEMENTS	XIII
CHAPTER 1	
INTRODUCTION	1
1.1 Gestational diabetes mellitus (GDM).....	2
1.1.1 Clinical manifestation.....	2
1.1.2 Morbidity and mortality for mother and infant.....	4
1.1.3 Gestational diabetes and future risk of diabetes.....	5
1.2 Placenta	9
1.2.1 Placental structure and function	9
1.2.2 Anatomy of placental membranes.....	13
1.2.3 Placental pathology complicated by GDM	15
1.3 Mesenchymal stem cells (MSC)	18
1.3.1 Stem cells in birth-associated tissues	18
1.3.2 Characterisation of MSCs in placenta	21
1.3.3 Amnion-derived stem cells	22
1.3.4 Chorion-derived stem cells.	24
1.3.5 Immunomodulation of amnion-/chorion- derived stem cells	26
1.4 Regenerative medicine	28

1.4.1 Placental membranes in clinical application	28
1.4.2 Placenta-derived MSCs in preclinical/clinical studies	29
1.4.3 Banking of neonatal tissues and stem cells	34
1.4.4 MSC therapy in type 2 diabetes	35
1.5 Introduction to microarray	42
1.5.1 Microarray technology	42
1.5.2 Applications of microarrays	43
1.6 Hypothesis and aims	44
 CHAPTER 2	
MATERIALS AND METHODS	46
2.1 Materials	47
2.2 Placental samples collection	51
2.3 Isolation and culture of AMSCs and CMSCs	53
2.4 Cell culture techniques	55
2.4.1 Cell passage, cryopreservation, and recovery	55
2.4.2 Morphological observation and measurement	56
2.4.3 Cell counting and doubling time	57
2.4.4 MTT assay	57
2.4.5 Production of conditioned media	58
2.5 Flow cytometry	59
2.6 Tri-lineage differentiation and assessment	61
2.6.1 Osteogenesis	61
2.6.2 Adipogenesis	61
2.6.3 Chondrogenesis	62
2.7 RNA extraction and reverse transcription	63
2.8 Real-time polymerase chain reaction (qPCR)	65

2.9 Immunology characterisation	70
2.9.1 Culture and stimulation of Jurkat cells	70
2.9.2 Supernatant collection.....	70
2.9.3 Culture and stimulation of THP-1 cells.....	71
2.9.4 Co-culture system	71
2.10 Elisa assay	72
2.10.1 IL-2, IL-10, TNF- α	72
2.10.2 Insulin and C-peptide.....	74
2.11 Live/dead viability assay	77
2.12 Beta-galactosidase senescence assay	77
2.13 Immunofluorescence staining	78
2.14 Migration assay	79
2.14.1 Transwell assay	79
2.14.2 Wound healing assay	79
2.15 ALDH activity assay	80
2.16 Detection of ROS	81
 CHAPTER 3	
CHARACTERISATION OF AMSCS/CMSCS FROM GDM AND HEALTHY PREGNANCIES.....	83
3.1 Introduction	84
3.2 Aim	86
3.3 Methods.....	87
3.4 Results	89
3.4.1 Morphological analysis	89
3.4.2 Cell proliferation and doubling time	94
3.4.3 Cell immunophenotype	97
3.4.4 Tri-lineage differentiation	99

3.4.5 Effect of conditioned media on Jurkat T cells	107
3.4.6 Co-culture system of CMSCs/AMSCs and macrophage.....	110
3.5 Discussion	115
3.6 Summary.....	123
CHAPTER 4	
GENERATION OF INSULIN PRODUCING CELLS FROM HEALTHY-/GDM- AMSCS/CMSCS	124
4.1 Introduction	125
4.2 Aim	131
4.3 Methods.....	132
4.4 Results	135
4.4.1 Pluripotent markers expression	135
4.4.2 High glucose effect on H-/G- AMSCs/CMSCs	137
4.4.3 High glucose induces pancreatic lineage markers	143
4.4.4 Stepwise differentiation and IPC morphology	145
4.4.5 Expression of pancreatic markers expression	148
4.4.6 Immunofluorescence staining and ELISA	153
4.5 Discussion	160
4.6 Summary.....	167
CHAPTER 5	
MICROARRAY STUDY OF HEALTHY- AND GDM- CMSCS TRANSCRIPTIONAL PROFILE	168
5.1 Introduction	169
5.2 Aim	172
5.3 Methods.....	173
5.4 Results	177
5.4.1 Identification of differentially expressed genes.....	177
5.4.2 Biological function analysis	179

5.4.3 Validation of enriched biological functions.....	186
5.4.4 Canonical pathway analysis	194
5.4.5 ALDH expression and function examination	202
5.4.6 ROS and oxidative stress	205
5.5 Discussion	210
5.6 Summary.....	215
 CHAPTER 6	
DISCUSSION, CONCLUSION AND FUTURE WORK	216
6.1 Summative discussion and conclusion.....	217
6.1.1 Human placenta – an attractive source of MSCs	217
6.1.2 IPC generation – an application of autologous MSCs for diabetes therapy.....	220
6.1.3 Microarray – insights of gene profile to functional molecular levels.....	223
6.2 Future work.....	228
CHAPTER 7 REFERENCES	230
APPENDIX – ETHICAL APPROVAL	277

Figures

FIGURE 1-1. INSULIN SENSITIVITY-SECRETION RELATIONSHIP	8
FIGURE 1-2. FORMATION OF THE PLACENTA.....	10
FIGURE 1-3. SCHEMATIC DRAWING OF THE PLACENTA	12
FIGURE 1-4. CROSS-SECTION OF PLACENTAL MEMBRANE.....	14
FIGURE 1-5. EFFECT OF MATERNAL NUTRIENTS ON FETAL DEVELOPMENT	17
FIGURE 1-6. STEM CELLS DERIVED FROM PLACENTAL MEMBRANES	23
FIGURE 1-7. NUMBERS OF CLINICAL TRIALS USING PERINATAL CELLS PER YEAR.....	34
FIGURE 1-8. MSC THERAPEUTIC EFFECTS ON TYPE 2 DIABETES	37
FIGURE 1-9. OVERVIEW OF DNA MICROARRAY	43
FIGURE 2-1. MSC ISOLATION FROM PLACENTAL MEMBRANES.	54
FIGURE 2-2. CELL MORPHOLOGY ANALYSIS	56
FIGURE 2-3. FLOW CYTOMETRY TECHNIQUE.....	60
FIGURE 2-4. REAL-TIME PCR AMPLIFICATION AND DISSOCIATION CURVE	66
FIGURE 2-5. ELISA STANDARD CURVES FOR IL-10, TNF- α , AND IL-2	73
FIGURE 2-6. ELISA STANDARD CURVES FOR INSULIN AND C-PEPTIDE	76
FIGURE 3-1. SUMMARY OF THE METHODOLOGY IN CHAPTER 3	88
FIGURE 3-2. OBSERVATION OF CELL MORPHOLOGIES	91
FIGURE 3-3. CELL LENGTH AND SURFACE AREA ANALYSIS	93
FIGURE 3-4. GROWTH CURVES AND DOUBLING TIME	95
FIGURE 3-5. CELL PROLIFERATION ASSESSED BY MTT ASSAY	96
FIGURE 3-6. IMMUNOPHENOTYPE OF H-/G- AMSCs AND CMSCs	98
FIGURE 3-7. TRI-LINEAGE DIFFERENTIATION – OSTEOGENESIS, ADIPOGENESIS, CHONDROGENESIS.....	100
FIGURE 3-8. OIL-RED-O STAIN AND ELUTION.....	102
FIGURE 3-9. BASAL ACTIVITY OF ADIPOGENESIS-REGULATING GENES	103
FIGURE 3-10. EXAMINATION OF ADIPOGENIC PROGRESSION THROUGH MARKER EXPRESSION.....	106
FIGURE 3-11. SUPPRESSION OF T-CELLS PROLIFERATION AND IL-2 SECRETION	109
FIGURE 3-12. SCHEMATIC REPRESENTATION OF MACROPHAGE POLARISATION.....	111
FIGURE 3-13. EXAMINATION OF M1/M2 MARKER EXPRESSION IN THP1	113
FIGURE 3-14. CYTOKINES RELEASE BY M1/M2 MACROPHAGES.....	114
FIGURE 4-1. TIME LINES OF MULTISTEP PROCEDURES FOR IPC DIFFERENTIATION.	127
FIGURE 4-2. DEFINED TRANSCRIPTION FACTORS FOR PANCREATIC DEVELOPMENT	130
FIGURE 4-3. SUMMARY OF THE METHODOLOGY IN CHAPTER 4	134
FIGURE 4-4. PLURIPOTENT MARKER EXPRESSION	136
FIGURE 4-5. MORPHOLOGICAL CHANGES IN HG CULTURE	138
FIGURE 4-6. DECREASED CELL VIABILITY IN HG CULTURE	140
FIGURE 4-7. CELLULAR SENESCENCE IN HG CULTURE	142

FIGURE 4-8. PANCREATIC MARKERS EXPRESSION IN HG CULTURE	144
FIGURE 4-9. OPTIMISED IPC DIFFERENTIATION APPROACH AND IPC MORPHOLOGY	147
FIGURE 4-10. INDUCTION OF PANCREATIC MARKERS BY IPC DIFFERENTIATION PROTOCOL	150
FIGURE 4-11. IMPROVING AMSC-IPC MATURATION BY BETACELLULIN	152
FIGURE 4-12. CONFOCAL IMAGES OF INSULIN AND PDX1 EXPRESSION	156
FIGURE 4-13. INSULIN AND C-PEPTIDE ELISA.....	158
FIGURE 4-14. ELISA OF INTRACELLULAR INSULIN	159
FIGURE 5-1. MICROARRAY EXPERIMENTAL FLOW	173
FIGURE 5-2. SUMMARY OF THE METHODOLOGY IN CHAPTER 5	176
FIGURE 5-3. VENN DIAGRAMS OF DEGs.....	178
FIGURE 5-4. ENRICHED MOLECULAR AND CELLULAR FUNCTION IN GDM-CMSCs	180
FIGURE 5-5. DOWNSTREAM EFFECTS IN MOLECULAR AND CELLULAR FUNCTION	182
FIGURE 5-6. ENRICHED PHYSIOLOGICAL SYSTEM DEVELOPMENT AND FUNCTION IN GDM-CMSCs	183
FIGURE 5-7 DOWNSTREAM EFFECTS IN CARDIOVASCULAR SYSTEM DEVELOPMENT	185
FIGURE 5-8. DOWNSTREAM EFFECTS IN PHYSIOLOGICAL SYSTEM DEVELOPMENT AND FUNCTION	186
FIGURE 5-9. REAL-TIME PCR VALIDATED THE GENES INVOLVED IN WOUND HEALING	188
FIGURE 5-10. TRANSWELL MIGRATION ASSAY	190
FIGURE 5-11. WOUND HEALING ASSAY.....	191
FIGURE 5-12 REAL-TIME PCR VALIDATED THE GENES INVOLVED IN CARDIOVASCULAR DEVELOPMENT	193
FIGURE 5-13. IPA CANONICAL PATHWAYS ANALYSIS.....	196
FIGURE 5-14. INTERACTION NETWORK OF POSITIVELY-REGULATED PATHWAYS.....	198
FIGURE 5-15. INTERACTION NETWORK OF NEGATIVELY-REGULATED PATHWAYS.....	201
FIGURE 5-16. REAL-TIME PCR VALIDATION OF ALDHs EXPRESSION	202
FIGURE 5-17. ALDH ENZYMATIC ACTIVITY	204
FIGURE 5-18. REAL-TIME PCR VALIDATION OF ANTIOXIDATIVE ENZYME EXPRESSION	205
FIGURE 5-19. DETECTION OF ROS PRODUCTION BY DCFDA	207
FIGURE 5-20. INHIBITION OF ALDH FUNCTION BY DEAB.....	209
FIGURE 6-1. SCATTER PLOT MATRIX OF MICROARRAY DATA	224

Tables

TABLE 1-1. RECOMMENDED MARKERS FOR PLACENTA-DERIVED MSCs	21
TABLE 1-2. SURFACE MARKERS OF AECs, AMSCs, AND CMSC	25
TABLE 1-3. FACTORS INVOLVED IN IPC DIFFERENTIATION.....	39
TABLE 2-1. LIST OF MATERIALS.....	47
TABLE 2-2. PLACENTA SAMPLE DETAILS	52
TABLE 2-3. PRIMER SEQUENCES	68

TABLE 3-1 MATERNAL AND FETAL CHARACTERISTICS	89
TABLE 5-1.TOP RANKED UP- AND DOWN- REGULATED GENES IN GDM-CMSCs VS. HEALTHY-CMSCs.....	179

Abbreviations

Abbreviations	
2-ME	2-mercaptoethanol
ALDH	Aldehyde dehydrogenase
AMSC	Amniotic mesenchymal stem cell
AEC	Amniotic epithelial cell
ADIPOQ	Adiponectin
AQP1	Aquaporin-1
BSA	bovine serum albumin
BM-MSC	Bone marrow mesenchymal stem cell
CCL	Chemokine (C-C motif) ligand
CELSR1	Cadherin EGF LAG seven-pass G-type receptor 1
CD	Cluster of differentiation
CMSC	Chorionic mesenchymal stem cell
CM	Conditioned media
CTGF	Connective tissue growth factor
CXCL	Chemokine (C-X-C motif) ligand
DAPI	4,6-diamidino-2-phenylindole
DEAB	N, N-diethylaminobenzaldehyde
DMEM	Dulbecco's Modified Eagle Medium
DMSO	Dimethylsulphoxide
ECM	Extracellular matrix
EDN1	Endothelin-1
EGF	Epidermal growth factor
FGF	Fibroblast growth factor
FLNB	Filamin B
GAPDH	Glyceraldehyde 3-phosphate dehydrogenase
GLUT	Glucose transporter
GLP-1	Glucagonlike peptide-1
GSIS	Glucose stimulated insulin secretion
GDM	Gestational diabetes mellitus
HBEGF	Heparin Binding EGF like growth factor

HCG	Human chorionic gonadotropin
HG	High glucose
HLA	Human leukocyte antigen
HMOX1	Heme Oxygenase 1
HPL	Human placental lactogen
HSC	Haematopoietic stem cell
IGF	Insulin-like growth factor
IFN-γ	Interferon gamma
ISL1	Insulin gene enhancer binding protein-1
IL	Interleukin
INS	Insulin
IPC	Insulin-producing cell
KGF	Keratinocyte growth factor
LG	Low glucose
LPS	Lipopolysaccharide
MRC1	Mannose receptor C-type 1
M-CSF	Macrophage colony-stimulating factor
MSC	Mesenchymal stem cell
MTT	3-(4,5-dimethylthiazol-2-yl)-2,5-diphenyltetrazolium bromide
NEAA	Non-essential amino acid
NEUROG3	neurogenin 3
NKX2.5	NK2 Homeobox 5
NOG	Noggin
NQO1	NAD(P)H quinone dehydrogenase 1
OCT-4	Octamer-binding transcription factor 4
OGTT	Oral glucose tolerance test
PAX6	Paired box gene 6
PDX1	Pancreatic and duodenal homeobox 1
PDGF	Platelet-derived growth factor
PPAR-γ	Peroxisome proliferator-activated receptor gamma
PHA	Phytohaemagglutinin
PMA	Phorbol 12-myristate 13-acetate
PDGFA	Platelet derived growth factor receptor alpha
RASIP1	Ras-interacting protein 1
RPMI	Roswell Park Memorial Institute medium
ROS	Reactive oxygen species
RSPO3	R-Spondin 3
STAT	Signal transducer and activator of transcription

SEM	Standard error of the mean
SD	Standard deviation
SOD2	Superoxide dismutase 2
T2DM	Type 2 diabetes mellitus
TNF-α	Tumor necrosis factor alpha
TGF	Transforming growth factor
TRA	T cell receptor alpha locus
VEGF	Vascular endothelial growth factor

Publications

Liyun C, Marwan MM, Nicholas RF, and Pensee W. Chorionic and amniotic membrane-derived stem cells have distinct, and gestational diabetes mellitus independent, proliferative, differentiation, and immunomodulatory capacities (Under review, Stem Cell Research)

Liyun C, Nicholas RF, and Pensee W. Insulin secreting cell differentiation of placental chorionic, not amniotic, membrane-derived mesenchymal stem cells from gestational diabetic women (Under review, Journal of Tissue Engineering and Regenerative Medicine)

Liyun C, Chungteng W. Nicholas RF, and Pensee W. Comparative microarray analysis of chorionic stem cells between healthy and gestational diabetes pregnancies identifies genes and regulatory mechanisms associated with regenerative potential (In preparation)

Acknowledgements

I would like to thank my supervisors, Dr. Pensee Wu and Prof. Nicholas Forsyth for their guidance and advice throughout this project and being supportive for every step of me PhD. Their expertise and research experience have helped to keep my project on track. Pensee provided the most wonderful support and help at the early stage of my project as well as my life in the UK. As an overseas student, I am truly grateful for having an amazing supervisor who I can share everything with. Special thanks to Nick for all the helpful and valuable input to my publications and thesis, particularly your tremendous academic support and unending patience when it comes to revising the manuscripts. I would also like to thank my viva examiners, Dr. Vinoj George and Dr. Catriona Kelly, for their very helpful comments and suggestions.

I would like to acknowledge and thank Marwan MM for his contributions to stem cell characterisation experiments and Chung-Teng for his invaluable help with microarray analysis and data interpretation. I would also like to thank Sue for giving me my first human placenta dissection lesson and Jess, who I used to share a short but lovely time together in Pensee's group, for her help with confocal microscope. Thanks to postdocs and PhDs in Guy Hilton, especially everyone in Nick's group, it was a pleasure to work with you and you have made every day at work enjoyable.

I would like to express my gratitude to my family who have always supported and believed in me. A great deal of thanks to my parents for encouraging me to pursue a PhD and my sister for always bringing me laughs through the ups and downs of my studies.

Finally, thanks to all of the women who have kindly donated their placentas for this project.

Chapter 1

Introduction



1.1 Gestational diabetes mellitus (GDM)

1.1.1 Clinical manifestation

Pathogenesis

Pregnancy is normally accompanied with progressive insulin resistance beginning at mid-pregnancy and progressing through the third trimester, as the result of maternal hyperglycaemia which is thought to facilitate nutrient flux from the mother to fetus¹. Placental hormones are the major factors that contribute to the disruption of glucose/insulin balance and lead to insulin resistance owing to the fact that insulin resistance rapidly abates following delivery. The secretion of human placental lactogen, human placental growth hormone, oestrogen, and cortisol during pregnancy attenuates the ability of maternal organs that respond to insulin². Insulin-desensitising effects along with increased maternal adiposity leading to insulin resistance, the need for maternal insulin is, therefore, increased during pregnancy. Pancreatic beta-cells increase their insulin secretion; however, when insulin secretion is inadequate to compensate for the insulin resistance of pregnancy, the development of gestational diabetes mellitus (GDM) occurs³.

Diagnosis

GDM is defined as glucose intolerance with onset or first diagnosed during pregnancy, usually beginning at the second trimester.⁴ The diagnostic thresholds of glucose intolerance for GDM vary from country to country. The criteria recommended by World Health Organization (WHO) are a 75g oral glucose tolerance test (OGTT) with fasting plasma glucose ≥ 5.1 mmol/l, OGTT 1 h ≥ 10.0 mmol/l and OGTT 2 h ≥ 8.5 mmol/l⁵. In the UK, the National Institute for Health and Care Excellence (NICE) has published updated guidance

for the diagnosis of GDM in 2015, involving a fasting plasma glucose concentration above 5.6 mmol/l and 7.8 mmol/l after administration of a 2-hour 75g OGTT⁶. Women with risk factors for GDM, such as obesity, family history of diabetes, glucose intolerance, and past GDM, are provided with OGTT at their first antenatal appointment⁷.

Prevalence

The incidence of GDM is increasing worldwide and varies among ethnic groups, which has been reported to be higher among Asian and Hispanic women⁸. The increasing prevalence is positively associated with the growth of advanced maternal age, obesity, and inactivity. Globally, the recently prevalence has increased to approximately 15% compared to the previous 8% in 1998⁹, while in Europe, the prevalence is around 12.6% reported in 2013¹⁰,¹¹. GDM accounts for the majority of pregnancies complicated by diabetes, 87.5%, with the remaining being due to type 1 diabetes (7.5%) and type 2 diabetes (5%)¹². Type 1 diabetes is an autoimmune disease resulting in the destruction of beta-cells and where lifetime insulin replacement is normally required while type 2 diabetes has a pathophysiological similarity with GDM; hyperglycaemia, insufficient insulin production, and insulin resistance¹³. Approximately 3.5% of pregnancy was complicated by GDM in the UK in 2008¹⁴; however, the number is likely to rise with the growing trend in obesity¹⁵. A cohort study published in 2012 measured the frequency of GDM based on various locations, with 2,376 participants in Manchester and 1,671 participants in Belfast indicating that 22.5% and 10.2% of those screened having GDM, respectively¹⁶. A recent report published in 2014 suggested that 7 million women were obese in the UK¹⁷, which is a major risk factor contributing to GDM with a 3 to 5-fold increased likelihood vs. non-obese women^{18, 19}.

Treatment

Diet control and lifestyle modification are generally provided as first-line treatments. Metformin, a common oral hypoglycaemic agent, is also widely prescribed to reduce hyperglycaemia in GDM and T2DM patients. Metformin can exert its function by reducing hepatic glucose production and enhancing insulin sensitivity²⁰. However, some concerns exist regarding the potential adverse effects on fetus due to its ability to pass the placenta have been raised²¹. Alternatively, insulin therapy has been shown to reverse insulin resistance and improve perinatal outcomes where disadvantages include the need for injection, weight gain, and hypoglycaemia^{22, 23}. The combination of insulin and metformin was proved to have superior glycaemic control and less insulin requirement or weight gain²⁴.

1.1.2 Morbidity and mortality for mother and infant

The risk of antepartum morbidity in women with GDM can be increased when combined with maternal hypertensive disorders, such as gestational hypertension, preeclampsia, and eclampsia^{25, 26}. The biological connection between GDM and hypertension is not fully understood; however, studies have suggested that excessive circulating glucose stimulated intracellular changes in stress signalling pathways and vascular remodelling which might result in the elevated risk of hypertension²⁷⁻²⁹. It is worth noting that the frequency of stillbirth is higher in GDM than healthy pregnancies, especially when it is complicated by hypertension. Therefore, screening for GDM and careful blood pressure monitoring are important during pregnancy and urinary protein excretion is recommended for GDM women at the second half of gestation³.

Apart from antepartum morbidity, there are many short and long term health concerns arising from GDM pregnancies. Fetuses in GDM pregnancies often have an accelerated growth pattern owing to the maternal hyperglycaemia. When an estimated fetal weight is

in excess of 4000-4500 g, it is considered as macrosomia. Infants with macrosomia have an abnormally low head circumference/abdominal circumference ratio due to the increased adiposity in the body³⁰. The excessive growth of fetus also leads to adverse perinatal outcomes, including birth trauma, shoulder dystocia, bone fractures, and nerve palsies. Caesarean section is usually recommended to reduce the risk of birth trauma³¹. Long-term outcomes result from metabolic disorders caused during pregnancy, leaving both mother and infant abnormal glucose tolerance, subsequent obesity, and strong risks for future metabolic syndrome, cardiovascular disease, and diabetes^{32, 33}.

1.1.3 Gestational diabetes and future risk of diabetes

Prevalence

Although the symptoms of GDM are usually resolved after delivery, GDM is associated with a long-term risk of developing type 2 diabetes mellitus (T2DM) later in life among both mother and their offspring. GDM represents the single largest risk factor for future development of diabetes, where 40-60% women with a GDM history develop T2DM over subsequent decades and approximately 5-10% are found to have T2DM immediately after pregnancy^{34, 35}. A population-based cohort study of approximately 9,000 women with GDM from 1990 to 2016 in the UK, indicated that women diagnosed with GDM were 20 times more likely to develop T2DM and an over 2.8 times increased incidence of ischemic heart disease later in life³⁶. The highest incidence of developing T2DM in women with a previous GDM occurs in the first 5 years after pregnancy³⁷. Therefore, postpartum follow-up glucose testing (typically performed 6-12 weeks after delivery) and an annual test are usually encouraged. Moreover, children born from GDM pregnancy have a high tendency of being overweight, obese and displaying abnormal glucose tolerance, resulting in T2DM in their

early adulthood³⁸. Exposure to hyperglycaemia in the uterus has adverse effects on fetal outcomes, from epigenetic modification to physical fetal programming, leading to the development of T2DM³⁹. A study conducted among Caucasian pregnant women, indicated that offspring from GDM women had a higher frequency of impaired glucose tolerance with a prevalence of 11.1% at 1-4 years and 20.0% at 5-9 years of age⁴⁰.

Implication for the pathogenesis

The underlying mechanisms of developing T2DM in GDM women have been investigated in various aspects. Physiologically, insulin resistance progresses during pregnancy and the level of insulin resistance almost reach T2DM levels in late pregnancy. Insufficient compensatory insulin secretion by beta-cells in GDM women reveals a deficiency in beta-cell function. The insulin requirement reduces after the delivery and GDM symptoms resolve; however, beta-cell dysfunction remains unsolved. The long-term deterioration of beta-cell function increases the likelihood of T2DM development⁴¹. As illustrated in Figure 1-1, insulin secretion is approximately 50% lower in GDM than healthy pregnancy at 3rd trimester.

At the molecular level; reduced insulin receptors, abnormal localisation of GLUT4 transporters, and impaired glucose transport caused by GDM may have an irreversible impact on insulin sensitivity^{42, 43}. Dysregulation of cytokines, such as increased circulating leptin, inflammatory cytokine tumor necrosis factor- α (TNF- α), and reduced levels of adiponectin all play a role in obesity and the progression to T2DM⁴⁴⁻⁴⁶.

GDM is known for its maternal inheritance transmitting to the next generation a genetic predisposition and permanently impaired glucose homeostasis during fetal growth caused by hyperglycaemic environment. Genetic studies indicated that GDM women carried T2DM

susceptibility genes which were transmitted to their offspring⁴⁷⁻⁴⁹. The increasing interest in epigenetic alternations in fetus where DNA methylation and histone modification of metabolic-associated genes is affected by hyperglycaemia⁵⁰. Non-genetic evidence has been demonstrated in several *in vivo* models, where, for example, the offspring from diabetic rats were observed to have decreased pancreatic weight, low pancreatic insulin content, and low beta-cell mass^{51, 52}.

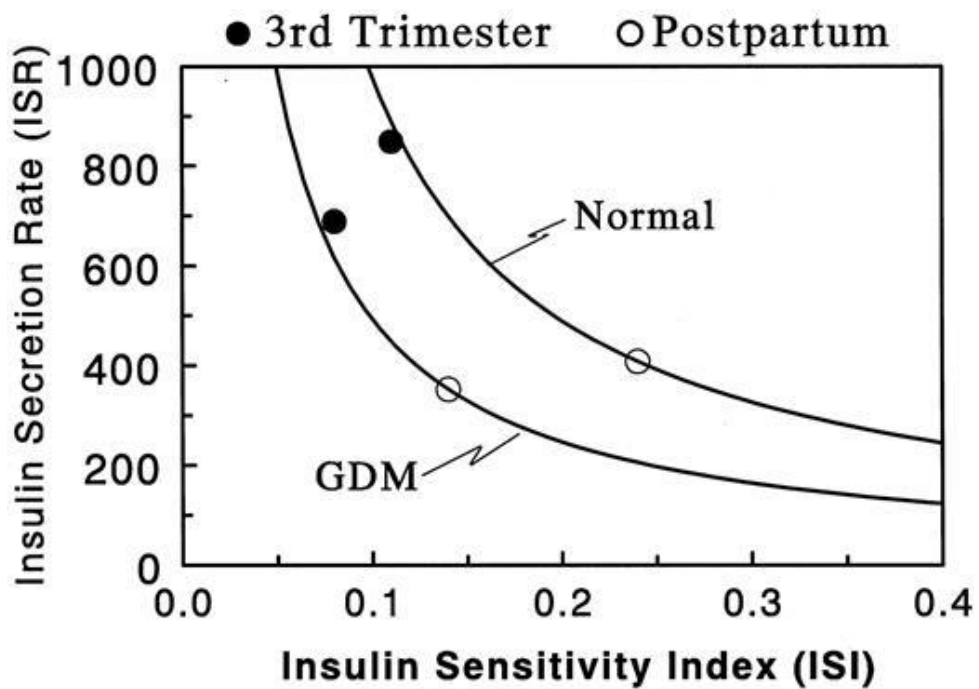


Figure 1-1. Insulin sensitivity-secretion relationship

The correlation between insulin sensitivity and secretion in GDM and healthy women. Insulin sensitivity index was calculated as the ratio of glucose disposal rate to steady-state plasma insulin concentration. Prehepatic insulin secretion rates were assessed from steady-state plasma insulin and C-peptide concentration. FFM, fat-free mass. Reprinted from Buchanan, 2001⁵³

1.2 Placenta

1.2.1 Placental structure and function

Placentation

The development of the placenta begins following on from fertilisation and once the fertilised ovum enters the uterus and becomes blastocyst. Immediately after attachment to the uterine lining, the blastocyst starts to enlarge while cells proliferate and differentiate. The outer layer of the blastocyst (trophoblast) becomes the cytotrophoblast and syncytiotrophoblast which will further develop into the placenta and fetal membranes while the inner cell masses will develop into embryo. The cytotrophoblast is the stem cell source of the placenta, which gives rise to most of the placental cell types while the syncytiotrophoblast is a specialised epithelium, which invades the endometrium (uterine mucosa) and establishes contact with maternal vessels forming a lacunar network. Lacunae is then surrounded by syncytial cells and filled with maternal blood and tissues^{54, 55} (Figure 1-2). Meanwhile, cytotrophoblastic stem cells penetrate into the syncytiotrophoblast layer and differentiate into the villous cytotrophoblast constituting primary chorionic villi, endovascular cytotrophoblast remodelling maternal spiral arteries, and interstitial cytotrophoblast invading the endometrium and eventually becoming placental-bed giant cells to anchor the growing fetus^{56, 57}.

Primary villi are formed of syncytiotrophoblast underlying cytotrophoblast and following the growth of extraembryonic mesodermal cells to the primary villi core turns them into secondary villi. Secondary villi expand and invade the maternal decidua while soon after vasculogenesis occurs, blood vessels begin to grow, and then differentiate rapidly to form

functional tertiary villi. Maternal and fetal vessels are connected at this stage and the placenta evolves to form a highly branched structure⁵⁵. Fetal and maternal vascularisation is complete by the 17th to 20th day and the thickness and circumference of placenta continues to increase until the fourth month. There is no obvious increase in thickness after the fourth month while circumference usually continues to grow.

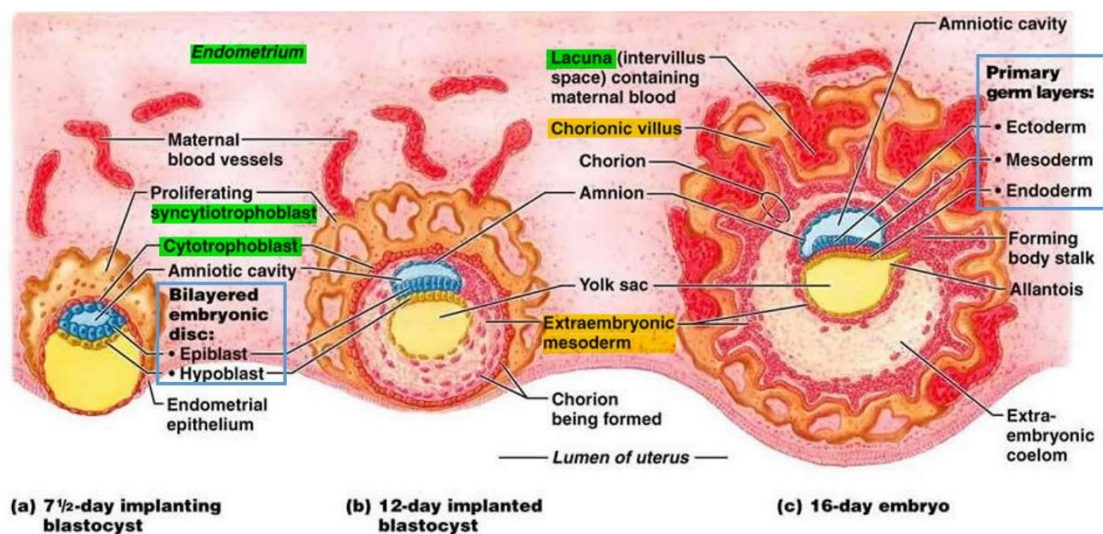


Figure 1-2. Formation of the placenta

(a) Implantation of blastocyst in the endometrium. Apoptotic maternal uterine cells are phagocytised by syncytiotrophoblast cells for proper implantation. (b) Maternal tissue fluid, uterine secretions, and blood from the erosion of the maternal capillaries are forming the lacunae. (c) Formation of primary germ layers and chorionic villi. Reproduced from Pearson Education Inc., publishing as Benjamin Cummings, 2004.

Structure

An average term placenta is approximately 22 cm in diameter, 2.5 cm central thickness, and a weight of 400-500 g, with a round disc-like appearance and an inserted umbilical cord⁵⁵. Figure 1-3 demonstrates the schematic structure of a full-term placenta. The chorionic plate and intervillous space are on the fetal side of placenta which is bathed in maternal blood. Umbilical vessels branch into the chorionic plate and supply the capillaries of chorionic villi forming a highly vascularised central core. Between the chorionic and basal plates is a large cavernous intervillous space, where the villi are in direct contact with maternal blood⁵⁸. The basal plate is on the maternal side of placenta, composed of fetal trophoblasts and maternal uterine decidua. Maternal arteries penetrate the myometrium (middle layer of the uterine wall) and divide into endometrial spiral arteries, highly coiled within the decidua basalis. The cytotrophoblastic shell is formed on the maternal surface of placenta, attaching firmly to endometrial tissues. A gap in the cytotrophoblast shell allows maternal endometrial arteries to reach the intervillous space and bath the chorionic villi in maternal blood^{59, 60}.

Function

Placenta, the interface between maternal and fetus circulation, plays an important role during fetal development by regulating gas exchange, nutrient transport, and waste elimination as well as the secretion of hormones during pregnancy. The fetal lung is filled with fluid in the uterus; therefore, the placenta is responsible for the gas exchange during the entire pregnant period. Oxygen and carbon dioxide can pass through the placenta by passive diffusion⁶¹. Nutrient transport is critical for fetal growth and includes, glucose, amino acids, fatty acids, ions, vitamins, and water. Glucose, functioning as the main source of energy, crosses the placenta through passive infusion and several types of glucose transporters. Amino acids and fatty acids are important for fetal proteins, essential fatty

acid, and lipids synthesis which can be transferred to fetus by active transport through various transporter proteins and fatty acid binding proteins. Sodium and chloride are transferred by passive transport while calcium ion, iron, and vitamins are transferred by active carrier-mediated transport^{59, 62}.

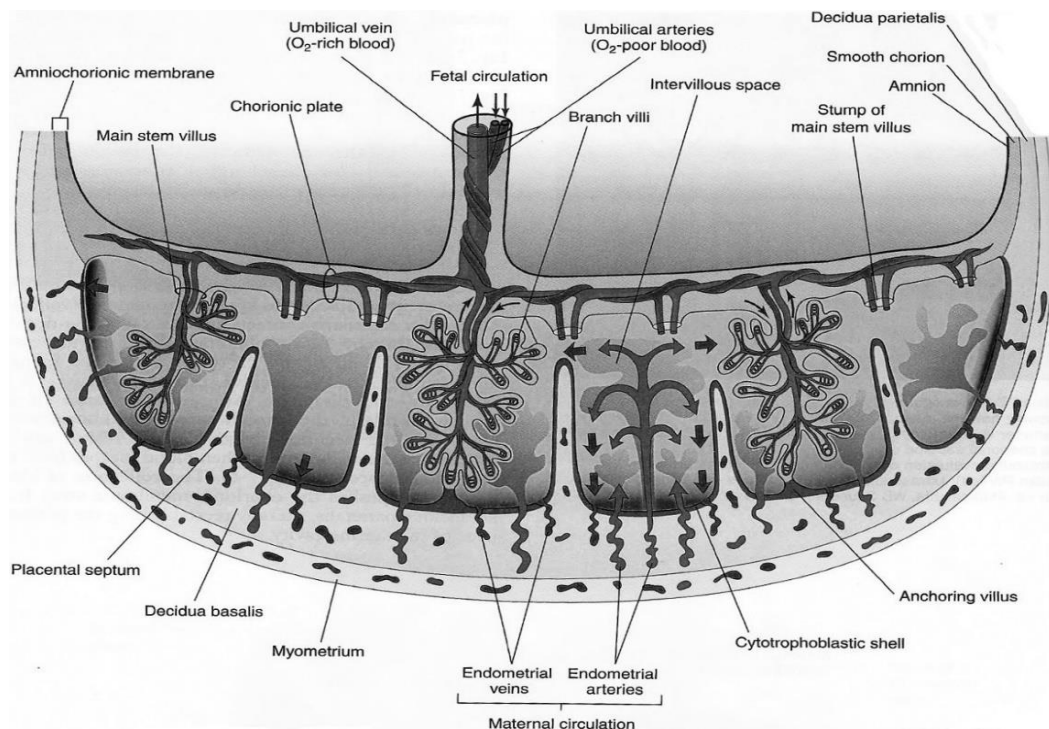


Figure 1-3. Schematic drawing of the placenta

Transverse section through a placenta illustrating the structure and fetal-maternal circulation at term. Reprinted from Moore et al., 2004⁶⁰ and Griffiths et al., 2015⁵⁹

Besides gas exchange and nutrient transport, another important function of the placenta is endocrine regulation which is involved in mediating placental growth, immune function, and fetal development. The placenta produces steroid hormones – oestrogen, progesterone and several protein hormones. The two major protein hormones secreted by placental trophoblast are human placental lactogen (HPL) and human chorionic gonadotrophin (HCG). The production of HCG peaks at the 10th week of gestation and slowly

decreases until the end of pregnancy, which plays a role in placental angiogenesis, immunotolerance, endometrial receptivity, and embryo implantation⁶³. HPL has both insulin-like and anti-insulin effects, which regulates maternal lipolysis, carbohydrate metabolism, and glucose homeostasis. Through the reduction of maternal insulin sensitivity, HPL promotes maternal body to use fatty acid and induces maternal insulin resistance in order to facilitate the mobilisation of nutrients and glucose for the fetus⁶⁴. In transgenic mice overexpressing HPL, the proliferation of pancreatic beta-cells showed significantly enhanced leading to an increased in insulin production. The enhanced secretion of HPL during pregnancy is associated with insulin resistance and contributing to the hyperglycaemia and hyperinsulinaemia in the maternal body⁶⁵. Steroid hormones are produced by ovaries until the 8th week of gestation and the placenta then takes over production of oestrogen and progesterone producing an increasing amount until before labour. Major functions of oestrogen and progesterone include stimulating uterine growth, promoting mammary gland development, preventing uterine contractions, and the onset of labour^{59, 65}.

1.2.2 Anatomy of placental membranes

The placental membrane is a bilayer structure composed of amniotic and chorionic membranes. During placental development, the amnion and chorion fuse early in the second trimester⁶⁶. The bilayer membrane migrates outwards from the placenta and encloses the amniotic cavity, where the fetus is growing and protected within the amniotic fluid⁶⁷.

The amnion is an avascular membrane, consisting of an epithelial monolayer, basement membrane, and amniotic mesoderm layer^{68, 69} (Figure 1-4). Nutrients and gas diffuse freely

from amniotic fluid and underlining decidua. The epithelial monolayer, also called amniotic epithelium, is a single layer of epithelial cells directly in contact with amniotic fluid and uniformly resting on the basement membrane. The basal membrane is composed of collagens secreted by mesenchymal cells situated beneath the basement membrane in the amniotic mesoderm. Interstitial collagens (type I and III) form parallel bundles for maintaining the mechanical integrity of the amnion. Filamentous connections between interstitial collagens and the epithelial membrane are formed by collagens type V and VI⁶⁹. Connecting between the amnion and chorion are formed via a spongy layer (intermediate layer) of loosely arranged glycoproteins and collagen fibres, mostly type III collagen⁷⁰.

The chorion is composed of a chorionic mesoderm and trophoblastic region (Figure 1-4). The former has a similar composition to the amniotic mesoderm, containing collagens and mesenchymal cells; the latter contains extravillous trophoblast cells. In between the chorionic mesoderm and trophoblast region is a basal membrane^{68, 71}.

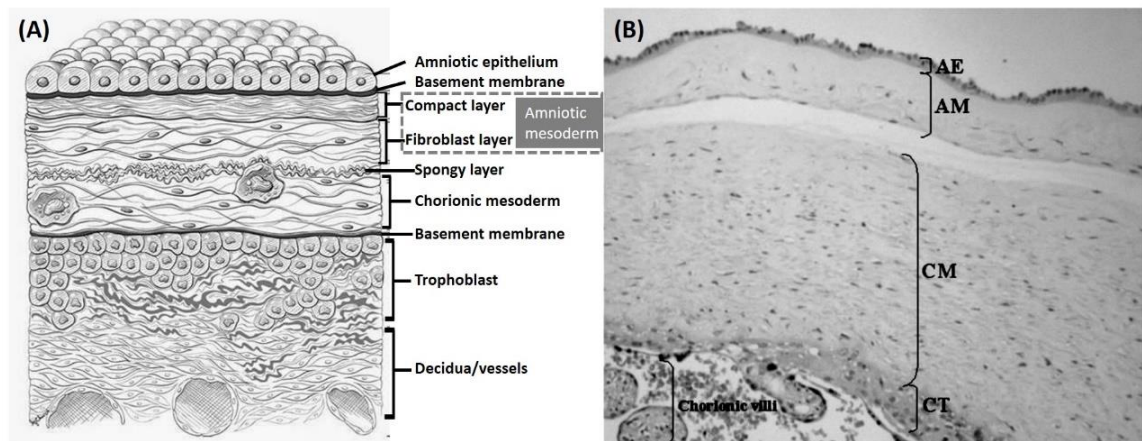


Figure 1-4. Cross-section of placental membrane

(A) Schematic presentation of the amniotic and chorionic membrane structure. (B) Layers of human placental membrane visualised by histology. AE, amniotic epithelium; AM, amniotic mesoderm; CM, chorionic mesoderm; CT, chorionic trophoblast. Reproduced from Baergen et al., 2005⁷² and Parolini et al., 2008⁶⁸

1.2.3 Placental pathology complicated by GDM

Structure and morphology

The composition of a healthy term placenta is 80-88% water, 10% protein, and 1% fat while diabetic placentas are found to have increased mass, DNA, glycogen, and lipids. The increase of glycogen and fat exceeds the relative amount of placental DNA, suggesting that each placental cell contains a higher level of glycogen and fat than a normal glucose-tolerant placenta⁷³. Increased placental weight happens in both GDM women with and without glycaemic control during pregnancy and also shows a positive correlation with fetal weight and fat mass^{74, 75}. Two common features of GDM placenta, hyperproliferation and hypervascularisation, lead to an enlarged placental surface and exchange area. Hyperglycaemia in early gestation induces trophoblast proliferation and structure modification. The thickening of the trophoblastic basement membrane results in increased diffusion distances between the maternal and fetal systemic circulations and which may be the consequence of trophoblast hyperproliferation at early gestation^{76, 77}. High incidences of abnormal villous development and branching in GDM placenta are observed where the cause and mechanism are still unclear. Low oxygen levels in the diabetic environment are suggested to have a profound influence on the upregulation of proangiogenic factors such as vascular endothelial growth factor (VEGF) and fibroblast growth factor (FGF)-2 in GDM placenta hence stimulating placental vascularisation^{76, 78}. Furthermore, the villous regions are likely to have accumulation of the placental resident macrophages promoting the release of leptin, TNF- α , and interleukins leading to alterations of placental metabolic and endocrine functions⁷⁹.

Nutrient transport

Maternal overweight, obesity, or GDM status all alter maternal circulating levels of glucose, fatty acids/cholesterol, and amino acids to the fetal circulation and ultimately, influence fetal growth and development. Glucose, the principal energy substance for both fetus and placenta, is supplied from the maternal circulation. It is reported that placental explants from GDM pregnancies exhibit 2- to 3- fold higher glucose uptake and a 40-50% reduction in fatty acid oxidation⁸⁰. Increased glucose transporter, GLUT-1, expression and activity affects the amount of glucose transport across the placenta⁸¹. Some studies indicate that the major mechanism affecting maternal-fetal glucose transport depends on glucose concentration gradient instead of glucose transporter expression^{82, 83}. The increased steepness of the glucose concentration gradient results in a higher glucose flux across the placenta. When fetal hyperinsulinaemia happens, glucose gradient will favour a persistently high glucose flux even though maternal blood glucose is under control by GDM treatment⁸⁴. Insulin sensitive glucose transporter, GLUT-4, which promotes glucose utilisation within cells, shows a reduction in activity in GDM women skeletal muscle cells^{85, 86}. Since fetal glucose consumption can be modified by maternal glucose concentration, the reduced glucose metabolism in the maternal body and increased uptake of glucose in placenta enhance the risk of excessive glucose transfer to the fetus in GDM pregnancies.

Amino acids are important for the formation of proteins and nucleic acids in the fetus. Most amino acids are transported in both directions between the maternal and fetal circulation. Upregulation of the placental syncytiotrophoblast amino acid transporters has been observed in GDM. These are responsible for alanine, glutamine, and serine transport and are associated with macrosomia⁸⁷. Increased lipid transport has also been noted in GDM pregnancies with the expression of receptors and regulators for fatty acid and cholesterol transport⁸⁸. Maternal lipoprotein transporting fatty acids and cholesterol requires lipoprotein receptors, lipases which are highly expressed in GDM placentas⁸⁹. Moreover,

maternal adipose tissues also play a role in regulating lipid transport and insulin resistance by secreting elevated levels of adipocytokines, such as leptin, adiponectin, and TNF- α ⁹⁰.

Studies on the pathophysiology of GDM between maternal and fetus are based on the hypothesis by Pedersen⁹¹ who stated that maternal hyperglycaemia leads to fetal hyperinsulinaemia and increased glucose utilisation, which is responsible for macrosomia and neonatal morbidity. The key features of the hypothesis are showed in Figure 1-5.

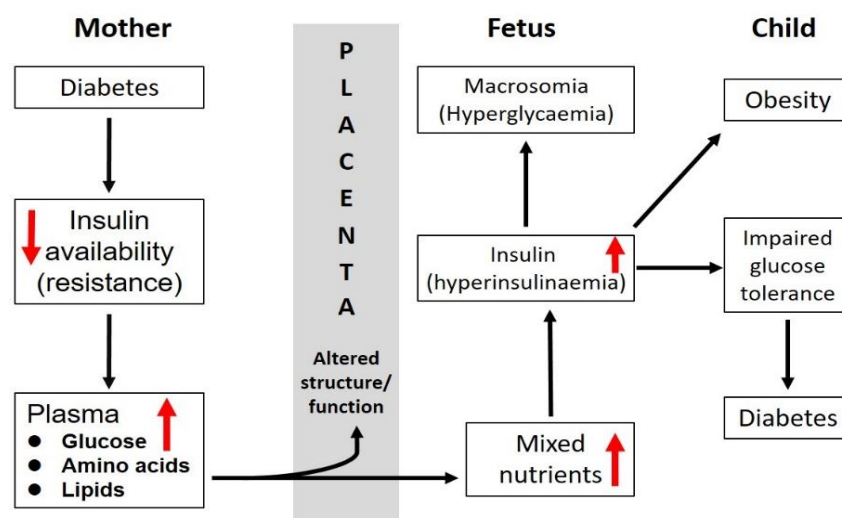


Figure 1-5. Effect of maternal nutrients on fetal development

The Pedersen's hypothesis⁹¹ of hyperglycaemia-hyperinsulinemia has been modified and indicated the contribution of maternal nutrients on fetal growth and development. Reproduced from Clinicalgate (<https://clinicalgate.com/>).

1.3 Mesenchymal stem cells (MSC)

1.3.1 Stem cells in birth-associated tissues

Stem cell population

Mesenchymal stem cells (MSCs) are defined as multipotent cells capable of differentiating into a variety of cell types. Originally, the MSC was referred to solely in respect of mesenchymal cell lineages differentiation ability; however, increasing studies have indicated a trans-differentiation potential in adult tissue-derived MSCs^{92, 93}. MSCs can be isolated from different parts of human placenta, which are thought to have a more primitive property due to their originating from inner cell mass of blastocyst giving them more potential in the three cell germ layer differentiation⁹⁴.

Haematopoietic stem cells (HSCs) are involved in haematopoiesis and give rise to many types of blood cells and generate the haematopoietic system. Being a highly vascularised organ mediating fetal-maternal exchanges the placenta and umbilical cord blood contain a large numbers of HSCs⁹⁵.

Umbilical cord and cord blood

The umbilical cord contains a gelatinous connective tissue used to protect umbilical vessels, which is known as Wharton's jelly. Several types of progenitor cells can be isolated from different regions of Wharton's jelly although whether these progenitor populations are equivalent is not yet clear^{96, 97}. Functioning as the connection between the placenta and fetus, when haematopoietic cells and MSCs circulate through the umbilical cord, these cells are likely to migrate and rest in Wharton's jelly. Migratory perivascular cells may also be

one of the MSC cell types in Wharton's jelly perivascular region^{96, 98}.

Fetal haematopoiesis starts at about 2 weeks after fertilisation in the yolk sac and gradually moves to the liver before moving to the bones and taking place in the bone marrow. Umbilical cord blood is a rich source of HSCs, which are more primitive than bone marrow derived HSCs or their counterparts in peripheral blood. Umbilical cord blood is considered as an effective alternative to bone marrow transplantation⁹⁹.

Amniotic fluid

Fetus is allowed to move freely in amniotic fluid, which acts in a protective and nourishing role during pregnancy. Amniotic fluid starts to appear immediately after the formation of the amniotic cavity and increases in volume through gestation. It contains proteins, carbohydrates, fats, and hormones to support nutrient and waste exchanges. Due to the direct contact with embryonic components, a variety of embryonic cells from three germ layers are present in the amniotic fluid¹⁰⁰. Multipotent MSC-like cells have been described within amniotic fluid; however, the characteristics may be various based on gestational ages^{101, 102}.

Placental membrane

Soon after the implantation of blastocyst, the inner cells mass (embryoblast) transforms into two distinct layers, epiblast and hypoblast, which is also known as bilaminar embryonic disc. The epiblast constitutes the amniotic epithelium between the outer layer (trophoblast) and embryonic disc. Subsequently, bilaminar embryonic disc develops into three germ layers (ectoderm, mesoderm, and endoderm) and the extraembryonic mesoderm surrounding the amniotic cavity gives rise to amniotic and chorionic mesoderm (Figure 1-

2). Given that the cells constituting amniotic and chorionic membranes are evolved from the embryoblast, it has been suggested that these cells retain a pluripotent phenotype. Studies have shown that these fibroblast-like cells derived from amnion and chorion have MSCs characteristics^{103, 104}.

Decidua and chorionic villi

The decidua is the maternal part of the placenta, essential for implantation, placenta formation and maintenance of pregnancy. During pregnancy, the placenta undergoes regeneration, differentiation, and shedding while stromal cells in decidua are thought to be responsible for the dynamic remodelling and thus found to have stem cell characteristics^{105, 106}. Chorionic villi are composed of syncytiotrophoblast, underlying cytotrophoblast, and a mesenchymal cell-filled central core. Therefore, some studies have successfully isolated MSCs from chorionic villi¹⁰⁷. However, extravillous trophoblasts invade into decidual tissue during villi formation. The characterisation of villi-derived MSCs and isolation process need to be further elucidated.

1.3.2 Characterisation of MSCs in placenta

MSCs derived from placenta share common criteria with bone-marrow MSCs and most of the MSCs derived from adult tissues (adipocytes, skin, lung). Most adult organs contain tissue-resident MSCs that contribute to tissue maintenance and repair of trauma, ageing, or disease. Although MSCs phenotypes can be altered due to different MSC niche/microenvironment, some general characteristics have been used to define human MSCs. Placenta-derived MSCs are plastic adherent, form fibroblast colony-forming units, undergo mesenchymal differentiation potential (bone, fat and cartilage), and display an appropriate range of surface antigen expression¹⁰⁸. Due to the lack of unique markers for the identification of the MSCs, there is an agreed specific panel of surface antigen – cluster of differentiation (CD)-90, CD73, and CD105 concurrent with the absence of CD45, CD34, CD14, and human leukocyte antigen (HLA)-DR¹⁰⁹ (Table 1-1).

Table 1-1. Recommended markers for placenta-derived MSCs

The signs (+) or (-) indicate the presence or absence of markers respectively.

Marker	Description	Expression
CD90 (+)	Thy-1 cell surface antigen	MSC marker
CD73 (+)	Ecto-5'-nucleotidase	MSC marker
CD105 (+)	Endoglin, TGF β receptor III	MSC marker
CD45 (-)	Protein tyrosine phosphatase, receptor type, C	Hematopoietic cells
CD34 (-)	Transmembrane phosphoglycoprotein	Hematopoietic stem cells
CD14 (-)	Myeloid cell-specific leucine-rich glycoprotein	Monocytes/Macrophages
HLA-DR	HLA Class II/MHC II receptor	Antigen presenting cells

1.3.3 Amnion-derived stem cells

There are two cell types can be isolated from amniotic membrane – amniotic epithelial cells (AECs) from the innermost layer of the amnion and amniotic mesenchymal stem cells (AMSCs) from mesoderm layer (Figure 1-6). AECs are developed at very early stage of gestation (8 days after fertilisation) and capable of secreting growth factors, such as basic fibroblast growth factor, epidermal growth factor¹¹⁰, keratinocyte growth factor, and hepatocyte growth factor. The epithelial nature of AECs is demonstrated by their ability to undergo epithelisation, their expression of several epithelial markers, and their secretion of growth factors. AECs are also able to regulate angiogenesis, fibroblast activation, and immunosuppression^{111, 112}. Moreover, research has reported stem cell characteristics of AECs, indicated by the expression of stem cell markers and possession of a differentiation ability. Pluripotency of AECs has been suggested following demonstration of pluripotent marker expression and evidence of three germ layers differentiation in mouse models^{113, 114}.

Similarly, AMSCs from the mesoderm layer have MSC characteristics and the capacity to differentiate beyond mesodermal lineages. In addition to skeletal, muscle, and cardiomyocytic differentiation (mesoderm), AMSCs also differentiate into neurogenic lineages¹¹⁵ (ectoderm), hepatocytes¹¹⁶ (endoderm), and endothelial cells¹¹⁷. Moreover, despite the pluripotent marker expression of AMSCs, including octamer-binding transcription factor 4 (*OCT4*), nanog homeobox (*NANOG*), protein antigens – T cell receptor alpha locus (TRA)-1-60 and TRA-1-81, AMSCs do not display any evidence of teratoma^{114, 115}.

Isolation and separation of AECs and AMSCs can be performed by trypsin digestion. AECs

can be released from the amnion and suspended in trypsin solution while AMSCs need further digestion of the collagen matrix to be isolated from mesoderm layer. Moreover, the cell surface markers are somehow different between AECs and AMSCs, where AECs display epithelial markers which are lacking in AMSCs¹¹⁸ (Table 1-2). The yield of AMSCs is approximately 1 million per gram of the placental membrane¹¹⁹.

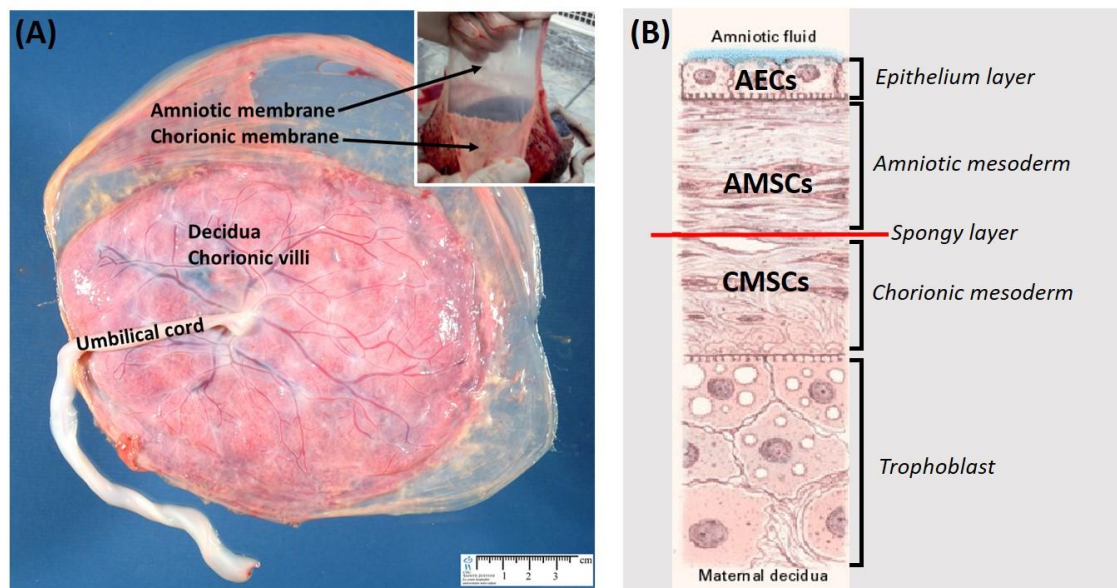


Figure 1-6. Stem cells derived from placental membranes

(A) Human placenta and manual separation of amniotic/chorionic membrane (B) Schematic representation of the placental membrane structure and MSCs from different membrane layers. AECs, amniotic epithelial cells; AMSCs, amniotic mesenchymal stem cells, CMSCs, chorionic mesenchymal stem cells.

Reproduced from Tabatabaei et al., 2014¹²⁰, Parry et al., 1998⁷⁰, and Humpath (<http://www.humpath.com/>).

1.3.4 Chorion-derived stem cells.

Chorionic MSCs (CMSCs) are derived from the chorionic mesoderm layer and share common characteristics with AMSCs (Figure 1-6). They both display plastic adherence, a mesodermal differentiation ability, and display MSCs markers (Table 1-2). In an *in vivo* study, CMSCs engrafted in neonatal swine and rats and did not induce a xenogeneic response indicating the immunoprivileged status of CMSCs^{121, 122}. CMSCs can be induced to neuron-like cells that showed comparable or even greater potential than AMSCs^{123, 124}. A study comparing CMSCs from early and late gestation found similar phenotypes and the expression of pluripotent markers in both stage derived CMSCs. It might indicate the retained pluripotency of CMSCs during gestation but when applying to an *in vivo* skin wound, early gestation-derived CMSCs accelerated the wound repair compared to late gestation-derived CMSCs¹²⁵. However, the literature on CMSCs is insufficient and limited characterisation of multi-lineage differentiation potential.

In addition, as the outermost layer of highly vascularised placenta lying adjacent to the decidual cells, the chorionic membrane was recently found to contain HSCs which are absent in the amnion. HSCs were observed in chorion at all gestational ages after 5-weeks of pregnancy and HSCs derived from mid-gestation showed superior engraftment potential in an *in vivo* model¹²⁶. However, if mechanical dissection of decidual tissues is insufficient, cross-contamination with maternal cells, blood cells, and decidual cells may be observed in CMSCs culture¹²⁷.

Table 1-2. Surface markers of AECs, AMSCs, and CMSC

Cell type	Phenotype	Cell
AECs	Epithelial markers: E-cadherin, CK7, CD49f, EpCAM Mesenchymal and embryonic markers: CD90+, CD105+, CD73+, CD44+, CD166+, CD29+, HLA-A,B,C+/-, CD13+, CD24+, SSEA-3+, SSEA-4+, TRA-1-60+, TRA-1-81+, NANOG+, SOX2+, SSEA-1-, CD117+/-, CD49e- Haematopoietic markers: CD34-, CD45-, CD14-, CD11-, HLA-DR-, CD31- Others: CD324+, CD349-	
AMSCs	Mesenchymal and embryonic markers: CD90+, CD105+, CD73+, CD44+, CD166+, CD29+, HLA-A,B,C+/-, CD13+, CD49d+, CD49e+, CD54+, Oct-3/4+ Haematopoietic markers: CD34-, CD45-, CD14-, CD31-, HLA-DR-, CD133-, CD3- Others: CD349+, CD140b+, CD324-	
CMSCs	Mesenchymal and embryonic markers: CD90+, CD105+, CD73+, CD44+, CD166+, CD29+, HLA-A,B,C+/-, CD13+, CD10+, CD49e+, CD54+, SSEA-4-/+ , NANOG+, SOX+, CD117- Haematopoietic markers: CD34-, CD45-, CD14-, CD31-, HLA-DR-, CD3-, CD133- Others: CD349+, CD140b+, CD324-	

surface antigens expressed on AEC, human amniotic epithelial cells; AMSCs, human amniotic mesenchymal stem cells; CMSCs, human chorionic mesenchymal stem cells. Reproduced from Kmiecik et al., 2013¹²⁴

1.3.5 Immunomodulation of amnion-/chorion- derived stem cells

MSC-modulated immune function can be categorised into immunosuppression and immunoprivilege. The former is defined as the ability to suppress immune cell (T-cells, B-cells, natural killer cells) function, such as proliferation and cytokine secretion while the latter describes that MSCs are able to protect themselves from immunological defence mechanisms.

AECs, AMSCs, and CMSCs lack or present very low expression levels of major histocompatibility complex (MHC) class I antigens (HLA-A, HLA-B, HLA-C) and an absence of MHC class II (HLA-DP, HLA-DQ and HLA-DR)^{128, 129} in order to avoid immune responses caused by T cells. Hence, placental membrane-derived stem cells (PM-SCs) have the ability to engraft and survive in immunocompetent neonatal swine, rats and rabbits, without a xenogenic response^{122, 130}. In an *in vitro* immune assay of AECs and allogeneic lymphocytes, no cytotoxic responses were observed whereas inhibition of lymphocyte proliferation was observed¹³¹. Placental membrane expresses high level of HLA-G, which is important for maternal-fetal tolerance, preventing rejection from the maternal immune system at implantation stage¹³². One unique characteristics of PM-SCs is the presence of HLA-G^{129, 133} which is mainly expressed in immunoprivileged organs (testis, ovary, and embryonic cells) and shows significantly higher levels in birth-associated MSCs than in adult tissue-derived MSCs^{134, 135}. HLA-G interacts with inhibitory receptors present on all immune cells and exerts its function by inducing apoptosis or arresting immune cells at the G0/G1 phase¹³⁶. This immunoprivileged status of AECs, AMSCs, and CMSCs may reflect their embryonic origin.

The immunosuppression of placental tissue-derived MSCs involves direct cell-cell contact

and secretory effects. In the presence of PM-SCs, the maturation of monocytes into dendritic cells is suppressed by preventing the expression of CD1a and reducing costimulatory molecules CD40, CD40 ligand, CD80 and CD86 expression for T cell activation¹³⁷. Without direct contact with PM-SCs in a trans-membrane co-culture system, PM-SCs are able to secrete soluble inhibitors to regulate immune cells¹³⁸ as well as the increased amount of prostaglandin 2 suppressing T cells proliferation¹³⁹. PM-SCs also secrete cytokines involved in angiogenesis, tissue repair or immune modulation, including VEGF, interleukin (IL)-6, IL-11, macrophage colony-stimulating factor (M-CSF)¹²⁴. In addition, AMSCs are found to suppress the production of C-X-C motif chemokine (CXCL)-10, CXCL9, and C-C motif chemokine (CCL)-5, demonstrating a significant anti-inflammation capacity¹¹¹. Immunomodulatory effects of AMSCs have been investigated on various *in vitro* experiments of natural killer, B cells, CD4⁺ T cells, CD8⁺ T cells regulatory T cells, and dendritic cells¹¹¹ while the understanding of CMSCs immunology is still limited.

1.4 Regenerative medicine

1.4.1 Placental membranes in clinical application

Historical background

Human amniotic membrane has been used for skin transplantation for over a hundred years. The first reported medical use of amniotic membrane dates back to 1910 with its use as a skin graft¹⁴⁰. Descriptions of amniotic membrane applied to burned and ulcerated skin surfaced was introduced appeared shortly after. They found that the amniotic membrane accelerated epithelialisation and reduced the pain on burned or ulcerated sites¹⁴¹. In the 1930s, amniotic membrane was applied in surgical reconstruction of vaginas¹⁴². The first report of using both amnion and chorion as a biological dressing material for conjunctival defects was described in 1940¹⁴³. Kim et al. further used amniotic membrane for corneal surface reconstruction in a rabbit model¹⁴⁴. Thereafter, more advanced studies on the clinical applications of placental membrane had begun and biological mechanisms were investigated.

Current application

Currently, placental membrane is used in a broad range of clinical applications due to its ability to reduce scarring and its immunomodulatory effect in suppressing inflammation in the healing process. There are numerous cytokines and growth factors found in the placental membrane making it an advantageous biomaterial for wound healing and regeneration¹⁴⁵⁻¹⁴⁷. Epidermal growth factor (EGF), vascular EGF (VEGF), basic fibroblast growth factor (bFGF), transforming growth factors (TGFs), keratinocyte growth factor (KGF), and many chemokines are important for the healing process and are contained within the

placental membrane. The chorion contributes 75% of the growth factor content in a amnion/chorion graft^{148, 149}. The amniotic and chorionic membrane products are commercially available via dehydration or cryopreservation techniques for their preservation and used in clinical practice, including cardiothoracic surgery (mainly for surgical closure)^{150, 151}, ocular surface reconstruction¹⁵², wound repair and management, especially for severe burns and chronic skin ulcers^{153, 154}. It is also suggested that stem cells derived from placental membrane retain their wound healing properties¹⁵⁵.

In recent years, using amniotic membrane in tissue engineering as a biological supporting matrix (scaffold) has gained increasing interest. It is described as improving cell proliferation, migration, differentiation, and as possessing antimicrobial properties, making amniotic membrane a good prospective scaffolding material^{69, 156}.

1.4.2 Placenta-derived MSCs in preclinical/clinical studies

MSC are a promising source for cell tissue engineering and cell-based therapies due to their ability to proliferate and differentiate into various functional cell types. The placenta is a reservoir of stem cells and due to its low immunogenicity, easy acquisition without invasive procedures and ethical concerns make placenta-derived MSCs an attractive source for regenerative medicine.

Cardiovascular repair

Myocardial infarction leads to irreversible damage to myocardial cells and is associated with high morbidity and mortality; therefore, cardiac regeneration has been widely investigated via gene therapy, cell therapy, and growth factors¹⁵⁷. MSCs have the ability to differentiate and regulate secretion of multiple growth factors as well as angiogenesis factors

demonstrating great therapeutic potential. AMSCs were induced to differentiate into cardiomyocytes and expressed cardiac-related genes as well as proteins in *in vitro* experiments¹⁵⁸. Human AMSCs labelled with a fluorescent marker and transplanted into rats were found to integrate into the myocardial infarct tissue region and differentiate into cardiomyocyte-like cells. Surprisingly, AMSCs survived for more than 2 months in the rat models, improving ventricular functions and enhancing capillary density¹⁵⁹. Another *in vivo* study evidenced the ability of AMSCs to transdifferentiate into cardiomyocytes in infarcted myocardium rats and indicated a strong association with the expression of HLA-G, IL-10, and progesterone that regulated fetal-maternal tolerance during pregnancy playing an important role in cardiac regeneration¹⁶⁰. A mixture of AMSCs and CMSCs expressed increased levels of cardiac-related genes and proteins than bone-marrow MSCs when treated with cardiogenic differentiation inducers¹⁶¹. In a chronic heart failure mouse model, placental MSCs enhanced cardiomyocyte proliferation and improved cardiac performance¹⁶². In addition, placental MSCs reduced apoptosis of cardiomyocytes at the infarcted border area and enhanced vascularity in pig models¹⁶³.

AMSCs and CMSCs are known to secrete angiogenic factors and modulate angiogenesis. Their secretion of HGF, IGF-1, and VEGF promoted blood flow and capillary density in mouse ischemia model¹⁶⁴. In particular, the VCAM-1⁺ subpopulation of CMSCs was suggested to have superior angiogenic potential *in vitro* and *in vivo*¹⁶⁵.

Neurological disorders

Owing to their stem cell characteristics, AECs have been studied in many neurological diseases, where AECs have demonstrated neuroprotective and neuroregenerative effects. Through the expression of neural markers - nestin, glial fibrillary acidic protein, and microtubule-associated protein 2 (MAP-2), AECs are inclined towards neuronal lineages¹⁶⁶.

Using AECs to treat peripheral nerve injuries in monkeys showed enhanced growth of host neurons and guided regenerative sprouting¹⁶⁷. AECs were differentiated into neuronal progenitors and transplanted to traumatic brain injury in rat models, which showed improved neurological function, brain tissue morphology, and elevated levels of neurotrophic factors, such as brain-derived neurotrophic factor and nerve growth factor¹⁶⁸.

Parkinson's disease is associated with the progressive loss of dopaminergic neurons in the brain. In a Parkinson's disease mice model, AMSCs were transplanted into the brain and the results indicated that AMSCs differentiated into neural progenitor cells and promoted endogenous neurogenesis¹⁶⁹. *In vitro* differentiation of placental MSCs into neural precursor cells was followed by transplantation into *in vivo* models. These placental MSC-derived neural precursor cells improved neuronal functions¹⁷⁰. Placental MSCs have been investigated for their therapeutic potential in multiple sclerosis and neurodegeneration of the central nervous system^{171, 172}.

Musculoskeletal diseases

Myogenic potential has been demonstrated with AECs, AMSCs, CMSCs, umbilical cord-derived MSCs, and placental tissue-derived MSCs. These MSCs differentiated into myogenic lineages *in vitro* and following *in vivo* implantation, showed positive results of treating skeletal muscle degeneration¹⁷³. Kawamichi *et al.*, (2010) demonstrated the intrinsic differentiation potential of placental MSCs into myotubes improving the efficiency of dystrophin delivery in muscle fibres upon implantation into mice¹⁷⁴.

CMSCs displayed therapeutic potential with osteogenesis imperfecta which is characterised by brittle bones in response to abnormal collagen composition and currently has no curable treatment. The intraperitoneal injection of CMSCs in osteogenesis imperfecta mice models

reduced fractures, increased bone ductility and bone volume along with the upregulation of endogenous genes involved in endochondral and intramembranous osteogenesis¹⁷⁵. Placental MSCs were used in bone tissue engineering, by inducing osteogenic differentiation, seeding on a scaffold, and transplanting to injured radius segmental bone in rabbits, while the results showed markedly enhanced bone repair¹⁷⁶.

Hepatic and pulmonary regeneration

AECs, AMSCs, and placental MSCs are capable of inducing liver regeneration and regulating cytokine expression to decrease inflammation, fibrosis, and hepatocyte apoptosis. AECs have been successfully differentiated to hepatocytes in several studies. The expression of hepatic-specific transcription factors, genes involved in drug metabolism, and functional enzymatic activities for drug degradation (Cytochrome P450 1A and 3A) were detected in AEC-derived hepatic-like cells^{177, 178}. It suggested the promising potential of using AEC-derived hepatocytes transplantation for liver disease therapy.

Apart from their differentiation ability, the cytokine regulatory effect of AECs, AMSCs, CMSCs plays a major role in suppressing fibrosis. Fibrosis is normally caused by a progressive accumulation of extracellular matrix (ECM) components resulting in the thickening and scarring of connective tissue and chronic tissue inflammation¹⁷⁹. The transplanted AECs in a carbon tetrachloride-4-induced liver fibrosis mouse displayed an ability to suppress MMPs that instigated fibrinolysis and to increase IL-10 concentrations¹⁸⁰. Infusing AMSCs in a carbon tetrachloride-4-treated mouse liver protected it from fibrosis and apoptosis¹⁸¹. Amniotic membrane also displayed anti-fibrotic properties with a reduction of ductular reaction and ECM deposition¹⁸².

Likewise, immune regulatory effect was demonstrated in a lung fibrosis model where AECs,

AMSCs, and CMSCs suppressed bleomycin-induced lung fibrosis with significant reductions in neutrophil infiltration^{183, 184}. Moreover, the application extended to cigarette-induced obstructive pulmonary disease. Intravenous injection of AMSCs was associated with a delay of the emphysema progression and alleviated lung damage¹⁸⁵. However, the inflammation was not entirely repressed and AMSCs were observed in heart, liver, and kidney. The homing efficiency of AMSCs to the target tissue needs to be further assessed.

Clinical trials

Currently, most of the clinical trials using birth-associated tissues are dedicated to cord blood HSCs. The first cord blood HSCs transplant was in 1988; thereafter, over 35,000 transplants have been performed worldwide¹⁸⁶. However, since MSCs have been found in various birth-associated tissues, the cell therapy using perinatal MSCs has become a growing field. Figure 1-7 shows the numbers of clinical trials registered worldwide per year by cell type, indicating the significantly increasing numbers in perinatal MSCs vs. cord blood cells transplantation¹⁸⁷. Some recent clinical applications using placental MSCs in phase 2 trials include severe aplastic anaemia, haemorrhagic cystitis, hypoxic ischaemic encephalopathy, stroke, rheumatoid arthritis, and graft-versus-host disease. Many clinical studies with placenta- or placental membrane- derived MSCs are still in phase 1 trial with small groups of participants. However, with great differentiation potential and immunomodulatory ability, there has been an increasing interest in regenerative medicine of birth-associated MSCs. Some challenges such as mixed cell populations upon differentiation, insufficient amount and purity of specialised cells, and route and timing of cell administration still need to be overcome to achieve therapeutic outcomes.

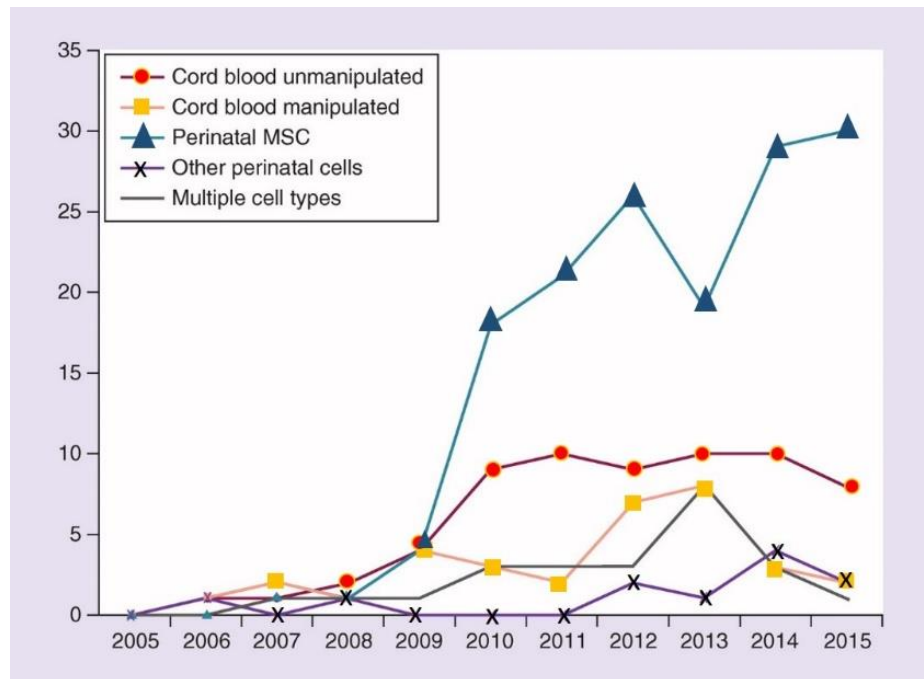


Figure 1-7. Numbers of clinical trials using perinatal cells per year

Numbers of cell therapy using perinatal MSCs/HSCs in clinical trials registered per year divided by the type of the cells: cord blood cells/HSCs that are unmanipulated or manipulated (specific cell type), perinatal MSC (Wharton's jelly, fetal membrane, amniotic fluid, placenta), other perinatal cells, multiple sources. MSC, mesenchymal stem cell; HSCs, haematopoietic stem cells. Reproduced from Couto et al., 2017¹⁸⁷

1.4.3 Banking of neonatal tissues and stem cells

Cord blood banking has been a popular option since 1993 when the first cord blood bank established¹⁸⁸. Banked cord blood has been successfully applied to clinical research and disease treatments while many biobanks have introduced a new type of service – the storage of birth-associated MSCs and new companies specialised in placental component banking have appeared. Pregnant women can choose to donate their placenta and placenta-derived cells to public banks such as UK Transplant Living Amniotic Membrane/Placenta Donation Programme for research purpose or privately store their own placental cells in commercial biobanks. Biobanking processes are required to follow

the principles and guidelines of good manufacturing practice (GMP) for medicinal products for human use¹⁸⁹. Although advancements in isolation and characterisation techniques allow scientists to obtain abundant MSCs from the placenta, the lack of specialised medical trainees in hospitals to ensure the quality and integrity of placenta and high costs ensuing from the import of biobanks using quality assurance system controls (such as International Organization for Standardization (ISO)) remain challenging for placental cell banking^{190, 191}. The storage of placental cells or components is also beneficial for discovery and screening of new drugs¹⁹². The establishment of placental cell biobanks shows exciting promise for future regenerative medicine and stem cell transplantation therapies.

1.4.4 MSC therapy in type 2 diabetes

Type 2 diabetes is characterised by a combination of a defect in beta-cell function resulting in insulin deficiency and insulin resistance. The frequency of diabetic comorbidities and complications, including cardiovascular disease, neuropathy, infections, and impaired wound healing are high when hyperglycaemia is uncontrolled¹⁹³. Although diabetes is a treatable disease, the existing therapeutic strategy can neither reverse insulin resistance nor the progression of beta-cell dysfunction¹⁹⁴. Lifelong monitoring of glucose level and treatment poses a burden on diabetic patients. Therefore, research is searching for new potentially curative therapies for diabetes.

The whole-pancreas transplant was first performed in 1966¹⁹⁵ while with the improvement in surgical techniques and immunosuppressive therapy in modern medicine, transplant obviates the need for lifelong insulin treatments and prevents diabetic complications¹⁹⁶. The necessity of major surgery and shortage of donors limit the availability of this therapeutic approach. In 1999, the transplantation of islet cells with minimally invasive

procedure was introduced¹⁹⁷. Transplanted islet cells successfully enhance insulin production, control blood glucose levels, and reduce the requirement of insulin. However, xenotransplantation of islets can introduce risk of zoonotic infections¹⁹⁸ while human allotransplantation is limited due to increased recipient demand greater than donor tissue supplies and the complications of immunosuppressive drugs¹⁹⁹.

MSCs, possessing immunosuppressive capacity and differentiation potential have generated a great interest in light of diabetic therapy. MSCs transplantation offers several advantages, such as lower risks, less complicated procedures, and abolishing the need for immunosuppressive therapy. Figure 1-8 summarises the potential of MSC-mediated type 2 diabetes therapy.

Regeneration and protection of islets

MSCs have been suggested to have the ability to promote pancreatic islet regeneration and to protect endogenous beta-cells from apoptosis. In streptozocin-induced diabetic mice, MSCs homed to and promoted the repair of pancreatic islets through enhancing endogenous cells to proliferate and regain their function²⁰⁰. MSCs express a set of chemokine receptors (CXCR4, CXCR6, CCR1, CCR7) in response to islet-secreted chemokines and allow them to migrate towards the damaged islet site²⁰¹. Through their paracrine mechanisms, MSC transplantation can modify the pancreatic microenvironment and thereby allow endogenous beta-cell regeneration.

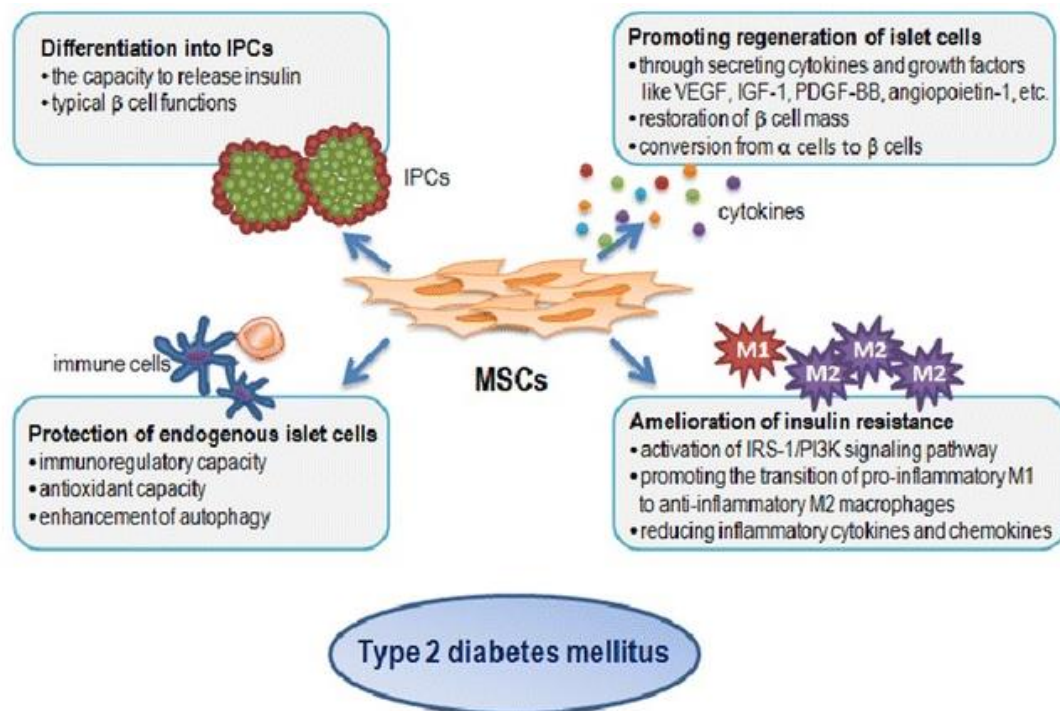


Figure 1-8. MSC therapeutic effects on type 2 diabetes

MSCs demonstrate beneficial effects through IPCs differentiation while undifferentiated MSCs promote islet cell regeneration, protect endogenous islet cells, and ameliorate insulin resistance. IPCs, insulin-producing cells; IGF-1, insulin-like growth factor-1; VEGF, vascular endothelial growth factor; PDGF, platelet-derived growth factor; IRS-1, insulin receptor substrate-1; PI3K, phosphoinositide 3-kinase. Reprinted from Zang et al., 2017²⁰²

Following MSCs intravenous injection, diabetic mice showed increased EGF expression in plasma and pancreas²⁰³. The secretion of EGF, insulin-like growth factor (IGF)-1, and platelet-derived growth factor (PDGF) are thought to be beta-cell mitogenic factors and other cytokines such as VEGF- α and angiopoietin-1 play a role in vascularisation²⁰². Additionally, different MSC subtypes may have different levels of therapeutic effect. Cell sorting based on aldehyde dehydrogenase (ALDH) activity reveals that bone-marrow MSCs with high ALDH expression have greater potential in improving hyperglycaemia and insulin secretion by increasing islet size, beta-cell mass, and vascularisation. The secretory activity of MSCs induces Wnt signal activation, the expression of matrix metalloproteases and

EGFR-activating ligands, contributing to islet regeneration²⁰⁴.

Increased oxidative stress and hypoxia are strongly associated with the diabetic environment leading to islet apoptosis. MSCs support islet survival and protect islets from oxidative stress-induced injury in order to maintain their normal functions. The increased viability through downregulation of apoptotic regulators (caspase 3, caspase 8, p53) and upregulation of anti-apoptotic genes enhance resistance to oxidative stress-induced apoptosis and dysfunction in islets²⁰⁵. Proinflammatory states of diabetes are characterised by increased levels of proinflammatory cytokines such as TNF- α , IL-6, interferon- γ ²⁰⁶. Co-culture of MSCs with pancreatic islets prevents beta-cell apoptosis induced by treatment with proinflammatory cytokines, suggesting the islet-protected role of MSC in inflammatory environment²⁰⁷.

Insulin-producing cell generation

Although MSC transplant has the aforementioned advantages, whether residual beta-cells and the remaining endogenous precursors could have enough numbers for regeneration to cope with hyperglycaemia and their regenerative efficiency remains unclear. Therefore, replacing damaged beta-cells by inducing MSC differentiation into insulin-producing cells (IPCs) may be a direct way to restore islet function.

Knowing that pancreatic cells derived from endodermal lineages, many studies have shown the capacity of MSCs to differentiate beyond mesenchymal lineage. Since MSCs do not spontaneously differentiate into pancreatic lineage *in vitro*, delicate reprogramming processes are required²⁰⁸. Particularly as, unlike embryonic stem cells, adult tissue-derived MSCs usually express low levels of pluripotent markers; therefore, MSCs reprogramming, examination of pancreatic markers, and evaluation of functions are important for IPC

differentiation. The differentiation approach for IPC generation can involve treatment with many molecules to induce MSC transdifferentiation into endocrine lineages and maturation of functional insulin-secreting cells. Table 1-3 lists the compounds commonly used in current IPC differentiation protocols. Three major stages of IPC differentiation described – definitive endoderm, pancreatic endoderm, and mature beta-cells are each characterised by lineage-specific gene expression; however, differentiation protocols depend on different MSC types and range from one step to multiple steps²⁰⁹.

The functions of MSC-generated IPCs have been investigated in many *in vivo* diabetic models. When transplanting IPCs into diabetic mice, hyperglycaemia was under control within two weeks and restored normal glycaemic condition as well as the co-expression of insulin, glucagon, and somatostatin in IPC-treated diabetic mice²¹⁰. The transplanted IPCs sustainably expressed insulin, c-peptide, and pancreatic-specific markers without apparent apoptosis *in vivo* for at least three weeks²¹¹. Longer survival time of transplanted IPCs was also reported, which maintained glucose regulatory function up to 5 weeks²¹².

However, the challenges are the percentage of mature IPCs is low and in most animal models, IPCs are implanted into the renal capsular space. The homing ability of differentiated MSCs to the injured organ will ease the cell transplant process in clinical practice.

Table 1-3. Factors involved in IPC differentiation

Compounds	Function in IPC differentiation
High glucose	Increases beta-cell replication
Activin A	Promotes beta-cell regeneration Increases insulin content
N2 and B27	Serum supplements in serum-free medium
FGF	Early stage differentiation Cluster formation

EGF	Accelerates beta-cell proliferation Increases insulin expression
HGF	Induces beta-cell cluster formation
Retinoic acid	Induces endocrine and ductal differentiation Induces insulin-positive differentiation
Nicotinamide	Induces insulin gene Enhances insulin content, DNA content
β -mercaptoethanol	Increases the potency of nicotinamide
Betacellulin	Promotes beta-cell regeneration Increases cell mass and maturation
GLP-1	Accelerates maturation of beta-cells towards glucose responsive insulin secretion
Exendin-4	Accelerates maturation of beta-cells towards glucose responsive insulin secretion
Pentagastrin	Expands beta-cell mass in combination with other factors

FGF, fibroblast growth factor; EGF, epidermal growth factor; HGF, hepatocyte growth factor; GLP-1, glucagon-like peptide-1

Amelioration of insulin resistance

In addition to beta-cell dysfunction, insulin resistance usually co-exists in type 2 diabetes which occurs when cells fail to respond normally to insulin and have impaired glucose uptake. MSCs were found to alleviate hyperglycaemia in high-fat diet-induced diabetic rats by activating insulin receptor substrate (IRS)-1 signal and Akt (protein kinase B) phosphorylation²¹³. Adipose tissue macrophage-induced chronic low-grade inflammation is also thought to play a role in exacerbating insulin resistance. MSCs infusion promoted insulin sensitivity in diabetic rat through converting inflammatory phenotype macrophages, M1 into anti-inflammatory phenotype M2. The study indicated that MSCs upregulated IL-4R expression and promoted phosphorylation of STAT6 (signal transducer and activator of transcription 6) in macrophage leading to polarisation of macrophage into M2 phenotype²¹⁴. However, the underlying mechanisms of MSC-mediated insulin sensitivity are not yet clear.

1.5 Introduction to microarray

1.5.1 Microarray technology

In the past, researchers used to discover genes based on one gene per experiment principle via mutations, selections, and cloning schemes. In the late 90's, tens of thousands of human cDNA sequences represented previously unseen genes²¹⁵ and brought us to think about the unexplored world of human genome. Thereafter, DNA microarray technology has progressed rapidly and introduced a new tool for genetic study with a slide or chip containing thousands of genes arrayed within a small surface area. Microarray technology provides a systematic and comprehensive way to explore the gene expression on genome-wide level²¹⁶. It has revolutionised biological science research in recent times, for instance, large numbers of publications describing data from microarrays, academia or industrial disease and drug discovery, clinical application for evaluating dosages of drugs²¹⁷.

The principle of microarray technology is based on DNA hybridization, a process in which the DNA strand binds to its unique complementary sequence (Figure 1-9A). The arrayed material (DNA strand) has generally been termed as probe. For DNA array, RNA isolated from two different samples, is converted to complementary DNA (cDNA) and labelled with two distinct fluorescent dyes (such as Cy5 and Cy3). Both samples are mixed in hybridization buffer and hybridized to a microarray chip that carries the probes of each specific gene. Two samples result in competitive binding of differentially labelled cDNA to its corresponding probe and through high-resolution confocal fluorescence scanning, relative signal intensity measured at each probe indicates the expression level of genes on the array²¹⁸ (Figure 1-9B). Based on this basic concept of microarray, today's technology has developed a wide range of DNA microarray platforms including one- and two-channel formats, cDNA and

oligonucleotide microarrays, spotted and in-situ synthesised microarrays, and commercially developed microarrays²¹⁹.

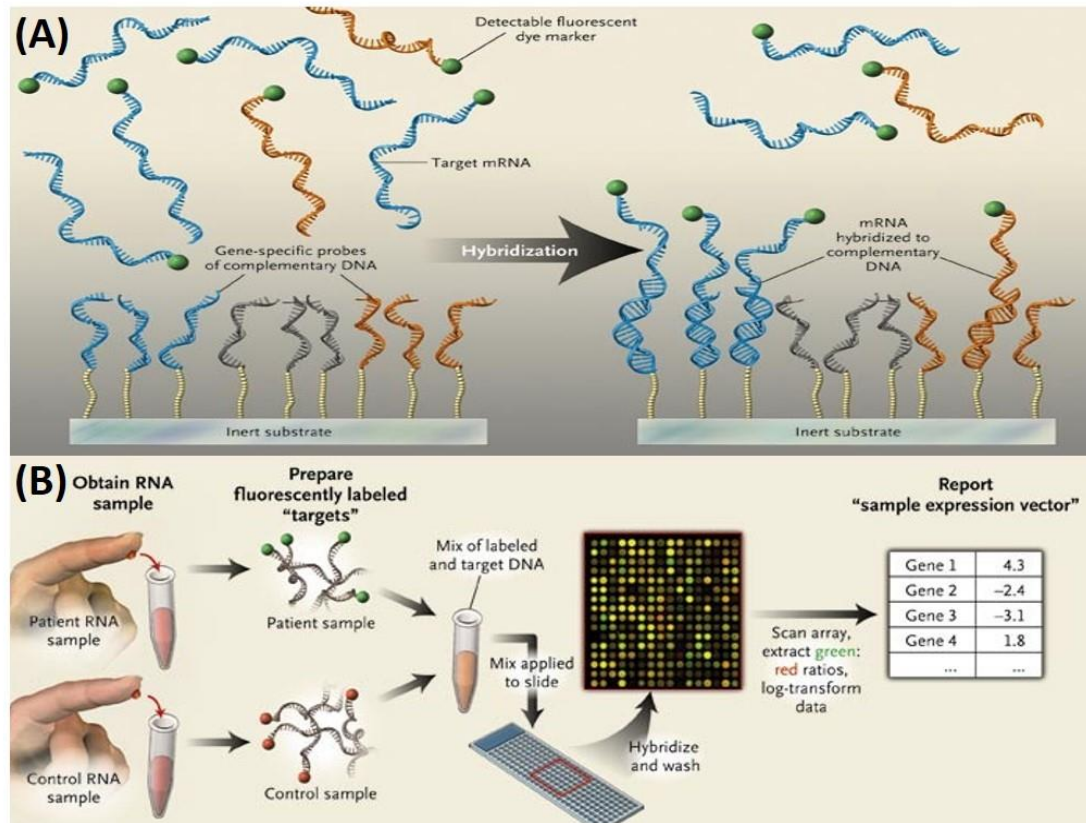


Figure 1-9. Overview of DNA microarray

(A) Hybridization with gene elements on a microarray. (B) Schematic overview of probe microarray with two samples. Fluorescent dye Cy3 (green) and dye Cy5 (red) having the fluorescence emission wavelength of approximately 570 nm and 670 nm, respectively. Reprinted from Quackenbush, 2006²²⁰.

1.5.2 Applications of microarrays

The predominate application of DNA microarrays has been to measure gene expression levels based on the abundances of RNAs in different tissues. Gene expression provides a key clue to a given alteration in phenotype and by looking at overall patterns of gene expression, helps to understand the genetic regulatory networks in order to identify co-

regulated genes with related functions. One of analytical methodologies to identify functionally related genes is cluster analysis which partitions genes into groups and clusters based on the similarity of expression patterns. By clustering, it is useful for elucidating the role of certain genes that appear in the same cluster and the relation of differentially expressed gene clusters in a particular phenotype²²¹.

Microarray technology has also been applied to transcription factor binding analysis and genotyping. The former is combined with chromatin immunoprecipitation to determine binding sites of transcription factors that regulate the activation or inhibition of gene expression²¹⁹. The latter usually refers to single-nucleotide polymorphism (SNP) genotyping, commonly used in discovering variation in a single nucleotide that occurs at a specific position in whole genome²²². Moreover, SNP genotyping is widely used in cancer research. Knowing that tumour formation involves simultaneous changes in cells and genes, SNP genotyping can identify single gene mutation, cancer biomarkers, target genes of tumour suppressors as well as the identification of genes associated with chemoresistance to provide information for drug discovery²²³.

Microarray has provided scientists with a convenient and useful tool for genome-wide analysis; however, with recent advancements and radical decline costs in next generation sequencing technologies, it offers another attractive option for genome-wide studies and may supersede many applications of microarray in the future.

1.6 Hypothesis and aims

Given that the placental environment is affected by pregnant complications, it would be important to investigate whether the biological properties of MSCs derived from GDM placenta were altered. On the other hand, the high risk of developing diabetes of women

with a GDM history and their offspring, placental MSCs come to be a valuable source for their future cell therapy. Therefore, we aim to characterise AMSC-/CMSC- derived from GDM and healthy placenta and investigate their differentiation potential for insulin-producing cell generation. Furthermore, we used DNA microarray technology to comprehensively understand the biological properties between healthy- and GDM- MSCs.

The aims of this study can be divided into three main objectives:

- Characterise AMSCs and CMSCs from GDM and healthy women via biological (morphology and immunophenotypes), functional (growth and tri-lineage differentiation), and immunological (T-cell and macrophage modulation) characterisation.
- Develop a feasible approach to generating insulin-producing cells from Healthy-/GDM-CMSCs and AMSCs in an attempt to explore their therapeutic potential in diabetes therapy.
- Perform DNA microarray to identify gene profiles and investigate benefits and disadvantages of using CMSCs from healthy and GDM women in future regenerative medicine.

Chapter 2

Materials and methods



2.1 Materials

Table 2-1. List of materials

	Catalogue number	Supplier
2-mercaptoethanol (Gibco)	21985023	ThermoFisher Scientific
2',7'-dichlorofluorescein diacetate (DCFDA)	ab113851	Abcam
3-(4,5-dimethylthiazol-2yl)-2,5diphenyltetrazolium bromide (MTT)	M6494	ThermoFisher Scientific
3-isobutyl-1-methylxanthine (IBMX)	I7018	Sigma-Aldrich
4',6-Diamidino-2-phenylindole (DAPI)	D9542	Sigma-Aldrich
ABTS Liquid Substrate Solution	A3219	Sigma-Aldrich
Acetic acid	A6283	ThermoFisher Scientific
Aldehyde dehydrogenase (ALDH) activity colorimetric assay kit	MAK082	Sigma-Aldrich
Alcian blue	A3157	Sigma-Aldrich
Alizarin red S	A5533	Sigma-Aldrich
Ascorbic acid phosphate	A8960	Sigma-Aldrich
Beta-glycerophosphate disodium salt hydrate	G5422	Sigma-Aldrich
Bicinchoninic acid (BCA) protein assays	23227	ThermoFisher Scientific
Bovine serum albumin (BSA) fatty acid free powder	11433164	ThermoFisher Scientific
Cellular senescence assay kit	KAA002	Merck Millipore
Chloroform	C/4960/17	ThermoFisher Scientific
Collagenase type IV	10780004	ThermoFisher Scientific
Corning Transwell polyester membrane cell culture inserts	CLS3460-48EA	Sigma-Aldrich
Crystal violet	C6158	Sigma-Aldrich
Dexamethasone	D2915	Sigma-Aldrich
Dimethylsulphoxide (DMSO)	D2650	Sigma-Aldrich

Dulbecco's Modified Eagle Medium (DMEM)- 4.5 g/L glucose	BE12-709F	Lonza
Dulbecco's Modified Eagle Medium (DMEM)- 1g/L glucose	LZBE12-707F	Lonza
DMEM, no glucose, no glutamine, no phenol red	A1443001	ThermoFisher Scientific
DMEM F12 1:1 mixture	BE04-687Q	Lonza
Exendin-4	E7144	Sigma-Aldrich
Ethanol (absolute)	E0650/17	ThermoFisher Scientific
Ethylene diamine tetra-acetic acid (EDTA)	BP2482-1	ThermoFisher Scientific
Foetal bovine serum (FBS)	FB-1001G/500	Biosera
Glycerol	G6279	Sigma-Aldrich
Glucose	G7021	Sigma-Aldrich
Human Betacellulin	100-50	PeproTech
Human EGF	AF-100-15	PeproTech
Human GLP-1 (7-36a.a)	130-08	PeproTech
Human/Murine/Rat Activin A (E.coli)	120-14E	PeproTech
High-Capacity cDNA Reverse Transcription Kit	4368814	ThermoFisher Scientific
Human IL-2 Mini ABTS ELISA Development Kit	900-M12	PeproTech
Human IL-10 Mini ABTS ELISA Development Kit	900-M21	PeproTech
Human TNF- α Mini ABTS ELISA Development Kit	900-M25	PeproTech
Human Insulin ELISA Kit	ab200011	Abcam
Human C-Peptide ELISA	80-CPTHU-E01.1-ALP	Stratech
Human TGF-beta 3 (E.coli)	100-36E	PeproTech
Hydrogen peroxide solution (H ₂ O ₂)	216763	Sigma-Aldrich
Indomethacin	I7378	Sigma-Aldrich
Insulin Antibody	sc-9168	Santa Cruz
Insulin, Transferrin, Selenium (ITS)	I3146	Sigma-Aldrich
Isopropanol	11398461	ThermoFisher Scientific
L-Glutamine	BE17-605E	Lonza
LIVE/DEAD Viability/Cytotoxicity Kit	L3224	ThermoFisher Scientific

L-Proline	P5607	Sigma-Aldrich
MEM Eagle NEAA (100X)	LZBE13-114E	Lonza
Methanol	10141720	ThermoFisher Scientific
Mouse anti-rabbit IgG-Texas Red	sc-3917	Santa Cruz
Nicotinamide	N0636	Sigma-Aldrich
Oil Red O	O0625	Sigma-Aldrich
PDX-1 Antibody (B-11) Alexa Fluor 488	sc-390792 AF488	Santa Cruz
Penicillin-Streptomycin	DE17-603E	Lonza
Phorbol 12-myristate 13-acetate (PMA)	P8139-5MG	Sigma-Aldrich
Phycoerythrin conjugated antibodies CD105	130-098-845	Miltenyi Biotec
Phycoerythrin conjugated antibody CD73	130-097-932	Miltenyi Biotec
Phycoerythrin conjugated antibody CD90	130-098-906	Miltenyi Biotec
Phycoerythrin conjugated antibody CD14	130-098-167	Miltenyi Biotec
Phycoerythrin conjugated antibody CD19	130-098-168	Miltenyi Biotec
Phycoerythrin conjugated antibody CD34	130-098-140	Miltenyi Biotec
Phycoerythrin conjugated antibody CD45	130-098-141	Miltenyi Biotec
Phycoerythrin conjugated antibody HLA-DR	130-098-177	Miltenyi Biotec
Phycoerythrin conjugated antibodies IgG1isotype	130-098-849	Miltenyi Biotec
Phycoerythrin conjugated antibodies IgG2a isotype	130-098-849	Miltenyi Biotec
Phytohaemagglutinin (PHA)	L166	Sigma-Aldrich
Phosphate buffered saline (PBS)	BE17-516F	Lonza
Radioimmunoprecipitation assay (RIPA) buffer	R0278-50ML	Sigma-Aldrich
Retinoic acid	R2625	Sigma-Aldrich
Rosewell Park Memorial Institute (RPMI1640)	12-918F	Lonza

RNAlater	R0901	Sigma-Aldrich
Sodium butyrate	B5887	Sigma-Aldrich
Sodium pyruvate	S8636	Sigma-Aldrich
Taurine	T8691	Sigma-Aldrich
TRIzol Reagent	15596026	ThermoFisher Scientific
Trypsin/Versene(EDTA)	BE02-007E	Lonza
Trypan blue	T8154	Sigma-Aldrich
Tween-20	P7949-100ML	Sigma-Aldrich
QuantiFast SYBR Green PCR Kit	204054	Qiagen
UltraPure DNase/RNase-Free Distilled Water	10977049	ThermoFisher Scientific

2.2 Placental samples collection

All placentas in our research were collected from Royal Stoke University Hospital, UK, after obtaining Research Ethics Committee and Health Research Authority approvals (Reference 15/WM/0342). Women undergoing Caesarean sections were consented to donate their placenta. Term placentas were collected from healthy donors (n=10) and donors with GDM (n=11). Individuals were classified as GDM after clinical diagnosis using an OGTT between 24 and 28 weeks pregnant. The OGTT was carried out by the measurement of fasting plasma glucose (FPG) concentration, and 2 hours after a 75 g solution of glucose was consumed, plasma glucose was measured again. If the patients exceeded the NICE clinical guidelines for glucose concentration thresholds (section 1.1.1) were diagnosed with GDM. The cell isolation process was performed within an hour of collecting the placenta from Caesarean section. Maternal and fetal details of the samples used in this study were listed in Table 2-2.

For each placenta, both amniotic mesenchymal stem cell (AMSCs) and chorionic mesenchymal stem cells (CMSCs) were isolated from the same placental membrane. Independent samples were grouped into Healthy-CMSCs, Healthy-AMSCs, GDM-CMSCs, and GDM-AMSCs for all the comparisons and statistical analysis in this thesis.

Table 2-2. Placenta sample details

Samples	Ethnicity	Age	Weeks	BMI	Infant/Weight	
Healthy01	Nigerian	46	38	38	Girl / 3380	Hypertension / GDM in last pregnancy
Healthy02	Caucasian	26	39	22	Girl / 3400	Hepatitis B
Healthy03	Caucasian	33	37	24	Girl / 3280	-
Healthy04	Caucasian	33	39	30	Girl / 3440	-
Healthy05	Caucasian	29	39	37	Girl / 3280	Previous smoker
Healthy06	Caucasian	41	39	22	Girl / 3720	-
Healthy07	Caucasian	30	39	20	Girl / 3095	Current smoker
Healthy08	Caucasian	24	39	21	Girl / 3540	Previous smoker
Healthy09	Caucasian	30	39	27	Girl / 3780	GDM in last pregnancy
Healthy10	Caucasian	26	39	29	Girl / 3100	-
Healthy11	Caucasian	32	39	25	Girl / 3630	-
GDM01	Chinese	35	38	25	Boy / 3740	-
GDM02	Caucasian	31	39	22	Girl / 4660	Addison's disease / received hydrocortisone before delivery
GDM03	Caucasian	31	37	42	Boy / 3120 & Boy / 3600	Non identical twins
GDM04	Caucasian	24	37	40	Boy / 3468	-
GDM05	Caucasian	23	37	34	Girl / 2920	Previous smoker
GDM06	Caucasian	43	39	44	Girl / 3860	GDM on metformin
GDM07	Caucasian	35	39	25	Boy / 3580	GDM on insulin
GDM08	Caucasian	32	36	29	Boy / 3581	GDM on insulin and metformin
GDM09	Caucasian	20	39	20	Boy / 3940	GDM on metformin
GDM10	Caucasian	32	39	36	Girl / 3380	-

2.3 Isolation and culture of AMSCs and CMSCs

The placenta dissection and cell isolation were conducted in a class II microbiological safety cabinet. All materials used in isolation process were sterile. The CMSCs/AMSCs isolation process was performed within an hour of collecting the placenta from Caesarean section, using the protocol described by Marongiu *et al.*, (2010)²²⁴. The placenta dissection process was demonstrated in Figure 2-1.

Umbilical cord was trimmed and cut an X-shaped incision onto the placental surface. Amniotic membrane was manually peeled from the underlying chorionic membrane and immediately washed with PBS for several times to remove blood clots. As chorionic membrane is attached to maternal tissues, a removal of decidual tissue was required. Decidual tissue and blood clots on chorionic membrane were carefully removed by forceps and washed with PBS. Following wash steps, membranes were placed in 20 ml prewarmed 0.05% trypsin/EDTA solution in 50 ml centrifuge tubes and incubated at 37°C for 1 hour. Membranes were then washed with PBS for 3-5 times to remove any residual trypsin solution. To release the cells, membranes were placed in freshly prepared digestion media containing 1 mg/ml collagenase type IV and 25 µg/ml DNase I in serum free Dulbecco's Modified Eagle Medium (DMEM) in 50 ml centrifuge tubes. Digestion media was filtered through a 0.2 µm filter and prewarmed before use. Membranes were digested at 37°C incubator for 1-1.5 h and during the digestion process, the membranes were checked every 15 minutes. Incubating on a rotator or shaking the tubes every 15 minutes was sometimes required to enhance the digestion process. The incubation stopped once the membranes were completely dissolved. Equal volume of PBS was added to the centrifuge tubes containing digestion media and dissolved membranes. The mobilised cells were pelleted by centrifugation at 200g for 5 minutes and then supernatant was discarded, the pellet was

washed with PBS, and pelleted again at 200 g for 5 minutes. Cell pellet was then re-suspended in growth media consisting of 10% FBS, 1% L-glutamine, 1% Penicillin-Streptomycin, and 1% non-essential amino acids (NEAA) in DMEM and seeded at the density of 1×10^5 cells/cm².

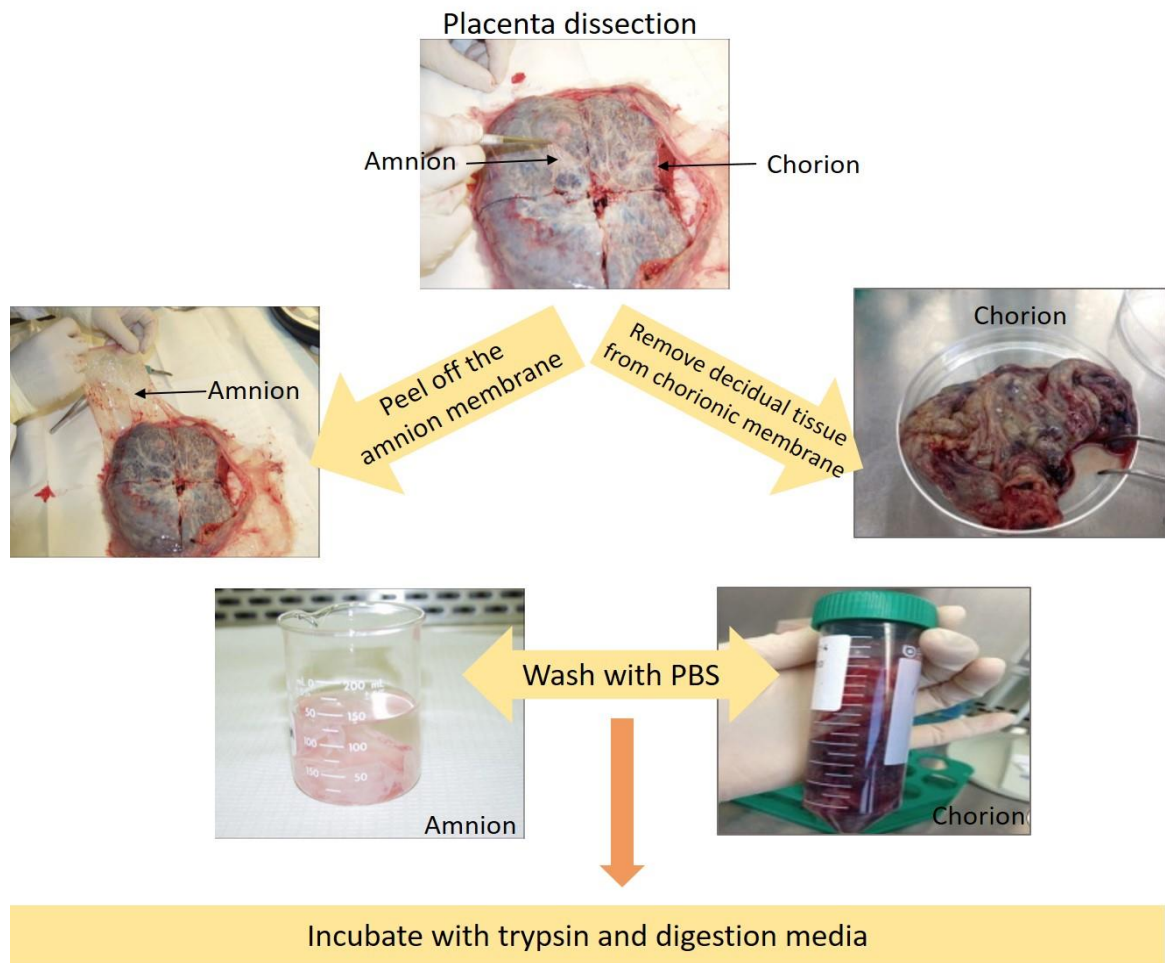


Figure 2-1. MSC isolation from placental membranes.

AMSCs and CMSCs were isolated from amniotic and chorionic membrane, respectively. Following trimming the umbilical cord and cutting an X-shaped incision on placental surface, amnion was peeled from the underlying chorion and washed with PBS. Blood clots and decidual tissue attached to chorion were removed by forceps and chorion was washed with PBS. After the washing step, both amnion and chorion were digested with trypsin and digestion media containing 1 mg/ml collagenase type IV and 25 µg/ml DNase I in serum free DMEM to release the AMSCs and CMSCs from the membranes. Reproduced from Marongiu *et al.*, 2010²²⁴ and Koo *et al.*, 2012²²⁵

2.4 Cell culture techniques

All cell cultured procedures were performing using disposable sterile consumables in a class II microbiological safety cabinet. Cells were cultured in standard tissue culture T25, T75 flasks or multi-well culture plates and maintained in 5% CO₂ at 37 °C incubators.

2.4.1 Cell passage, cryopreservation, and recovery

For adherent cell lines, cells were sub-cultured when its growth reached 80-90% confluence. Media were aspirated, monolayer cells were rinsed with PBS, and sufficient amount of trypsin/EDT (0.05% trypsin/0.02% ethylenediaminetetraacetic acid (EDTA) diluted 1 in 10 in PBS) was added to cover cells. Cells were then incubated at 37 °C for about 10 minutes until detached. Cell maintenance media added to halt the trypsin activity in an equivalent volume of trypsin/EDTA solution and cell suspensions were transferred to a centrifuge tube for pelleting at 1,000 rpm for 5 minutes. Cell pellet was re-suspended in fresh maintenance media for seeding.

To cryopreserve the cells for future use, cells were detached using trypsin/EDTA and re-suspended in freezing media (10% FBS DMEM supplemented with 10% DMSO). 1 ml of freezing media containing approximately 2×10^6 cells was transferred into a cryovial and placed in Mr. Frosty for slowly cooling to -80 °C before transferred to liquid nitrogen for further storage.

To recover frozen cells, cryovials taken out from liquid nitrogen were immediately placed into a 37 °C water bath. Thawed the cells by gently swirling the cryovials and transferred thawed cells to the desired amount of growth media in a centrifuge tube. Cells were pelleted at 1,000 rpm for 5 minutes, supernatant was aspirated, and pellets were re-

suspended in growth media for seeding.

2.4.2 Morphological observation and measurement

Changes in cell morphology were detected by a light microscope and images were processed with ImageJ software to analysis cell length and surface area. For analysis, 5 images were taken from each sample from passage 0-2. The images were open by ImageJ and to calibrate the images, scale was set based on a known distance. Images were adjusted by modifying the contrast and sharpening the images until the shapes of cells clearly appeared. To measure cell lengths, line tool in ImageJ was used to draw a line based on the longest axis from cell periphery and length of the line was measured to represent each cell length. At least 100 single cells were measured in each image. Cell surface area was measured by ImageJ through automatically circling the outline of cells and the edged cells were excluded (Figure 2-2).

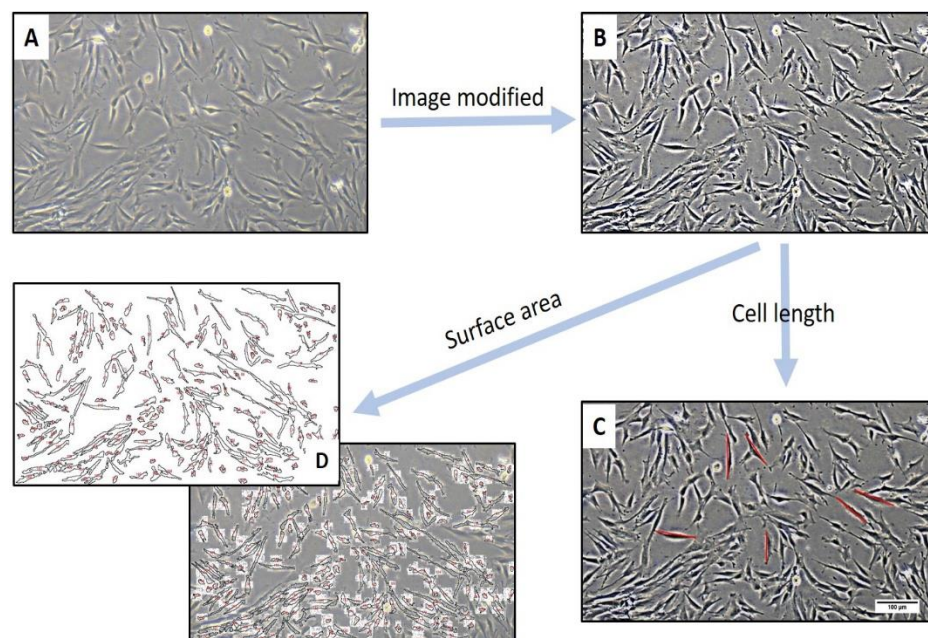


Figure 2-2. Cell morphology analysis

(A) Original image (B) Contrast and brightness adjustment (C) Cell length measurement (D) Cell surface area measurement. All images were analysed by ImageJ.

2.4.3 Cell counting and doubling time

Cells were suspended and diluted in culture media, if trypan blue was used, a small amount of cell suspension was mixed with the equal volume of trypan blue. 10 μ l of the cell suspension was loaded into a haemocytometer adhered with a coverslip. Cells were counted from 4, 1 mm² corner squares under a microscope and each square represents a volume of 0.1 μ l. To determine the number of cells/ml, the mean number of each square was multiplied by 10⁴ while if cell suspension was diluted 1:1 with trypan blue, the dilution factor was also taken into account by multiplying 2 in the calculation.

Cell numbers were counted every 2 days and the doubling time was calculated at passage 3. Equation for doubling time = $(T_2 - T_1) \times \log 2 / (\log N_2 - \log N_1)$, where: T1, final time (hours); T2, initial time; N1, initial cell numbers; and N2, final cell numbers.

2.4.4 MTT assay

The 3-(4,5-dimethylthiazol-2-yl)-2,5-diphenyltetrazolium bromide (MTT, ThermoFisher) assay has been widely used to determine cell viability and proliferation since its development by Mosmann in the 1980's²²⁶. The measurement of MTT is based on mitochondrial function of cells by measuring activity of mitochondrial enzymes such as succinate dehydrogenase²²⁷. The increased measurement of MTT represents enhanced metabolic activity, which can be affected by cell proliferation, different conditions, chemical treatments, and cell death²²⁸. Therefore, MTT assay can only indirectly reflect the viable cell numbers and proliferation. Viable cells with active metabolism can convert soluble yellow-coloured MTT into an insoluble purple-coloured formazan product through NAD(P)H-dependent cellular oxidoreductase enzymatic activity, indicating mitochondrial activity²²⁹. The MTT compound was prepared in PBS at a concentration of 5 mg/mL, filtered through a

0.2 μm filter, and stored at $-20\text{ }^{\circ}\text{C}$. Cells were seeded at 3,000 cells/well in a 96-well plate in triplicate and performed MTT assay every 2 days for a 12-day period. When performing MTT assay, media was aspirated and added 90 μl serum-free media plus 10 μl MTT solution into each well. Following incubating the plates at $37\text{ }^{\circ}\text{C}$ for 4 hours, 100 μl DMSO was added and incubated at $37\text{ }^{\circ}\text{C}$ for 30 minutes to dissolve purple formazan crystals. Plates were wrapped in foil and shaken on an orbital shaker for 5 minutes before reading the absorbance at wavelengths of 570 nm using a plate reader. As phenol red present in the media can generate background, wells without cells contained same proportion of serum free media, MTT solution, and DMSO was used as a blank. The results are presented as mean \pm SD of triplicates, taking time as the horizontal axis and optical density (OD) as the longitudinal axis.

2.4.5 Production of conditioned media

Cells at passage 3 were seeded in T75 flasks and when reaching 80–90% confluence, cells were washed with PBS and then 15 ml of fresh media without FBS was added. After incubating for 48 hours, conditioned media was collected by transferring supernatant to a centrifuge tube and filtering through a 0.2 μm filter to remove cell debris. Supernatant was stored at $-80\text{ }^{\circ}\text{C}$ until further use.

2.5 Flow cytometry

Flow cytometry is a technique to investigate cell populations at the single-cell level through labelling cells with fluorescent antibodies and suspending cells in dynamic fluidics to pass through the flow cytometer. As the cells traverse the laser beam, fluorescent light emission from the cells is detected and converted to electronic signals, subsequently processed and visualised on a monitor for analysis (Figure 2-3).

Flow cytometry was used to investigate the cluster of differentiation (CD) surface antigens for MSC characterisation. Cells were obtained from a T75 flask at 90% confluence, trypsinised using trypsin/EDTA, and re-suspended in flow cytometry buffer (0.5% BSA and 2 mM EDTA in PBS). Suspension cells were equally divided into 10 Eppendorf tubes and centrifuged at 300 g for 10 minutes in preparation for antibody conjugation. Phycoerythrin conjugated antibodies (CD14, CD19, CD34, CD45, CD73, CD90, CD105, HLA-DR, and isotype controls IgG₁ and IgG_{2a}) were diluted in flow cytometry buffer. The diluted concentration of each antibody was based on manufacturer's suggestion (Miltenyi Biotec). After centrifuging cell suspension, supernatant was discarded and cell pellets were re-suspended in 50 µl diluted antibody followed by incubation in the dark at 4 °C for 15 minutes. 1 ml of flow cytometry buffer was added to each tube and cells centrifuged at 300 g for 10 minutes, removed supernatant, re-suspended in 300 µl buffer for flow cytometry analysis. Flow cytometry was carried out using Beckton Dickinson FC500 and at least 50,000 events were acquired for each assessment. Data were analysed using Flowing Software to produce colour dot plots, histogram plots and set gates for analysing percentage of positive events. Isotype control IgG₁ was used for CD19, CD73, CD90, CD105; IgG_{2a} was for CD14, CD34, CD45, HLA-DR analysis.

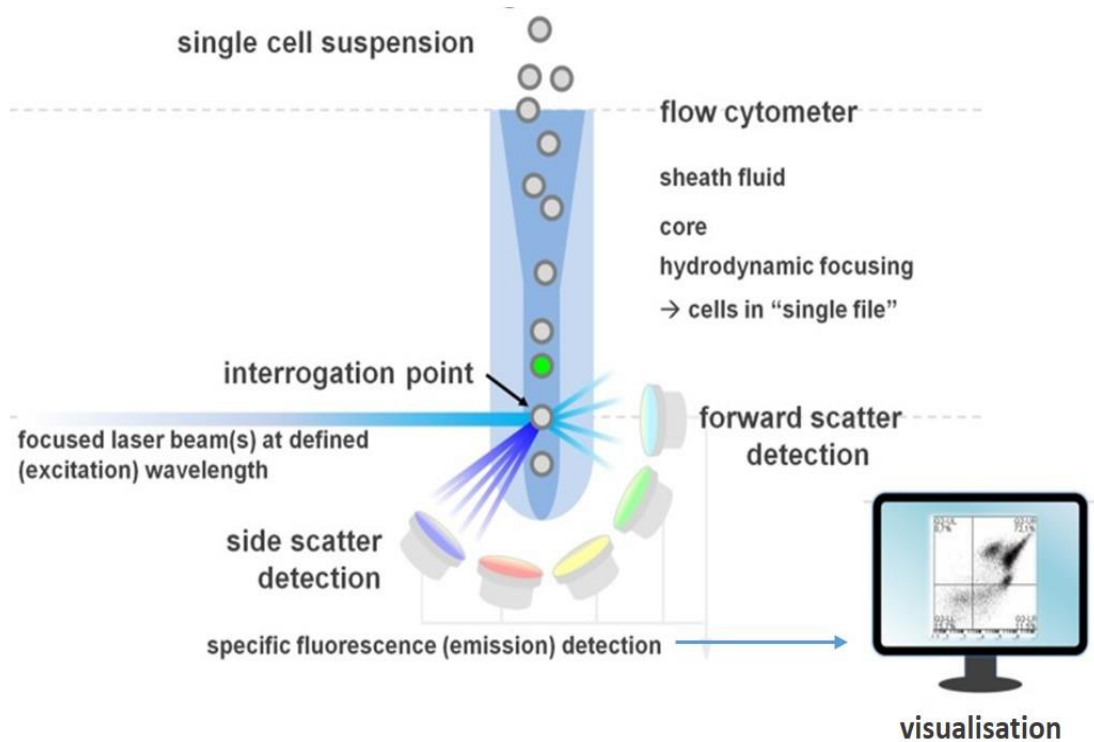


Figure 2-3. Flow cytometry technique

The sheath fluid mobilises cell suspension and directs it through laser beam as a single event per time. Forward scatter, associated with the size of the particle, and side scatter, reflecting the granularity of the cell can be detected without the requirement of specific labelling. The appropriate lasers should be assigned for the corresponding excitation and emission spectra which can identify the positive staining of fluorescent markers. Reproduced from Menon *et al.*²³⁰

2.6 Tri-lineage differentiation and assessment

Cells at passage 3 were seeded in a 24-well plate in complete growth media (DMEM with 10% FBS, 1% L-glutamine, and 1% NEAA) overnight to allow attachment. Following cell adherence, the medium was replaced with a differentiation medium, which was changed every 3 days during the 21-day culture. All images of differentiation were monitored with an inverted optical microscope (Olympus).

2.6.1 Osteogenesis

To induce osteogenic differentiation, 2×10^4 cells/well were seeded in a 24-well plate and cultured in differentiation media consisting of 50 μ M ascorbic acid, 10 mM β -glycerol phosphate, and 0.1 μ M dexamethasone in complete growth media²³¹.

Osteogenesis was evaluated by the stain of mineral deposition in differentiated osteoblasts with alizarin red S. Following removing the differentiated media, cells were fixed by 500 μ l/well of 10% formalin for 20 minutes, washed with PBS, and incubated in 2% alizarin red S solution for 10 minutes. Alizarin red S was prepared in distilled water (dH₂O) and paper filtered. Stained wells were then washed gently using tap water and allowed to dry for imaging.

2.6.2 Adipogenesis

For adipogenesis, 2×10^4 cells/well were seeded and cultured in complete growth media supplemented with 0.5 μ M dexamethasone, 0.5 mM 3-Isobutyl-1-methylxanthine (IBMX), 10 μ g/ml insulin, and 100 μ M indomethacin^{232, 233}.

Adipogenesis was assessed by Oil Red O stain for intracellular lipid droplets. Oil Red O stock

solution was prepared by dissolving 350 mg of Oil Red O in 100 mL isopropanol and shaking overnight on a rotator. Oil Red O working solution was prepared freshly prior to staining by mixing 6 parts of Oil Red O stock solution with 4 parts of dH₂O and filtered through a 0.2 µm filter. For staining, cells were washed, fixed with 10% formalin as described in osteogenesis assessment, and rapidly washed with 60% isopropanol. Filtered Oil Red O working solution was added and incubated for 10 min, which was then washed 3 times with dH₂O and imaged immediately.

For quantitative analysis of positive staining, 500 µl of 100% isopropanol was added to each well and incubated for 10 minutes with gently shaking to ensure all the Oil Red O staining was eluted. 100 µl of the solution was transferred to each well in a 96-well plate and measured the absorbance at 500 nm. 100% isopropanol was used as blank.

2.6.3 Chondrogenesis

To induce chondrogenic differentiation, 1×10^5 cells were re-suspended in 8 µl of medium and dropped in the centre of the well as a micromass. After 1-hour incubation in the standard culture condition to allow cells to attach to the culture surface, micromass was then replenished with chondrogenic differentiation media, supplemented with 1% ITS, 0.1 µM dexamethasone, 50 µM ascorbic acid, 40 µg/mL L-proline, 1% sodium pyruvate, and 10 ng/mL TGF-β3 in complete growth media with reduced FBS to 1%^{234, 235}.

After 21-day differentiation period, cells were fixed and proteoglycan-rich matrix accumulation was detected by Alcian blue for chondrogenesis evaluation. 1% Alcian blue solution was prepared by dissolving 0.5 g Alcian Blue 8GX in 50ml of 3% acetic acid (pH 1.5) and paper filtered. Fixed cells were incubated with 1% Alcian blue solution overnight, washed gently with tap water, and images were captured immediately.

2.7 RNA extraction and reverse transcription

Total RNA was extracted by TRIzol reagent, a monophasic solution of phenol, guanidine isothiocyanate, and proprietary components for suppressing RNase activity and isolating RNA from large or small numbers of cells and tissue samples.

RNA isolation process was conducted in a biosafety cabinet. Cell monolayer was rinsed with PBS and 1 ml of TRIzol reagent (ThermoFisher) per well in a 6-well plate was added to lyse the cells. Cell lysate was transferred to a 1.5 ml Eppendorf tube, vortexed thoroughly and incubated for 10 minutes to permit complete dissociation of the nucleoproteins complex. 0.2 ml of chloroform was added and samples were vortexed for 15 seconds repeating for 2-3 times. Following centrifuging at 12,000 g for 15 minutes at 4 °C, the mixture separated into a lower red phenol-chloroform, an interphase, and an upper aqueous phase where RNA remained exclusively. The upper aqueous phase was then transferred to a new Eppendorf tube containing 0.5 ml of isopropanol, mixed and incubated for 10 minutes before centrifuging at 12,000 g for 10 minutes at 4 °C to allow RNA precipitation. A white small pellet at the bottom of the tube was washed with 1 ml 75% ethanol twice by briefly vortexing and pelleting at 7,500 g for 5 minutes at 4 °C. Supernatant was discarded and air dried the RNA pellet for 10 minutes, followed by re-suspending the pellet in 20 µl of RNase-free water. To solubilise the pellet, Eppendorf tubes were incubated in a 55 °C water bath for 10–15 minutes. RNA was stored at -80 °C for further applications.

RNA concentration and purity was determined by Nanodrop spectrophotometer (ND-2000). 1 µl of RNA was used for measurement and the ratio of A_{260}/A_{280} was around 1.8-2.2 which is generally accepted as good RNA quality. For microarray experiments, in order to obtain high purity of RNA, 1×10^7 cells were pelleted at 1,000 rpm for 5 minutes and stored in 1 ml of RNeasy lysis solution (Qiagen) at 4 °C. Samples were sent to Welgene Biotech Company for

RAN extraction and microarray analysis (section 5.3).

Complementary DNA (cDNA) was prepared from 1 µg of total RNA using High-Capacity cDNA Reverse Transcription Kit (ThermoFisher). RNA was diluted to a desired concentration in RNase-free water with a total volume of 10 µl. Equal volume of reverse transcription master mix was prepared based on manufacturer's instruction and mixed with diluted RNA samples. Samples were briefly centrifuged and loaded to a thermal cycler (MJ Research PTC-200). The program for reverse transcription: 25 °C for 10 minutes, 37 °C for 2 hours, 85 °C for 5 minutes, and cooling down to 4 °C before removing the samples from thermal cycler. The cDNA samples were stored in -20 °C for further applications.

2.8 Real-time polymerase chain reaction (qPCR)

Gene expression analysis was evaluated by real-time PCR using QuantiFast SYBR Green PCR Kit (Qiagen). All cDNA was diluted 1:4 in RNase-free water and used to perform real-time PCR. 2 µl of diluted cDNA was mixed with an appropriate amount of SYBR Green master mix based on manufacturer's instruction alongside 250 nM of respective forward and reverse primers. Primers were designed to be fully complementary to template DNA sequences using NCBI Primer-BLAST online tool. Primers were 18 - 25 nucleotides in length, containing 40 - 60% GC content, and lacking lack significant secondary structures, and primer pairs were approximately the same length. Regions of complementarity at the 3' end of primers were minimised to reduce the potential for the formation of primer dimer²³⁶.

SYBR Green generates a fluorescent signal when bound to double stranded DNA during the course of amplification. The fluorescent signal represents the relative abundance of product determined by the comparison of the cycle number that each sample has accumulated sufficient fluorescence to cross an arbitrary threshold value. The threshold level is set in the exponential phase of product amplification and above background levels for all samples (Figure 2-4A). A melting curve (dissociation curve) analysis shows the change in fluorescence observed when double-stranded DNA with incorporated dye molecules (SYBR Green) dissociates into single-stranded DNA as the temperature of the reaction is raised²³⁷. Primer-dimers, non-specific or mismatched sequences generally have a lower melting temperature than the specific PCR product of the reaction (Figure 2-4B). Therefore, melting curves analysis was used to check real-time PCR reactions for primer-dimers and to ensure reaction specificity during assay optimisation. Real-time PCR used in this study depended on relative quantification and was unaffected by the lack of quantitative DNA standards, as the ratio of two targets was assessed within the same assay and many of the sources of

measurement uncertainty similarly affected both determinations, and thus did not influence the final result²³⁸.

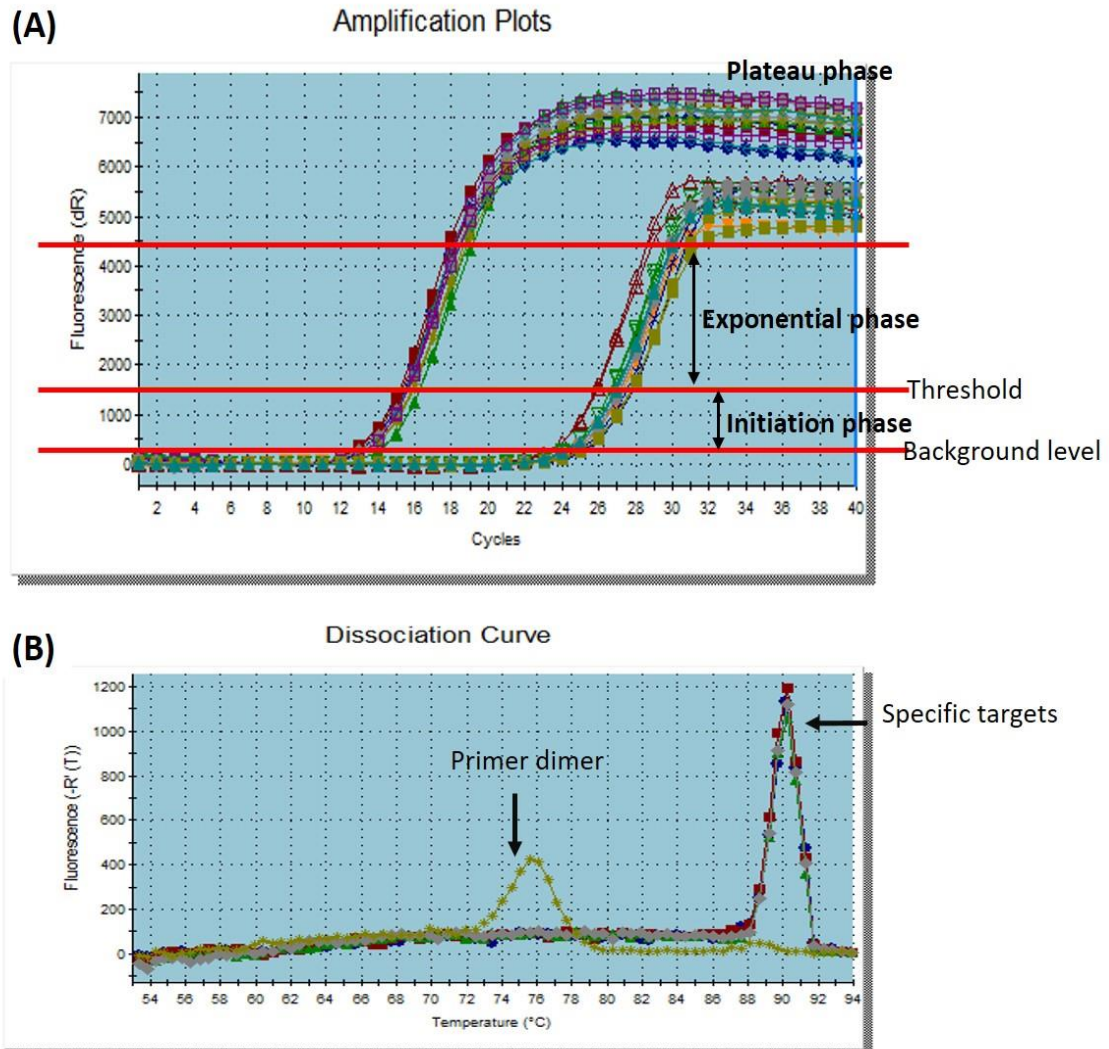


Figure 2-4. Real-time PCR amplification and dissociation curve

(A) The three phases of fluorescence accumulation across cycles during a real-time PCR amplification – initiation phase (early exponential), exponential phase (log-linear), and plateau phase. A threshold is set on the log-linear phase of amplification curve. (B) The post-amplification melting curve (dissociation curve) analysis to differentiate specific PCR products from primer dimers.

The cycle at which the threshold is passed (CT) was normalised for all samples using the CT

value for the housekeeping reference gene GAPDH (glyceraldehyde 3-phosphate dehydrogenase). The choice of GAPDH as the reference gene was validated for every sample and confirmed that it remained constant in all samples being compared at all points of the experiment. All runs included a no-template control (NTC) which contained all reaction components except the cDNA sample. If an amplification curve appears in NTC, it indicates the existence of primer-dimers or contamination with completed PCR reaction product, which can lead to inaccurate expression levels. Every pair of primers used in this study was optimised for its ideal melting temperature (T_m , Table 2-3), which results in the lowest variation in replicates, a negative NTC, a melting curve analysis revealing detection of a specific product and high reproducibility between replicate reactions (Figure 2-4B). All primers were optimised via a test run, including three experimental samples in triplicates and a NTC control.

The total volume of each reaction mixture was 15 μ l and real-time PCR was carried out in real-time PCR system (Agilent Stratagene Mx3000P). Primer sequences for each gene are shown in Table 2-3. All samples were amplified at 95 °C for 10 minutes followed by 40 cycles of a denaturation step at 95°C for 10 seconds, and a 30-second annealing step at the optimised temperature for the primers (Table 2-3). The expression levels of genes were normalised to the reference gene, *GAPDH* ($\Delta Ct = Ct_{(target)} - Ct_{(reference)}$), and compared with controls to generate the $2^{-\Delta\Delta Ct}$ ($\Delta\Delta Ct = \Delta Ct_{(experimental)} - \Delta Ct_{(control)}$) for calculating relatively fold changes.

Table 2-3. Primer sequences

Gene ID	Forward sequence	Reverse sequence	Tm
ADIPOQ	AGGCCGTGATGGCAGAGATG	CTTCTCCAGGTTCTCCTTTCCTGC	60
ALDH1A1	TCAAACCAGCAGAGCAAAC	TAGGCCCATACCAGGAACA	60
ALDH2	CTGCTGACCGTGGTTACTT	CTCCCAACAACCTCCTCTATG	60
ALDH3B1	GCTGAAGCCATCGGAGATTAG	GCTCCCTGTGAAGAAGATGTAG	60
AQP1	CTGCATGGTCAAGCCTCTTA	TCAAGGGAGTGGGTGAATTG	60
CCL-17	CGGGACTACCTGGGACCTC	CCTCACTGTGGCTCTTCTTCG	60
CD24	CTCCTACCCACGCAGATTATTC	AGAGTGAGACCACGAAGAGAC	60
CELSR1	TACTTCTGCGGTGCTGGTTT	GTCCGTAAACCGTCCCTTCC	58
CTCF	GCCTGTTCCAAGACCTGTG	GGCGGCTCTGCTTCTCTA	60
CXCL8	CTGGCCGTGGCTCTCTTG	CCTTGGCAAACTGCACCTT	60
CXCL12	ATGAACGCCAAGGTCG	GGGCTACAATCTGAAGGG	60
EDN1	CCATGAGAAACAGCGTCAAATC	CGAAGGTCTGTCACCAATGT	60
FLNB	TGATCTATGTGCGCTTCGGT	GACATGCATTTACCGGTGCC	60
GAPDH	ACTTCAACAGCACACCCACT	GCCAAATTCGTTGTCATACCAG	58
GLUT2	ACTTCAACAGCACACCCACT	GCCAAATTCGTTGTCATACCAG	58
HBEGF	AATCTGGCTTAGTGCCACCC	GCACTCTGACCACGGAAGAT	60
HMOX1	TCTTGGCTGGCTTCCTTACC	GGATGTGCTTTTCGTTGGGG	60
IL-18	ATTCTCTTCAGCCAATCTTCA	TATCCCATGTGTGGAAGAAG	60
IL-10	TCAGCAGAGTGAAGACTTTC	CCTTGCTCTTGTTTTCACAG	60
IL-12	AAAGGACATCTGCGAGGAAAGTTC	CGAGGTGAGGTGCGTTTATGC	60
INS	TGCCCACAATCTCATACTCAA	TACAGACAGGGACCAGAGCAT	58
ISL1	GCAGCCTTTGTGAACCAACA	TTCCCCGCACACTAGGTAGAGA	58
MET	TGGTGCAGAGGAGCAATGG	CATTCTGGATGGGTGTTCCG	60
MRC1	ACCTCACAAGTATCCACACCATC	CTTTCATCACCACACAATCCTC	58
NANOG	CAACTGGTCAATTTTTCAGAAGGA	TTGAGAGGACATTGATGCTACTTCAC	55
NEUROG3	CCCAGCCTTTACTCTTCTTACCAC	GATTCTCTCCACAGTTATAGAAGGGA	60
NKX2.5	CAACATGACCCTGAGTCCCC	TAATCGCCGCCACAACTCT	60
NOG	CATGCCGAGCGAGATCAAA	CAGCCACATCTGTAACCTCCTC	60
NPPB	TGGAAACGTCCGGGTACAG	GACTTCCAGACACCTGTGGG	60
NQO1	GGGATGAGACACCACTGTATTT	AGTGATGGCCACAGAAAG	60
OCT4	CTATTCTTTTGCGCCGGTAGA	CTCACGGGTCACTTGGACAGT	55
PAX6	GTCCGAGTGTGGTTCTGTA	CTCAGTTTGAATGCATGGGA	58
PDGFA	GGAACGCACCGAGGAAGA	GCCAGGAGGAGGAGAAACAG	58
PDX1	TGTCCAACGGATGTGTGAGTA	TCCCGCTTATACTGGGCTATT	60
PPARG	GCAGGAGATCTACAAGGACTTG	CCCTCAGAATAGTGCAACTGG	58

<i>RASIP1</i>	CGTCTCCTTGAGAACCAATACC	CATTCCACGCGGGATAAGAA	60
<i>RSPO3</i>	CACCTTTATCTGAGCCAATGGA	ATGCAGGGGGATCTGACATA	60
<i>SOD2</i>	GGACAAACCTCAGCCCTAAC	GCCGTCAGCTTCTCCTTAAA	60
<i>SOX2</i>	TTCCGGAAGAAAAAGAGCCA	AAACAGGTCCAAGGTGGAGT	57
<i>TGFB2</i>	ATGCGGCCTATTGCTTTAGA	ACCCTTTGGGTTCGTGTATC	60

2.9 Immunology characterisation

2.9.1 Culture and stimulation of Jurkat cells

Jurkat T cells were originally cultured in 10% FBS RPMI 1640 and gradually adapted to 10% FBS DMEM through culturing in a mixture of RPMI and DMEM at the ratio of 4:1, 2:1, 1:1, 0.5:1, and 0:1 with each subculture. For subculture, suspension Jurkat T cells were transferred to a centrifuge tube, pelleted at 1,000 rpm for 5 min, removed supernatant, and re-suspended in fresh growth media. Cells were seeded at a density of 1×10^5 cells/ml in 25 ml growth media in a T75 flask.

To induce activation of Jurkat T cells, 5×10^5 cells/ml were stimulated with 5 μ g/ml phytohaemagglutinin (PHA, stock solution 0.5 mg/ml in PBS) and 50 ng/ml phorbol 12-myristate 13-acetate (PMA, stock solution 100 μ g/ml in DMSO) and control samples (without PHA and PMA) were received same amount of DMSO treatment. PHA is a lectin that binds to the T cell receptor and leads the stimulation of signal transduction for IL-2 secretion. Likewise, PMA is a small organic compound, which can diffuse through cell membrane into cytoplasm and directly activate protein kinase C leading to IL-2 production. The combination of PHA and PMA strongly enhanced Jurkat cells IL-2 production²³⁹.

2.9.2 Supernatant collection

The secretion of cytokine interleukin 2 (IL-2) is considered as an active state of Jurkat cells. Activated Jurkat cells were cultured in conditioned media from CMSCs or AMSCs for 24, 48, and 72 hours. Supernatant was collected at each time point for IL-2 ELISA assays, centrifuged at 1,500 rpm for 5 minutes to remove cell debris and transferred to a new Eppendorf tube for storage in a -80 °C freezer. CMSC and AMSC conditioned media

incubated in an empty well without Jurkat cells was used as a blank control.

2.9.3 Culture and stimulation of THP-1 cells

Human monocytes THP-1 cells were maintained in DME containing 10% FBS, 1% L-glutamine, 1% Penicillin-Streptomycin. As both Jurkat cells and THP-1 monocytes are suspension cell lines, the same sub-cultured method described in section 2.9.1 was applied to THP-1.

To simulate THP-1 cells for microphage polarisation, THP-1 cells were treated with 50 ng/ml PMA for 24 hours. Roughly 80% of suspension THP-1 attached to flask after 24 hours, indicating a differentiated state (M0 macrophage) and the suspension cells were removed by media change. M0 macrophages were polarised to M1 macrophages by incubation with 20 ng/ml of interferon- γ (IFN- γ) and 10 pg/ml of lipopolysaccharide (LPS). Macrophage M2 polarisation was induced by incubation with 20 ng/ml of interleukin 4 (IL-4).

2.9.4 Co-culture system

In co-culture experiments, 5×10^5 THP-1 cells were placed to a well in 12-well plates and treated with PMA for 24 hours. Media was gently aspirated and changed to 1.5 ml fresh media. The Transwell inserts (membrane pore size of 0.4 μ m, Corning) were then placed into each well and 5×10^5 CMSCs or AMSCs in 0.5 ml media were added to the Transwell insert. Following incubation for 24 hours, supernatant was collected, centrifuged at 1,500 rpm for 5 minutes, and transferred to a new Eppendorf tube for storage at -80 °C. The adherent THP-1 cells at the bottom of the wells were lysed with TRIzol reagent (ThermoFisher) for RNA extraction.

2.10 ELISA assay

ELISA (enzyme-linked immunosorbent assay) is designed for detecting and quantifying peptides, proteins, and hormones. ELISA assays performed in this study were sandwich ELISA, which involved an attachment of a capture antibody to a microplate, binding of target protein to the capture antibody, and then the detection of signals via a conjugated antibody and an enzymatic substrate. ELISA was performed in a 96-well plate and all samples were performed in duplicate.

2.10.1 IL-2, IL-10, TNF- α

The human IL-2, IL-10, and TNF- α development kits were purchased from PeproTech containing a recombinant protein, standards, capture antibody, detection antibody (biotinylated antibody). For ELISA assay, every wash step mentioned in this protocol was performed by adding 300 μ l wash buffer (0.05% Tween-20 in PBS) per well, flicking the plate for aspiration, patting the plate on a paper towel and the entire procedure was done in 3-4 repeats.

To coat the plate with capture antibody for targeting the specific antigen in the samples, monoclonal capture antibody (IL-10, IL-2, TNF- α) was diluted in PBS to a concentration of 1 μ g/ml and added 100 μ l to each well. The plate was sealed and incubated overnight at room temperature. Following the wash step, 300 μ l blocking buffer (1% BSA in PBS) was added to each well and incubated for 1 hour. The plate was then washed and ready for protein (antigen) detection from supernatant collected in section 2.9. The standard was serially diluted from 0.01 μ g/ml to zero in diluent (0.05% Tween-20, 0.1% BSA in PBS). 100 μ l of standard or samples was added to each well and incubated at room temperature for 2 hours. For signal detection, the plate was washed and incubated with 100 μ l diluted detection

antibody (IL-10, IL-2, TNF- α ; 0.5 μ g/ml in diluent) recognising a different epitope on the target protein for 2 hours, followed by Avidin-HRP conjugate through incubation with diluted Avidin-HRP secondary antibody (1:2000 in diluent) for 30 minute. To read the signal by plate reader, the plate was washed and 100 μ l of ABTS-substrate (2,2'-Azino-bis (3-ethylbenzothiazoline-6-sulfonic acid)) was added to each well, which changed the colour from yellow to green/blue-ish during reaction, indicating the presence of the protein-of-interest in the samples. The plate was read every 5 minute intervals until desired OD readings were obtained for a maximum 40-minute period. The signal was read at 405 nm with wavelength correction set at 650 nm by a plate reader. The standard curves used to determine the concentration of the samples were shown in Figure 2-5. The best fitting trendline and equation was calculated by Excel using a second- or third- degree polynomial equation based on the R^2 value. R^2 evaluates the scatter of the data points around the fitted regression line. The R^2 value >0.99 was used for standard curve equation.

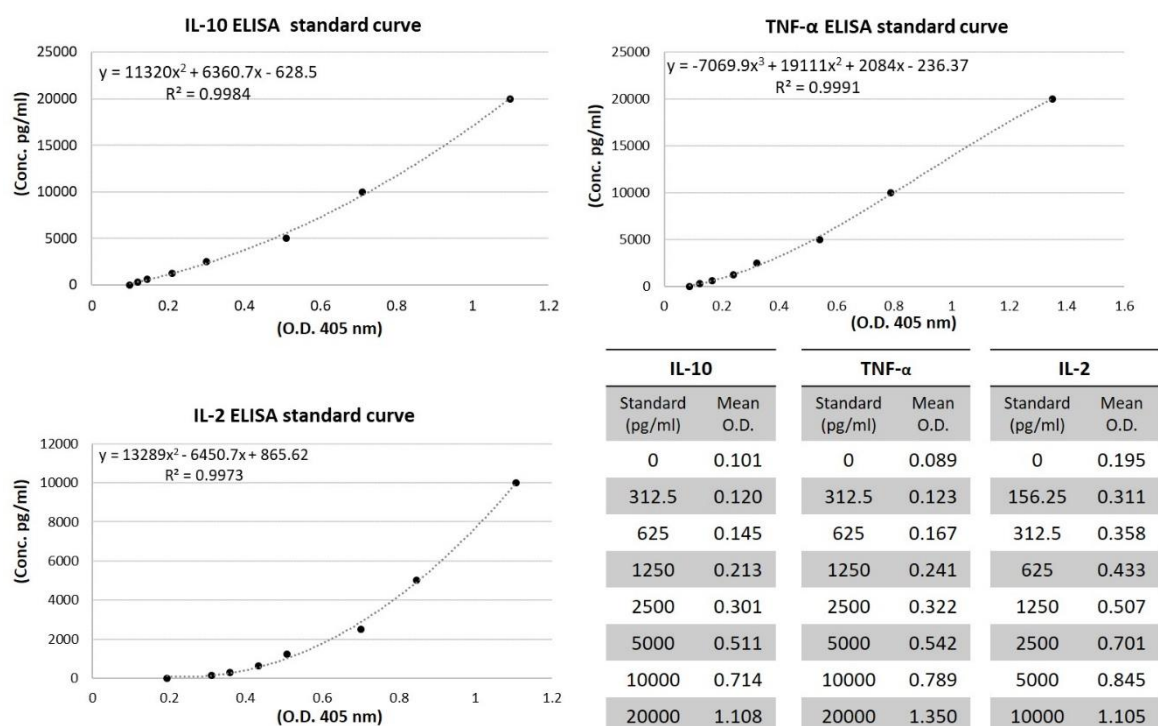


Figure 2-5. ELISA standard curves for IL-10, TNF- α , and IL-2

The mean O.D. values of the standards (X-axis) obtain from duplicate absorbance were plotted against the known concentration of the standard (Y-axis). The best fitting standard curves and equations were calculated based on the R^2 value greater than 0.99.

2.10.2 Insulin and C-peptide

The secreted insulin, C-peptide, and intracellular insulin content was measured by commercialised specific insulin or C-peptide ELISA with pre-coated plate and highly specific capture antibody. To induce insulin/C-peptide release, undifferentiated CMSCs/AMSCs (controls) or CMSC/AMSC-derived insulin producing cells were washed with PBS and pre-incubated for 1 hour in phenol red-free DMEM without glucose and then media was switched to phenol red-free DMEM with glucose at different concentration for glucose challenge. The media volume for glucose challenge was 1 ml/well in a six well plate. Cells were first incubated in 5.5 mM glucose (low glucose) phenol red-free DMEM for 1 hour and supernatant was collected by centrifuging at 1,500 rpm for 5 minute to remove cell debris and stored in -80 °C for measurement of released insulin/C-peptide with ELISA assays. Cells were then incubated in 25 mM glucose (high glucose) phenol red-free DMEM for 2 hours and supernatant was collected for ELISA analysis. The phosphodiesterase inhibitor, IBMX (0.5 mM) known to stimulate insulin secretion was added together with 5.5 mM or 25 mM glucose in phenol red-free DMEM. After subsequently incubating with low and high glucose media, cells were trypsinised and lysed in 200 µl RIPA buffer (radioimmunoprecipitation assay buffer) for measuring the intracellular insulin content by ELISA. The protein concentration was measured using Thermo BCA (bicinchoninic acid) protein assays and absorbance was detected by a plate reader against a BSA standard. All samples (supernatant and protein) were stored at -80 °C until use.

The insulin ELISA was performed following the manufacturer's instructions (Abcam). All the solutions were provided with the kit. Briefly, 50 µl of all samples and serially diluted

standards was added to each well and incubated with 50 µl antibody cocktail for 2 hours on a plate shaker at 400 rpm. Antibody cocktail was prepared by diluting the capture and detector antibody in diluent. The plate was washed 3 times and 100 µl of 3,3',5,5'-Tetramethylbenzidine substrate (TMB) was added for a 30-minute incubation in the dark on a plate shaker. Following the addition of 100 µl stop solution to each well, an endpoint reading was recorded at 450 nm using a plate reader.

The C-peptide ELISA was performed by ALPCO C-peptide ELISA kit, using the test procedure for 25 µl sample volume as per the manufacturer's instructions. 50 µl of assay buffer was added to each well and the plate was incubated on a shaker at 800 rpm for 2 hours. Following incubation, each well was washed and samples were incubated with 100 µl enzyme conjugate solution. For signal detection, the plate was washed, 100 µl TMB was added to the well, and incubated for 30 minutes on a plate shaker. 100 µl of stop solution was then added to each well and absorbance measured at 450nm by a plate reader. The insulin and C-peptide ELISA standard curves were shown in Figure 2-6 and the calculation methods were described in section 2.10.1.

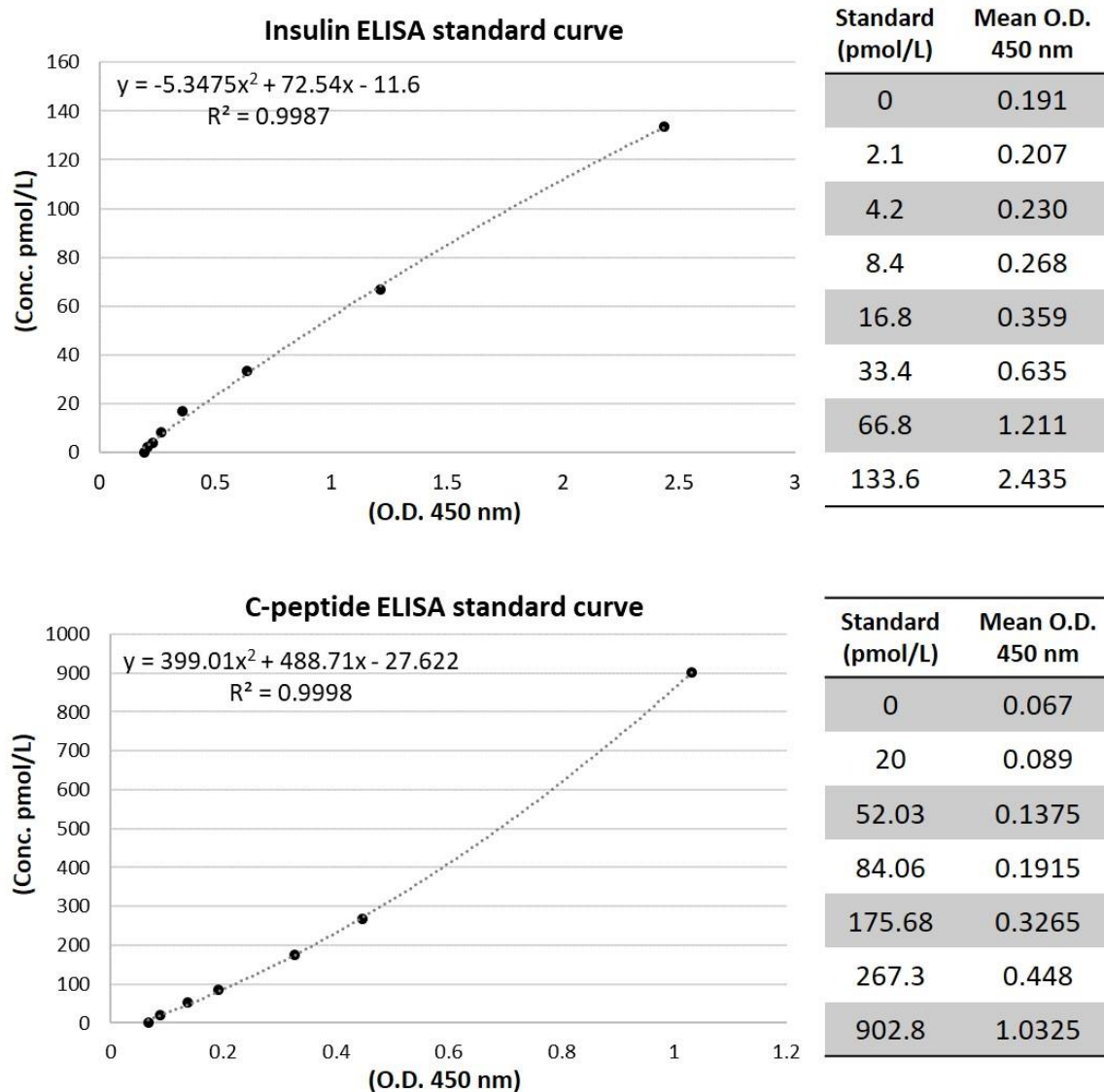


Figure 2-6. ELISA standard curves for insulin and C-peptide

The mean O.D. values of the standards (X-axis) obtain from duplicate absorbance were plotted against the known concentration of the standard (Y-axis). The best fitting standard curves and equations were calculated based on the R2 value greater than 0.99.

2.11 Live/dead viability assay

Cell viability assay was assessed using two-colour fluorescence LIVE/DEAD viability/cytotoxicity assay kit (ThermoFisher) and fluorescent images were captured by confocal microscope. The calcein-acetoxymethyl (calcein-AM, ThermoFisher) indicates intracellular esterase activity while ethidium homodimer-1 (EthD-1, ThermoFisher) indicates the loss of membrane integrity. Adherent cells were washed with PBS and incubated with calcein-AM (1 μ M) and EthD-1 (4 μ M) in PBS at 37 °C in the dark for 20 minutes. Cells were then gently rinsed with PBS to remove residual fluorescent dyes and viewed under a confocal microscope. Images were taken immediately and fluorescence emission was detected at 530 nm for calcein-AM (live cells) and at 645 nm for EthD-1 (dead cells).

2.12 Beta-galactosidase senescence assay

Senescence was characterised by the induction of senescence-associated β -galactosidase (SA- β -gal) activity, which is present only in senescent cells, not in quiescent or proliferating cells. Senescence was confirmed by the catalytic activity of SA- β -gal which catalyses the hydrolysis of Xgal (5-bromo-4-chloro-3-indolyl-beta-D-galactopyranoside, Merck) and results in the accumulation of blue precipitate.

To detect SA- β -gal activity, cells were washed with PBS before being fixed using fixation solution supplied with the cellular senescence kit (Merck) for 15 minutes at room temperature. The SA- β -gal detection solution was prepared following the manufacturer's instruction by diluting the Xgal in staining solution and PBS. After fixation, cells were washed with PBS and incubated with the detection solution at 37 °C in the dark for at least 4 hours or overnight. The detection solution was then removed and cells were washed with

PBS. However, sometimes salt crystals were observed when incubating overnight while excess amount of salt crystals could be removed by briefly incubating the stained samples with DMSO for 10 seconds. Images were obtained under bright-field microscope and blue stained cells were counted from several random fields of each samples.

2.13 Immunofluorescence staining

The staining was performed on insulin producing cells (IPCs) to confirm the differentiated state of CMSCs/AMSCs. Cells were cultured in an 8-well chamber slide for IPC differentiation and fixed with 4% paraformaldehyde in PBS for 20 minutes at the end of differentiation period to inhibit degradative process of proteins. Fixed cells were either covered in PBS and stored in 4 °C up to a week or performed immunostaining straight away.

Before any antibodies were introduced, cells were permeabilised with 0.3% TritonX-100 in PBS for 15 minutes and blocked potential nonspecific binding sites by incubation with blocking buffer (1% BSA, 0.1% TritonX-100 in PBS) for 1 hour at room temperature. The primary antibody was diluted in 1% BSA in PBS. The appropriate amount of diluted primary was added into the samples and incubated overnight at 4 °C. After washing with PBS, the samples were then incubated with secondary antibodies diluted in 1% BSA in PBS and incubated at room temperature for 2 hours following by counterstained with 4,6-diamidino-2-phenylindole (DAPI) for 10 minutes. The samples were washed with PBS before taking images by confocal microscope.

The following antibodies and dilutions were used – anti-insulin (1:100, Santa Cruz Biotechnology, sc-9168), anti-PDX-1 conjugated to Alexa Fluor 488 (1:100, Santa Cruz Biotechnology, sc-390792 AF488), and Alexa Fluor 594 secondary antibody (1:200, Invitrogen).

2.14 Migration assay

2.14.1 Transwell assay

Transwell assay was performed at passage 3. Cells were trypsinised and re-suspended in serum free DMEM. Transwell filters with 8 µm pores were placed in a 24-well plate and 2×10^5 cells in 200 µl serum free media were added to a Transwell chamber. The plate was incubated in 37 °C incubator for 10 minutes and then 550 µl of complete growth media containing 10% FBS was added to the lower chamber. Cells were allowed to migrate for 8 or 24 hours at 37 °C.

To assess the migration, at the end of incubation period, Transwell inserts were carefully transferred to a new empty well and cells that did not migrate through the pores remaining on the upper side of the filter were removed with a cotton swab. This process was repeated 3-4 times to completely remove cell debris and every time a clean cotton swab was moisturised with dH₂O to avoid breaking Transwell membrane when wiping off the cells. Cells that migrated through the membrane were fixed by placing Transwell inserts in 100% methanol for 15 minute and rinsed with PBS. Cell staining was performed by placing Transwell inserts in 0.1% crystal violet dissolved in 20% ethanol/PBS solution for 15 minutes. The excess crystal violet was removed by briefly washing with dH₂O for few seconds and the upper side of the membrane was gently wiped with a cotton swap. The membrane was allowed to dry for one hour and images were captured by light microscope. Cell migration was quantified by counting migrated cells in five randomly selected fields in each sample.

2.14.2 Wound healing assay

A number of 5×10^5 cells was seeded into each well in a 6-well plate and cultured for 2 days

until reaching confluence as a monolayer. Wound was created by scratching with a 200- μ l pipette tip across the surface of the well. After scratching, wells were washed twice with media to remove suspension cells and cell debris. In order to obtain the same field during image acquisition at different time points, the reference point was made by marking the plate with a fine tip marker on the outer bottom of the plate. The plate was then incubated at 37 °C for 6 or 12 hours and cell migration towards the gap area was recorded using a light microscope. Relative cell migration was calculated by measuring final wound area compared to initial area using ImageJ.

2.15 ALDH activity assay

Aldehyde dehydrogenase (ALDH) enzymatic activity was quantified by Sigma's ALDH Activity Assay Kit. In ALDH activity measurement, acetaldehyde was oxidised by ALDH generating nicotinamide adenine dinucleotide (NADH), which reacted with a probe and generated a colorimetric (450 nm) coloured product proportional to the ALDH activity present. According to manufacturer's instruction, one unit of ALDH is the amount of enzyme that will generate 1.0 μ mole of NADH per minute at pH 8.0 at room temperature.

1×10^6 cells were homogenised in 200 μ l of ice-cold ALDH assay buffer and centrifuged at 13,000 g for 10 minutes to remove insoluble cell debris. The supernatant was transferred to Eppendorf tubes and kept on ice. Reaction mix was prepared by adding an appropriate proportion of ALDH assay buffer, ALDH substrate mix, and acetaldehyde supplied with the kit based on manufacturer's instruction. For background signal correction, a blank was set up for each sample by omitting the acetaldehyde from reaction mix. 50 μ l of supernatant from each sample or serially diluted standard was added into a 96-well plate and then the equivalent volume of reaction mix was added to each well. The plate was protected from light and incubated on a plate shaker for 5 minutes. Changes in absorbance for ALDH activity

were measured at 450 nm every 5 minutes over a 30-minute period. The plate was protected from light during the entire incubation period. All samples were performed in duplicate.

The absorbance was corrected to the blank and the activity of ALDH was calculated by the following equation:

$$\text{ALDH activity} = (T_{\text{final}} - T_{\text{initial}}) / (\text{Reaction time (minutes)}) \times V$$

The absorbance at 450 nm at the initial (T_{initial}) or final (T_{final}); the amount (nmole) of NADH generated between initial and final ($T_{\text{final}} - T_{\text{initial}}$); duration time between initial and final (Reaction time); sample volume added to the well (V). ALDH activity is described as nmole/min/mL = milliunit/mL

2.16 Detection of ROS

Reactive oxygen species (ROS) was indicated by 2',7' - dichlorofluorescein diacetate (DCFDA, also known as H2DCFDA, Sigma). After diffusion into cells, DCFDA is deacetylated by intracellular esterases and oxidised by ROS converting into 2', 7' - dichlorofluorescein (DCF). DCF is a highly fluorescent compound which can be detected by fluorescence spectroscopy with an excitation and emission spectra of 485 nm and 535 nm, respectively.

Cells were seeded at 10,000 cells/well in a 96-well plate and allowed attachment for overnight incubation at 37 °C. The DCFDA working solution was prepared by diluting 20 mM DCFDA/DMSO in assay buffer to a concentration of 25 µM. After attachment, cells were washed with PBS and incubated with 25 µM DCFDA solution for 45 min at 37 °C in the dark. DCFDA solution was then removed and cells were treated with glucose to induce metabolic activity for the desired time period. Tert-Butyl Hydrogen Peroxide (TBHP) solution supplied

with the kit was used as positive control.

For florescent images, ROS detection was observed by confocal microscope. Images were taken from randomly selected fields in each sample. The intensity of florescence was measured by a fluorescence plate reader (SpectraMax i3x) and signal was read at excitation/emission: 485/535 nm. A blank well containing no cells (media only) was used as background signal.

Chapter 3

Characterisation of AMSCs/CMSCs from GDM and healthy pregnancies



3.1 Introduction

Cell therapy and tissue engineering using mesenchymal stem cells (MSCs) have emerged as an attractive option in disease treatments seeking to maintain, restore, or enhance tissue regenerate and function. Safe, effective, and reliable cell sources remain a major issue for use in regenerative medicine clinical applications. Bone marrow MSCs have now been widely and successfully used in clinical applications for a number of decades²⁴⁰, however some limitations have caused concerns, such as their limited expansion capacities, scarcity within bone marrow, and the invasive and labour intensive isolation process which can associate with an increased risk of infection for the donor²³³. Thus far, MSC derivation has been reported from a wide range of adult tissues including; fat, dental, lung tissue and peripheral blood²⁴¹.

The human placenta, generally discarded post-partum, is now becoming recognised as a plentiful and alternative source of stem cells²⁴². Placental MSCs are phenotypically similar to BM-MSCs, in terms of plastic adhesion, immunophenotype, and lineage differentiation potential. It has also been suggested that the placental MSC provides a substantial expansion potential and delayed senescence^{243, 244}. Moreover, the ease of access, reduced ethical conflicts, and reduced age-acquired DNA damage makes them a promising source for stem cell therapy²⁴⁵.

The placenta plays a vital role in fetal development and maternal health by regulating the metabolic interaction between the mother and fetus. As the intrauterine environment is closely related to placental state, pregnant complications have been associated with abnormal placentation^{246, 247}. Gestational diabetes mellitus (GDM), the common pregnancy complication, affects both the mother and fetus during pregnancy, where maternal hyperglycaemia influences fetal programming and leaves mother and child with high a risk

of developing type 2 diabetes later in life^{33, 34}. The GDM environment is also known to have an impact on placental pathology, as discussed in section 1.2.3, implying that the characteristics of stem cells and progenitor cells in GDM placenta are likely to be affected. For example, Hadarits *et al.* (2003) reported the increased proportion of haematopoietic stem cells in cord blood of new-born from GDM pregnancies²⁴⁸; another study showed that perivascular stem cells from umbilical cord of GDM pregnancies had lower cell yield and proliferative rate when compared to healthy pregnancy²⁴⁹. Environmental factors can cause significant effects on cell populations and behaviours; therefore, understanding the biological properties of stem cells is important before applying these cells in clinical applications.

In this study, MSCs were isolated from different sides of the placental membrane – amnion and chorion in healthy and GDM placenta. Due to the higher risk of developing diabetes in women who have had GDM and children from GDM pregnancies, autologous amniotic and chorionic MSCs (AMSCs/CMSCs) free of ethical conflicts and immune rejection hold great therapeutic potential for diabetes therapy. Recent examples include the transplantation of MSC-derived islet cells²⁵⁰ and the use of MSC secretome cytokines to promote the regeneration of pancreatic cells^{251, 252} (section 1.4.4). However, the application of MSC therapy to the treatment of human disease requires extensive studies. Establishing biological properties is an essential first step to evaluate the therapeutic potential of each type of MSCs.

3.2 Aim

Considering that the placental environment is affected by pregnant complications and having an impact on placental cells, it would be important to investigate whether the CMSCs and AMSCs derived from GDM placenta are an ideal candidate for cell therapy. Therefore, we aimed to investigate biological differences between AMSCs and CMSCs obtained from GDM and healthy pregnancies for exploring the fundamental differences and environmental impacts on AMSCs and CMSCs.

The main objectives of the chapter:

- Isolate and expand AMSCs/CMSCs from healthy and GDM placental membrane.
- Characterise MSCs via morphological analysis and surface marker expression.
- Examine cell proliferation and tri-lineage differentiation ability (osteogenesis, adipogenesis, chondrogenesis).
- Investigate immunomodulatory capacity of MSCs secretome via conditioned media and co-culture system.

3.3 Methods

Following informed consent placenta was collected from 10 healthy and 10 GDM women undergoing elective caesarean sections, as described in section 2.2. MSCs were isolated from amniotic and chorionic membranes processed in sterile conditions (section 2.3) and cultured in DMEM supplemented with 10%FBS, 1% L-glutamine, 1% NEAA and 1% Penicillin-Streptomycin. Morphologically changes were examined at every passage (section 2.4.2) and all characterisation was performed at passage 3.

Experiments performed in this chapter are summarised in Figure 3-1. Cell morphology was analysed from passage 0-3 and proliferation capacity was examined via cell count, doubling time calculation, and MTT assay during a 12-day period (section 2.4). Surface marker characterisation for MSCs was performed via flow cytometry as described in section 2.5. Tri-lineage differentiation was performed by inducing osteogenesis, adipogenesis, and chondrogenesis in specific differentiation media for 21 days and followed by histological staining with alizarin red, Oil Red O, and alcian blue, respectively (section 2.6). Adipogenic potential was further assessed through destaining of Oil Red O and marker examination by real-time PCR (section 2.6 - 2.8). Immunosuppression of AMSCs/CMSCs was characterised by MSC conditioned media via modulation of Jurkat T cell proliferation and cytokine secretion. Conditioned media was collected from CMSCs/AMSCs and stored at -80°C until further ELISA analysis (section 2.9.2). Co-culture system was used to investigate the immunomodulation of MSCs on THP1 monocyte polarisation and cytokine secretion, as described in section 2.9.

AMSCs/CMSCs from 10 healthy and 10 GDM placenta undergoing characterisation assays at passage 3		
Morphology <ul style="list-style-type: none"> Cell length (section 2.4.2) Surface area (section 2.4.2) 	Proliferation <ul style="list-style-type: none"> Cell count (section 2.4.3) Doubling time (section 2.4.3) MTT assay (section 2.4.4) 	Immunophenotype <ul style="list-style-type: none"> Surface marker examination via flow cytometry (section 2.5)
Differentiation <ul style="list-style-type: none"> Osteogenesis (section 2.6.1) Adipogenesis (section 2.6.2) Real-time PCR for adipogenic marker examination (section 2.7 - 2.8) Chondrogenesis (section 2.6.3) 	T cell modulation <ul style="list-style-type: none"> Jurkat culture (section 2.9.1) Jurkat proliferation via MTT assay (section 2.4.4) ELISA for IL-2 secretion (section 2.10.1) 	Macrophage co-culture <ul style="list-style-type: none"> THP1 culture (section 2.9.3) Co-culture system (section 2.9.4) ELISA for IL-10, TNF-α secretion (section 2.10.1)

Figure 3-1. Summary of the methodology in chapter 3

Statistical analysis

One-way ANOVA and Tukey post-hoc tests or two-way ANOVA where appropriate were used to determine the statistical significance of observed differences in the mean values among different groups by GraphPad Prism (GraphPad Software). The comparison within two groups was analysed by the simple t-test. The data was presented as mean \pm SEM. Each data point represents the average of at least three independent experiments with three repeats in each experiment. A p-value below 0.05 was indicated as statistically significant (* $p \leq 0.05$, ** $p \leq 0.01$, *** $p \leq 0.001$ and **** $p \leq 0.0001$).

3.4 Results

3.4.1 Morphological analysis

AMSCs and CMSCs have distinct morphologies independent of disease state

AMSCs and CMSCs lines derived from healthy (n=10) and GDM (n=10) placenta were used in this study. The details of each pregnancy are shown in Table 3-1. Statistical analysis demonstrated that there were no significant differences between healthy and GDM groups.

Table 3-1 Maternal and fetal characteristics

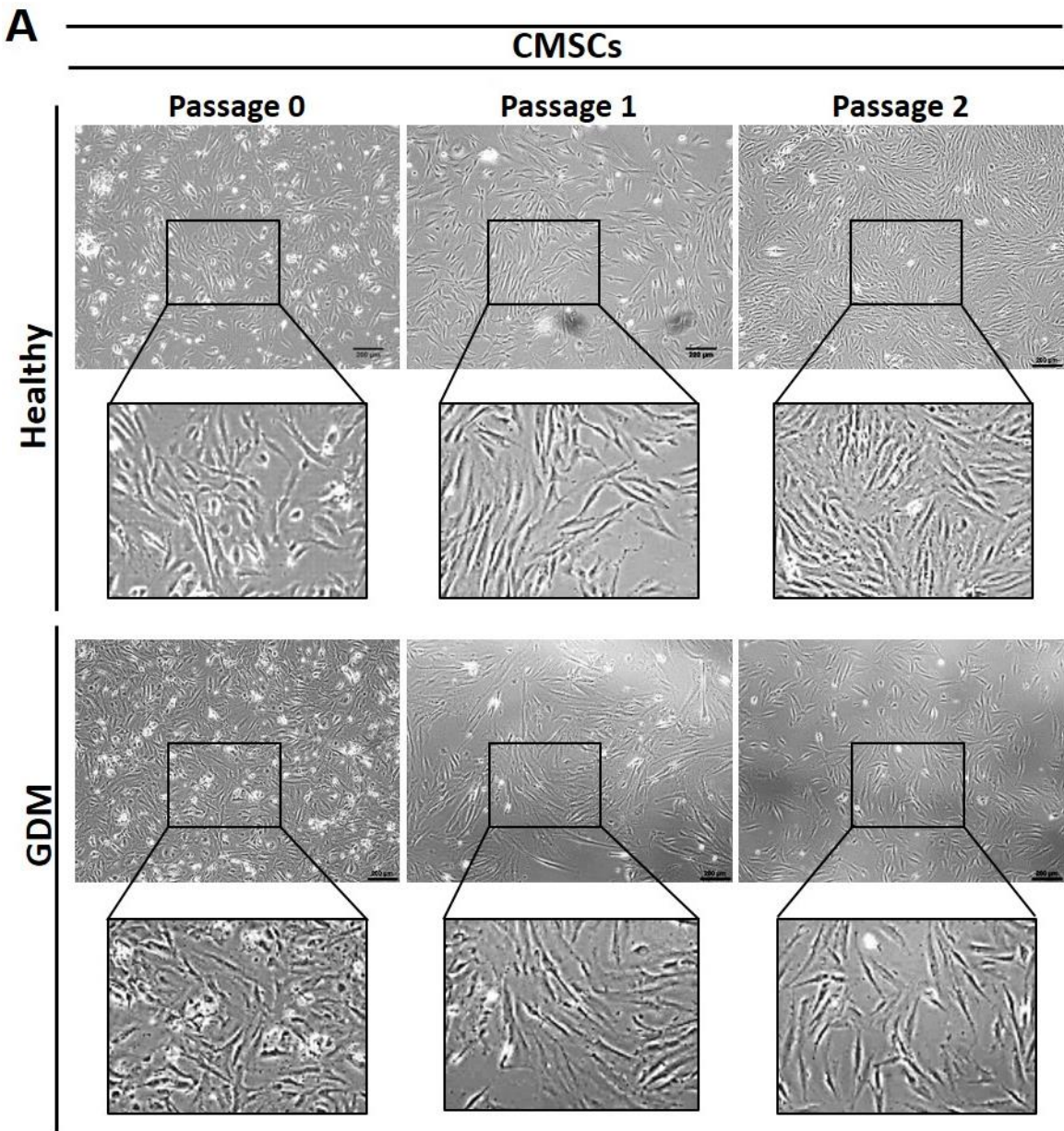
	Healthy (n=10)	GDM (n=10)	P value
Age (years)	30.1 ± 1.68	30.1 ± 2.32	0.38
BMI (kg/m ²)	25.2 ± 1.76	32.4 ± 2.95	0.17
Gestational age (weeks)	38.7 ± 0.22	38 .0 ± 0.41	0.11
Infant weight (g)	3425 ± 85.43	3611 ± 151.5	0.09
Gender (female/male)	10/0	4/7*	-

*Included one non-identical twins placenta.

Data are presented as mean (± standard deviation)

Morphological observation was performed from passage 0-3 indicating that CMSCs from healthy (H-MSCs) and GDM (G-CMSCs) pregnancies exhibited similar fibroblast-like morphologies from passage 0 and maintained stable morphological features during subsequent culture (Figure 3-2A). Conversely, AMSCs morphology differed between healthy (H-AMSCs) and GDM (G-AMSCs) groups where the H-AMSCs displayed a triangular or spindle shape post-seeding for 24 hours while the G-AMSCs, which attached more slowly, displayed reduced adherence and a more cuboidal shape. Typical MSC morphology of H-

/G- AMSCs was observed at later passages (Figure 3-2B).



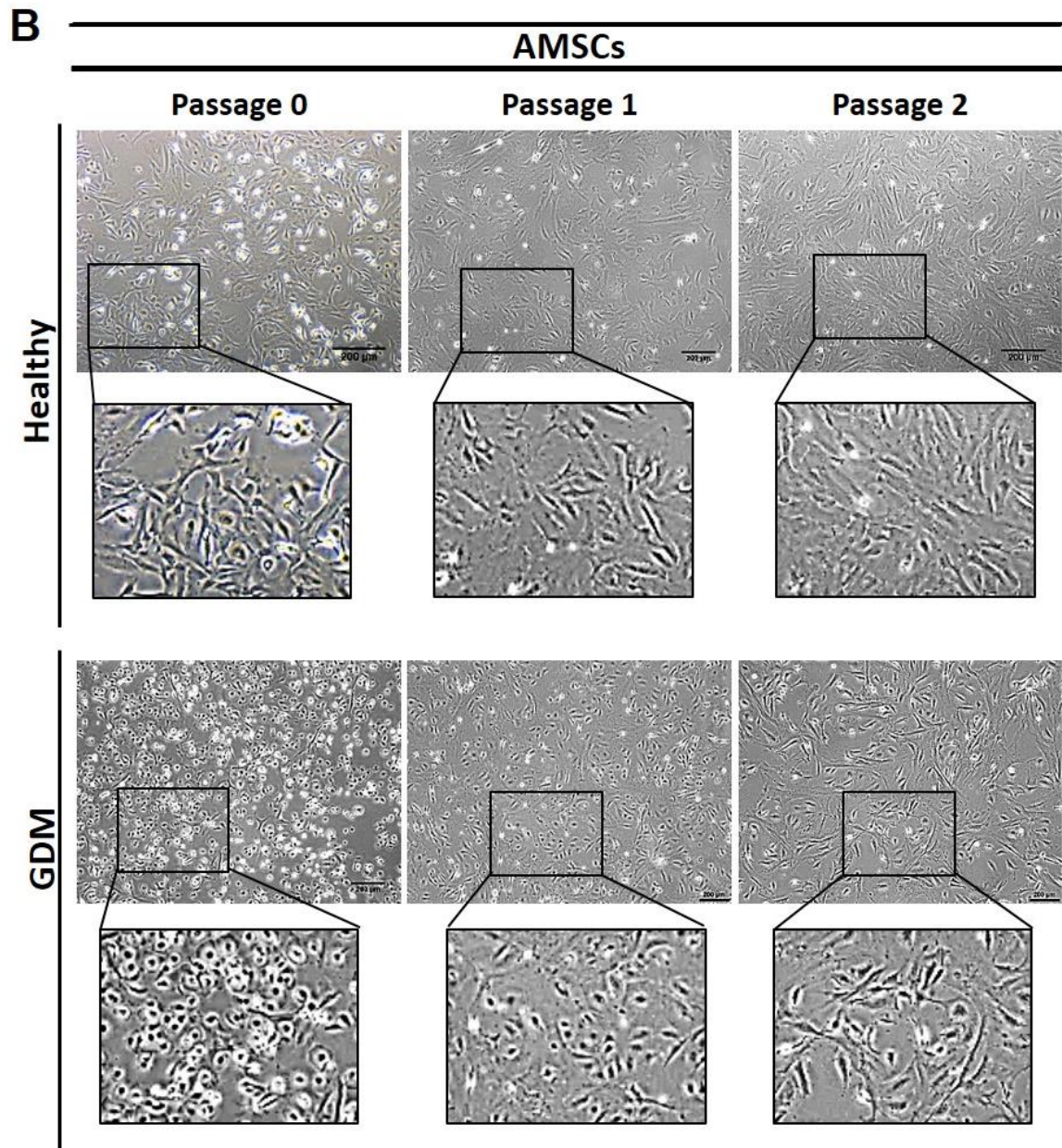


Figure 3-2. Observation of cell morphologies

The morphology of human H-/G- (A) CMSCs and (B) AMSCs from primary culture to passage 2. Images of passage 0 were taken after seeding for 7 days; images of passage 1 and 2 were taken 5 days after subculture. Scale bar = 200 µm.

Although human MSCs, derived from many different tissues, are characterised by a fibroblast-like morphology, cell length could be various depending on different origins²⁵³. The CMSC length (the longest axis from the cell periphery) gradually increased and was longer than AMSCs between passage 0 to 2. The morphology of AMSCs became elongated in the subsequent passages, where more fibroblast-shaped cells were detected. Comparison between GDM and healthy pregnancies demonstrated that G-CMSC displayed comparable length to H-CMSCs (Figure 3-3A), while G-AMSCs were shorter than H-AMSCs (Figure 3-3B). Surface area measurement indicated that AMSCs displayed a larger and broader surface area than CMSCs. There was no significant difference in surface area between CMSCs or AMSCs taken from healthy and GDM pregnancies (Figure 3-3C).

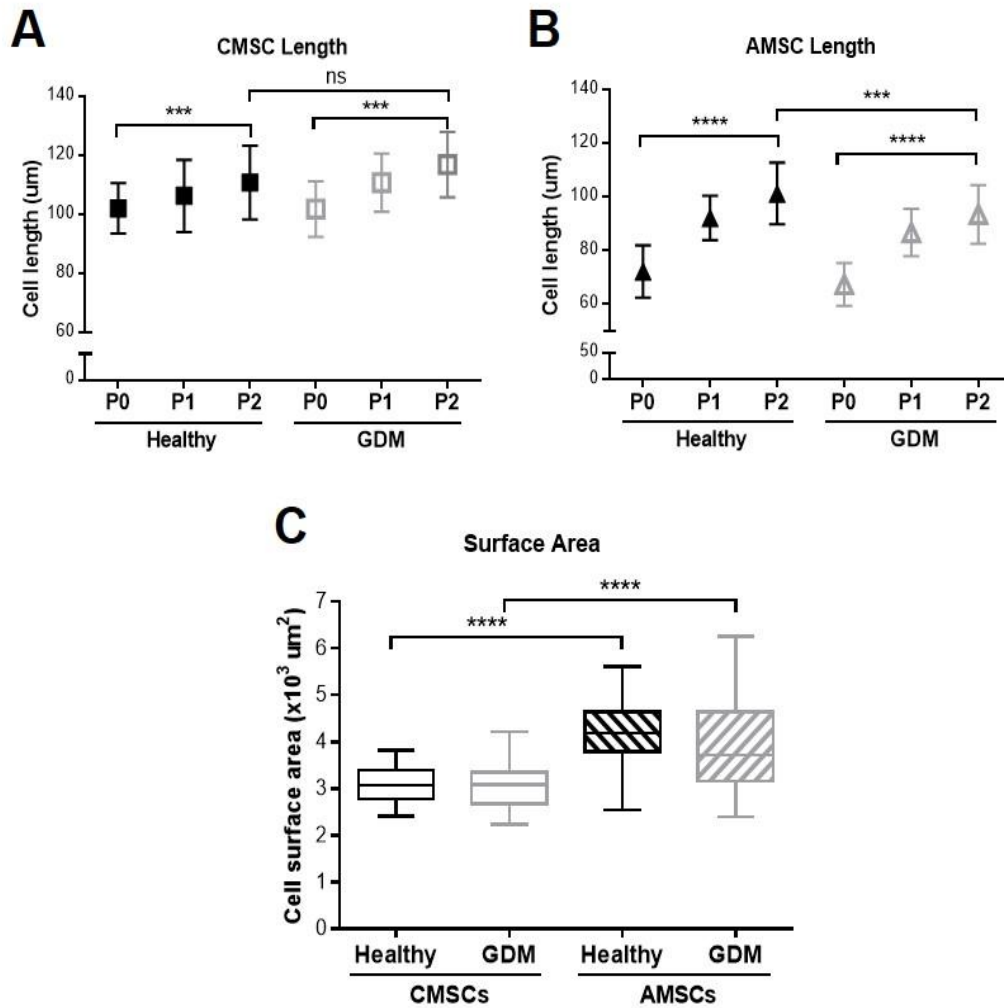


Figure 3-3. Cell length and surface area analysis

Cell length of H-/G- (A) CMSCs and (B) AMSCs was measured from passage 0-2. Data are expressed as the mean \pm SEM. One-way ANOVA and post-hoc test were conducted to determine the significant differences. (C) Box and whiskers plot of cell surface area measured at passage 2 of each group. Whiskers indicate minimum and maximum, box area the interquartile range with the median indicated by the mid-point line. Data of cell length and area was based on 150 cells per population from 5 independent experiment and analysed by Image J. *** $p < 0.001$, **** $p < 0.0001$

3.4.2 Cell proliferation and doubling time

CMSCs display a faster proliferative rate than AMSCs while GDM has an opposite impact on CMSCs and AMSCs doubling rates

The proliferation capacity was evaluated every 2 days during a 12-day culture window via cell counting and both H-/G- CMSCs and AMSCs were seeded at 10,000 cells/well in a 24-well plate. H-CMSCs and G-CMSCs both evidenced a short lag-phase at day 0-4, followed by an exponential growth curve from days 4-12. The exponential growth kinetics showed a more significant increase in H-CMSCs than G-CMSCs (Figure 3-4A). On the other hand, the cell numbers of H-AMSCs and G-AMSCs slowly increased for the initial 8 days and gradually reached plateau from day 8-12 with more cell numbers in G-AMSCs than H-AMSCs (Figure 3-4B). Cell doubling time was calculated when H-/G- CMSCs and AMSCs reached exponential growth phase at passage 3. A lower proliferation capacity was exhibited in H-/G- AMSCs with a doubling time of 91.4 hours for H-AMSCs and 81.6 hours for G-AMSCs compared to CMSCs from healthy and GDM placenta with doubling times of 37.9 hours and 44.0 hours, respectively (Figure 3-4C). The data indicated that CMSCs proliferate more rapidly than AMSCs and when comparing the healthy and GDM group, G-CMSCs showed a lower growth ability than H-CMSCs while AMSCs displayed the converse.

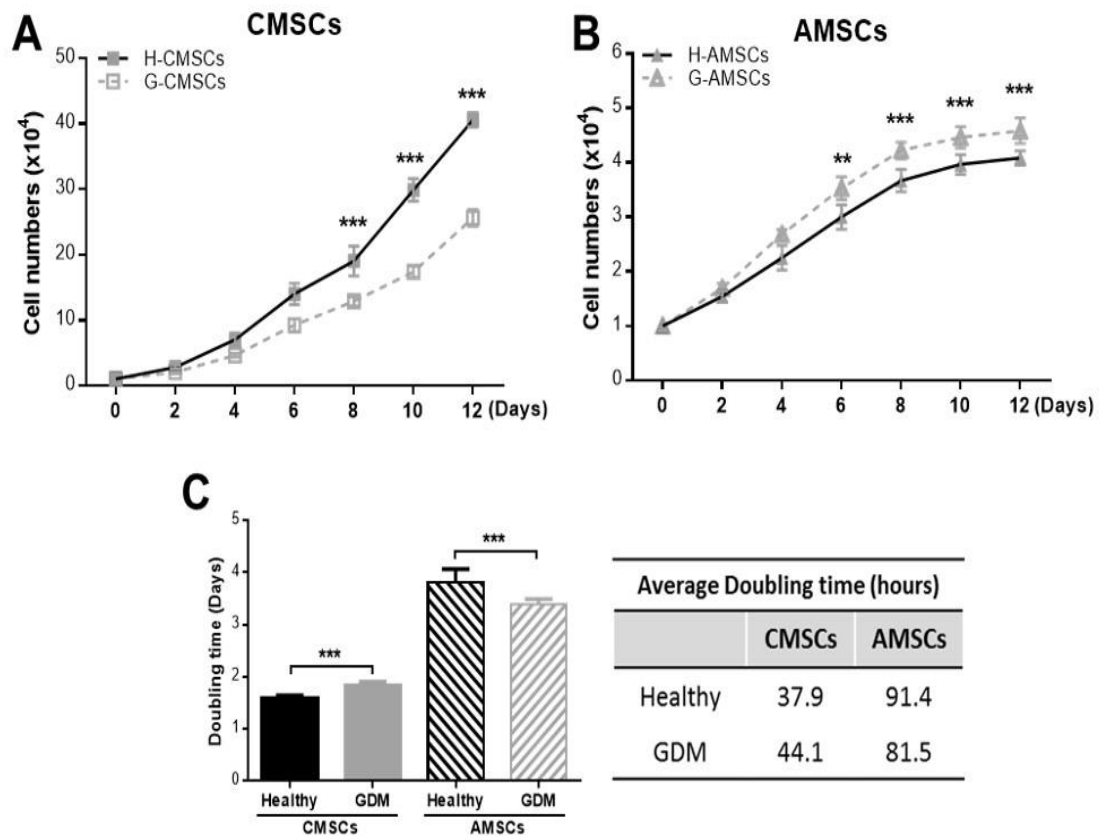


Figure 3-4. Growth curves and doubling time

10,000 cells at passage 3 were plated in 24-well plates and cell numbers were counted every 2 days. Growth curves of H-/G- (A) CMSCs and (B) AMSCs were shown for a 12-day period. Results are presented as mean from three replicates. (C) Cell doubling time for CMSCs/AMSCs from healthy and GDM placenta was calculated based on cell counts at passage 3. Results represent mean \pm SEM. One-way ANOVA was conducted to determine the significant differences, ** $p < 0.01$, *** $p < 0.001$.

MTT assay was used to indirectly reflect viable cell numbers based on the measurement of mitochondrial metabolic rate²²⁸. A reduced metabolic activity in G-CMSCs was observed from day 4 when compared to H-CMSC through the detection of cleaved MTT by metabolically active cells (Figure 3-5A). This may reflect the reduced cell counts observed in the G-CMSCs population (Figure 3-4A). Between H-AMSCs and G-AMSCs the converse was noted where G-AMSCs showed a relatively higher metabolic level than H-AMSCs which was consistent with both previous cell number and doubling time observations (Figure 3-5B and 3-4B). However, no obvious increase in the numbers H-/G-AMSCs at day 8-12 was observed, but the OD value of MTT results continued to increase with time, which may infer that H-/G-AMSCs were still slowing metabolising but not in active cell division phase.

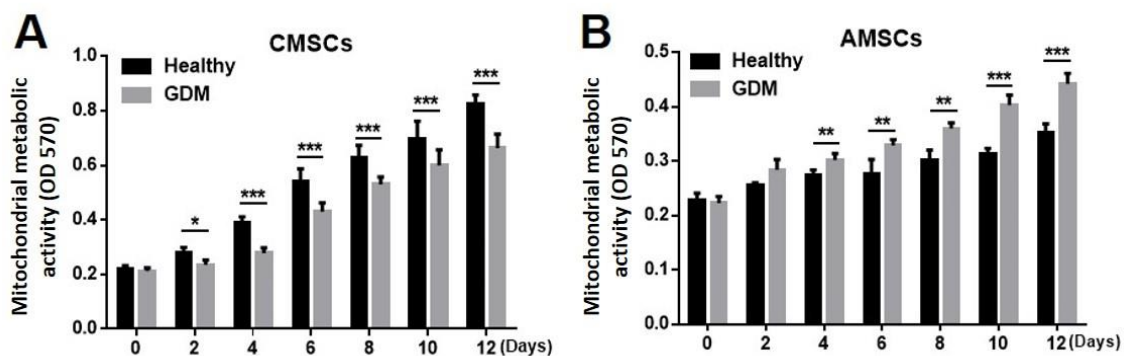


Figure 3-5. Cell proliferation assessed by MTT assay

Metabolic activity was assessed by measuring the MTT dye absorbance in a 12-day period. H-/G- CMSCs and AMSCs were seed at a number of 1,000 cells per well in a 96-well plate and performed MTT assay every 2 days. All assays were conducted in triplicate. OD was read at wavelength of 570 nm. Results represent mean \pm SEM, $n=6$. One-way ANOVA was conducted to determine the significant differences, * $p < 0.05$, ** $p < 0.01$, *** $p < 0.001$

3.4.3 Cell immunophenotype

Healthy- and GDM- CMSCs/AMSCs immunophenotypes are broadly comparable

Immunophenotypes of AMSCs and CMSCs were characterised by surface marker expression according to the International Society for Cellular Therapy minimal definition criteria¹⁰⁹. H-/G- CMSCs and AMSCs were incubated with antibodies to CD19, CD73, CD90, CD105, CD14, CD34, CD45, HLA-DR and the recommended non-specific isotype control, either IgG₁ or IgG_{2a}. Representative histograms of fluorescence intensity for all markers by flow cytometry are shown in Figure 3-6A. The immunophenotype of H-/G- CMSCs and AMSCs were comparable and displayed high levels of expression of typical MSC markers; CD73, CD90, CD105, and low levels of CD14, CD19, CD34, CD45 and HLA-DR. There was no significant difference between CMSCs and AMSCs in either GDM or healthy groups. However, CD45 expression was slightly higher in G-CMSCs/AMSCs when compared to their healthy counterparts; $17.5\% \pm 2.06\%$ in G-CMSCs, $7\% \pm 2.6\%$ in H-CMSCs (Figure 3-6B) and $19\% \pm 1.02\%$ in G-AMSCs, $6.33\% \pm 1.45\%$ in H-AMSCs (Figure 3-6C).

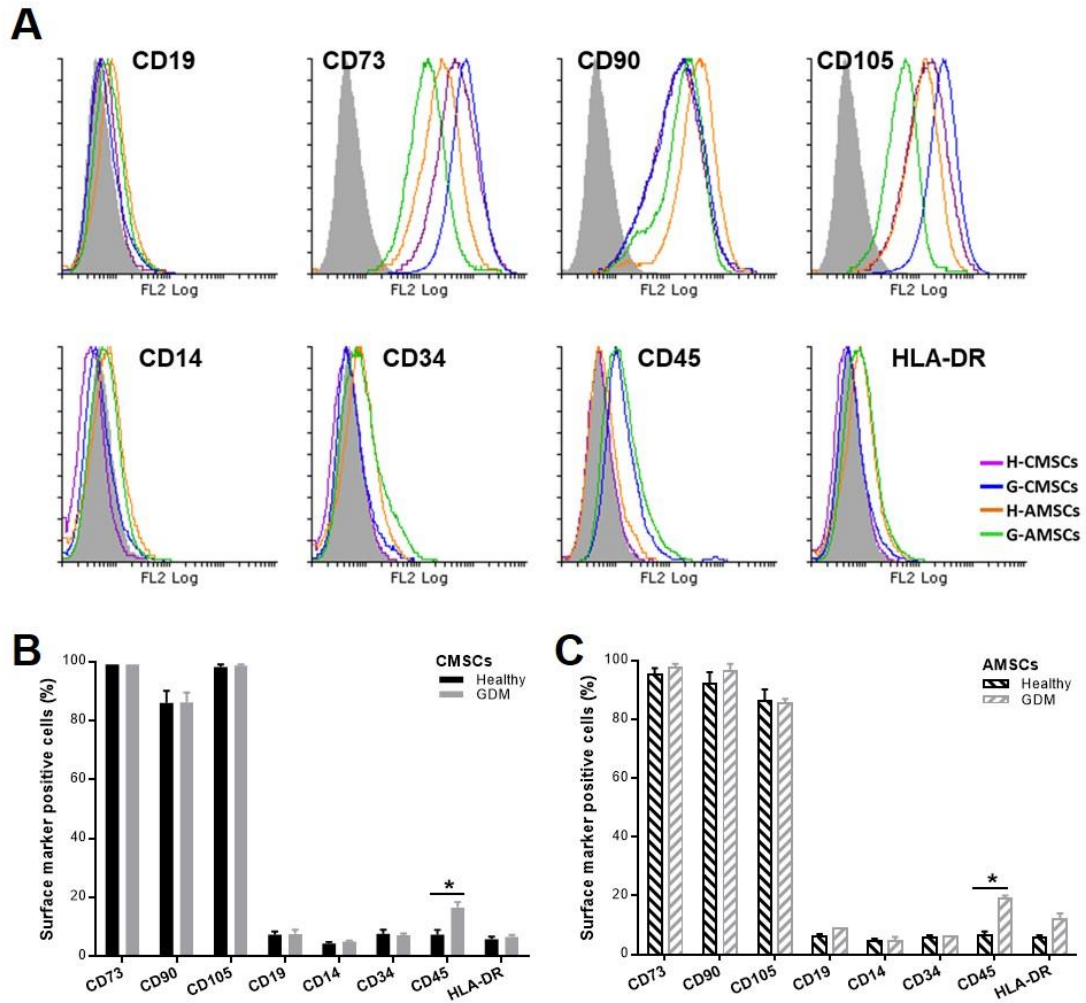


Figure 3-6. Immunophenotype of H-/G- AMSCs and CMSCs

Immunophenotypic characterisation of H-/G- CMSCs and AMSCs at passage 3 was assessed by FACS to examine the expression of typically negative (CD14, CD19, CD34, CD45, HLA-DR) and typically positive (CD73, CD90, CD105) MSC markers. (A) Representative histograms of MSC markers. Filled histogram, isotype control IgG₁ or IgG_{2a}; coloured-line histogram, G-/H-CMSCs or AMSCs samples. (B and C) The graph compared the positive percentage of MSC marker expressions between H-CMSCs and G-CMSCs or H-AMSCs and G-AMSCs. Similar levels of CD marker expressions were observed in GDM and healthy MSC except for the marginally higher CD45 expression. Results represent mean \pm SEM, n=6. Two-sample t-test was conducted to determine the significant differences, * $p < 0.05$.

3.4.4 Tri-lineage differentiation

GDM environment promotes MSC lineage commitment toward adipogenesis

To investigate differentiation potential, H-/G- CMSCs and AMSCs were exposed to specific differentiation media to induce tri-lineage differentiation as identified by histological staining (Figure 3-7). Following culture in osteogenesis differentiation media, evidence of mineralisation in H-/G- CMSCs and AMSCs was evidenced by alizarin red S stained bone nodules. CMSCs and AMSCs from both GDM and healthy samples had similar level of stained mineralised regions, indicating comparable osteogenic potential.

For chondrogenesis, Alcian blue was used to stain glycosaminoglycans produced during differentiation. H-/G- CMSCs and AMSCs had partly detached from culture plate, formed condensations, showing positive Alcian blue staining, although H-/G- CMSCs formed condensations to a greater extent than H-/G- AMSCs.

Adipogenic potential was assessed by Oil-Red-O stain of lipid droplets produced by cells undergoing adipogenesis. Following culture in adipogenesis differentiation media, H-CMSCs and G-CMSCs stained strongly with Oil-Red-O, especially in G-CMSCs with more stained lipid vesicles. In contrast, H-AMSCs and G-AMSCs appeared to have reduced staining of lipid droplets.

Overall, CMSCs from healthy and GDM samples both exhibited a tri-lineage differentiation capacity while H-AMSCs and G-AMSCs displayed bi-lineage differentiation ability and very limited capacity toward adipogenesis.

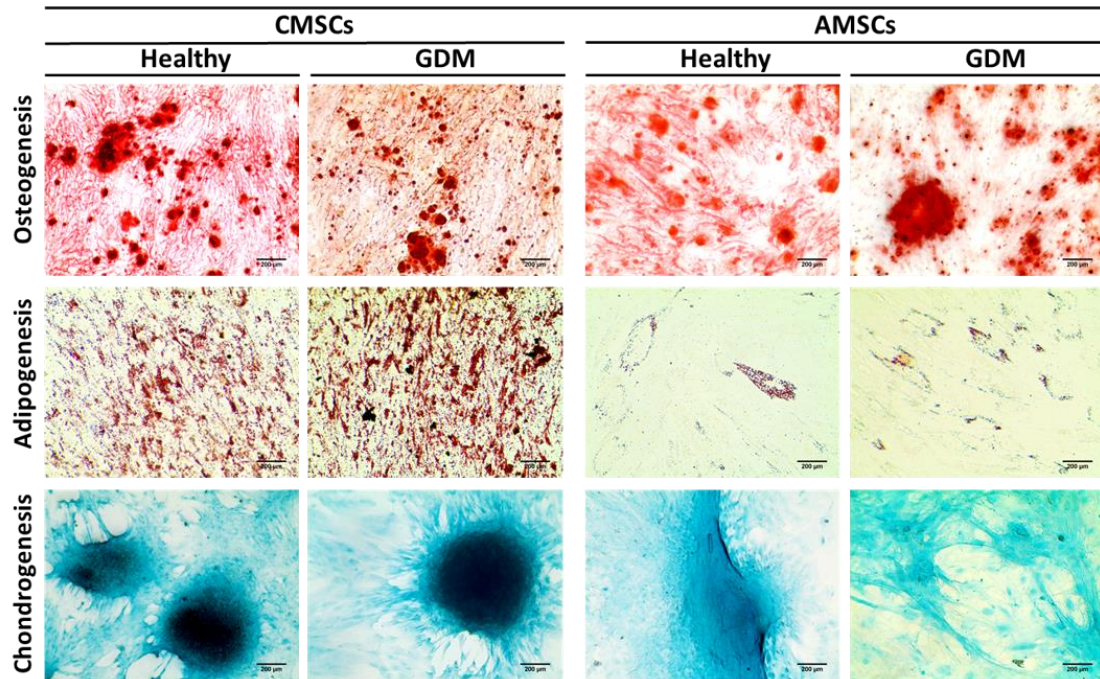


Figure 3-7. Tri-lineage differentiation – osteogenesis, adipogenesis, chondrogenesis

Representative images of tri-lineage differentiation of H-/G- CMSCs and AMSCs following culture in monolayer for 21 days in differentiation media. H-/G- CMSCs/AMSCs were induced to differentiate towards osteogenic lineage and stained with Alizarin Red S to identify calcified matrix, adipogenic lineage verified by Oil-Red-O for lipid accumulation, and chondrogenic lineage detected by Alcian blue for glycosaminoglycans. Scale bar = 200 μ m.

The enhanced adipogenic capacity in G-CMSCs was confirmed with other GDM samples undergoing 21-day culture in differentiation media and the results of Oil-Red-O stain were displayed in Figure 3-8. Abundant Oil-Red-O positive lipid vacuoles were exhibited in both H-CMSCs and G-CMSCs while more lipid droplets accumulation could be observed in GDM groups (Figure 3-8A). In contrast, only a few or small Oil-Red-O-stained granules were detected in H-AMSCs and G-AMSCs (Figure 3-8B).

To quantify the lipid droplets produced during adipogenesis, positive stain of Oil-Red-O was eluted with 100% isopropanol and the absorbance of the elutes was measured at 500 nm using a plate reader. H-/G- CMSCs and AMSCs cultured in growth media were used as control and adipogenic differentiation was examined on day 14 and day 21 after inducing differentiation. Quantitative analysis in Figure 3-8C indicated no significantly increased amount of lipid droplet formation in H-/G- CMSCs or AMSCs in the initial 14 days of induction. Lipid content significantly increased in H-CMSCs and G-CMSCs on day 21 while in H-AMSCs and G-AMSCs, no significant changes was detected by Oil-Red-O elution. However, smaller and reduced numbers of stained lipid droplets were observed from histological staining (Figure 3-8B). Quantification of Oil-Red-O confirmed the histological observations with significantly more intense staining in G-CMSCs after differentiation for 21 days (Figure 3-8C).

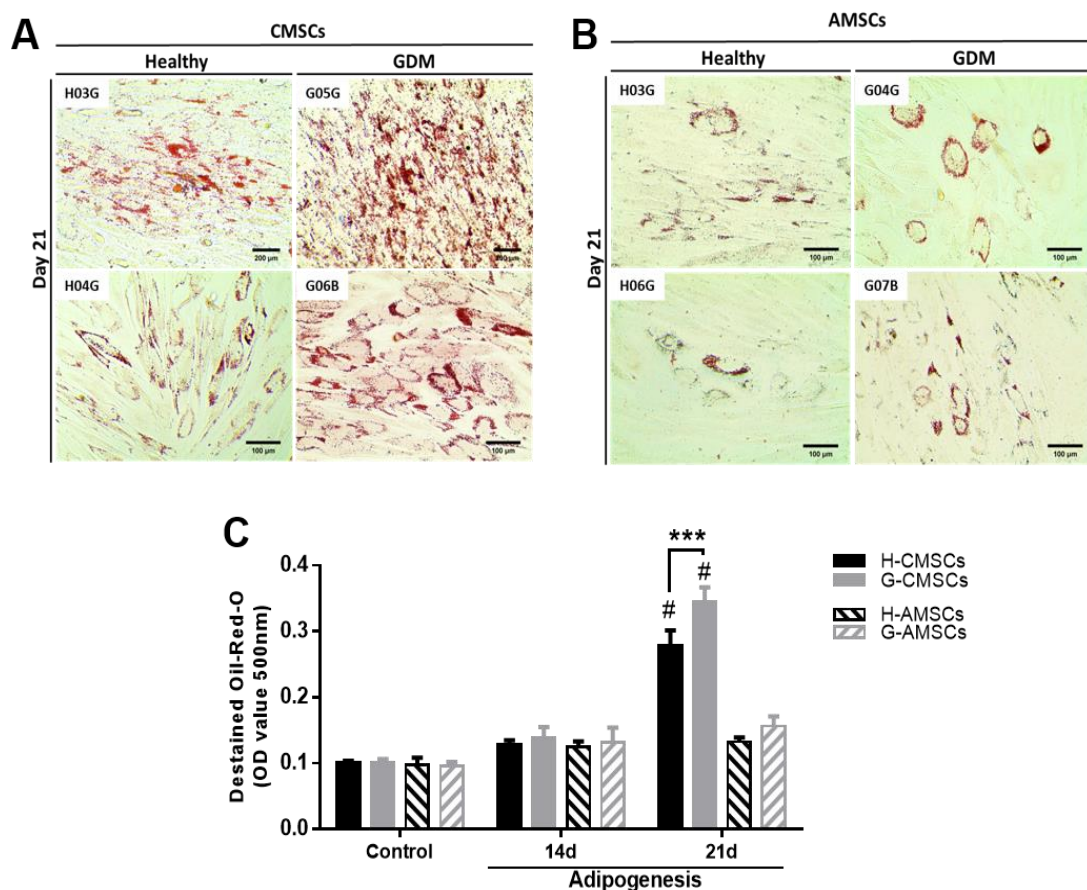


Figure 3-8. Oil-Red-O stain and elution

(A and B) Adipogenic potential in H-/G- CMSCs and AMSCs was examined by Oil-Red-O stain after 21 day of differentiation. Scale bar = 100 μ m. (C) Quantification of lipid accumulation by detecting the absorbance of Oil-Red-O extracts with isopropanol. The mean OD values were obtained from 5 independent experiments and expressed as mean \pm SEM. One-way ANOVA was used to determine statistical significance. *** $p < 0.001$ indicates G-CMSCs vs. H-CMSCs; # $p < 0.001$ indicates H-/G- CMSCs vs. control.

To further investigate enhanced adipogenic potential in MSCs from GDM placenta, the basal RNA levels of two major factors involved in adipogenesis, peroxisome proliferator-activated receptor (PPAR)- γ and adiponectin (*ADIPOQ*), were examined. *PPAR* γ is a nuclear receptor that functions as a transcription factor regulating adipocyte-specific genes and triggering adipogenesis²⁵⁴. *ADIPOQ* is usually expressed late in adipogenesis and also functions as an autocrine factor promoting differentiation and lipid accumulation²⁵⁵. The expression of *PPAR* γ and *ADIPOQ* was examined in H-/G- CMSCs and AMSCs before the induction of adipogenesis. G-CMSCs and G-AMSCs both showed a 2 to 3-fold increase in *ADIPOQ* basal expression levels vs. Healthy- CMSCs/AMSCs (Figure 3-9A). Likewise, higher *PPAR* γ expression was exhibited in G-CMSCs than H-CMSCs but not in G-AMSCs (Figure 3-9B).

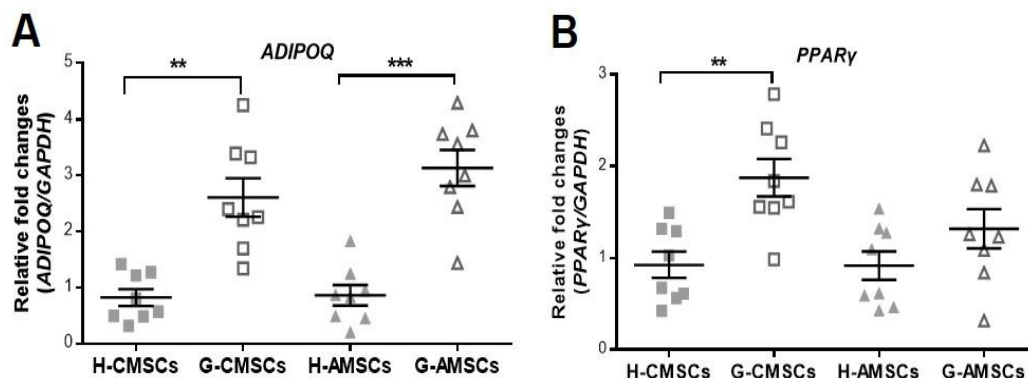


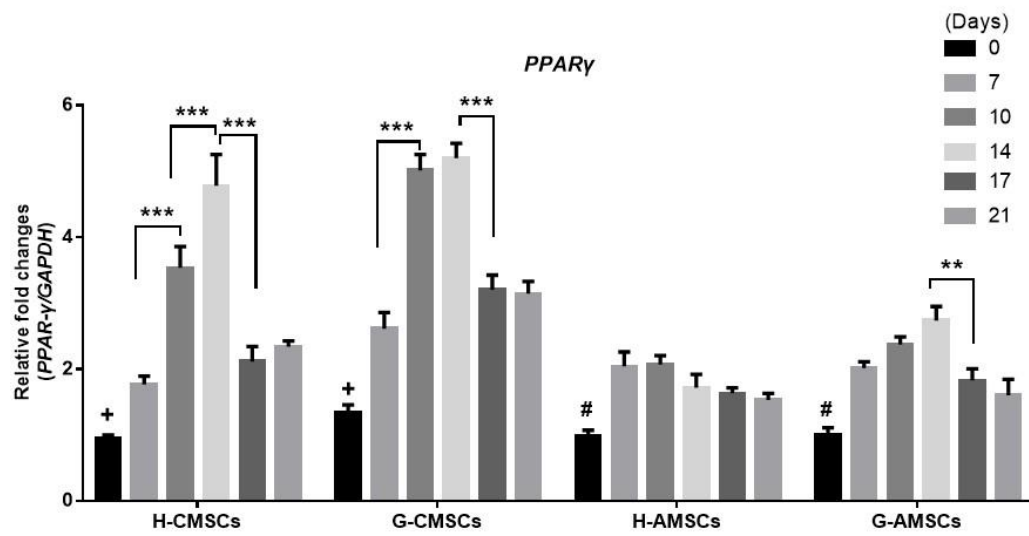
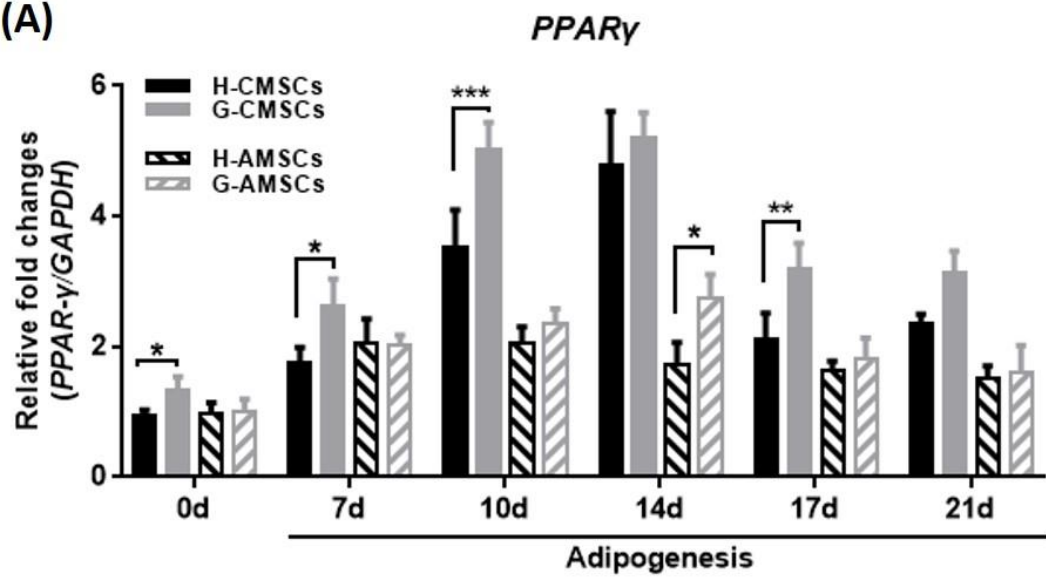
Figure 3-9. Basal activity of adipogenesis-regulating genes

Basal expression levels of (A) *ADIPOQ* and (B) *PPAR* γ were examined before inducing differentiation. The data were normalised to *GAPDH* and expressed as mean \pm SEM of 8 independent experiments. The fold changes were calculated by comparing the relative expression levels in GDM vs. Healthy groups. One-way ANOVA was used to determine statistical significance. ** $p < 0.01$, *** $p < 0.001$.

PPAR γ and *ADIPOQ* closely reflect adipogenic progression; therefore, the expression of *PPAR γ* and *ADIPOQ* during adipogenesis at passage 3 were examined at five different time points (days 7, 10, 14, 17, 21). The data was normalised to *GAPDH* and compared with undifferentiated H-/G- CMSCs/AMSCs on day 0. *PPAR γ* and *ADIPOQ* expression in H-/G- CMSCs displayed elevation across the differentiation time course, peaking at around day 10-14 and *PPAR γ* decreasing thereafter while *ADIPOQ* remaining elevated (Figure 3-10). During adipogenic differentiation G-CMSCs expressed significantly higher levels of both *PPAR γ* and *ADIPOQ* than H-CMSCs at almost all time points. *PPAR γ* displayed some upregulation in H-/G- AMSCs but not to levels seen with H-/G- CMSCs. The gradual increase of *PPAR γ* was observed in H-AMSCs and G-AMSCs from day 0-10 and day 0-14, respectively (Figure 3-10A). Notably, *ADIPOQ* was initially higher in G-AMSCs than H-AMSCs but no significant induction during the differentiation period was seen (Figure 3-10B).

The *PPAR γ* and *ADIPOQ* RNA levels were determined in adipogenically differentiated H-/G- CMSCs/AMSCs and then correlated to lipid accumulation within the cells shown in Figure 3-8. It suggested that increased expression of *PPAR γ* and *ADIPOQ* during early stage induced adipogenesis initiation and the lipid formation happened at later stage of adipogenesis which may be associated with elevated level of *ADIPOQ* expression. Overall, the results once again confirmed that G-CMSCs have enhanced adipogenic capacity whereas H-/G- AMSCs have a limited adipogenic capacity in spite of G-AMSCs displaying increased basal expression levels of adipogenesis-regulating genes.

(A)



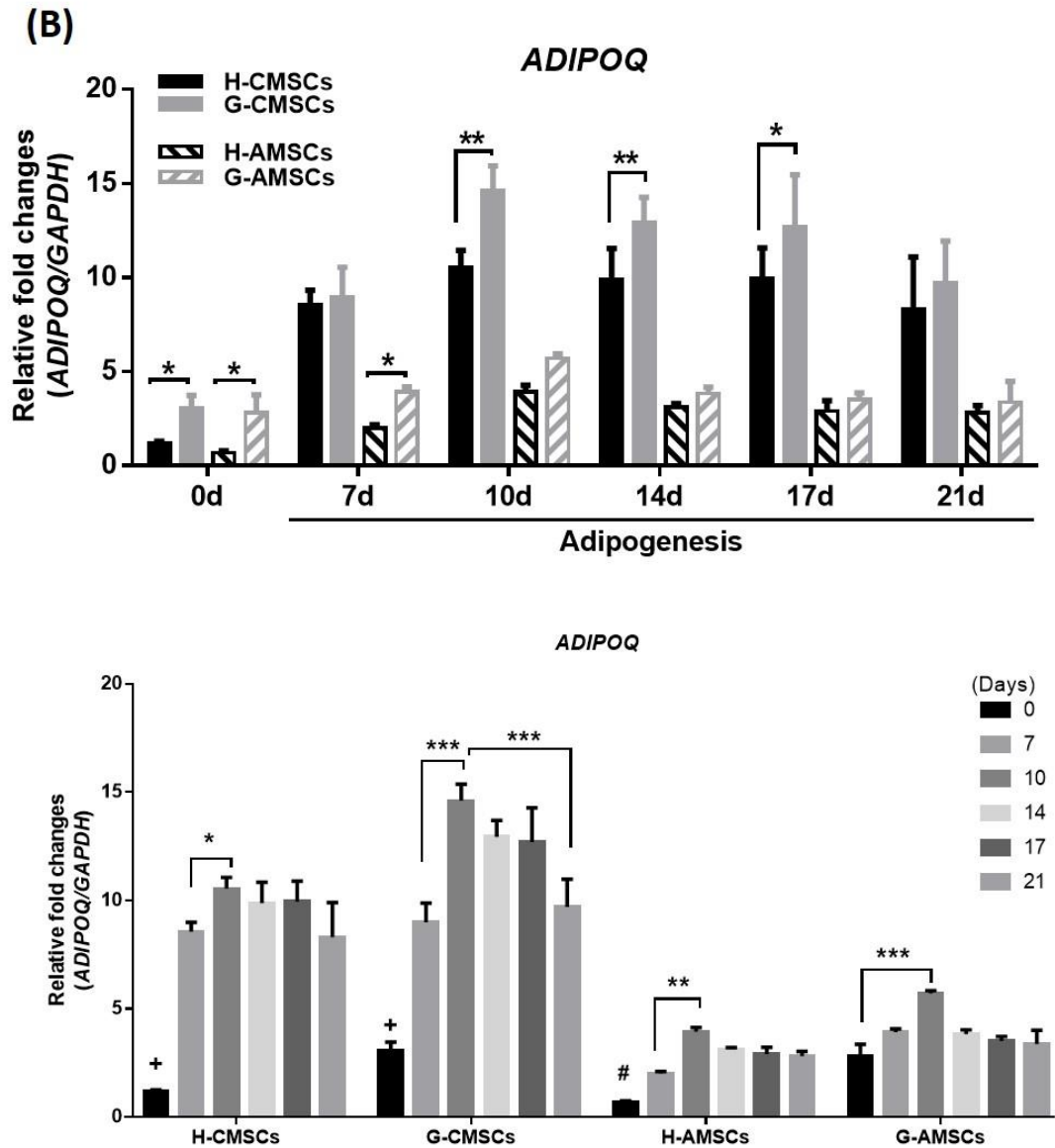


Figure 3-10. Examination of adipogenic progression through marker expression

Time course of adipogenic marker expressions – (A) *PPAR γ* and (B) *ADIPOQ* during differentiation process were analysed by real-time PCR. The above graph shows the comparison between GDM and Healthy groups; the below graph shows the comparison of gene expression changes within the same group over 21 days. Relative levels of gene expression were normalised to *GAPDH* and displayed as fold changes over day 0. Each data represents mean \pm SEM of 5 independent experiments. Two-way ANOVA was used to determine statistical significance, continuous variable - days, * $p < 0.05$, ** $p < 0.01$, *** $p < 0.001$, + $p < 0.001$ differentiated H-/G- CMSCs (day 7, 10, 14, 17, 21) vs Day 0 (undifferentiated H-/G- CMSCs), # $p < 0.05$ differentiated H-/G- AMSCs (day 7, 10, 14, 17, 21) vs Day 0 (undifferentiated H-/G- AMSCs)

3.4.5 Effect of conditioned media on Jurkat T cells

Conditioned media from H-/G- CMSCs and AMSCs has a significant antiproliferative effect on T-cells

MSCs are known to mediate immune cell activity through cell-cell contact and the production of paracrine factors. To evaluate the immunoregulatory properties of secreted factors from Healthy- and GDM- CMSCs/AMSCs, conditioned media (CM) were collected at passage 3 after culturing in serum free media for 48 hours. 10% of FBS were later on added to CM when exposure Jurkat T cells to H-/G- CMSCs/AMSCs CM while 10%FBS DMEM without H-/G- CMSC/AMSCs CM was used as controls. The proliferation and inflammatory cytokines secretion of Jurkat T cells were investigated to compare the immunomodulatory effect of H-/G- CMSCs/AMSCs.

Jurkat T cells cultured in complete growth media (10%FBS) showed a steady increase in proliferation and stable growth rate. A significant reduction in Jurkat T cells was noted following on from exposure to either H-/G- CMSC or AMSCs CM. In comparison to the inhibitory effect of H-/G- AMSCs CM, both Healthy- and GDM- CMSCs CM showed more significant reduction in Jurkat T cell proliferation which maintained a consistent inhibitory effect for 3 days. The growth of Jurkat T cells cultured in H-/G- CMSCs/AMSCs CM resumed on day 4 and day 5 (Figure 3-11A).

Jurkat T cells were stimulated with phytohemagglutinin (PHA) and phorbol 12-myristate 13-acetate (PMA) to induce T cell activation and immune responses. The PHA/PMA activated Jurkat T cells had a slow growth rate even when culturing under complete growth media which exhibited more than 50% reduction in proliferation upon activation. However, PHA/PMA activated Jurkat T cells still displayed a sensitivity to H-/G- CMSCs and AMSCs CM and similarly displayed a reduced proliferation rate following on from exposure. Likewise,

CM from both H-/G- CMSCs and AMSCs suppressed Jurkat T cells proliferation to a significantly greater extent with CM from H-/G- CMSCs. No differences in proliferative suppression by CMSCs/AMSCs CM were noted between healthy and GDM groups (Figure 3-11B).

Interleukin-2 (IL-2), produced upon PHA/PMA stimulation, regulates proliferation of activated T-cells and leads to immune response. As the significant inhibitory effect of H-/G- CMSCs/AMSCs CM on Jurkat T cells proliferation was observed from day 0-3 and cell growth resumed, the secretion of IL-2 was measured for a 3-day period. Jurkat T cells released sustainable levels of IL-2 and showed increased secretion over 3 days. In the first 24 hours after stimulating Jurkat T cells with PHA/PMA, IL-2 secretion did not show significant suppression by H-/G- CMSCs or AMSCs CM. However, the supernatant from activated Jurkat T cells cultured in H-/G- CMSCs CM contained significantly reduced levels of secreted IL-2 on day 2 and 3. H-/G-AMSCs CM also suppressed IL-2 secretion but the suppressive effect was lower than that of H-/G-CMSCs CM (Figure 3-11C).

The immunosuppressive capacity in H-CMSCs vs. G-CMSCs and H-AMSCs vs. G-AMSCs were rather comparable where no significant difference in inhibitory effect on Jurkat T cell proliferation and IL-2 secretion was observed. Healthy- and GDM- CMSCs showed a more pronounced effect on suppressing Jurkat T cell proliferation and diminishing the secretion of IL-2 than H-/G- AMSCs.

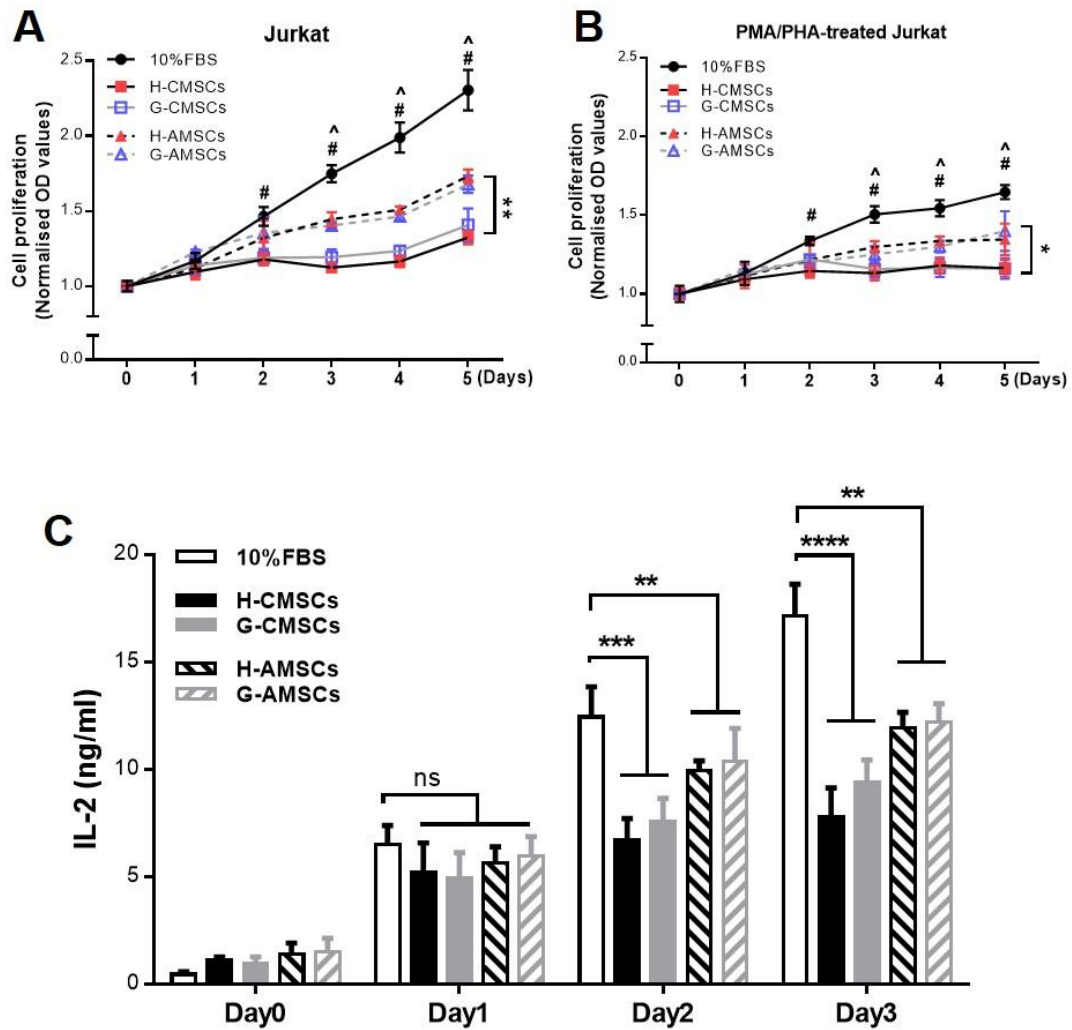


Figure 3-11. Suppression of T-cells proliferation and IL-2 secretion

Jurkat T cells were cultured in the presence of Healthy- and GDM- CMSCs/AMSCs CM (A) without activating with PMA/PHA or (B) with 50 ng/ml PMA and 5 μ g/ml PHA. Cell proliferative ability was measured by MTT assay in a 5-day period. # $p < 0.001$ H-/G-CMSCs vs. 10%FBS, ^ $p < 0.001$ H-/G-AMSCs vs. 10%FBS (C) IL-2 secretion after PHA/PMA stimulation was measured by ELISA from day 0-3. Results were normalised to IL-2 secretion without PHA/PMA stimulation and presented as mean \pm SEM of 5 independent experiments. Two-way ANOVA was conducted to determine the significant differences, continuous variable – days, ** $p < 0.01$, *** $p < 0.001$, **** $p < 0.0001$.

3.4.6 Co-culture system of CMSCs/AMSCs and macrophage

Distinct immunoregulatory properties of H-/G- CMSCs and AMSCs evaluated by macrophage modulation

MSCs modulate immune cell function through a variety of mechanisms. In addition to T cell regulation, MSCs are also known to modulate macrophage-mediated inflammatory responses. Macrophages are key regulators of initiation and control of inflammation, and are typically divided into two types: classically activated type 1 macrophages (M1), characterised by the production of pro-inflammatory cytokines with an acute inflammatory phenotype, and alternatively activated type 2 macrophages (M2), secreting anti-inflammatory cytokines and promoting wound healing²⁵⁶. THP-1 is a human immortalised monocyte-like cell line derived from an acute monocytic leukemia patient²⁵⁷.

The secretome of MSCs has known to mediate immune responses and modulate macrophage population. Bone marrow MSC-derived soluble factors showed the ability to promote the conversion on monocytes or inflammatory M1 macrophage into anti-inflammatory M2 macrophage^{258, 259}. To investigate the immunomodulatory function of H-/G- CMSCs' and AMSCs' secretome on macrophage polarisation, H-/G- CMSCs/AMSC were cultured in a co-culture Transwell with THP-1 monocytes without direct contact. Suspension-cultured THP-1 monocytes were differentiated into macrophages (M0) in the presence of PMA (PMA-THP1) where they adhere to the culture plate and can be further polarised into M1 or M2 macrophages. For M1 and M2 polarisation control²⁶⁰, PMA-THP1 (M0) was activated by interferon- γ (IFN- γ) and lipopolysaccharide (LPS) in order to obtain inflammatory M1 macrophages while interleukin 4 (IL-4) was used to induce anti-inflammatory M2 macrophages. To investigate H-/G- CMSCs/AMSCs paracrine effects on M0 macrophage polarisation, PMA-THP1 (M0) without any stimulation was seeded in the

lower chamber and co-cultured with H-/G- CMSCs or AMSCs in the upper Transwell inserted chamber (Figure 3-12).

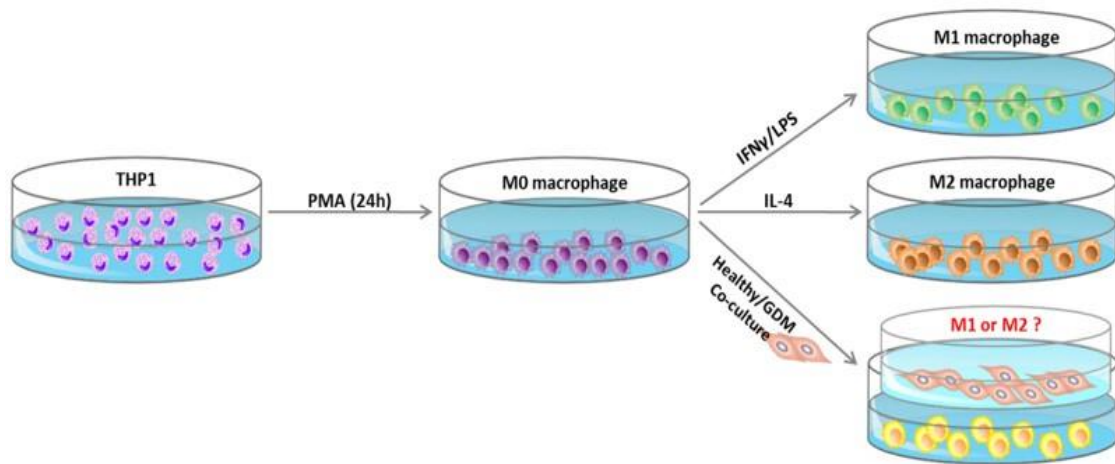


Figure 3-12. Schematic representation of macrophage polarisation

A co-culture system of the macrophage polarisation procedure. THP-1 cells were pre-treated with 50 ng/ml PMA for 24 hours to obtain M0 macrophage. For M1 and M2 macrophage phenotype controls, M0 macrophages were stimulated with 20 ng/ml IFN- γ and 10 pg/ml LPS to obtain M1 polarisation while stimulated with 20 ng/ml IL-4 for M2 polarisation. To examine the effect of H-/G- CMSCs'/AMSCs' secretome on M0 polarisation, 5×10^5 H-/G- CMSCs/AMSCs were seeded in an upper Transwell chamber and 5×10^5 M0 macrophages were seeded in the lower chamber. After co-culture for 24 h, supernatant was collected from all samples for ELISA analysis, and RNA was extracted from H-/G- CMSCs/AMSCs-co-cultured M0 macrophages and M1/M2 controls for further characterisation of macrophage phenotypes.

Following co-culture of H-/G- CMSCs or AMSCs with PMA-THP1, PMA-THP1 were collected to examine the macrophage polarisation through gene expressions. M1 macrophages are characterised by the expression of inflammation-related genes and the production of inflammatory cytokines. High level of inflammatory marker expression, including *IL-1 β* , *IL-12*, and *CXCL8* were detected in IFN- γ /LPS-treated PMA-THP1, suggesting the induction of M1 polarisation (Figure 3-13A). When PMA-THP1 co-cultured with H-/G- CMSCs or AMSCs,

there was no significant increase in inflammatory marker - *IL-1 β* , *IL-12*, and *CXCL8* expression, compared to PMA-THP1 (M0) and M1 macrophages (Figure 3-13A). Notably, *CXCL8* was significantly induced in PMA-treated THP1 (M0) while the expression was significantly suppressed after co-culturing with H-/G- CMSCs/AMSCs. Although the expression of *CXCL8* was higher in H-/G- AMSCs-co-cultured than H-/G- CMSCs-co-cultured PMA-THP1, the expression levels were significantly lower than M1 macrophages controls. Thus, the data suggested that the secretome of H-/G- CMSCs and AMSCs did not promote M1 macrophage polarisation of THP1 cells.

On the other hand, anti-inflammatory M2 macrophages are characterised by increased expression of *IL-10*, *MRC1*, and *CCL-17* which were detected in IL-4 stimulated PMA-THP1, suggesting the induction of M2 polarisation (Figure 3-13B). High levels of M2 macrophage markers were also observed PMA-THP1 when co-cultured with H-/G- CMSCs or AMSCs, indicating that PMA-THP1 were polarising towards M2 phenotypes through the regulation of H-/G- CMSCs'/AMSCs' secretome. PMA-THP1 co-cultured with H-/G- CMSCs expressed significantly higher levels of *MRC1* and *CCL-17* than co-cultured with H-/G- AMSCs, which suggested that H-/G- CMSCs had a more profound effect on promoting M2 marker expression in PMA-THP1 than H-/G- AMSCs. Moreover, no significant difference was detected in the ability to induce M2 macrophage polarisation in H-/G- AMSCs but in CMSCs higher *MRC1* and *CCL-17* expression could be observed when PMA-THP1 co-cultured with H-CMSCs than with G-CMSCs (Figure 3-13B).

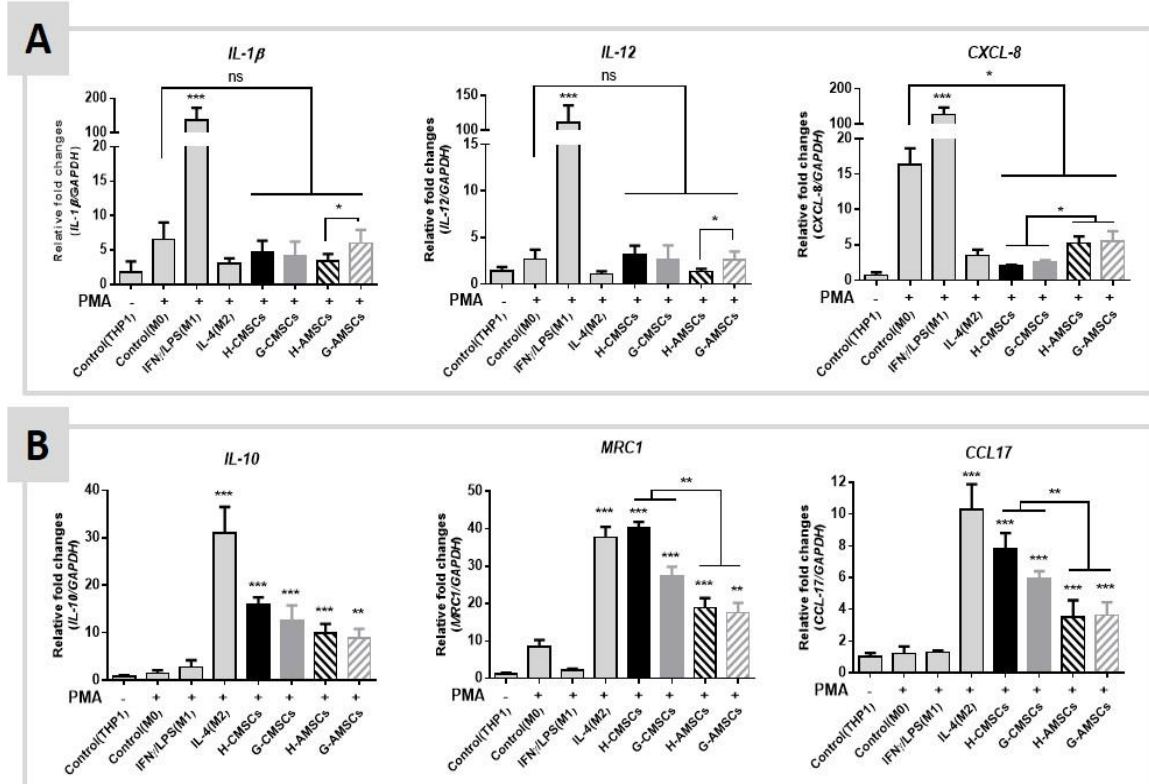


Figure 3-13. Examination of M1/M2 marker expression in THP1

THP1 monocytes polarisation was examined by M1/M2 marker gene expression. Apart of negative control (THP1), all groups were treated with PMA for 24 hours to induce M0 macrophages. M1 phenotypes were further induced with IFN- γ and LPS while M2 phenotypes were induced with IL-4. To examine the effect of H-/G- CMSCs/AMSCs on THP1 polarisation, PMA-treated THP1 were co-cultured with H-/G- CMSCs/AMSCs for 24 hours and RNA from THP1 cell were extracted for gene expression analysis. All cells were cultured in the same basal media, 10% FBS DMEM. (A) M1 macrophage markers - *IL-1 β* , *IL-12*, *CXCL8* and (B) M2 macrophage marker - *IL-10*, *MRC1*, *CCL-17* expressions were examined by real-time PCR. The values were normalised to *GAPDH* and fold changes were calculated by comparing to THP1 control. Each data shown represents mean \pm SEM of 6 independent experiments. One-way ANOVA was conducted to determine the statistical significance, * $p < 0.05$, ** $p < 0.01$, *** $p < 0.001$ relative to PMA-treated control.

Macrophages exert their functions by releasing a series of cytokines to activate and recruit other immune cells during immune responses. Cytokines secretion bias the macrophage's phenotypes towards M1 or M2 macrophage. M1 macrophages secrete pro-inflammatory cytokines TNF- α , IL-1 β , IL-6, IL-12, IL-23 while M2 macrophages secrete high levels of

immunosuppressive cytokine IL-10 and also a little amount of pro-inflammatory cytokines. Supernatant from co-culture of PMA-THP1 and H-/G- CMSCs/AMSCs was collected to examine TNF- α and IL-10 release for identifying M1 or M2 phenotypes. No significant increase in TNF- α secretion (Figure 3-14A) was seen but an upregulation in IL-10 (Figure 3-14B) was detected when co-culturing PMA-THP1 with H-/G- CMSCs or AMSCs. Comparing with M2 markers gene expression (Figure 3-13B), though H-/G- AMSCs co-cultured PMA-THP1 expressed lower levels of M2 markers, the IL-10 secretion was comparable to H-/G- CMSCs co-cultured PMA-THP1. Overall, CMSCs and AMSCs derived from healthy or GDM placenta were equally capable of promoting PMA-THP1 towards M2 polarisation. The GDM environment did not significantly alter macrophage regulation ability in G-CMSCs and G-AMSCs, compared to their healthy counterparts.

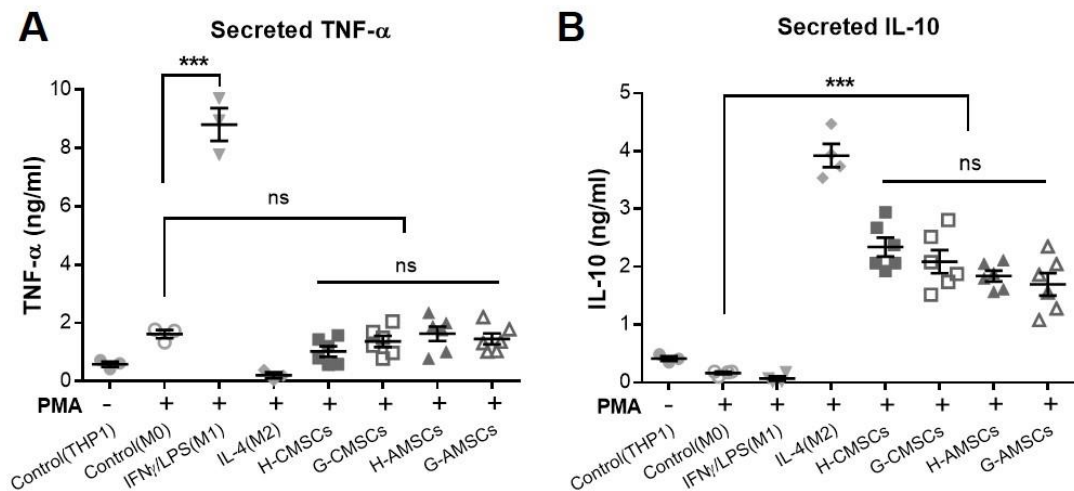


Figure 3-14. Cytokines release by M1/M2 macrophages

Cytokines secretion from PMA-THP1 in H-/G- CMSCs or AMSCs co-culture was examined by ELISA. Supernatant was collected after 24 h co-culture and measured the levels of TNF- α and IL-10 secretion. Each data shown represents mean \pm SEM of 6 independent experiments. One-way ANOVA was conducted to determine the statistical significance, *** p < 0.001.

3.5 Discussion

The placenta, usually discarded after delivery, is a valuable source of plentiful perinatal MSCs for regenerative medicine without ethical concerns. Cell therapies using placental-derived MSCs have already been applied to various disorders treatment in animal models²⁶¹ and some clinical trials, such as ischaemic stroke, Crohn's disease, and idiopathic pulmonary fibrosis^{242, 262, 263}. However, few studies have investigated differences in therapeutic potential of placenta-derived MSCs from women with pregnancy complications. In this study, we provided a thorough comparison of CMSCs vs. AMSCs and reported the effects of GDM environment on CMSCs and AMSCs biological properties.

Biological characterisation of H-/G- CMSCs/AMSCs

Derived from different layers of the same placental membrane, CMSCs and AMSCs show diverse cell biological characteristics. AMSCs have been widely studied as the clinical applications of amniotic membrane began several years ago. The isolation process of AMSCs has also been well-established; however, the role of CMSCs remained unclear until recent years. The observation of the reduced proliferation rate of AMSCs compared with CMSCs in our study is consistent with some recent reports. A study demonstrated the limited *ex vivo* expansion potential of AMSCs, where CMSCs were found to have higher proliferation ability than AMSCs and BM-MSCs²⁶⁴. Likewise, Araujo et al. compared the growth kinetics of amniotic (AMSCs), chorionic (CMSCs), placental decidua (DMSCs) and umbilical cord MSCs. They found the superior proliferation ability in CMSCs and DMSCs which were able to maintain a steady growth rate until passage 10 while AMSCs had a short lifespan, low doubling time, and were unable to expand after passage 5²⁶⁵. Indeed, we also noticed the difficulty in AMSCs expansion at late passages.

We further investigated differences in growth ability between GDM and healthy CMSCs/AMSCs via direct counting of viable cells and measurement of metabolic activity. It has been suggested previously that umbilical cord derived-MSCs from GDM women displayed decreased cell growth with early cellular senescence accompanied by the expression of p16 and p53²⁶⁶. Alternatively, Pierdomenico et al. described MSCs obtained from umbilical cord of both healthy and diabetic mothers where the later demonstrated an increased proliferative ability along with an upregulation of CD44, CD29, CD73, CD166, SSEA4 and TERT²⁶⁷. We found that GDM had distinct effect on CMSCs and AMSCs proliferation, where G-CMSCs displayed reduced rates when compared to H-CMSCs while G-AMSCs, by contrast, showed higher proliferation rates than H-AMSCs. As AMSCs are derived from the amniotic membrane adjacent to the fetus, the higher proliferation rate of diabetic AMSCs may reflect features of GDM including heavier fetal weights on resultant cell phenotype.

Immunophenotypic analysis characterised H-/G- CMSCs/AMSCs surface marker expression (positive for CD90, CD73, CD105; negative for CD14, CD19, CD34, CD45 and HLA-DR). Overall, H-/G- CMSCs and AMSCs express similar levels of surface markers and all meet the minimal criteria for MSC definition. However, the surface protein expression profile may vary depending on different MSC sources. The level of CD45 expression was higher in both G-CMSCs and G-AMSCs compared to healthy counterparts. CD45 is a transmembrane protein tyrosine phosphatase that regulates signal transduction in immune cells and mainly expressed on hematopoietic stem/progenitor cells (HSCs)²⁶⁸. CD45 also plays a role in regulating the motility of bone marrow progenitor cells and their retention. CD45 knockout bone marrow progenitors showed increased cell adhesion and defective motility, mediated by reduced matrix metalloproteinase 9 secretion and imbalanced Src kinase activity²⁶⁹. Our study showed that approximately 17% of G-CMSCs and 19% of G-AMSCs were positive for

CD45 expression. Although we were unclear whether higher CD45 expression in G-CMSCs/AMSCs was associated with cell motility, the enhanced migration in ability in G-CMSCs was demonstrated in chapter 5 via microarray analysis and *in vitro* migration assays. In fact, CD45 is a typical HSC marker but BM-MSCs can still express some degree of CD45 under certain condition. The CD45 expression was found around 15% in BM-MSC derived from older donor at passage 1 while the expression decreased at later passage²⁷⁰. Approximately 15% of decidual MSCs²⁷¹ and 17% of AMSCs²⁷² shown positive for CD45 expression were also reported in some studies. However, we performed immunophenotyping at passage 3 and did not examine the possible expression change at later passage.

GDM pregnancy and adipogenesis tendency in MSCs

Emerging research has highlighted the importance of the intrauterine environment as a risk factor in the likelihood of offspring developing obesity and metabolic diseases^{273, 274}. The underlying biological mechanism for the link between GDM and the increased risk of future diabetes is poorly understood, although the GDM environment has potential to modify the epigenetic state of fetal genes. Increased methylation of *PYGO1* and *CLN8* genes in offspring exposed to a GDM environment is proposed as being associated with long-term adverse effects on fetal health^{275, 276}. GDM is associated with newborn hyperinsulinemia with effects on offspring fat mass seen until 6 weeks. Elevated preperitoneal adipose tissue in newborns is linked with increased risk of obesity in later life²⁷⁷. We found that the CMSCs and AMSCs differentiation potential are influenced by maternal environment during gestation. Under the same culture condition, elevated adipogenic differentiation was found in GDM-MSCs than with MSCs from healthy pregnancies. Moreover, higher basal expression levels of adipogenic transcription factors in G-CMSCs and subsequent lipid content associated with

increased transcription factor expression during differentiation indicated an enhanced adipogenic potential when compared to H-CMSCs and H-/G- AMSCs. This suggests that the GDM environment itself may have less of a role in affecting fetal cell properties than that of the membrane itself.

In addition, although H-/G-CMSCs demonstrated adipogenic potential verified by substantial lipid droplet accumulation and increased adipogenesis-associated gene expression, the reduced expression in *PPAR γ* and *ADIPOQ* was noticed on day 21. The adipogenic transcription factor, *PPAR γ* plays a critical role in initiating adipogenesis and *ADIPOQ* is involved in adiponectin formation²⁷⁸. The reduced expression may reflect the loss of adipocyte phenotype. For instance, the deletion of *PPAR γ* in adipose tissues contributed to impaired adipocyte function and maturation, adipocyte death, and reduced fat weights or lipodystrophy^{279, 280}. On day 14 and 17, *PPAR γ* and *ADIPOQ* showed high expression levels in differentiated H-/G- CMSCs, which may suggest the optimal induction period. Some studies demonstrated adipocyte maturation during 14-day adipogenesis protocols from bone marrow MSCs²⁸¹, umbilical cord MSCs²⁸², and placental MSCs²⁸³. As adipogenesis protocols for different cell types may vary from 14-21 days, our data might suggest that a 17-day culture period with adipogenesis media might be ideal for H-/G- CMSCs differentiation. However, it is still unclear whether H-/G- CMSCs differentiated into fully mature adipocytes or remained in immature state. To optimise the ideal differentiation protocol, it may benefit from the comparison between human adipocytes and MSC-differentiated adipocytes at different time points during adipogenesis process.

Immunosuppression of H-/G- CMSCs/AMSCs

For successful clinical application of MSC therapy, the immunoregulatory potential of H-/G- CMSCs and AMSCs is an important area of consideration. The immune responses mediated

by T-cells may lead to cell transplant rejection or Graft-versus-Host disease²⁸⁴. MSCs have been reported to modulate the proliferation and function of immune cells by both cell-to-cell contact and the secretion of growth factors, cytokines, and chemokines²⁸⁵. Immunosuppressive capacity of MSCs is a therapeutic option for the treatment of various immunological disorders. Given that the placenta plays a critical role in fetal-maternal tolerance and contains cells that display immunomodulatory properties, MSCs derived from placenta not only have superior immunomodulatory potential but also have therapeutic potential for the mothers and offspring²⁸⁶. In our study, H-/G- CMSCs and AMSCs displayed differential levels of immunosuppressive capacities in T-cell regulation. Both H-/G- CMSCs and AMSCs suppressed T cell proliferation while H-/G- CMSCs showed superior inhibitory effect than H-/G- ASMCs. The mechanism of MSCs suppressing T-cell proliferation has been widely investigated. BM-MSCs are able to inhibit T-cell proliferation through the induction of cell division arrest²⁸⁷, apoptosis via Fas ligand-dependent apoptotic pathway²⁸⁸, and blocking T cell effector function via contact-dependent interaction²⁸⁹.

Moreover, T-cell mitogenic cytokine IL-2 is released upon T-cell activation. The suppressive effect of IL-2 production was more profound in H-/G- CMSCs CM than H-/G- ACMSC CM while GDM environment did not show significant alteration in CMSCs/AMSCs ability to suppress T cell activation. IL-2 is associated with various immune responses, including T cell proliferation, survival, differentiation, supporting the activation of natural killer cells, and promoting activation-induced cell death²⁹⁰. The reduction of IL-2 secretion by MSCs suppresses immune reactions triggered by T cells and improves engraftment in cell transplant²⁹¹.

Apart from well-studied mechanisms of MSC-mediated T-cell activity, there is an increasing interest in MSCs immunomodulation on macrophages over the past few years. MSCs

involve in regulating innate immune response by modulating macrophage polarisation and inhibiting the secretion of inflammatory cytokines^{292, 293}. M1 macrophage induced by intracellular pathogens, tissue damage and infection, is associated with inflammation, along with the secretion of inflammatory cytokines. M2 macrophages have high phagocytosis capacity, tissue remodelling ability, and involve in producing extracellular matrix (ECM) components and anti-inflammatory factor, IL-10. Transferring M2 macrophages into autoimmune type 1 diabetes mouse models showed protection against inflammation and the transferred M2 macrophages homed to the inflamed pancreas, promoting β -cell survival²⁹⁴. The transplantation of MSCs into an *in vivo* model showed increased recruitments of M2 macrophages to the wound site and enhanced damaged tissue repair²⁹⁵. More and more evidences indicate the interaction between MSCs and macrophages recently, for instance, increased expression of M2 macrophage makers was observed following the injection of MSCs to rat infarct myocardium which was initially infiltrated with M1 macrophage²⁹⁶.

In our finding, H-/G- CMSCs and AMSCs were evidenced to divert the differentiation of naïve macrophages (M0) into M2 phenotypes through a co-culture system, which also implied that CMSCs/AMSCs were able to regulate macrophage differentiation through their secretome functions without the need of direct cell-cell contact. Several soluble factors secreted by MSCs have been considered as mediators to regulate immune cells, such as IL-6, prostaglandin E2 (PGE₂), indoleamine 2,3-dioxygenase (IDO), and lactate^{297, 298}. Moreover, some studies have demonstrated the possibility of MSCs-mediated macrophage activation shift from M1 to M2 phenotypes²⁹⁶. BM-MSCs attenuated M1 macrophage function with a concomitant shift towards M2 state through the alteration in AMPK and mTOR pathway activities²⁹⁹. These findings could be beneficial for the treatments of inflammatory diseases such as rheumatoid arthritis, asthma, or fibrosis where M1 macrophages play a vital role in

disease progression.

Although H-/G- CMSCs and AMSCs were capable of promoting M2 polarisation, the higher expression of *MRC1* and *CCL17* were found in H-/G- CMSCs than H-/G- AMSCs co-cultured macrophages, particularly the highest expression in H-CMSCs. MRC1 (C-type mannose receptor 1), also known as CD206, is a typical M2 macrophage marker which binds to glycoproteins and collagen ligands. A recent study showed that CD206⁺ M2-like macrophages in adipose tissues created a microenvironment that inhibited growth and differentiation of adipocyte progenitors. In the *in vivo* mouse model, the reduction in the numbers of CD206⁺ M2-like macrophages resulted in a down-regulation of TGFβ signalling, together with upregulated adipocyte progenitors differentiation³⁰⁰. M0 macrophages under H-CMSCs co-culture displayed significantly upregulated levels of CD206 expression than G-CMSCs co-cultured macrophages. The increased adiposity in GDM pregnancy may somehow reflect the significantly lower CD206 expression in G-CMSC-induced than H-CMSC-induced M2 macrophages. However, immune functions of CD206 has not yet fully understood while CD206 is also involved in migration, pro-inflammatory cytokine secretion, and fetal-maternal immunological tolerance³⁰¹. Besides, CCL-17 and IL-10 released by M2 macrophage are known to have a critical role in inhibiting M1 macrophage polarisation³⁰². Although CCL-17 was lower in M2 macrophage under H-/G- AMSCs than H-/G- CMSCs co-culture, the secretion of IL-10 was comparable in all groups.

Notably, the GDM environment had no significant effects on the immunosuppressive ability of MSCs in all aspects. Despite an increase in M2 marker expressions after co-culturing PMA-THP1 with H-CMSCs, which might suggest a better macrophage modulation potential in H-CMSCs than G-CMSCs, G-CMSCs showed a comparable ability in regulating Jurkat T cells activity and modulating cytokine secretion. Likewise, the responses from Jurkat cells

treated with G-AMSCs conditioned media or macrophages co-cultured with G-AMSCs were similar to the results from H-AMSCs.

3.6 Summary

In summary, human placenta is comprised of several stem cells niches that mostly originate from extraembryonic tissue, and connect to maternal tissues, which may be a promising autologous source for cell therapy in both the mother and her offspring. Bone marrow MSCs isolated from elder donors have been reported to have reduced biological activity, thus leading to poor therapeutic potential³⁰³. Insufficient numbers of MSCs or impaired MSCs function from patients with rheumatoid arthritis and diabetes, respectively, have also been reported ^{304, 305}. Therefore, an understanding of MSC behaviours under different growth environment is essential. In this study, we provide a comparison between CMSCs and AMSCs from healthy and GDM placenta, and evaluate the biological characteristics of both. CMSCs and AMSCs have distinct biological properties. The superior proliferation, differentiation and immunomodulatory properties in CMSCs than AMSCs make them a promising alternative source for autologous cell transplantation. In addition, we demonstrated the importance of the maternal GDM intrauterine environment and its differential effects on CMSCs and AMSCs

Chapter 4

Generation of insulin producing cells from Healthy- and GDM- AMSCs/CMSCs



4.1 Introduction

Women with a history of GDM have an increased risk of developing type 2 diabetes postnatally compared with women without previous GDM. Roughly 5-10 years following on from a GDM-affected pregnancy approximately half of these women are diagnosed with type 2 diabetes^{34, 37}. GDM is associated with gestational programming in the fetus and may predispose offspring to an increased incidence of childhood obesity and impaired glucose tolerance, leading to type 2 diabetes later in life^{306, 307}. Evidence has demonstrated a positive correlation between GDM and the risk of developing type 2 diabetes in women with a history of GDM, as well as children from GDM pregnancies^{308, 309}.

Patients with type 2 diabetes require lifelong anti-diabetic drug or insulin treatment. However, neither of these either reverse the disease or correct the beta cell dysfunction^{310, 311}. Transplantation of cadaveric islet cells has therefore become a promising therapeutic strategy for diabetes, and though first conducted in 1999³¹² a shortage of donors and immune rejection have limited its clinical usage. Nowadays, mesenchymal stem cells (MSCs) which possess a multi-lineage differentiation potential coupled to immunomodulatory properties offer an alternative to β -cell replacement therapy³¹³.

IPC generation protocols

Several studies have reported the generation of insulin-producing cells (IPCs) from adult tissue-derived MSCs, such as bone marrow^{314, 315}, adipose tissue²¹⁰, and liver³¹⁶. However, these existing approaches lack a consistent protocol applicable to all source of MSCs³¹⁷. The IPC differentiation method was originally developed from mouse embryonic stem cells (mESCs)³¹⁸ and then modified for generating IPC from human ESCs (hESCs)³¹⁹. The successive exposure of hESCs to different growth factors and small molecules in order to

mimic the environment during pancreagenesis *in vivo* has successfully generated endocrine-like tissue from hESCs. Figure 4-1 lists a variety of multistep procedures to induce differentiation of hESCs into IPCs.

Due to the limited availability and ethical concerns of using hESCs, some studies have modified and applied IPC generation method to bone-marrow MSCs (BM-MSCs). However, a major limitation of MSCs derived from adult tissues is that they are considered more likely to differentiate toward mesenchymal lineages due to their mesodermal origin, while β -cells are of endodermal origin³²⁰. Inducing definitive endoderm is an essential step for IPCs generation. To do this, activin A is commonly used for definitive endoderm formation³²¹ although administration concentrations may vary depending on different conditions. Other challenges include the low generation rate of IPCs from BM-MSCs or the immature state of the IPCs where they fail to release insulin^{322, 323}.

MSCs from fetal origins, such as placenta and amniotic fluid, on the other hand have been demonstrated to express endoderm lineage and embryonic markers^{324, 325}. This is suggestive of a less restricted potency of fetal-related tissue derived MSCs and a potentially broader differentiation potential.

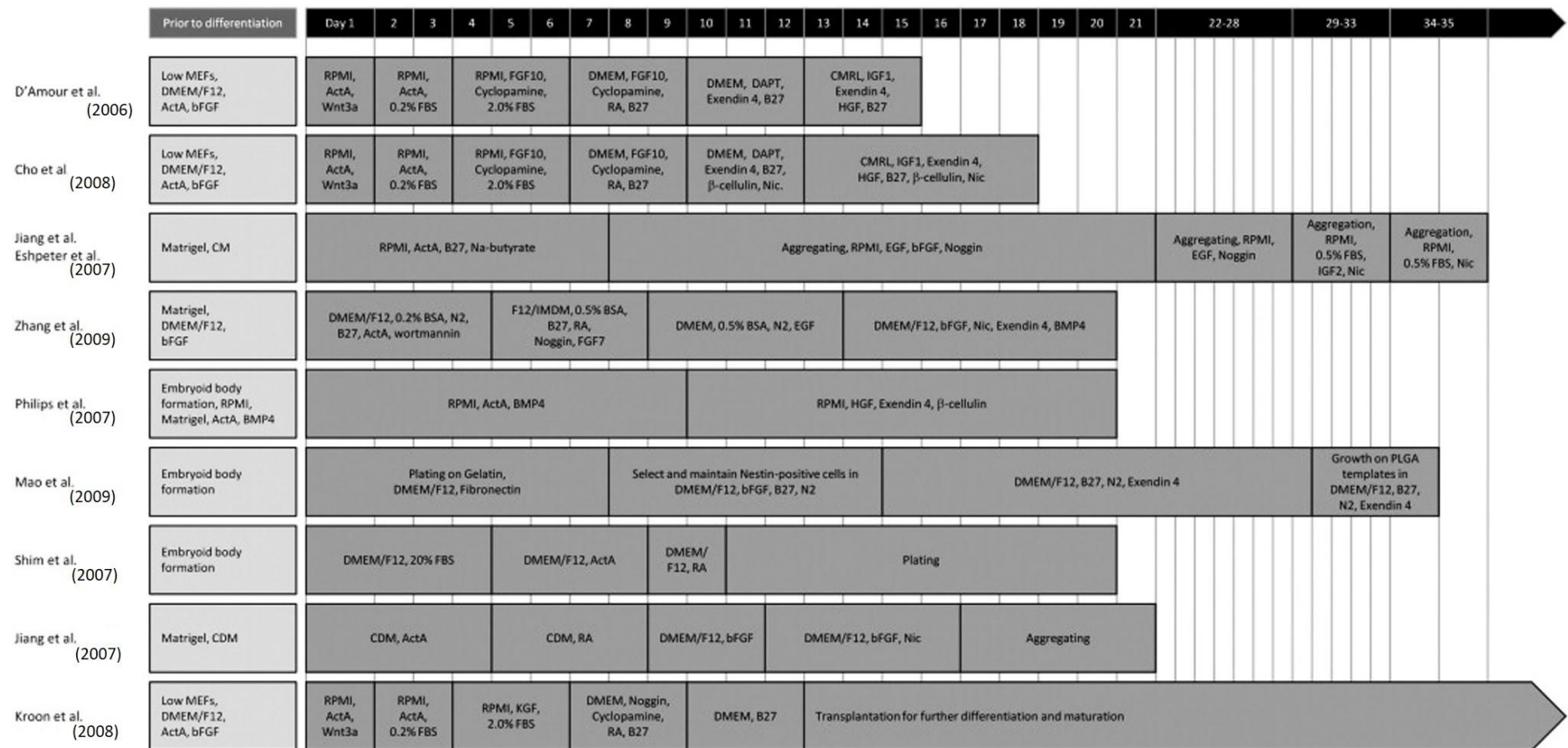


Figure 4-1. Time lines of multistep procedures for IPC differentiation.

Various protocols to induce IPC differentiation from hESCs. ActA, Activin A; bFGF, basic fibroblast growth factor; BMP4, bone morphogenetic protein 4; CM, conditioned media; DAPT, γ -secretase inhibitor; EGF, epidermal growth factor; HGF, hepatocyte growth factor; IGF1/2, insulin-like growth factor 1/2; KGF, keratinocyte growth factor; MEFs, mouse embryonic fibroblast feeders; Nic, nicotinamide; RA, retinoic acid. Reprinted from Van Hoof *et al.*, 2009³¹⁹

A common feature of the various strategies described for the differentiation of MSCs into IPCs is a high glucose culture environment^{326, 327}. During pancreatic islet development multiple stimuli are required including hormones, growth factors, and nutrients³²⁸. Within all these stimulators, glucose is suggested to play an important regulatory role in β -cell growth, survival, and proliferation³²⁹. In the human body, elevated blood glucose level is a primary activator of β -cell expansion in situations where β -cell compensation is required due to increased metabolic demand³³⁰. A glucose concentration of 20-30-mM was sufficient to significantly enhanced β -cell replication in both *in vitro* and *in vivo* models³³¹. With human bone marrow MSCs a culture environment containing 23.3 mM glucose for 15 days was shown to stimulate expression of pancreatic-related genes; *PDX1*, *PAX4*, *GLUT2*, and *INS* and induce the formation of β -cell precursors³³². Collectively, glucose seems to be an essential factor for IPC generation. GDM-CMSCs/AMSCs are under prolonged exposure due to hyperglycaemia during pregnancy, the suitability of the high glucose concentration, applied in many IPC differentiation protocols, used to mimic the β -cell development environment, for GDM-CMSCs/AMSCS remains to be determined.

Makers for beta-cell maturity

A human islet cluster contains not only insulin-secreting β -cells but also several endocrine cell types which secrete different hormones, including α -cells, δ -cells, PP-cells, and ϵ -cells that express glucagon, somatostatin, pancreatic polypeptide, and ghrelin, respectively³³³. Given the common origin and the similar environment for these pancreatic cells development, the examination of marker expressions is hence useful for identifying different pancreatic cell types and staging the differentiation of MSCs to β -cells whether *in vivo* or *in vitro*. The expression of pancreas-associated transcription factors at intermediate developmental stages are shown in Figure 4-2. Some of the markers used in this chapter

are described in detail below.

The expression of transcription factor neurogenin 3 (*NGN3* or *NEUROG3*) induces endocrine lineage development and functions as an activator of several endocrine gene transcriptions in progenitor cells³³⁴. The *NGN3* expression peaks at endocrine stage and reduces in mature β -cells³³⁵. Insulin gene enhancer binding protein-1 (*ISL1*) is one of the endocrine lineage markers that controls the proliferation and survival of endocrine cells during islet developmental stage³³⁶. *ISL1* also involves in cell fate specification regulating the endocrine cells lineage commitment into different pancreatic cell subtypes³³⁷.

With regard to pancreatic development, insulin promoter factor 1 (*PDX1*) is the most studied marker, expressed during early development of endocrine cells and sustained presence in mature islets³¹⁹. *PDX1* is involved in several regulations of β -cell function and survival. The deficiency of *PDX1* is associated with pancreatic agenesis, β -cell dysfunction, and increases cell death and diabetes both in rodent and human³³⁸. The transcription factor paired box protein *PAX6* is generally expressed in terminally differentiated endocrine cells in the process of developing into pancreatic hormone-producing cells³³⁹. Both *PAX6* and *PDX1* are crucial for insulin synthesis in β -cells through the transcriptional regulation of insulin gene^{340, 341}.

The insulin (*INS*) and major glucose transporter *GLUT2* are expressed in mature β -cells and essential for glucose stimulated insulin secretion (GSIS). The genetic inactivation of *GLUT2* significantly suppressed glucose uptake and GSIS pathways³⁴², suggesting an important role of *GLUT2* in glucose sensing and homeostasis³⁴³.

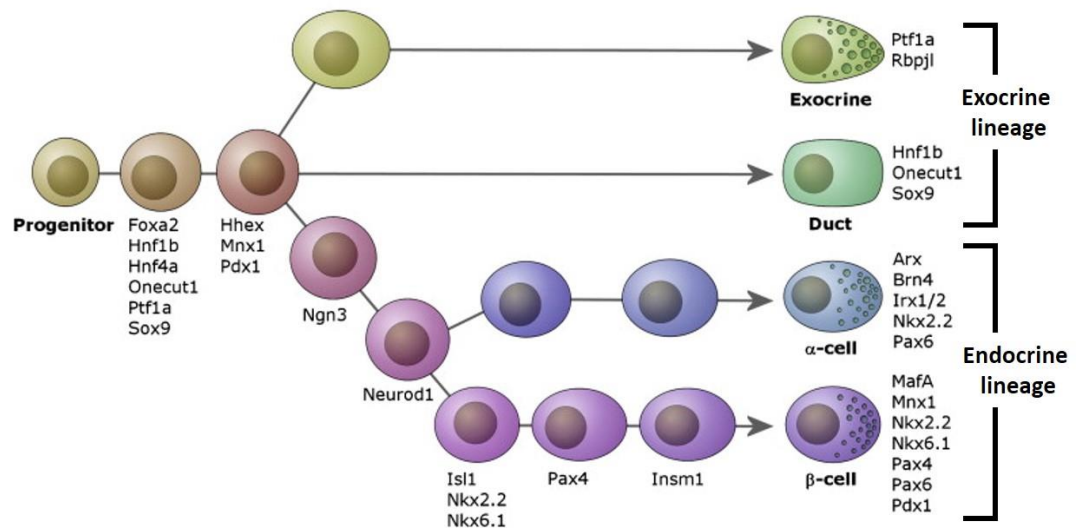


Figure 4-2. Defined transcription factors for pancreatic development

Different cell types in pancreatic islets are derived from a common precursor. The developmental stages are marked by expression of a number of pancreas-associated transcription factors. Reproduced from Van Hoof *et al.*, 2009³¹⁹

4.2 Aim

Given that both the woman and child from a pregnancy affected by GDM have an increased risk of developing diabetes, autologous AMSCs and CMSCs provide a potentially valuable source as a cell therapy. In an attempt to establish a therapeutic use potential of autologous placental membrane-derived MSCs for diabetes treatment, we aimed to establish a feasible approach for the generation of IPCs from CMSCs/AMSCs and determine the role, if any, of GDM in this capacity.

The main objectives of the chapter:

- Investigate high glucose culture effect on H-/G- CMSCs and AMSCs
- Establish a step-wise approach for IPC generation from H-/G- CMSCs/AMSCs
- Characterise H-/G- CMSC/AMSC derived IPCs via morphological changes, marker expression, and insulin release.

4.3 Methods

All maternal and fetal details of placentas used in this chapter were described in chapter 2 section 2.2. Pluripotent marker expression of CMSCs and AMSCs were analysed by real-time PCR for pluripotent gene expressions (section 2.8) and performed with all placenta samples. For high glucose effect investigation, healthy samples used for analysis were from Healthy03, 06, 07, 08 and GDM samples were from GDM05, 06, 07, 08 (Table 2-1). Prior to high glucose exposure, Healthy- and GDM- CMSCs/AMSCs were cultured in 5.5 mM glucose DMEM supplemented with 10% FBS, 1% L-glutamine, 1% NEAA and 1% Penicillin-Streptomycin from passage 0-3. At passage 3, media were switched to 25 mM glucose DMEM. Cells were cultured for indicated periods (10, 20, 30 days) and then examined for cell death/survival by cell viability assay (section 2.11) and cellular senescence by β -galactosidase activity assay (section 2.12).

For three-stage IPC differentiation protocol development, 6 healthy samples (Healthy03, 06, 07, 08, 10, 11) and 7 GDM samples (GDM03, 04, 05, 06, 07, 08, 10) were used. Molecules and growth factors used in differentiation protocols are described in detail in section 4.4.4. Briefly, cells at passage 3 were pre-cultured in 25 mM glucose DMEM for 10 days and then trypsinised, re-suspended in stage 1 differentiation media, and seeded at a density of 1×10^6 cells/well in a six-well plate. For stage 1, cells were cultured in serum-free 17.5 mM glucose DMEM/F12 that contained 1% BSA, 50 μ M 2-mercaptoethanol, 1mM sodium butyrate, and 50 ng/ ml activin A for 3 days before adding 2 μ M retinoic acid to the media and culturing for an additional 3 days. At stage 2, cell media was switched to DMEM/F12 containing 1% BSA, 20 ng/ml EGF and 0.3mM taurine for 3 days. At stage 3, 10 mM nicotinamide and 50 nM glucagon-like peptide (GLP)-1 were added to stage 2 media to induce IPC maturation and insulin formation, and 1% NEAA were added to support cell

growth. Cells were cultured in stage 3 media for another 7 days. To further induce AMSC-IPC maturation, exendin-4 and betacellulin known to induce insulin secretion were used at stage 3 to replace GLP-1. The purpose of exendin-4 or betacellulin supplementation is described in result section 4.4.5.

IPC characteristics were assessed by cell morphological observation (section 2.4.2), pancreatic marker examination through real-time PCR (section 2.8), immunofluorescence staining (section 2.13), and ELISA (section 2.10.2). The experimental flow and methodology adopted in this chapter are summarised in Figure 4-3.

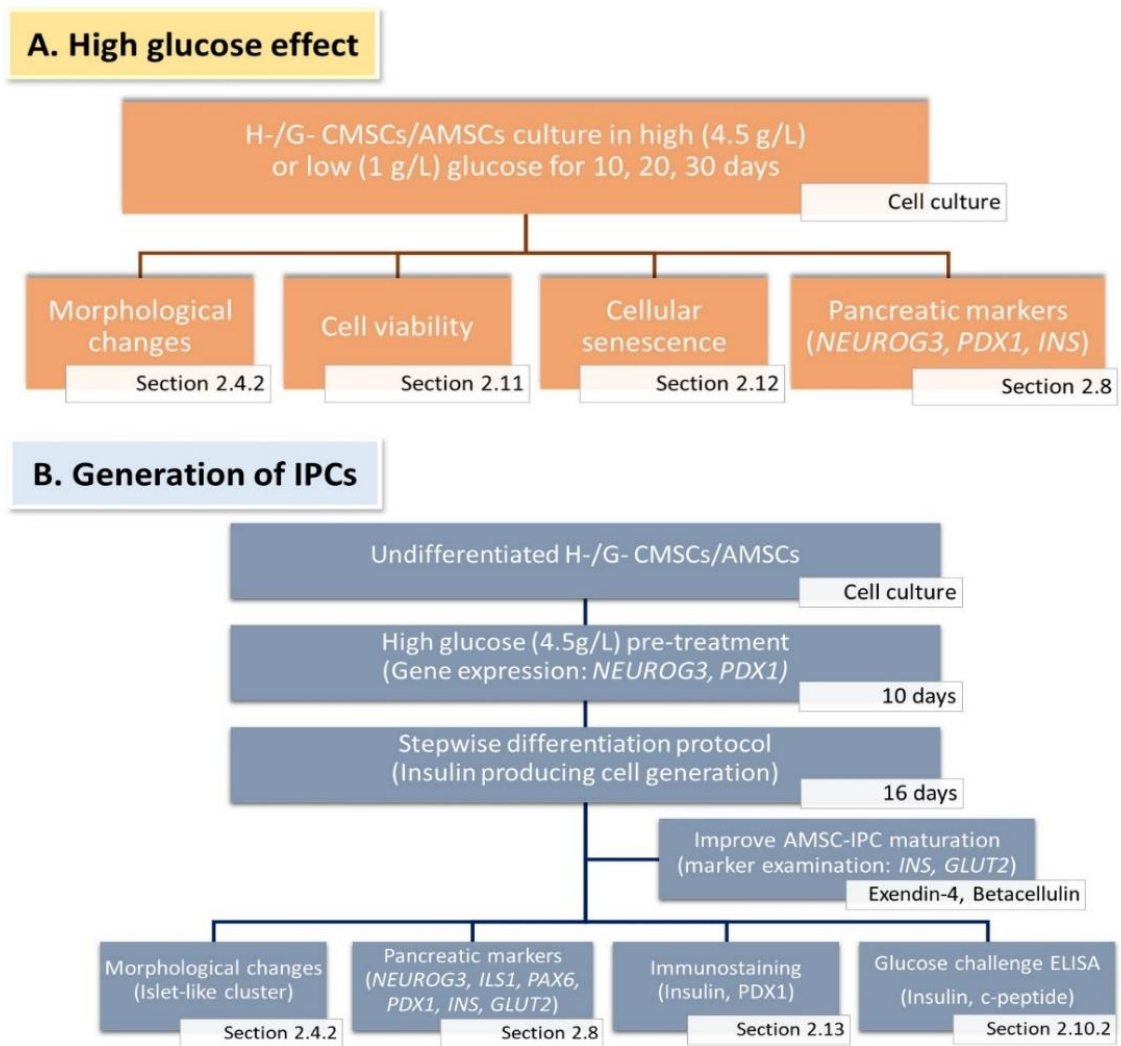


Figure 4-3. Summary of the methodology in chapter 4

Statistical analysis

The percentage of SA- β -gal-positive cells, cell viability, real-time PCR results of IPCs marker expression, and ELISA for protein secretion were compared using one-way ANOVA and Tukey post-hoc tests. 30-day high glucose treatment on pancreatic gene expression changes were analysed by two-way ANOVA to determine the statistical significance among different groups, p-value below 0.05 was considered significant. Analysis was performed using GraphPad Prism (GraphPad Software). The data was presented as mean \pm SEM.

4.4 Results

4.4.1 Pluripotent markers expression

Transcription factors which help to maintain the pluripotent state in stem cells include *NANOG*, *SOX2*, and *OCT4*. These are highly expressed in undifferentiated embryonic stem cells (ESCs) and provide an indication of the capacity of self-renewal, proliferation, survival, and multi-lineage differentiation potential. The expression of pluripotent markers is usually low in adult tissue-derived MSCs and gradually decreases further as the passage number increases³⁴⁴. The gene expressions of *NANOG*, *SOX2*, and *OCT4* in H-/G- CMSCs/AMSCs were examined and compared to ESCs and BM-MSCs.

ESCs expressed significantly higher levels of *NANOG* and *OCT4* than BM-MSCs. Similarly, placental MSCs (H-/G- CMSCs/AMSCs), *NANOG* and *OCT4* expression were also significantly lower than ESCs. The *NANOG* expression in H-/G- CMSCs and AMSCs was comparable and significantly higher compared to BM-MSCs (Figure 4-4A). Likewise, the placental MSCs expressed significantly higher levels of *OCT4* than BM-MSCs; in addition, G-AMSCs showed an increased *OCT4* expression than H-AMSCs (Figure 4-4B).

Placental MSCs expressed high levels of *SOX2*, particularly in H-/G- CMSCs which showed significantly increased *SOX2* expression than in H-/G- AMSCs, ESCs, and BM-MSCs (Figure 4-4C). Overall, H-/G- CMSCs and AMSCs showed higher level of *NANOG*, *SOX2*, and *OCT4* than BM-MSCs which may indicate a broader differentiation capacity.

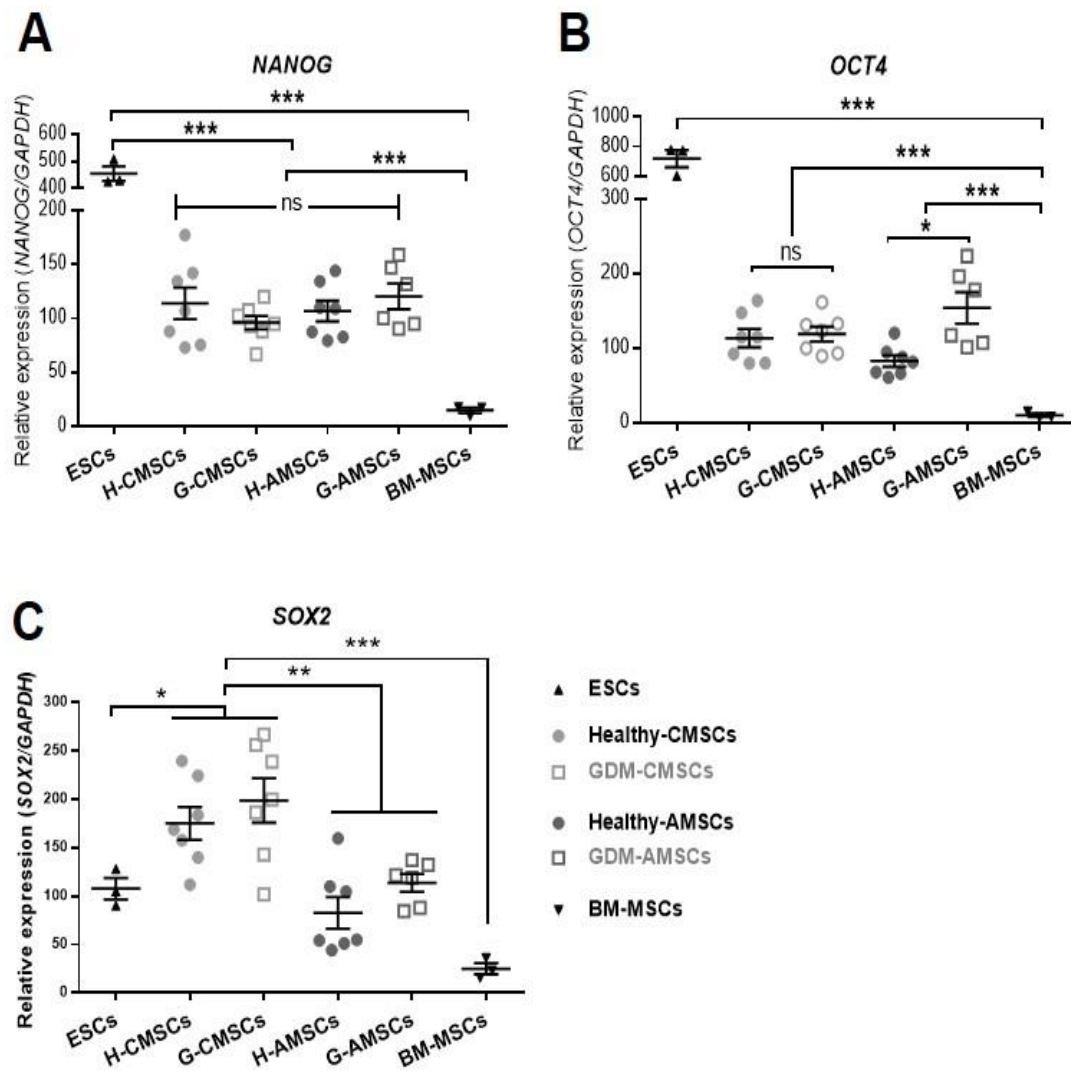


Figure 4-4. Pluripotent marker expression

Gene expression levels of pluripotent markers – *NANOG*, *OCT4*, and *SOX2* in H-/G- CMSCs and AMSCs compared with embryonic stem cell line (SHEF2) and BM-MSCs. Results represent mean \pm SEM. One-way ANOVA was conducted to determine the significant differences, * $p < 0.05$, ** $p < 0.01$, *** $p < 0.001$. ESCs, embryonic stem cells; BM-MSCs, bone marrow MSCs, *NANOG*, nanog Homeobox; *OCT4*, octamer-binding transcription factor 4; *SOX2*, SRY (sex determining region Y)-box 2.

4.4.2 High glucose effect on H-/G- AMSCs/CMSCs

Prolonged exposure of CMSCs/AMSCs to high glucose culture induces morphological changes, premature senescence , and decreased cell viability

As glucose concentration is crucial for β -cell growth, replication, and widely used in the IPC generation process, we investigated the effect of high glucose on H-/G- CMSCs/AMSCs as a first step in determining a suitable environment for IPC differentiation from placental MSCs. CMSCs and AMSCs were cultured in high glucose (HG) DMEM (25 mM) and low glucose (LG) DMEM (5.5 mM) media containing 10% FBS for a 30-day period. H-CMSCs cultured under HG conditions began to form condensations after day 20 where the number and dimension of cell condensations continued to increase until day 30. Similar, though less pronounced, changes were also observed in G-CMSCs under the same conditions whereas no apparently morphological change was observed after 10-day HG culture in either H-CMSCs or G-CMSCs (Figure 4-5).

H-/G- AMSCs demonstrated less obvious morphological changes in HG culture. Some small cell condensations were detected in H-AMSCs whereas no distinguishable difference in morphology of G-AMSCs was observed during the 30-day culture period in either HG or LG conditions (Figure 4-5).

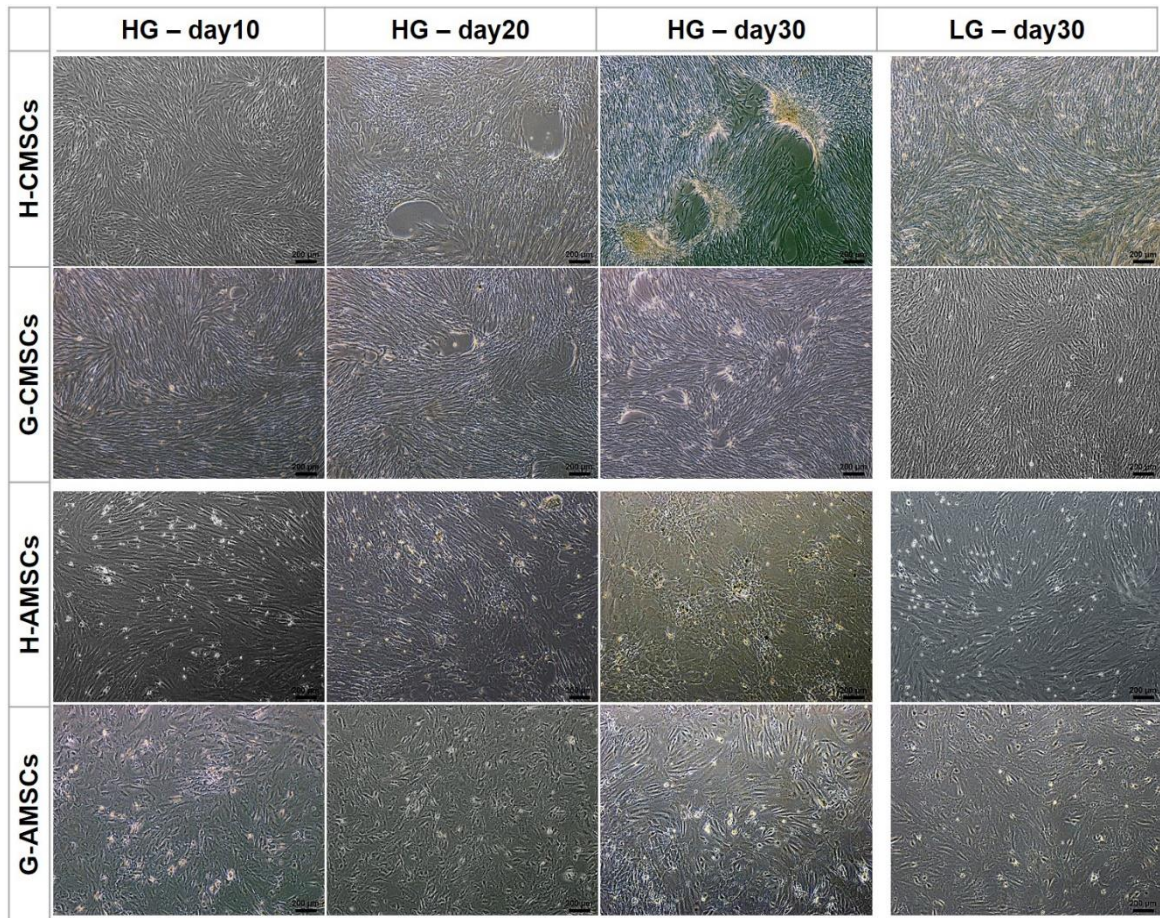


Figure 4-5. Morphological changes in HG culture

H-/G- CMSCs/AMSCs were cultured in 5.5 mM glucose DMEM until passage 2 and then exposed to 25 mM glucose (HG) DMEM to investigate the effect of glucose on morphological changes. Controls were maintained in 5.5 mM glucose (LG) DMEM. Phase contrast images of H-/G- CMSCs/AMSCs in HG culture over 10, 20, 30 days. H-/G- CMSCs/AMSCs in LG condition showed steady growth in the same time period and remained adherent fibroblast-like morphology. Representative image was from one of four independent experiments. Scale bar, 200 μ m; HG, high glucose; LG, low glucose.

In addition, live/dead fluorescence staining indicated that long-term HG exposure contributed to significantly reduced cell viability. Intracellular esterase activity discriminates live from dead cells by staining with calcein-AM (green) while ethidium homodimer-1 (red) indicates dead cells with loss of plasma membrane integrity. The reduced cell viability was observed in H-CMSCs and G-CMSCs under HG culture for 20 and 30 days. (Figure 4-6A). Viable H-CMSCs percentage declined from $97.7 \pm 2.1\%$ on day 20 to $90.6 \pm 3\%$ on 30 while viable G-CMSCs were also reduced with the percentage of $93.5 \pm 3.6\%$ and $87.8 \pm 2.5\%$ on day 20 and 30, respectively. There was no significant difference in decreasing rate of cell viability between H-CMSCs and G-CMSCs.

Likewise, H-AMSCs and G-AMSCs exposed to HG concentration resulted in lower viable cell numbers when compared with LG control (Figure 4-6B). Significant reductions in H-/G-AMSC viability was observed from day 20-30 with the percentage decreasing from 93.2-80.6% in H-AMSCs and 92.5-77.8% in G-AMSCs. The reduction was more marked in H-/G-AMSCs than CMSCs. Although HG culture contributed to significantly reduced cell viability, H-/G- CMSC and AMSC viability was maintained around 99-100% in 10-day HG culture.

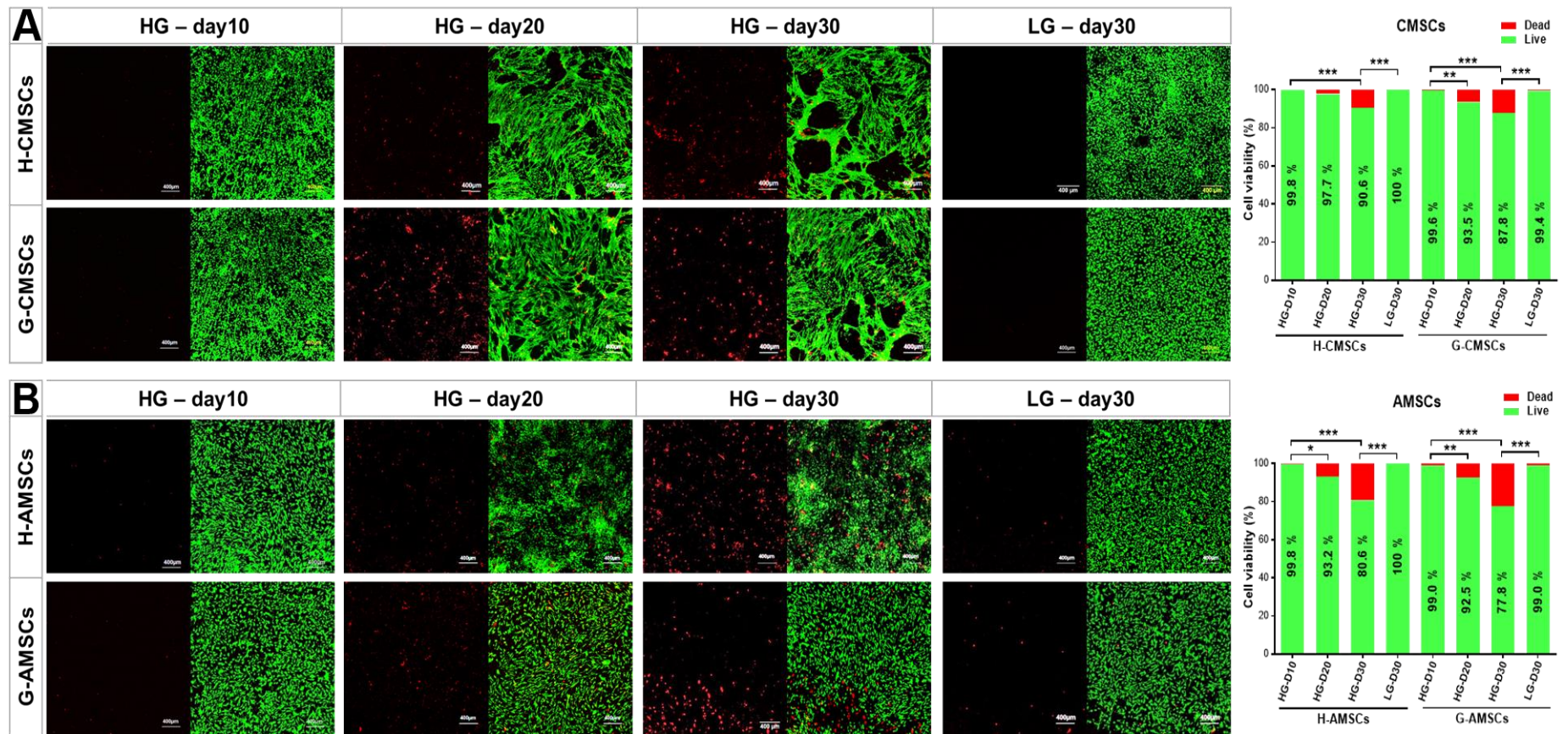


Figure 4-6. Decreased cell viability in HG culture

Left panel: Fluorescent images of the viable or dead H-/G- CMSCs/AMSCs using calcein-AM (green, alive cells) and ethidium homodimer-1 (red, dead cells) Scale bar, 400 μ m. Right panel: the mean percentage of live and dead cells calculated from 3 independent experiments.

Cellular senescence is considered as an irreversible cellular state of growth arrest. HG was noted to induce senescence in H-/G- CMSCs and AMSCs with increased incubation time. The staining of senescence-associated-beta-galactosidase (SA- β -Gal) activity is used to identify the occurrence of senescence³⁴⁵. Significantly elevated SA- β -Gal was first detected after 20 days of HG culture in G-CMSCs rising to approximately 30% of cells by day 30. On the other hand, significant elevation of SA- β -Gal was only seen at day 30 in H-CMSCs with around 15% of the population staining positively (Figure 4-7A and C). G-CMSCs showed an earlier and more profound HG-induced senescence response than H-CMSCs on both day-20 and day-30 HG culture.

H-AMSCs and G-AMSCs both displayed elevated SA- β -Gal from day 10 onwards with markedly elevated and significant increases seen thereafter (Figure 4-7B). A greater number of senescent cells were detected in G-AMSCs than in H-AMSCs from day 20 onwards reaching 75% by day 30 vs. 55% with H-AMSCs (Figure 4-7C).

Prolonged HG culture contributed to higher levels of SA- β -Gal staining in GDM- than Healthy- CMSCs/AMSCs. However, this did not occur in LG culture with SA- β -Gal activity in H-/G- CMSCs remaining unchanged during the culture period while an increase in SA- β -Gal activity was observed in H-/G- AMSCs on day 30 (Figure 4-7C).

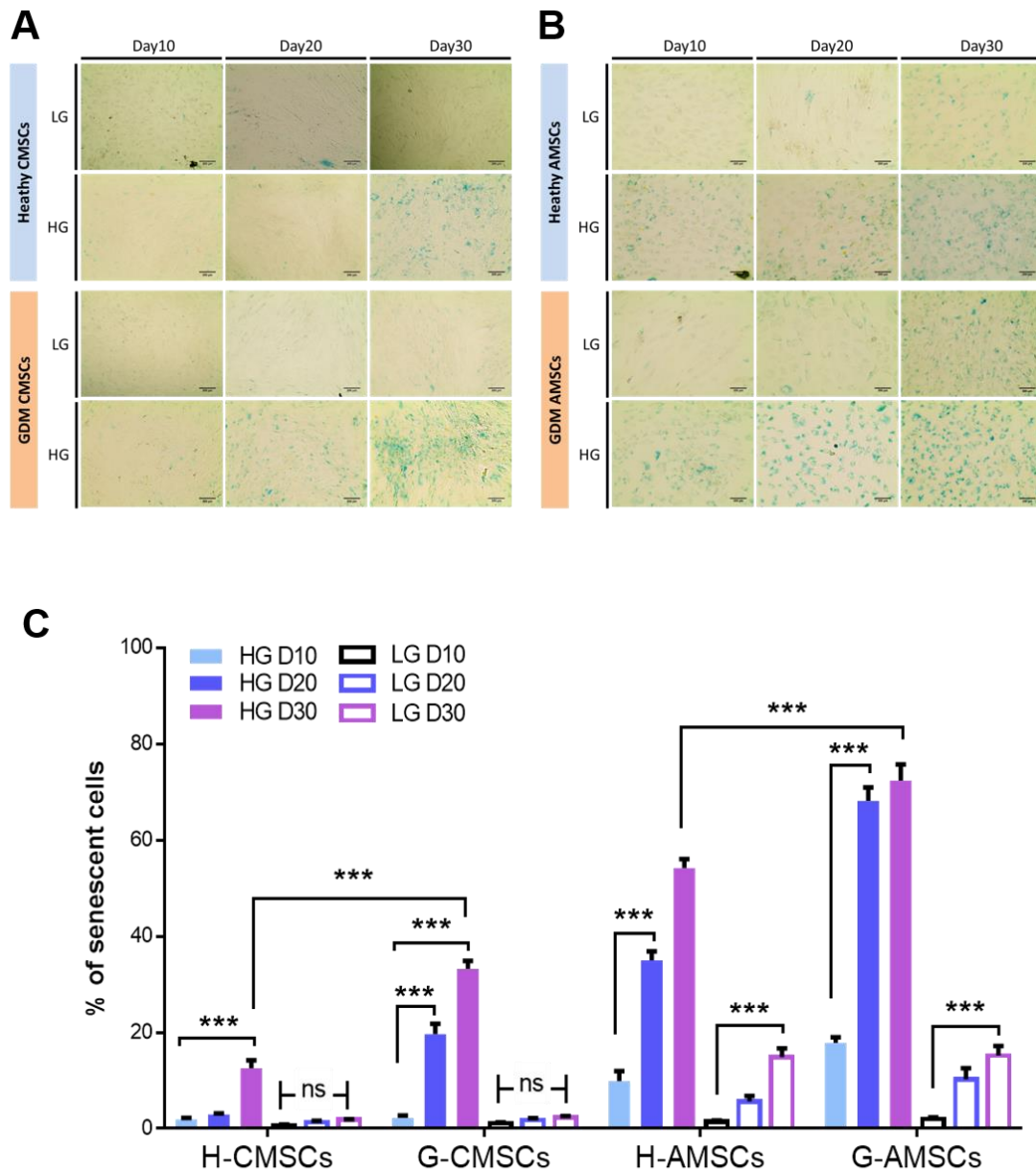


Figure 4-7. Cellular senescence in HG culture

(A and B) Representative images of cellular senescence was examined on day 10, 20, 30 in both HG and LG culture. Senescent cells showed positive staining of SA-β-Gal. Scale bar, 200μm. (C) Quantification of SA-β-Gal-positive cells. The SA-β-Gal-positive cells of 100 random cells was counted from at least three images of each sample (n=3) using phase-contrast microscopy. Data are expressed as mean ± SEM. Statistical significance were calculated by one-way ANOVA, *** $p < 0.001$

4.4.3 High glucose induces pancreatic lineage markers

MSCs exposed to HG condition has been suggested to induce endocrine lineage markers expression and promote β -cell differentiation³⁴⁶. Thus, the expression of pancreatic lineage genes (*NEUROG3*, *PDX1*, *INS*) under HG culture were examined by real-time PCR. The fold changes of genes were calculated by comparing with the expression level on day 0 and the significant upregulation was compared to LG-Day30.

When exposing H-/G- CMSC to HG condition for 10 days, there was an induction in *PDX1* (Figure 4-8A) and *NEUROG3* (Figure 4-8B) expression. *PDX1* expression in H-CMSCs was significantly elevated at day 10 and gradually increased until day 30. *NEUROG3* expression in H-CMSCs was also significantly elevated at day 10 and thereafter. G-CMSCs similarly displayed upregulated *PDX1* and *NEUROG3* expression at day 10 but which both then declined with continued culture. HG-cultured H-AMSCs and G-AMSCs had similar expression patterns of *NEUROG3* and *PDX1*. *PDX1* and *NEUROG3* in H-/G- AMSCs were both significantly increased after initial HG culture with both undergoing reductions across the remaining time course (Figure 4-8A and B). Moreover, mature β -cell marker, insulin (*INS*) expression was examined (Figure 4-8C). The expression of *INS* showed no increase in G-CMSCs and H-/G-AMSCs over the 30-day HG culture period; however, H-CMSCs had an approximately 5-fold increase in *INS* expression. Taken together this is suggestive that while HG culture was inductive for pancreatic lineage differentiation conversion of H-/G- CMSC and AMSCs into mature insulin producing cells (IPCs) required additional factors.

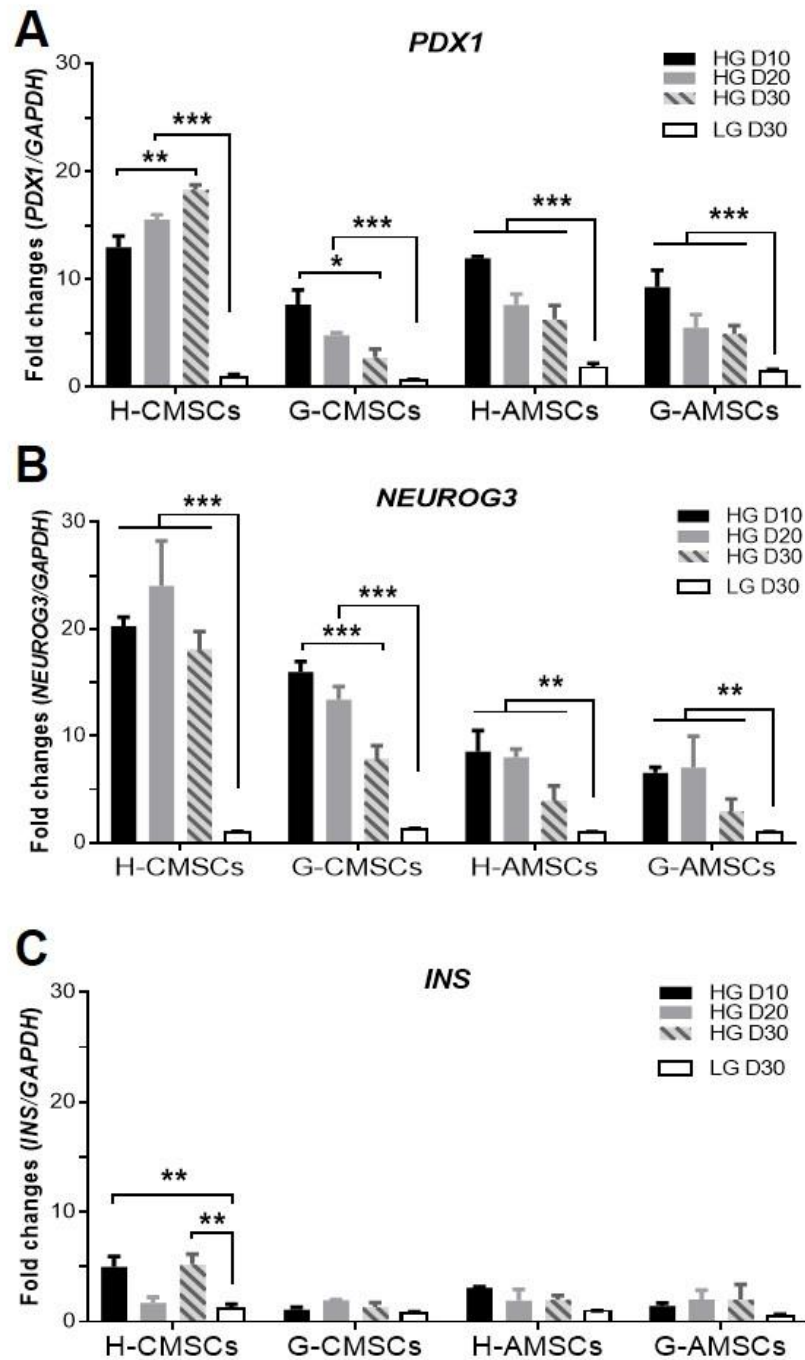


Figure 4-8. Pancreatic markers expression in HG culture

Gene expression (*NEUROG3*, *PDX1*, *INS*) was analysed by real-time PCR at day 10, 20, and 30 of HG culture. The expression was normalised to *GAPDH* and the fold change was calculated by comparing to the expression level on day 0. There was no change in *PDX1*, *NEUROG3*, and *INS* expression under LG culture in each group. Data are expressed as mean \pm SEM of 4 independent experiments. One-way ANOVA was used to determine statistical significance, * $p < 0.05$, ** $p < 0.01$, *** $p < 0.001$

4.4.4 Stepwise differentiation and IPC morphology

A three-stage differentiation protocol for reprogramming H-/G- CMSCs and AMSCs into IPCs after high glucose pre-culture

HG culture promoted formation of H-/G- CMSC condensations and while H-CMSCs displayed elevated pancreatic β -cell marker, G-CMSCs did not. Further, neither H-AMSCs nor G-AMSCs formed condensations or displayed upregulated β -cell markers. Long-term HG culture resulted in cell death and accelerated cellular senescence; however, the critical transcription factors for β -cell development were induced after 10-day HG culture. Therefore, we primed H-/G- CMSCs and AMSCs in 25mM glucose media for 10 days and sequentially stimulated cells with small molecules and growth factors to induce IPC maturation.

To induce definitive endoderm cell populations were then switched into a 17mM glucose DMEM/F12 containing bovine serum albumin (BSA), sodium butyrate, 2-mercaptoethanol base media for 3 days with Activin A³⁴⁷ followed by 3 days with Retinoic Acid³⁴⁸. The base media was used to protect against cellular stress induced by serum free media and promote chromatin rearrangements^{349, 350}. Next, cells were cultured for a further three days in DMEM/F12 supplemented with BSA, EGF and Taurine. EGF was used to enhance the growth of endocrine progenitor cells and Taurine, a beta-sulfonic acid, was known to induce insulin production and release at different concentrations in pancreatic beta cells *in vitro* culture³⁵¹ as well as type 1 diabetic and obese-induced diabetic mouse models³⁵². It has been suggested that using Taurine at low concentration promoted pancreatic specialisation in endocrine lineage cells^{317, 353, 354}. Thus, Taurine was used at 0.3 mM at stage II media and increased to 3 mM at stage III with the additional supplementation of GLP-1, nicotinamide, and NEAA to induce the maturation and proliferation of IPCs^{355, 356} (Figure 4-9A). GLP-1,

with many important physiological functions in fetal beta-cell development, insulin synthesis, and secretion³⁵⁷ has been widely used in IPC differentiation protocols, including embryonic stem cells³⁵⁸ and bone-marrow MSCs³⁵⁹ while the supplement of 10 mM nicotinamide was showed to increase the function of GLP1 in insulin production³⁵⁵.

H-CMSCs and G-CMSCs were seeded and grown in adherent monolayers for HG pre-treatment before stimulating with IPC differentiation media. After the exposure to stage 1 differentiation media, H-/G- CMSCs formed small condensations which seemed to loosen but yet to detach from the substrate. The subsequent incubation with stage 2 differentiation media promoted suspension cell clusters formation in both H-CMSCs and G-CMSCs. In stage 3 increased dimension and mass of spheroid clusters was accompanied by detachment from the substrate and continued culture as organoids. H-CMSCs and G-CMSCs had similar morphological changes at each stage of the differentiation process (Figure 4-9B).

In contrast, H-/G- AMSCs cultured under the same differentiation condition displayed evidence of condensation formation during stage 1 and 2 whereas the adherent condensations showed no sign of detaching. The increasing size of condensations was observed at subsequent differentiation stages, along with some single cells suspending in the media. Suspension cells were collected during media change and transferred to a new culture plate; however, these cells did not grow, form clusters, or re-attach to culture plate. The suspension H-/G- AMSCs observed during IPC differentiation from were removed with differentiation media change. At the end of 3-stage differentiation process, H-/G- AMSCs still remained adherent without any detached spheroid formation (Figure 4-9B).

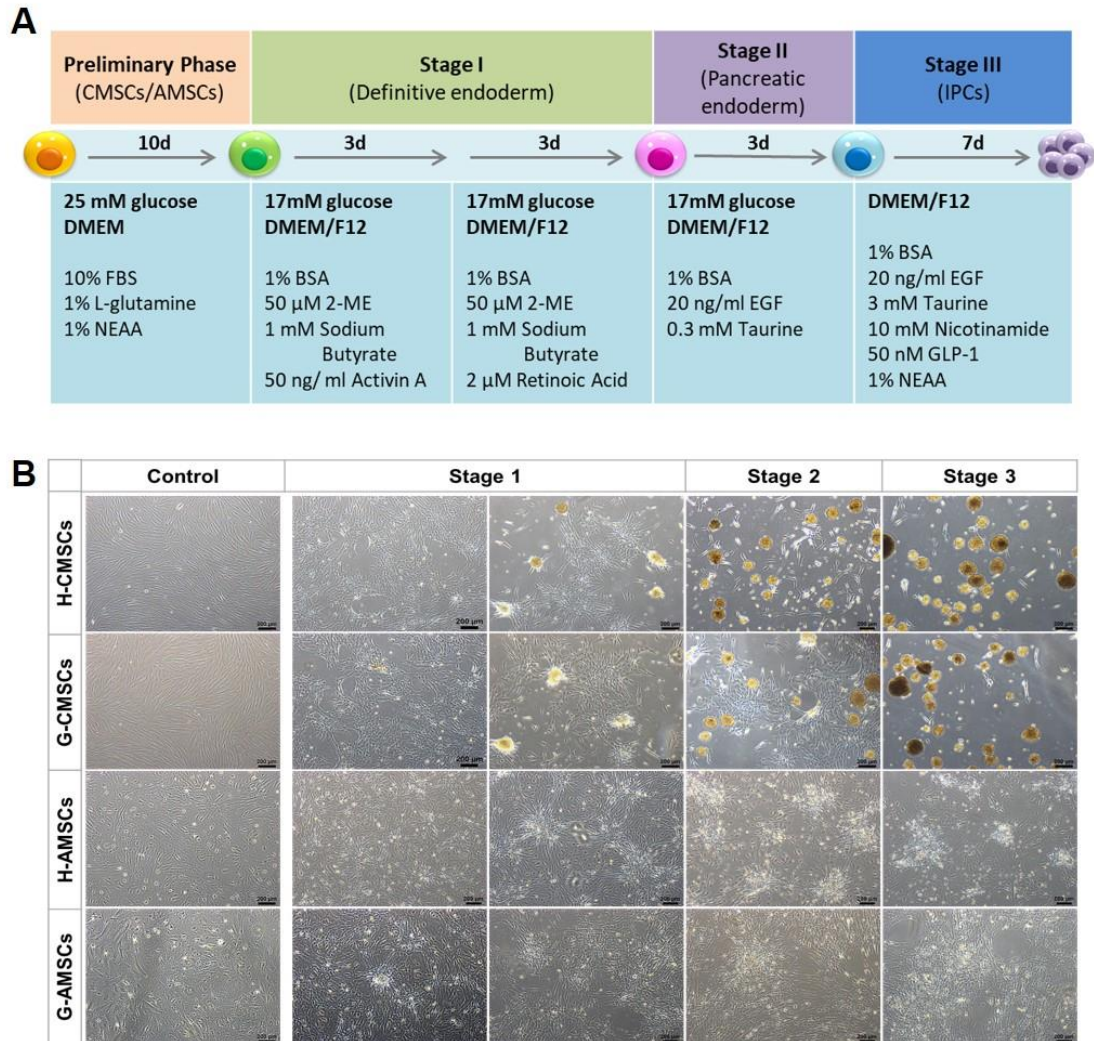


Figure 4-9. Optimised IPC differentiation approach and IPC morphology

(A) Differentiation scheme for IPC generation illustrates the growth factors, small molecules, and incubation time at each stage. BSA, bovine serum albumin; 2-ME, 2-mercaptoethanol; EGF, epidermal growth factor; GLP-1, glucagonlike peptide-1; NEAA, non-essential amino acids; IPC, insulin-producing cell. (B) Morphological changes during IPC differentiation. Control images were undifferentiated H-/G- CMSCs/AMSCs cultured in complete growth media (5.5 mM glucose DMEM containing 10% FBS) which remained fibroblast-like morphology. The image was a representative image of six independent experiments (scale bar, 200 μ m).

4.4.5 Expression of pancreatic markers expression

H-/G- CMSC-IPCs exhibited high level of pancreatic lineage markers whilst the lack of mature beta-cell markers in H-/G-AMSC-IPCs was improved by betacellulin

To determine whether H-/G- CMSCs/AMSCs were programmed into endocrine hormone-producing cells, pancreatic lineage marker expression was examined by real-time PCR. The differentiated H-/G- CMSCs and AMSCs showed evidence of IPC differentiation by the expression of endocrine progenitor markers (*NEUROG3*, *ILS1*) and pancreatic lineage transcription factors (*PDX1*, *PAX6*). Gene expression was examined at the end of 3-stage differentiation process and the increased fold changes of each gene were calculated by comparing to undifferentiated H-/G- CMSCs/AMSCs.

NEUROG3 and *ILS1*, promoting endocrine lineage differentiation, expression was noted in H-/G-CMSC-IPCs and showed comparably upregulated levels in both healthy and GDM group with approximately 13-fold increase in *NEUROG3* and 10-fold in *ILS1*. The upregulation of *NEUROG3* and *ILS1* displayed significantly enhanced levels in H-/G-AMSC-IPCs vs. H-/G-CMSC-IPCs. H-AMSC-IPCs and G-AMSC-IPCs both showed an 18-20-fold increase in *NEUROG3* and *ILS1* expression (Figure 4-10A).

Pancreatic lineage differentiation and β -cell development transcriptional markers, *PAX6* and *PDX1*, were also significantly induced in differentiated groups. H-CMSC-IPCs expressed higher level of *PAX6* induction than G-CMSC-IPCs while the expression of *PAX6* in H-AMSC-IPCs and G-AMSC-IPCs were comparable. Notably, there was a significantly increased expression of *PDX1* in H-/G-AMSC-IPCs compared with H-/G-CMSC-IPCs (Figure 4-10B).

The induction of endocrine progenitor and pancreatic lineage markers was previously

shown to be enhanced in 10-day HG culture without further stimulation by any compounds. The 3-stage differentiation protocol did not enhance the induction of these markers in H-/G- CMSCs but had a significant effect on promoting H-/G- AMSCs pancreatic markers expression. However, the 3-stage differentiation protocol was intended to promote the maturation of IPCs that failed to achieve in HG culture.

Mature β -cell markers, *INS* and *GLUT2* were examined by real-time PCR. Significantly elevated expression of *INS* and *GLUT2* were observed in H-/G- CMSC-IPCs (vs. H-/G- AMSC-IPCs) with approximately 30-fold and 10-15-fold induction, respectively. On the other hand, H-/G-AMSC-IPCs expressed significantly lower levels of mature β -cell marker expression. The expression of both *INS* and *GLUT2* displayed no significant changes vs. undifferentiated H-/G- AMSCs (Figure 4-10C).

Direct comparison of IPCs generated from GDM- and Healthy- CMSCs established that, with the exception of *PAX6* which was lower in G-CMSC-IPCs, both expressed comparable level of progenitor and, pancreatic transcription factors, and mature β -cell genes. Given the level of endocrine progenitor markers expression (*NEUROG3*, *ISL1*, and *PDX1*) and β -cell markers (*INS* and *GLUT2*) in H-/G- AMSC-IPCs vs. CMSC-IPCs it remains possible that the IPCs derived from H-/G- AMSCs may reflect an immature β -cell state.

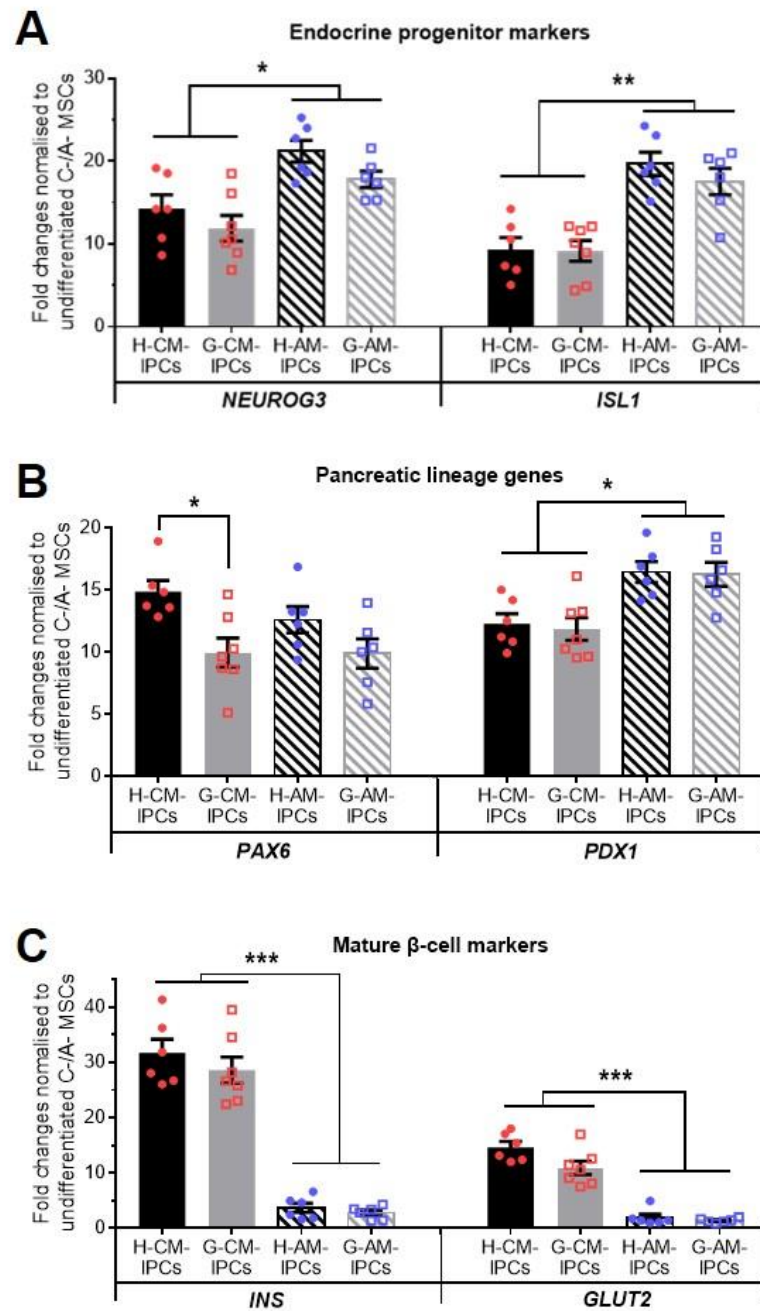


Figure 4-10. Induction of pancreatic markers by IPC differentiation protocol

Gene expression was analysed by real-time PCR. The relative expression level of (A) endocrine progenitor markers, *NEUROG3* and *ISL1* (B) pancreatic lineage transcription factors, *PDX1* and *PAX6* (E) mature β -cell makers – *INS* and *GLUT2*, were normalised to *GAPDH* and compared with undifferentiated CMSCs/AMSCs. Data are expressed as mean \pm SEM of 6 independent experiments. One-way ANOVA was used to determine statistical significance, * p < 0.05, ** p < 0.01, *** p < 0.001.

The basal induction of mature β -cell marker expression in H-/G- AMSC-IPCs was inconsistent with endocrine and pancreatic lineage gene expression. To explore induction further we explored additional supplementation with three molecules to improve their maturation; GLP-1, Exendin-4, and Betacellulin. GLP-1 was incorporated at Stage III of our original protocol (at the concentration of 50 nM) to promote IPC maturation Both exendin-4, a synthetic stable GLP-1 analogue, and betacellulin, a member of the epidermal growth factor family, have been demonstrated to improve β -cell maturation, proliferation and increase insulin content^{360, 361}. Dosage used in the screening was based on literature finding.

Figure 4-11 showed the result of *INS* and *GLUT2* expression in H-/G- AMSC-IPCs when replacing GLP-1 with exendin-4 or betacellulin at stage 3. GLP-1 induced *INS* expression with an approximately 5-fold increase in H-/G- AMSC-IPCs compared to undifferentiated AMSCs while the induction showed no dose-dependent effect on *INS* expression levels. There was no significant induction of *GLUT2* expression under either 50 nM or 100 nM GLP-1 supplementation.

Exendin-4 at the concentration of 10 nM was reported to induce insulin expression in umbilical cord MSCs³⁶². We showed that the induction of *INS* expression showed a 5-fold increase in H-/G- AMSC-IPCs vs. undifferentiated AMSCs at 10 nM exendin-4 supplementation while there was no dose-dependent effect with higher exendin-4 concentration. Exendin-4 at 10 nM induced *GLUT2* expression in H-AMSC-IPCs but no effect on *GLUT2* expression in G-AMSC-IPCs.

Betacellulin was used in many IPCs differentiation protocols, including bone-marrow MSCs, embryonic stem cells, and umbilical cord MSCs at various concentrations³⁶³⁻³⁶⁷. Whilst 1 nM betacellulin was the most common concentration used in literature, we investigated the effect of betacellulin at the concentration of 1 and 2 nM on H-/G-AMSC-IPCs maturation.

The expression of *INS* and *GLUT2* was significantly improved by 1 nM betacellulin and with higher concentration of betacellulin (2 nM), further enhanced expression of *INS* was observed in H-/G-AMSC-IPCs. H-/G-AMSCs were found to be more responsive to betacellulin stimulation for β -cell maturation than GLP-1 or exendine-4.

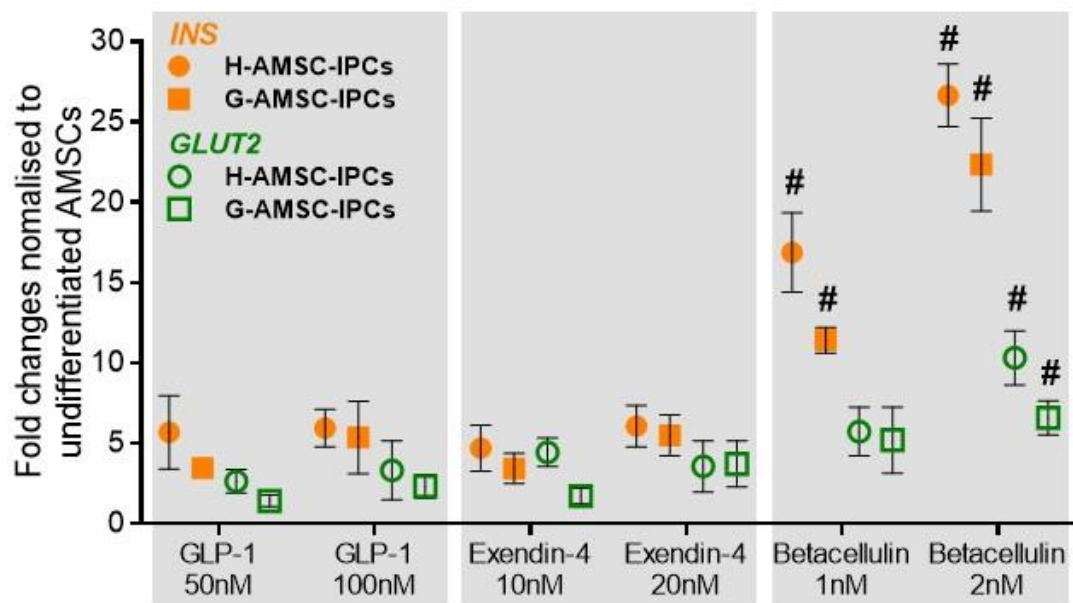


Figure 4-11. Improving AMSC-IPC maturation by betacellulin

The improvement of *INS* and *GLUT2* expression in H-/G-AMSC-IPCs by GLP1, exendin-4, or betacellulin supplementation. The gene expression was normalised to *GAPDH* and y-axis shows the fold increase by comparing with undifferentiated H-/G-CMSCs/AMSCs. Data represent mean \pm SEM. One-way ANOVA was used for statistical significance, # $p < 0.001$ indicates significantly increased gene expression under betacellulin compared with GLP-1 or Exendin-4 supplementation.

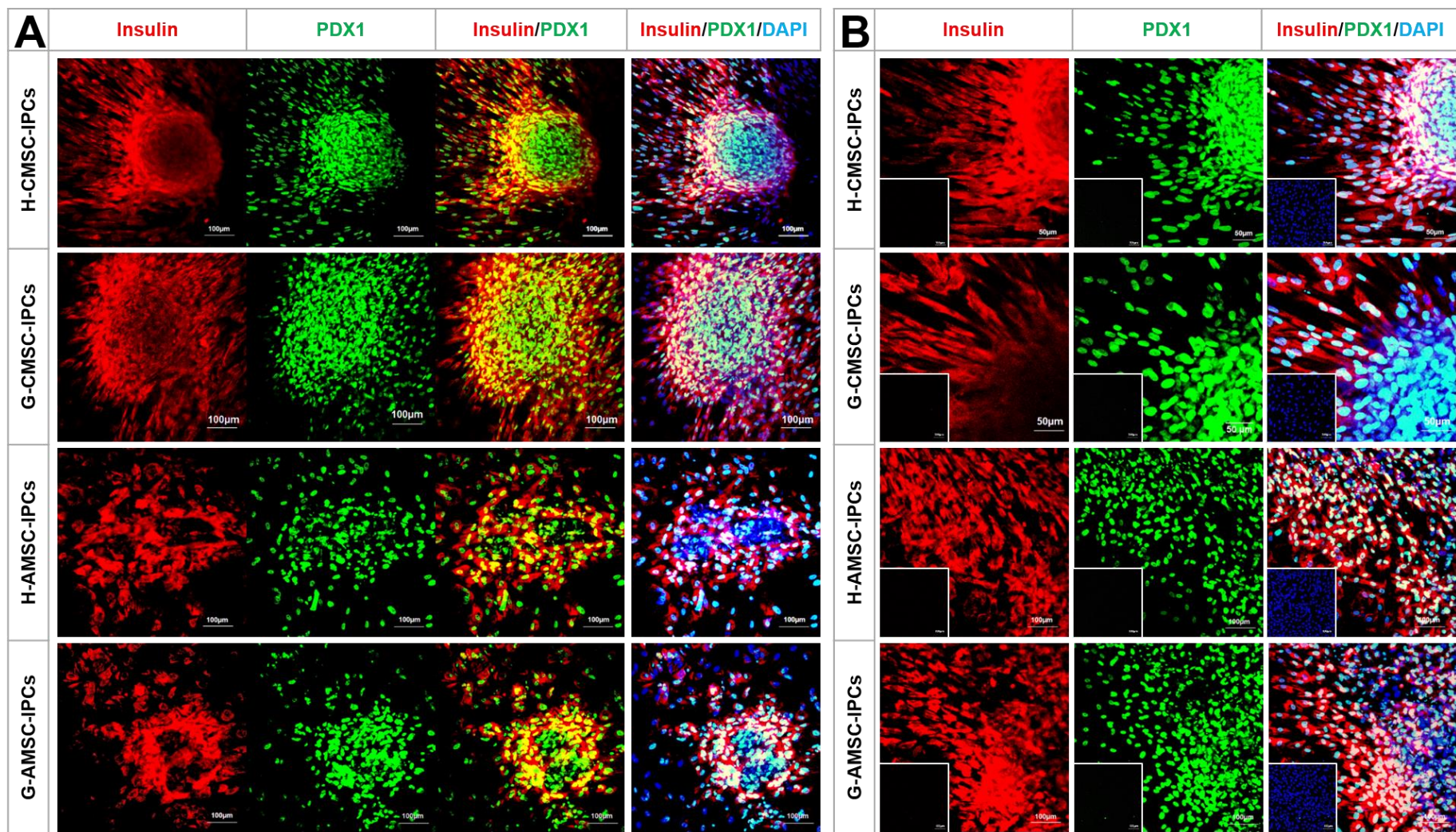
4.4.6 Immunofluorescence staining and ELISA

Comparable insulin protein expression in H-/G- CMSC-IPCs and AMSC-IPCs but insufficient insulin secretion function in AMSC-IPCs

Immunofluorescence staining was used to verify protein expression of β -cell markers but is not a precise measurement of protein expression levels due to variations from staining and imaging procedures depending on morphological differences. H-/G- CMSCs were differentiated to IPCs using original protocols with the stimulation of GLP-1 at stage 3 while H-/G- AMSCs was induced to IPCs via optimised protocol where GLP-1 was replaced with betacellulin at the last differentiation stage. Cells were fixed on the last day of differentiation and stained for insulin (red) and transcription factor PDX1 (green) expression (Figure 4-12).

Immunofluorescence labelling indicated that Insulin was co-expressed with transcription factor PDX1 in both Healthy- and GDM- CMSC-IPC spheroids. On the other hand, suspension spheroid cultures were not observed with H-/G- AMSC-IPCs with little progression beyond cell condensations at the end of differentiation process. However, irrespective of above co-expression of insulin and PDX1 was noted in H-/G- AMSC-IPCs (Figure 4-12).

The result confirmed the mature IPC differentiation and suggested that the upregulated pancreatic lineage genes were also expressed on protein levels in differentiated groups (H-/G- CMSC-/AMSC- IPCs) compared to undifferentiated H-/G- CMSCs/AMSCs.



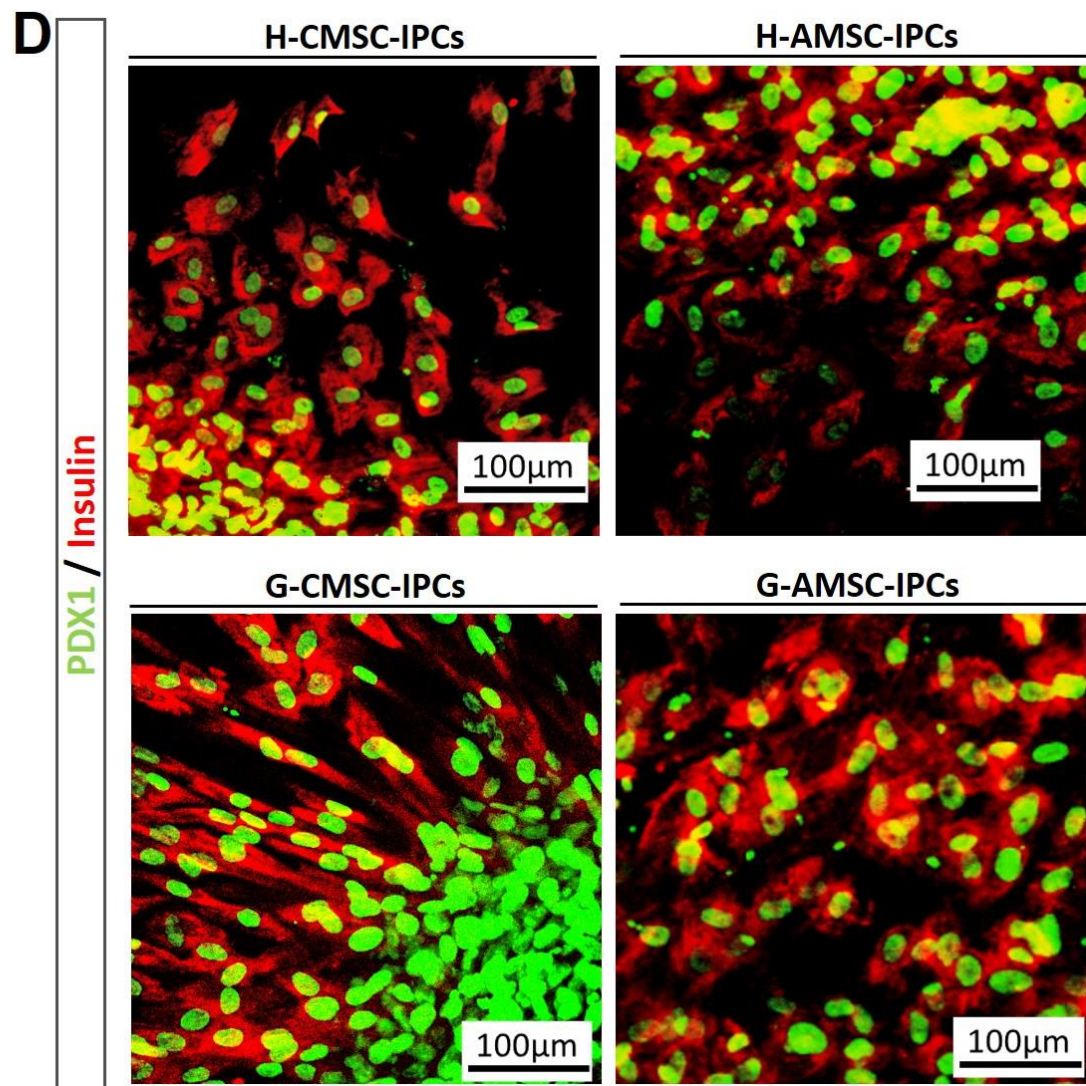
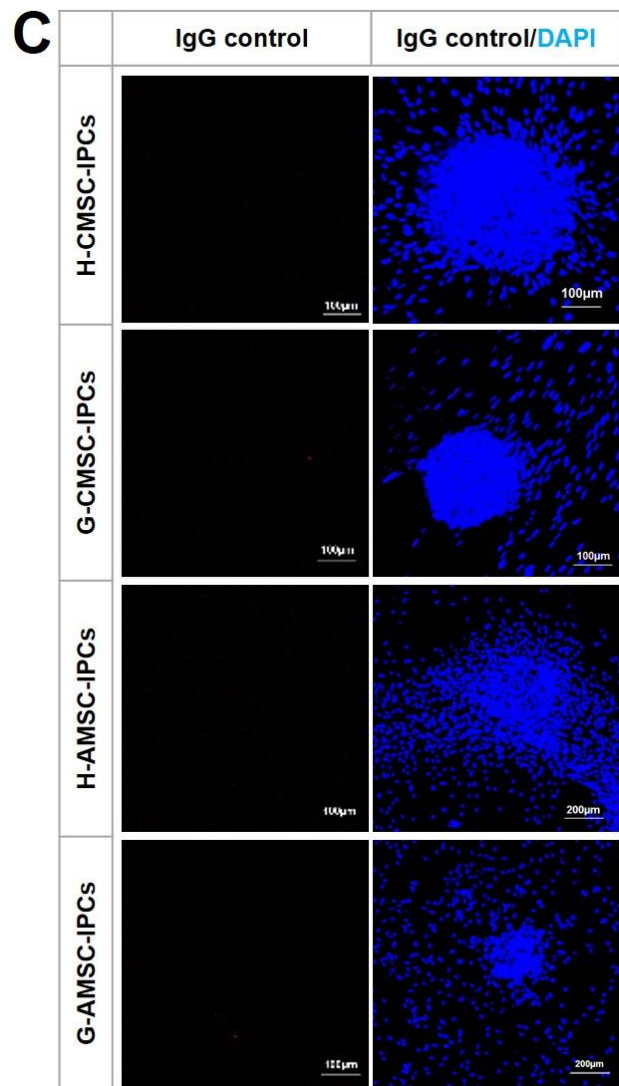


Figure 4-12. Confocal images of insulin and PDX1 expression

(A) Fluorescence microscopic imaging of immunostaining for insulin and PDX1. After 3-stage IPC differentiation, cells were stained with antibodies against insulin (red) and PDX1 (green), followed by appropriate secondary antibodies conjugated. Merged images show localisation of insulin and PDX1 co-expression in H-/G- CMSC/AMSC IPCs. DAPI was used as nuclear counterstain in blue. (scale bar, 100 μ m) (B) 20x magnification images and undifferentiated H-/G- CMSCs and ASMCs staining image of insulin and PDX-1 expression showed at the bottom left corner. (scale bar, 50 μ m) (C) secondary antibody IgG control (D) 40x magnification images of insulin and PDX1 localisation

Functional β -cells are characterised by the ability to secrete adequate amounts of insulin in response to a glucose challenge. To establish functionality of IPC, we performed ELISA assays to investigate the secretion of insulin and C-peptide following glucose challenge (Figure 4-13). C-peptide is a by-product from the maturation process of insulin which is stored and released in equimolar quantities with insulin granules. H-/G- CMSC-IPCs and AMSC-IPCs were incubated in glucose free media for 2 hours prior to sequentially challenging with low glucose (5.5mM) for 1 hour and high glucose (25mM) for 2 hours, followed by measurement of insulin release into supernatants. The phosphodiesterase inhibitor, 3-isobutyl-1-methylxanthine (IBMX) known to induce insulin secretion³⁶⁸ was supplemented at the concentration of 0.5 mM to 5.5 mM and 25 mM glucose media.

Undifferentiated H-/G- CMSCs and AMSCs released low or undetectable basal level of insulin and C-peptide into the media. H-CMSC-IPCs and G-CMSC-IPCs secreted insulin to low glucose challenge and released an increased amount of insulin in response to glucose content changes (Figure 4-13A). Likewise, a similar result was demonstrated in C-peptide release, where the increased C-peptide production was observed from low to high glucose challenge (Figure 4-13B). The insulin and C-peptide release levels showed no statistical

differences between H-CMSC-IPCs and G-CMSC-IPCs.

In contrast, IPCs derived from H-/G- AMSCs released insulin and C-peptide in response to low glucose challenge but failed to produce increased amount of insulin at high glucose stimulation. Similar levels of insulin release in H-/G- CMSC-IPCs and AMSC-IPCs were noted when challenging with 5.5 mM glucose concentration. However, when increasing the glucose to 25 mM, around 50% of H-AMSC donor samples displayed evidence of glucose sensitivity while G-AMSC-IPCs failed to consistently produce insulin responsive to glucose concentration changes (Figure 4-13A). The C-peptide expression was consistent with insulin release in H-/G-AMSC-IPCs (Figure 4-13B).

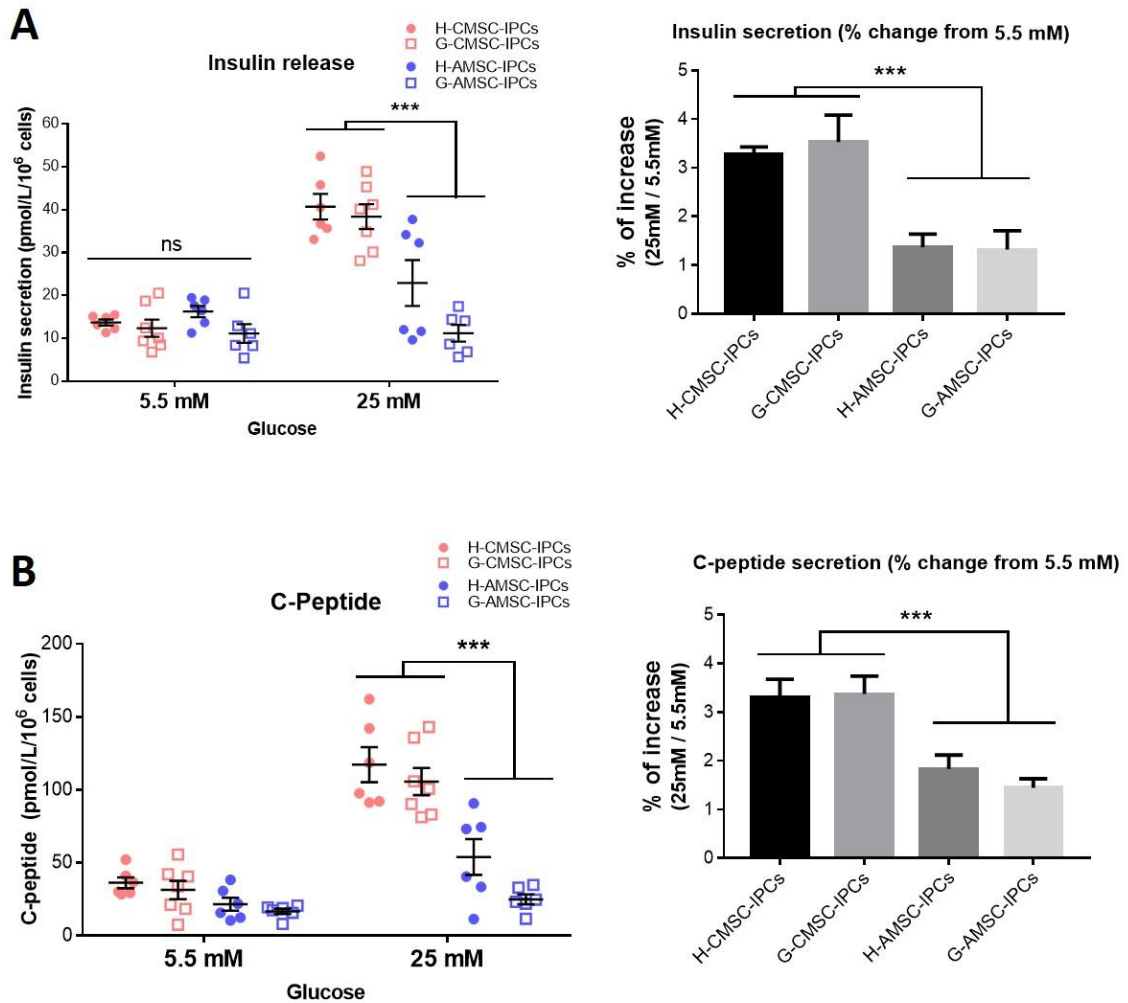


Figure 4-13. Insulin and C-peptide ELISA

Functional IPCs were accessed by insulin releasing capacity upon glucose challenge. IPCs were subsequently incubated with 5.5 mM glucose DMEM containing 0.5 mM IBMX for 1 hour and switched to 25 mM glucose DMEM containing 0.5 mM IBMX for 2 hours. The supernatant was collected and measured for (A) insulin and (B) C-peptide release by ELISA. Left panels show the secretion level measured by ELISA and right panels show the percentage of increased insulin/C-peptide secretion in 25 mM glucose vs. 5.5 mM glucose. Data were normalised to undifferentiated H-/G- CMSCs/AMSCs and expressed as mean \pm SEM. Each data point was conducted in duplicates. One-way ANOVA was used for statistical significance, *** $p < 0.001$.

Finally, we examined the intracellular insulin protein content to further understand whether the poor response to glucose stimulation in H-/G- AMSC-IPCs was caused by low insulin synthesis during differentiation. H-/G- CMSC-IPCs and AMSC-IPCs were lysed and insulin content was measure by ELISA normalising to total protein content within the cells. Significantly increased insulin content was observed in IPC groups compared to undifferentiated H-/G- CMSCs/MASCs. Surprisingly, no significant difference in intracellular insulin level was observed across all IPCs suggesting a broad comparability in insulin synthesis ability (Figure 4-14). The insufficient insulin secretion from H-/G- AMSC-IPCs might due to impaired glucose uptake or inadequate insulin exocytosis rather than insulin synthesis.

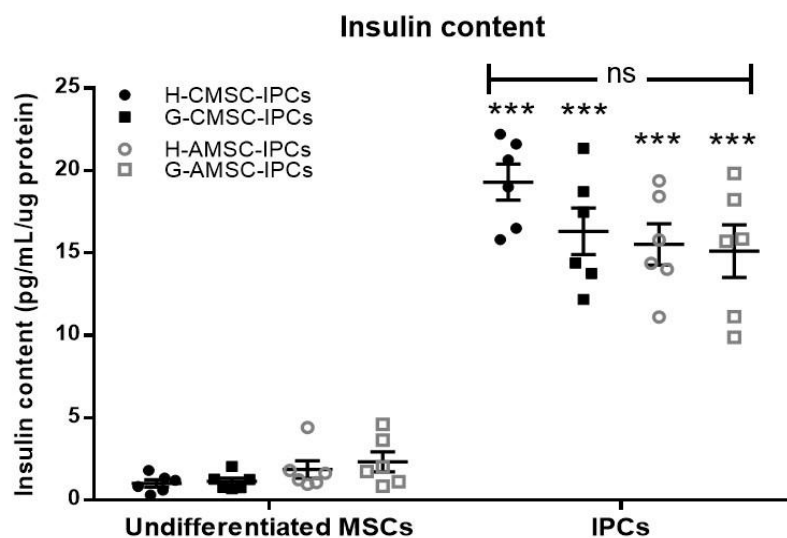


Figure 4-14. ELISA of intracellular insulin

Insulin content in H-/G- CMSC-/AMSCs- IPCs were measured by ELISA after incubating with 25 mM glucose challenge. The expression levels were normalised to total protein content. Each data point was conducted in duplicates. One-way ANOVA was used for statistical significance, *** $p < 0.001$ indicates significant difference compared to undifferentiated MSCs; ns, no significant difference between each group.

4.5 Discussion

Embryonic stem cells normally express high levels of *NANOG*, *SOX2*, and *OCT4*. We demonstrated that H-/G- CMSCs and AMSCs showed either higher or comparable levels of *SOX2* expression than embryonic stem cells although the high expression levels were not found in *NANOG* and *OCT4*. Notably, H-/G- CMSCs/AMSCs showed significantly increased expression of *NANOG*, *SOX2*, and *OCT4* than bone marrow MSCs. Neonatal tissue-derived MSCs have been reported to express higher levels of stemness markers than bone marrow MSCs in some studies. For instance, amniotic epithelial cells and mesenchymal cells showed more *OCT3/4*, *NANOG*, and *KLF4* expression than bone marrow MSCs²⁷². Chorion stem cells were highly positive for OCT-4, *NANOG*, SSEA-3, and TRA-1–60 expression³⁶⁹. Our results show that AMSCs and CMSCs from both healthy and GDM women have higher levels of stemness markers than bone-marrow MSCs.

Glucose effect on pancreatic development

Adult β -cells are mostly quiescent with only a small proportion having the ability to proliferate in response to hyperglycaemia³⁷⁰. Owing to the limited regenerative capacity of endogenous β -cells, researchers have been looking for alternative approaches to restore or promote β -cell function for diabetes patients. Generation of functionally mature β -cell from MSCs is one of the attractive alternative for β -cell replacement therapies. Various extrinsic factors have been used to mimic the environment in order to facilitate β -cell differentiation.

Glucose is a critical factor for pancreatic islet development *in vitro* and *in vivo*³⁷¹. During pregnancy, maternal glucose levels raise to allow fetus to have sufficient nutrients for development in the late second to third trimester, which is also the crucial period for pancreatic islet development while the remodelling and maturation of fetal pancreas

continues until early childhood³⁷². In *in vivo* animal studies, elevated maternal glucose levels contributed to increased fetal pancreatic insulin content, promoted β -cell proliferation, and enhanced insulin secretion in response to glucose^{373, 374}. The influential role of glucose in β -cell development, survival and insulin biosynthesis and secretion has also been evidenced in many studies^{375, 376}. Therefore, glucose is considered as an inducer for β -cell differentiation and commonly used in IPC generation protocols³⁷⁷.

Although glucose availability regulates fetal islet development, it is known that abnormal maternal hyperglycaemia may lead to adverse effects and cause β -cell exhaustion³⁷⁸. Given that GDM-MSCs were under prolonged exposure to hyperglycaemia during pregnancy, to know whether glucose is a suitable factor for IPC generation from GDM-MSCs, we exposed H-/G- CMSC/AMSCs to HG culture for a 30-day period. Reports have indicated that with a glucose concentration at 20-30, β -cell replication was significantly enhanced³⁷⁹. The starvation of bone-marrow MSCs in serum-free LG media prior to 7 days 25 mM glucose (high glucose) culture resulted in the formation of small spheroid clusters and upregulated expression of GLUT2, glucagon, and insulin³⁸⁰. We did not observe 7-day HG culture-induced spheroid cluster formation with either H-/G- CMSCs or AMSCs. The obvious cell condensations formed around 20-day of HG culture in H-/G- CMSCs while the morphological changes were not profound in H-/G- AMSCs. However, we did note upregulated pancreatic transcription factor expression following on from short-term HG exposure. The increased expression of *PDX1* and *NEUROG3* in HG-cultured H-/G- CMSCs/AMSCs indicated the formation of endocrine progenitor cells while the lack of *INS* expression suggested that those progenitor cells failed to differentiate into mature endocrine cells. *PDX1* and *NEUROG3* were reported to be essential factors for beta-cell development, where the expression of *PDX1* remained high over the entire pancreatic islets development period and also in mature beta-cells³⁸¹ whereas *NEUROG3* was induced

during endocrine progenitor cells formation and the expression slightly reduced in mature beta-cells³⁸². Although we detected the increase in *PDX1* and *NEUROG3*, little or no increase in *INS* expression was observed across all populations under HG culture indicating failure to mature under HG culture alone even though HG concentration induced *INS* expression was shown in some studies^{380, 383, 384}.

In addition, long-term HG culture led to cell death in both Healthy- and GDM-CMSCs/AMSCs. HG is associated with reactive oxygen species production and induced cell apoptosis³⁸⁵. In BM-MSCs, HG was found to affect cell proliferation, mitochondrial function, and result in apoptosis³⁸⁶. Direct comparison of our findings to other studies is not possible though noteworthy comparisons are provided via elevated caspase-3 and caspase-8 pro-apoptotic activity in adipose-derived MSCs from type 2 diabetes patients³⁸⁷.

Cellular senescence is a state of growth arrest and an inability to proliferate which is generally present in primary MSCs culture, especially at late passage³⁸⁸. We found that prolonged HG exposure accelerated cellular senescence in both H-/G- CMSCs and AMSCs, but showed its greater effect on GDM samples than Healthy counterparts. Glucose at the concentration of 25 mM promoted BM-MSCs premature senescence through the expression of p16 and p21 over 28 days culture³⁸⁹. In many IPC differentiation studies, MSCs were under a long period of HG culture from a couple of weeks to four months^{346, 390, 391}. Although some research showed positive results of IPC generation through HG culture, we pointed out the adverse effect of long-term HG culture, including increased cell death and cellular senescence which might affect the differentiation capacity for IPC generation. High glucose environment leading to cell senescence and impaired beta-cell survival was reported in many *in vivo* studies. In high-fat diet-induced diabetic mice, hyperglycaemia resulted in beta-cell senescence with reduced beta-cell mass and insufficient insulin

release³⁹². The glycaemic level changes in obesity mice were associated with beta-cell death and dedifferentiation, leading to loss of functional beta-cell population³⁹³. Glucose is an important factor for pancreatic beta-cell development but long-term exposure may cause adverse effects.

Optimised IPC generation approach

Short-term HG culture provided a balance point with low levels of cell death, senescence, and elevated β cell-linked transcripts for priming of placental membrane MSCs followed by incubation and induction of mature IPC differentiation following our three-stage differentiation process.

Our three-stage protocol was modified from previously published protocol by Chandra *et al.*³⁵³ who generated IPCs from adipose derived-MSCs. The protocol has also been applied to umbilical cord-derived MSCs by Wang *et al.*³⁹⁴. However, several steps were modified in our study. Firstly, the ITS (insulin-transferrin-selenium) used in Chandra's differentiation media was withdrawn in our protocol. ITS is commonly used in serum free media to maintain cell growth whereas BSA and 2-mercaptoethanol were sufficient to support most of CMSC/AMSCs survival in serum free media. The insulin contained in ITS may enhance the chance of taking up insulin from differentiation media instead of insulin synthesis in IPCs. Secondly, after stimulating with activin A, an inducer for definitive endoderm formation³²¹ at the stage 1, the additional 2-day retinoic acid (RA) stimulation combined with activin A improved morphological changes towards condensations and spheroid cluster formation at later stages (Figure 4-9B). RA signalling is essential for pancreatic development that induces the generation of endocrine progenitors and functions as an effective inducer for pancreatic transcription factor *PDX1* expression while the disruption of RA signalling leads to pancreatic agenesis^{361, 395, 396}. Thirdly, Chandra's protocol established a 10-day maturation

protocol for IPC generation; however, it was not reproducible with H-/G- CMSCs or AMSCs. A longer incubation time was required especially for the last maturation stage, as well as the additional supplementation with EGF and nicotinamide to enhance the growth and maturation of IPCs^{397, 398}.

In the present three-stage IPC differentiation approach, among all various factors GLP-1 plays a crucial role in promoting the maturation of IPC. GLP-1 has important physiological functions in fetal β -cell development, insulin synthesis, and secretion^{399, 400}; therefore GLP-1 has been widely used at the last differentiation stage in many IPC differentiation protocols. H-/G-CMSCs displayed good responsiveness to our IPC induction protocol with enhanced mature beta-cell marker expression and the ability to secrete insulin. However, in immunostaining, we found that some cell populations showed PDX-1 positive but not insulin. These cell populations may be at immature differentiation stage or other endocrine cell types. PDX1-expressing progenitor cells give rise to β -cell and also α -cells and δ -cells that secrete glucagon and somatostatin, respectively⁴⁰¹. It is likely that the cell clusters formed in H-/G-CMSC-IPCs may contained different endocrine cell types.

Given the low expression of mature beta-cell markers in H-/G-AMSCs, we further optimised our protocol for promoting AMSC-IPCs maturation. We explored the supplementation with either exendin-4 or betacellulin as a substitute for GLP-1 in the last IPC maturation stage. Exendin-4 is a GLP-1 agonist which improves glucose tolerance in diabetes patients via enhanced insulin secretion^{402, 403}. A previous report has indicated that exendin-4 supplementation promoted β -cell gene transcription in mouse embryonic stem cell-derived IPCs⁴⁰⁴. In this instance we saw no significant, or dose-dependent, induction of either *INS* or *GLUT2* transcription in H/G-AMSC-IPCs following exendin-4 supplementation.

In contrast, we noted significant increases in both *INS* and *GLUT2* in H-/G- AMSCs following

betacellulin supplementation. Betacellulin is an epidermal growth factor (EGF) family member with demonstrable regulation of pancreatic regeneration through activation of EGF receptors (EGFR), ErbB1 and ErbB2⁴⁰⁵. Further, in β -cell development from human embryonic stem cells the addition of betacellulin sustained *PDX1* expression and improved the differentiation process⁴⁰⁶. In present study, H-/G-AMSCs were more responsive to betacellulin than GLP-1 or exendin-4. GLP-1 and exendin-4 interact with the high affinity receptor, GLP-1R, while GLP-1R lacks kinase activity and depends on EGFR to activate its downstream pathways⁴⁰⁷. In turn, signal transduction of GLP-1R via EGFR require the proteolytic processing of membrane-anchored betacellulin or other EGF-like ligands⁴⁰⁸. Therefore, the direct treatment of betacellulin likely had a more direct effect on EGFR regulation of insulin expression.

Irrespective of above, successful induction of insulin gene and protein expression was not reflected in significant increases in insulin secretion from H-/G-AMSC-IPCs upon glucose challenge, regardless of their comparable pancreatic gene and intracellular insulin expression levels with H-/G-CMSC-IPCs. Notably, three H-AMSC-IPCs samples (Healthy 03, 06, 10) were able to release insulin in response to high glucose environment but AMSC-IPCs derived from Healthy 07, 08, and 11 failed to secrete increased insulin. Although Healthy 07 and 08 had a history of smoking which might affect cell biological properties, such as DNA methylation⁴⁰⁹, we were unable to identify whether smoking has a direct effect on poor insulin secretion. However, cigarette and nicotine were found to have impacts on impaired insulin secretion and insulin resistance^{410, 411}. Moreover, we noticed that AMSC-IPCs derived from Healthy 08 and 11 had lower expression of *GLUT2* gene. The glucose transporter, GLUT2 plays an important role in glucose sensing and homeostasis⁴¹². The low expression of *GLUT2* may reflect the less responsiveness to high glucose environment in H-AMSC-IPCs.

A notable difference between H-/G-AMSC-IPCs and H-/G-CMSC-IPCs during differentiation was that the former displayed a morphology of attached cell condensations which did not progress into suspension spheroids. Current perspectives have suggested β -cell glucose stimulation requires the formation of small spheroid clusters either in suspension or loosely adhered to extracellular matrix and that single cells are not responsive^{413, 414}. This reflects our observations where spontaneously detached, spheroid cultures, supported IPC differentiation and maturation in H-/G-CMSCs

4.6 Summary

Coupled to the growing interest in autologous, and allogeneic, cell therapy, an understanding of how disease state impairs the regenerative capacity of endogenous MSCs is crucial. In this study we have provided three key observations; the first being the description of a comprehensive protocol for the generation of IPCs from placental chorionic membrane-derived MSCs, the second being that amniotic membrane-derived MSC are refractory to IPC differentiation, and the third being that the above primary characteristics are GDM-independent. GDM-derived CMSCs were capable of transdifferentiation into IPCs, expressing β -cell markers and functionally indistinguishable from healthy CMSC-IPCs but G-AMSCs failed to differentiate into mature IPCs. This suggests that the pathophysiological state of GDM may cause irreversible impairment in the differentiation capacity of AMSCs. Notably, G-CMSCs possessed comparable IPC differentiation potential to H-CMSCs.

Chapter 5

Microarray study of Healthy- and GDM- CMSCs transcriptional profile



5.1 Introduction

Mesenchymal stem cells (MSCs) are present in many adult tissues and responsible for tissue regeneration and maintenance. Their regenerative potential provides numerous benefits for disease treatment. In terms of differentiation potential toward multiple lineages and immunomodulatory capacity MSC may share certain levels of common transcriptional signature⁴¹⁵. However, transcriptional profile can also be unique to MSCs derived from different tissues. Stem cell therapies are somehow hampered by our incomplete knowledge of their fundamental differences⁴¹⁶. Unlike embryonic stem cells, MSCs niche in adult tissues may affect and determine the gene expression in specific tissue-derived MSCs. It is likely that many genes critical to regenerative functions of MSCs or altered gene signature in different MSC sources are not yet fully understood. A better knowledge of MSCs gene profile provides more effective strategies for using MSCs in regeneration medicine.

DNA microarray is a powerful tool to study genomic-scale transcriptome profiling and through various bioinformatic methods, image data can be processed and converted to gene expression values. Even when the microarray data is processed to gene expression value, thousands of genes expressed within the cells make the analysis of these complex datasets challenging. There are a number of commercially or open source bioinformatic software available to assist microarray studies and analyse biological significance⁴¹⁷. In this chapter, analysis methods, including identification of differentially expressed genes, clustering of data, relevant biological function analysis, and interaction networks were used via different bioinformatics tools. Other bioinformatics analysis techniques such as biomarker identification has been widely used in cancer research and toxicogenomics is commonly used in drug screening.

However, when microarray data is obtained from different platforms, the procedures can

vary greatly with gene expression. Reliability and reproducibility of microarray data has raised concerns. For example, two studies attempted to investigate survival after chemotherapy for diffuse large B-cell lymphoma by gene expression profiling using different microarray platforms. The results showed different gene classifiers with a low number of overlapping genes⁴¹⁸⁻⁴²⁰. Likewise, inconsistent results were found in some stem cell studies on exploring gene signature of embryonic and adult stem cells⁴²¹⁻⁴²³. Since the inconsistency issue has been addressed, the MicroArray Quality Control project initiated by the US Food and Drug Administration attempted to enhanced intra-platform and cross-platform consistency⁴²⁴ which has improved nowadays microarray technology.

In addition, verification of microarray results through laboratory experiments is considered as a reliable method to validate the accuracy of microarray data. As DNA microarray analyses transcriptome activity, using semi-quantitative reverse transcription PCR or real-time PCR to examine gene expression is a common first step to verify microarray data⁴²⁵. However, with the increasing availability of microarray chips and affordable prices, some studies are able to enhance the accuracy of microarray data and reduce sample-to-sample variance by improving sample size. These studies can thereby provide more powerful evidence and forgo performing validations through laboratory gene analysis assay⁴²⁶. Given that biological functions mainly depend on protein activities, validating array results at the protein level corresponding to gene expression is equally important^{425, 427}. Validation of protein expression and its relevant biological functions revealed by microarray analysis can be carried out through immunoblotting, immunostaining, function assays, or *in vivo* experiments.

Owing to the fact that umbilical cord blood-derived MSCs/HSCs (U-SCs) have been studied and applied in clinical therapies for many years, there are many U-SCs microarrays or gene

sequencing data available on GEO database (GEO, gene expression omnibus, <https://www.ncbi.nlm.nih.gov/geo/>). However, very few studies have investigated whether the genomic profile of these perinatal tissue-derived stem cells are altered by pregnancy complications. A microarray study on umbilical vein endothelial cells (HUVEC) derived from GDM pregnancies indicated altered gene expression in insulin sensing and extracellular matrix reorganisation⁴²⁸. Another study performed microarrays on umbilical cord tissue from diabetic pregnancies and found alterations in genes associated with vascular development and function⁴²⁹. However, the gene profiling research on regenerative ability of MSCs from GDM women is limited. Moreover, microarray data of CMSCs is yet to be found on GEO database.

In chapter 3, we showed that CMSCs can be isolated in high numbers, with steady growth and proliferation rate under a standard culture environment. In addition, CMSCs derived from GDM and healthy women demonstrated comparable regenerative potential towards tri-lineage differentiation. These findings leading to conclude that the GDM environment did not significantly hamper the differentiation ability of CMSCs. GDM-CMSCs were able to behave similarly to healthy CMSCs and successfully reprogrammed into insulin producing cells as demonstrated in chapter 4. GDM-CMSCs seem to have promising potential to be used in regenerative medicine. Therefore, to further evaluate the therapeutic potential of CMSCs, we performed DNA microarray to comprehensively understand their gene profiles and investigate the potential clinical application based on their transcriptional signature.

5.2 Aim

With increasing interest in the utilisation of placental MSCs and their banking for clinical purposes, understanding the characteristics and regenerative potential of placental MSCs has become an important subject. Thus, we sought to explore gene expression profiles between CMSCs from healthy and GDM placenta by DNA microarray analysis. Moreover, we aimed to investigate the biological differences or similarities based on gene expression and validate these changes in functionality through experimental assays to provide a comprehensive understanding of healthy and GDM CMSCs.

The main objectives of the chapter:

- Perform DNA microarray with 3 healthy and 3 GDM CMSC samples
- Analyse microarray data using bioinformatic software
- Validate gene expressions with 10 healthy and 11 GDM samples
- Investigate biological differences through *in vitro* functional assays

5.3 Methods

DNA microarray

Samples used for microarray analysis were 3 H-CMSCs (Healthy03, 07, 08) of similar ages and BMI, and 3 GDM-CMSCs (GDM06, 07, 08) treated with either metformin (06), insulin (07), or both (08), representing the different severity of GDM. Cells were collected at passage 2 for microarray analysis. Apart from RNA extraction and microarray raw data collection conducted by Welgene Biotech Company, all analysis and validation experiments in this chapter were carried out by the author for this thesis.

Microarray experimental flow is showed in Figure 5-1 conducted by Welgene Biotech Company. The 0.2 µg of total RNA was amplified and labelled with Cy3 (CyDye, Agilent Technologies) for in vitro transcription process. 0.6 µg of Cy3-labeled cRNA was fragmented to an average size of about 50-100 nucleotides and then pooled and hybridized to Agilent SurePrint Microarray (Agilent Technologies) at 65 °C for 17 hours. After washing process by nitrogen gun blowing, microarrays were scanned with an Agilent microarray scanner and images were analysed by Feature extraction10.7.3.1 software (Agilent Technologies).

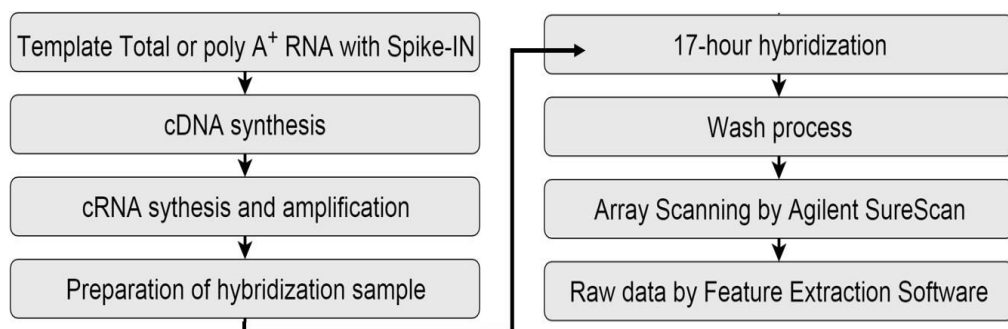


Figure 5-1. Microarray experimental flow

A common external RNA control, poly A⁺ RNA with Spike-IN, is a set of unlabelled, poly-adenylated transcripts of known sequence and quantity used to calibrate measurements in RNA hybridization assays⁴³⁰. Microarray experiments were performed using Agilent

SurePrint technology by Welgene Biotech Company.

Microarray analysis using bioinformatics software

Venn diagram and hierarchical clustering heat maps were created by AltAnalyze software (Gladstone Institution, UCSF) used to identify commonly up-regulated or down-regulated genes and illustrate the differentially expressed gene lists of interest.

Ingenuity Pathway Analysis (IPA, Qiagen; www.qiagen.com/ingenuity) was used to analyse the genes with fold changes greater than 1.5 in GDM samples vs. healthy samples (differentially expressed genes, DEGs). Overrepresented and underrepresented biological functions and canonical pathways were identified based on the DEGs involved in Ingenuity Knowledge Database (Qiagen). The chi-squared test and Fisher's exact test are used to compare statistical significance between two variables when the comparing groups are independent and not correlated. The chi-squared test applies when the sample size is large, while the Fisher's exact test runs an exact procedure as the chi-squared test but for a small sample size⁴³¹. In this study, the two variables in the microarray analysis are the total DEGs (up-/down- regulated genes) and associated biological functions/pathways, when the independent comparing groups are Healthy and GDM. Due to the small-sized samples in our study, the Fisher's exact test was used for analysing significance via IPA software. The p-value is calculated by considering the number of DEGs that participate in a specific biological function vs. the total number of genes that are known to be associated with that biological function in the IPA database (Ingenuity Knowledge Base, Qiagen). The p value < 0.05 indicates statistical significance.

The downstream function analysis was used to identify biological functions that are expected to be increased or decreased based on the activation Z-score. The activation Z-

scores were calculated by IPA, which assess the potential activation state of a biological function by using information about (1) the up- or down- regulatory state of each gene involved (2) the statistical significance of these genes in the biological function. The positive activation Z-score indicates increased activation and the negative activation Z-score indicates decreased activation.

Pathway network visualisation was created by Cytoscape v.3.6.1. Enriched gene sets identified by IPA pathway analysis were selected and used as input nodes. The interaction network was generated according to literature findings and public database. The network was manually curated and distributed with circles for easier visualisation.

The experimental workflow of microarray analysis and validation was demonstrated in Figure 5-2.

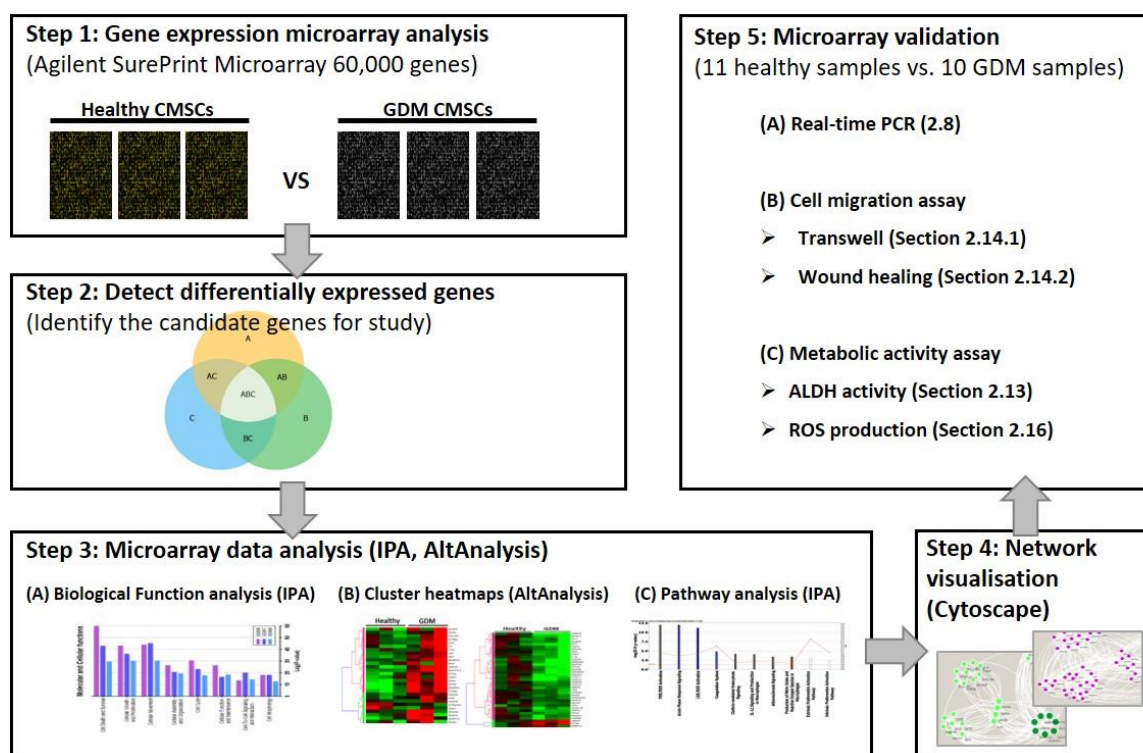


Figure 5-2. Summary of the methodology in chapter 5

Validation and statistical analysis

10 Healthy and 11 GDM CMSC samples were used for validating microarray data through gene expression and functional assays. The selected upregulated/downregulated genes in microarray data were validated by real-time PCR (Section 2.8). Functional assays were used to validate enriched biological function in GDM-CMSCs, including Transwell migration assay (Section 2.14.1), wound healing assay (Section 2.14.2), ALDH activity analysis (Section 2.15) and ROS detection (Section 2.16). Real-time PCR and migration results were compared using Student's t-test to determine the statistical significance between two groups. ALDH activity and ROS detection was analysed using one-way ANOVA to compare the significance between two groups at different time points. Analysis was performed using GraphPad Prism (GraphPad Software).

5.4 Results

5.4.1 Identification of differentially expressed genes

Gene expression profiling of CMSCs derived from 3 healthy (H-CMSCs) and 3 GDM women (GDM-CMSCs) were assessed by DNA microarray analysis at passage 2. The details of samples used for microarray analysis (Healthy03, 07, 08 and GDM06, 07, 08) are listed in Table 2-2. The 3 H-CMSCs (Healthy03, 07, 08) were chosen based on similar ages and BMI. GDM samples were selected from GDM patients that had received glycaemic control treatments during pregnancy, as this cohort showed excessive physiological glucose levels vs. healthy women or untreated GDM patients, and could be more representative cohort to explore hyperglycaemic effects on GDM-CMSCs. Two GDM samples (GDM 06 and 07) were treated with metformin and insulin, respectively while a severe GDM sample (GDM08) received a combined treatment with both metformin and insulin.

Within the thousands of genes analysed in microarray, a small number of informative genes which display altered expression patterns and are mostly responsible for the differences between two biological conditions under investigation, are defined as differentially expressed genes (DEGs)⁴³². DEGs can be identified by specific selection criteria. In this study, a cut-off of $P < 0.05$ and 1.5-fold change in gene expression were used to identify the DEGs between H-CMSCs and GDM-CMSCs. Compared to H-CMSCs, there is a total of 431 DEGs, including 162 up-regulated and 269 downregulated genes in all 3 GDM samples (Figure 5-3). The sample from the women received both metformin and insulin treatment (GDM08) exhibited the highest number of total DEGs.

The top 10 differentially upregulated or downregulated genes are listed in Table 5-1 with the expression \log_2 fold change. Functional interpretation of top ranked genes was defined

by Gene Ontology Consortium (<http://www.geneontology.org/>). In the down-regulated genes, *PRKCB*, *FAM20A*, *ALDH1A1*, and *ATP8B4* were associated with catalytic activity; *GJA8* and *ATP8B4* were involved in transport activity; and *CXCL12*, *CXCL3*, *CXCL*, and *RSPO3* in chemokine activity. The majority of the top 10 up-regulated genes were related to protein or ion binding and *RPS4Y1*, *COL17A1*, *SPRR3*, *KRT5*, *HAPLN1* were also involved in structural molecule activity.

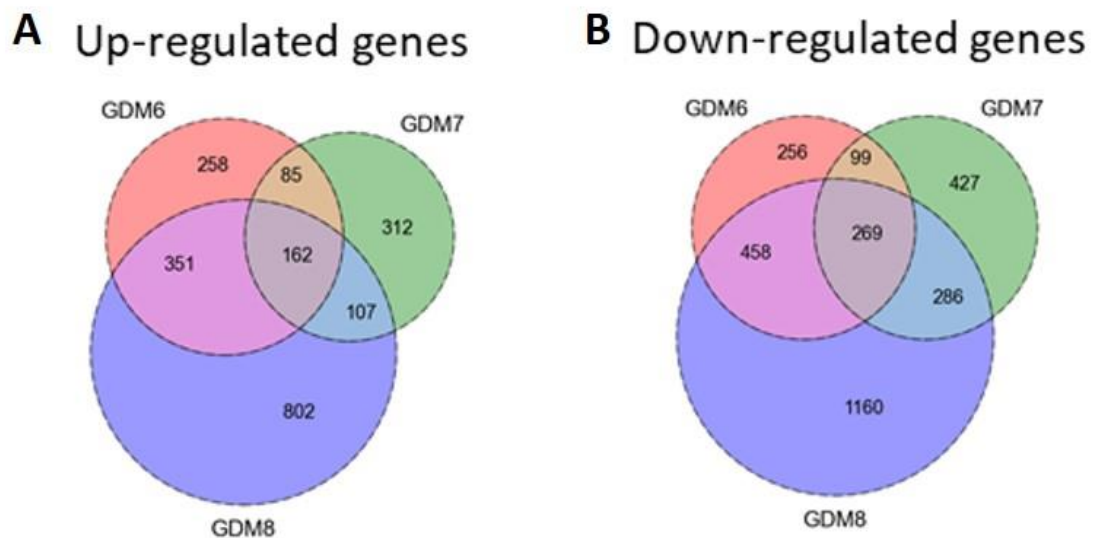


Figure 5-3. Venn diagrams of DEGs

Venn diagrams show the numbers of genes that are up- or down- regulated 1.5-fold more in GDM-CMSCs vs. H-CMSCs. The overlapping areas of 3 circles were co-regulated genes in GDM-CMSCs, defined as differentially expressed genes (DEGs).

Table 5-1. Top ranked up- and down-regulated genes in GDM-CMSCs vs. Healthy-CMSCs

Top 10 Down-regulated genes	Average log ₂ ratio	Top 10 Up-regulated genes	Average log ₂ ratio
<i>PRKCB</i>	-5.566	<i>RPS4Y1</i>	9.873
<i>GJA8</i>	-4.166	<i>COL17A1</i>	9.344
<i>CXCL12</i>	-3.436	<i>DDX3Y</i>	8.528
<i>FAM20A</i>	-3.379	<i>CDH1</i>	8.376
<i>ALDH1A1</i>	-3.315	<i>KRT5</i>	8.308
<i>PRRX2</i>	-3.227	<i>SCEL</i>	8.207
<i>ATP8B4</i>	-3.040	<i>SPRR3</i>	7.823
<i>RSPO3</i>	-2.927	<i>PLD5</i>	7.293
<i>CXCL3</i>	-2.925	<i>HAPLN1</i>	7.102
<i>CXCL1</i>	-2.914	<i>L1TD1</i>	6.996

5.4.2 Biological function analysis

Wound repair and altered cardiovascular function in GDM-CMSCs

Biological function analysis using DEGs that were identified in all 3 GDM-CMSCs samples was performed with Ingenuity Pathway Analysis (IPA) through two categories: “molecular and cellular functions” and “physiological system development and functions”. The “molecular and cellular functions” most represented in GDM-CMSCs were related to cell death and survival, cellular growth and proliferation, and cellular movement (Figure 5-4).

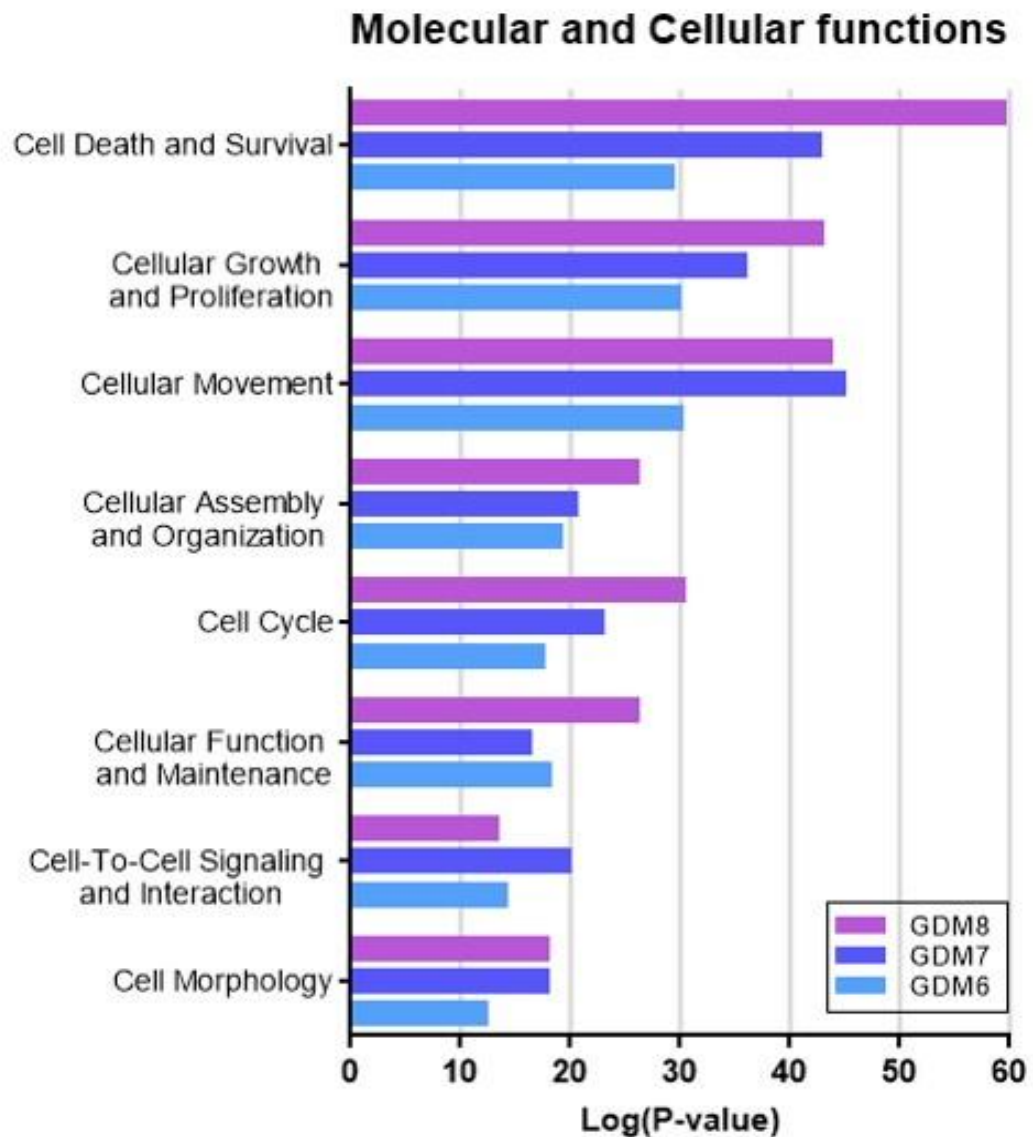


Figure 5-4. Enriched molecular and cellular function in GDM-CMSCs

Each pair of bars displays the significant state of over-represented functions in GDM-CMSCs compared to H-CMSCs and each colour represents each GDM sample. The p-value, calculated with the Fisher's exact test.

To further identify the altered cellular process of the most represented biological functions, downstream effects analysis was used to understand key biological processes influenced by DEGs. The activation z-score computed by IPA indicated the activation or inhibition state and gene enrichment of each downstream cellular process. A positive z-score indicates increased functional activity in GDM-CMSCs relative to H-CMSCs while a negative z-score indicates a reduction in activity.

As indicated by IPA, genes enriched in GDM-CMSCs were related to enhanced abilities in cell survival, cellular motility, assembly and organization of cytoskeleton, and skin formation, which are critical functions in wound repair and tissue remodelling (Figure 5-5A). The positive associated downstream cellular processes in “molecular and cellular functions” revealed the potential of GDM-CMSCs in wound healing process. Although some negative activation was found in colony formation, proliferation, cellular infiltration, and homing, due to the smaller z-score value it would suggest less significance of gene enrichment and effect.

To gain insight into the gene expression level of GDM and healthy samples, multiple functional gene clusters involved in cell movement and survival (Figure 5-5B), cellular assembly (Figure 5-5C), and development of epithelium (Figure 5-5D) were displayed on the clustering heat maps. The upregulated expressions of these gene sets were demonstrated in GDM-CMSCs associating with an increased function in healing process.

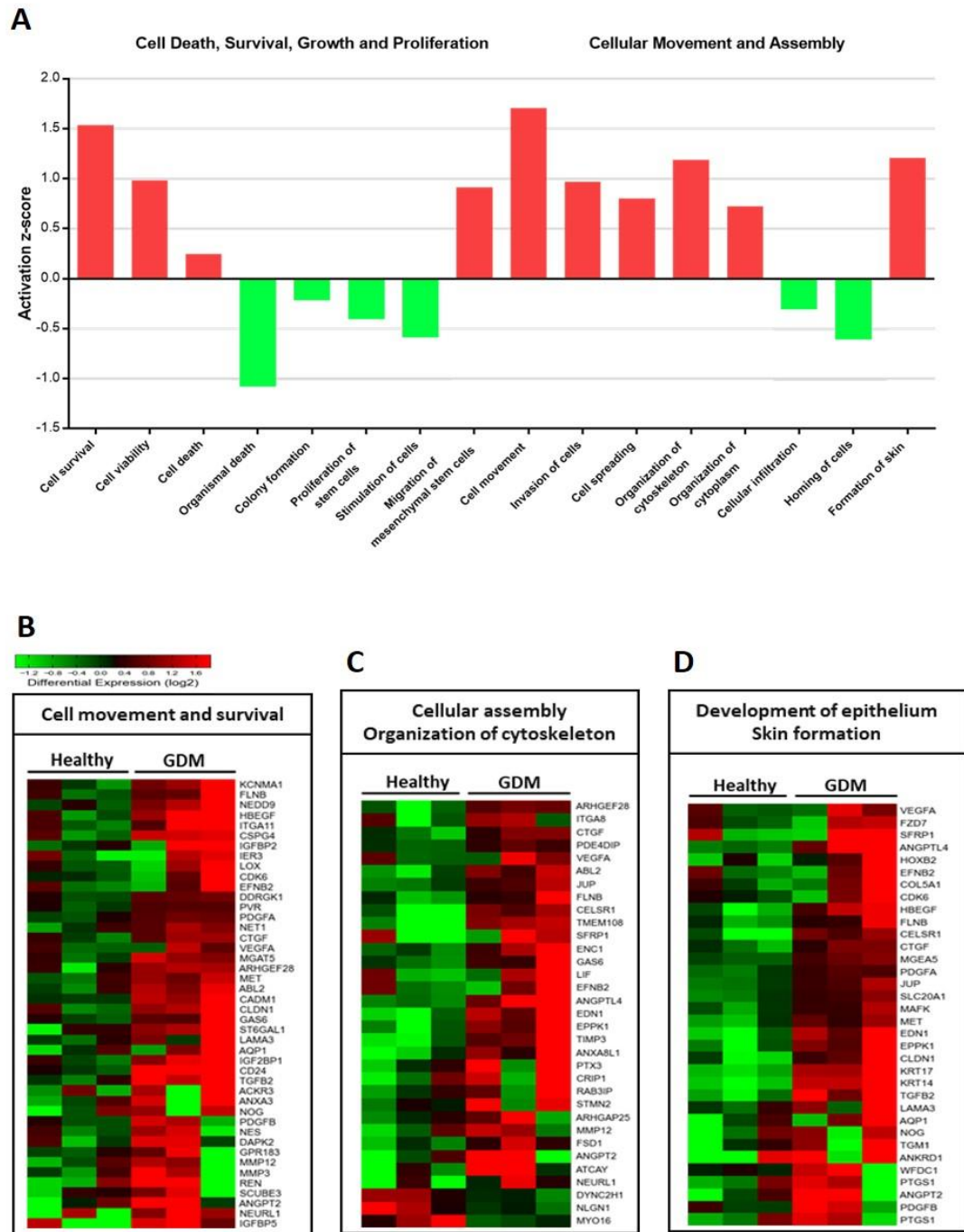


Figure 5-5. Downstream effects in molecular and cellular function

(A) Activation state of top enriched downstream cellular processes in “molecular and cellular functions” using IPA activation z-score to identify the increased (positive z-score) or decreased activity (negative z-score) in GDM-CMSCs compared to H-CMSCs. (B-D) Hierarchical clustering heat maps of DEGs involved in cellular functions related to healing process. Expression levels are represented by log₂ fold change (expression value in each sample vs. mean expression value in H-CMSCs). Colours are according to the scale representing high expression (red) and low expression (green) genes.

In order to explore the development/differentiation potential of GDM-CMSCs, DEGs were used to performed “physiological system development and function” analysis by IPA. The most represented biological function included cardiovascular system development and function, connective tissue development and function, and organ morphology. (Figure 5-6).

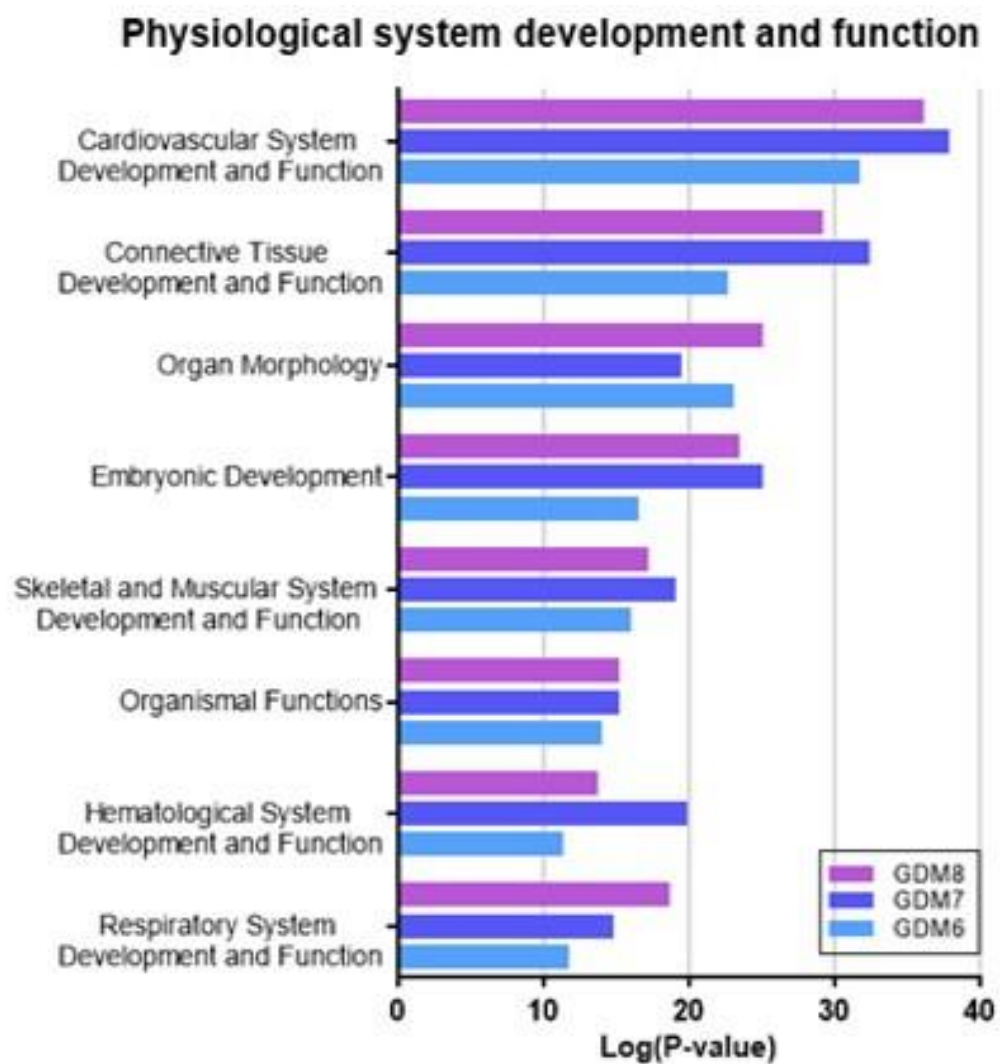


Figure 5-6. Enriched physiological system development and function in GDM-CMSCs

The most relevant biological functions in “physiological system development and function” category in GDM-CMSCs were identified by IPA. The p-value, calculated with the Fisher's exact test.

Further in-depth analysis of the downstream functional activation performed in relation to cardiovascular system development showed that cardiogenesis was the most significantly over-represented downstream cellular process with the highest positive z-score. Along with the positive association with development of cardiovascular tissue, it could imply the possibility of GDM-CMSCs giving rise to cardiogenic progenitors and their development into cardiomyocytes (Figure 5-7A). The heat map illustrated a set of genes involved in cardiogenesis that were highly expressed in GDM-CMSCs compared to H-CMSCs, contributing to greater potential in cardiac regeneration (Figure 5-7B).

Cardiogenesis potential is what generates cardiac cells which can replace the loss of cardiomyocytes or insufficient endogenous regeneration of cardiomyocytes in some heart diseases. On the other hand, the ability of stem cells to promote angiogenesis is a reason for successful cell therapies in cardiac regeneration^{433, 434}. However, in GDM-CMSCs the cellular processes of vasculogenesis and angiogenesis in cardiovascular development were identified to have decreased activation with negative z-score (Figure 5-7A). The heat map showed that the regulators in vasculogenesis and vasculature development, such as *PRRX2*, *RSPO3*, *KITLG*, and *CXCL1*, had lower expression in GDM-CMSCs compared with H-CMSCs (Figure 5-7C).

Moreover, other enriched downstream cellular processes in the “physiological system development and function” category included respiratory system development, formation of lung and kidney with positive z-score while development of exocrine gland and connective tissue with negative z-score in GDM-CMSCs (Figure 5-8).

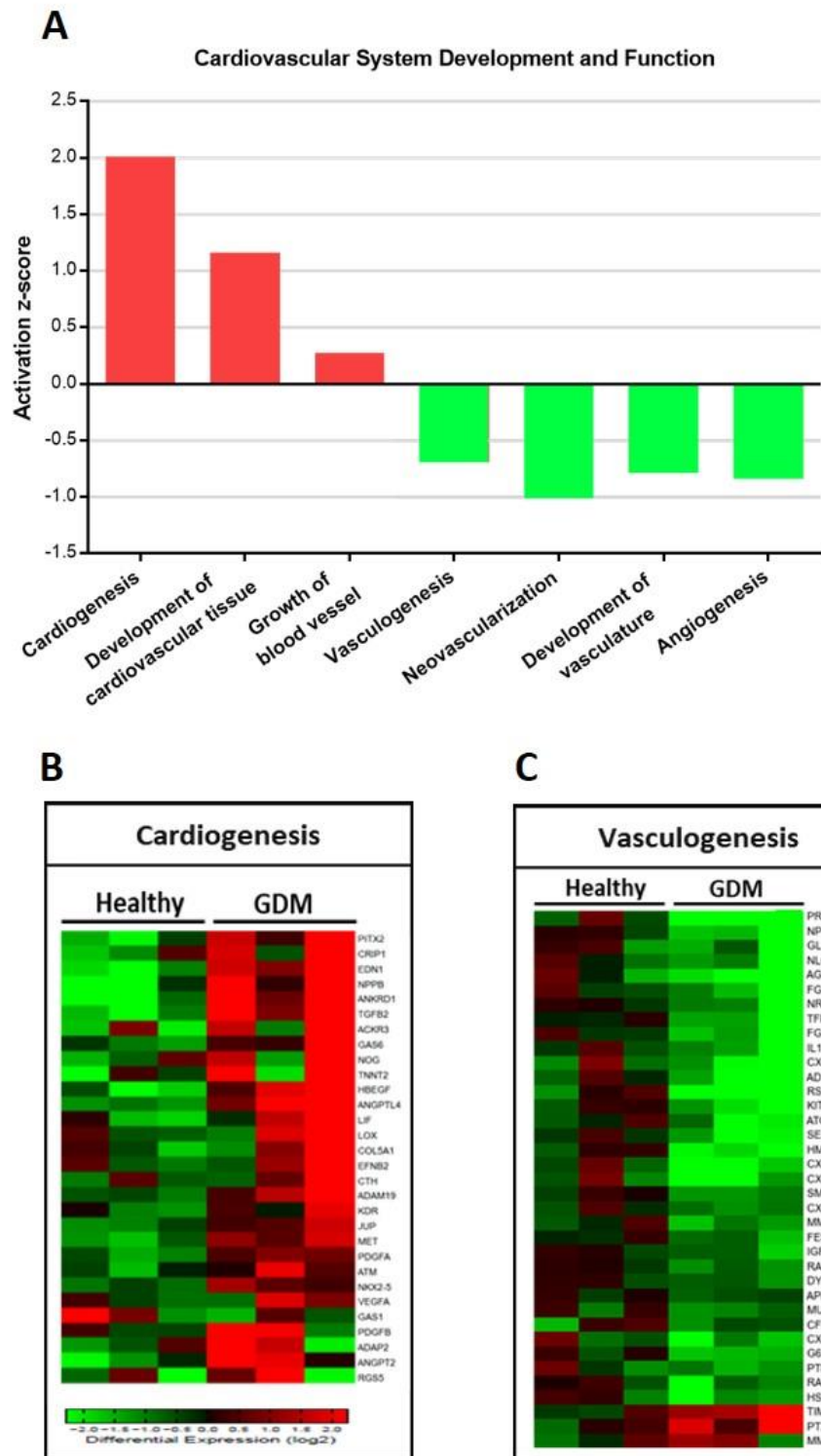


Figure 5-7 Downstream effects in cardiovascular system development

(A) Enriched downstream cellular processes associated with “cardiovascular system development and function” in GDM-CMSCs. Activation state was calculated by IPA activation z-score. (B-C) Heat maps summarized DEGs involved in cardiogenesis and vasculogenesis. Colours indicates high expression (red) and low expression (green)

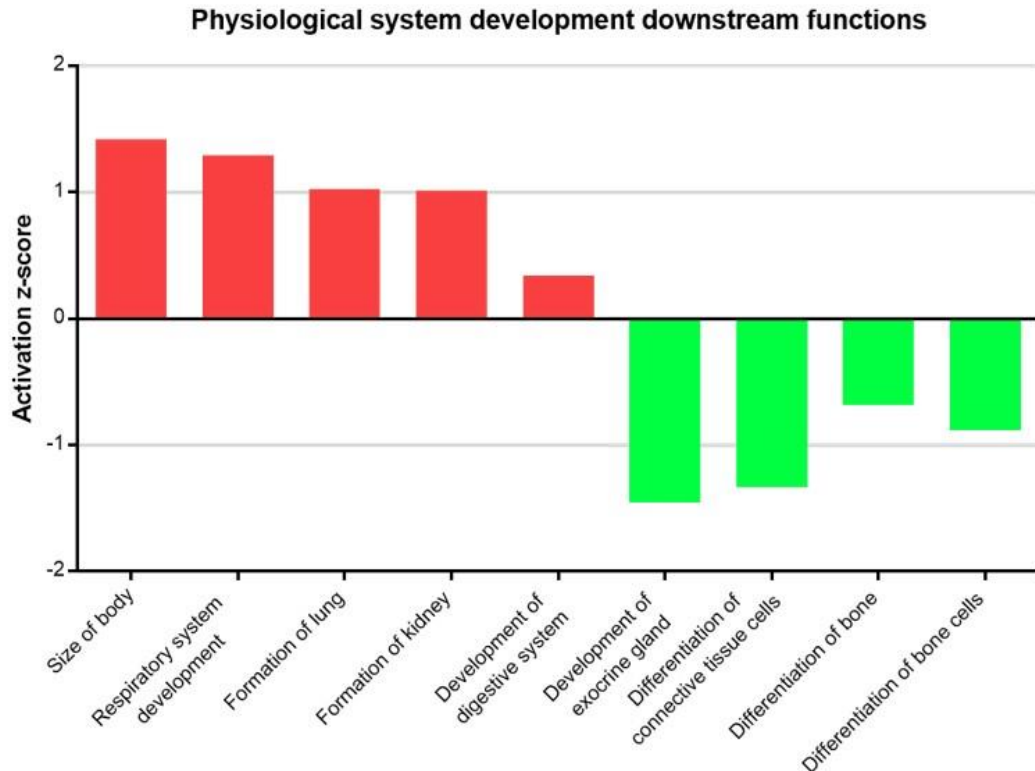


Figure 5-8. Downstream effects in physiological system development and function

The relevant cellular processes related to development were identified and ranked by the IPA analysis based on DEGs. Activation state was calculated by IPA activation z-score.

5.4.3 Validation of enriched biological functions

Increased migration ability, wound healing potential, and cardiac development in GDM-CMSCs

To evaluate microarray data and functional differences between H-CMSCs and GDM-CMSCs, enhanced expression in genes involved in migration, survival, and cellular assembly ability in GDM-CMSCs were validated through real-time PCR analysis. Validated genes were selected mainly based on the significance of increased levels in microarray data and also the importance of the gene in the biological function.

In all 3 GDM-CMSCs microarray data, the highly glycosylated protein CD24 showed more than 10-fold increase. The expression of CD24 has been suggested to regulate cell migration in various cell types^{435, 436}. A microarray study of overexpression and suppression of CD24 in BM-MSCs indicated the regulatory role of CD24 in transforming growth factor (TGF)- β signal⁴³⁷ which is known to involve in many cellular functions, including cell growth, survival, and wound healing. Real-time PCR confirmed the significantly upregulated CD24 expression in GDM-CMSCs while the increased level varied from 5 to 15 folds (Figure 5-9A). Approximately 2 times higher expression of *CELSR1*, a membrane of cadherin superfamily involving in regulating adhesion and wound repair signalling, was found in GDM-CMSCs vs H-CMSCs. Filamin B (*FLNB*) and aquaporin 1 (*AQP1*) are involved in cytoskeleton arrangement and cellular assembly which showed a 2-3-fold increase in GDM06 and GDM07 microarray data while GDM08 had 3.7-fold upregulation in *FLNB* and 40-fold increase in *AQP1*. Real-time PCR verified the increased expression of *FLNB*, *AQP1*, *CELSR1* in GDM-CMSCs but the relatively high increase in *AQP1* expression in GDM08 was not detected by real-time PCR analysis (Figure 5-9A).

The selected genes related to skin formation, epithelial development, and healing process included endothelin 1 (*EDN1*) which was evidenced to accelerate wound healing processes⁴³⁸, and several growth factors; transforming growth factor (TGF), heparin-binding EGF-like (HBE)-GF, and connective tissue (CT)-GF which are known to promote wound repair and epithelium growth. The validation of *EDN1*, *HBEGF*, *TGFB2*, *CTGF* expression was consistent with microarray result, showing significantly upregulated in GDM-CMSCs compared to H-CMSCs (Figure 5-9B).

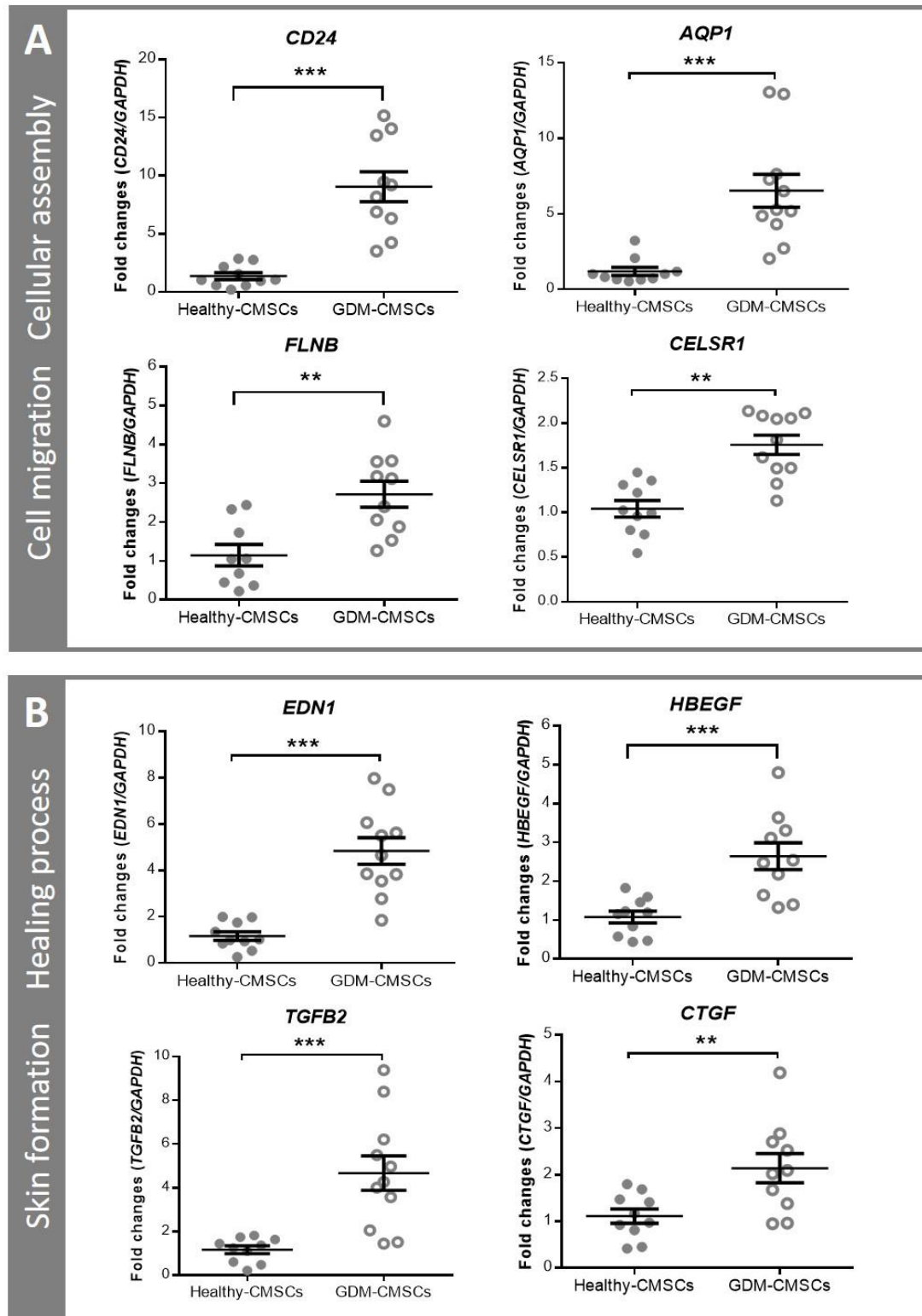


Figure 5-9. Real-time PCR validated the genes involved in wound healing

Expression level of each gene was normalised to *GAPDH* expression. Results represent mean \pm SEM. Statistical significance was determined by Student's t-test, * $p < 0.05$, ** $p < 0.01$, *** $p < 0.001$.

To examine biological differences on a functional level *in vitro* assays were performed to evaluate the migration ability. The Transwell migration assay was used to analyse the motility of single cell to respond toward attractants. H-CMSCs or GDM-CMSCs were placed into the upper compartment of a Transwell in serum free media and the lower compartment was filled with complete growth media containing FBS as an attractant. After allowing migration for 8 hours, enhanced migration ability was observed in GDM-CMSCs with a greater numbers of cells having migrated across the membrane. Cells were continually incubated for 24 hours and both H-CMSCs and GDM-CMSCs were observed to pass through the Transwell filter, where more migrated GDM-CMSCs were observed than H-CMSCs. After either 8 or 24 hours of incubation, GDM-CMSCs had a significant increase in the number of migrated cells vs. H-CMSCs which verified the more mobile state of GDM-CMSCs (Figure 5-10).

Wound healing assay was used to determine the migration ability of cell populations. A wound was created by scratching with a pipette tip through a confluent monolayer of cells and the migration ability determined by wound closure percentage. The result showed that higher numbers of GDM-CMSCs migrated into the wound field at every observed time point (6, 12, 24 hours) than H-CMSCs. The closure percentages were significantly increased, with approximately 30% in GDM-CMSCs and 20% in H-CMSCs after 12 hours and increasing up to 60% in GDM-CMSCs and 40% in H-CMSCs after 24 hours (Figure 5-11). Collectively, both the Transwell migration and wound healing assay validated the enhanced migration ability in GDM-CMSCs.

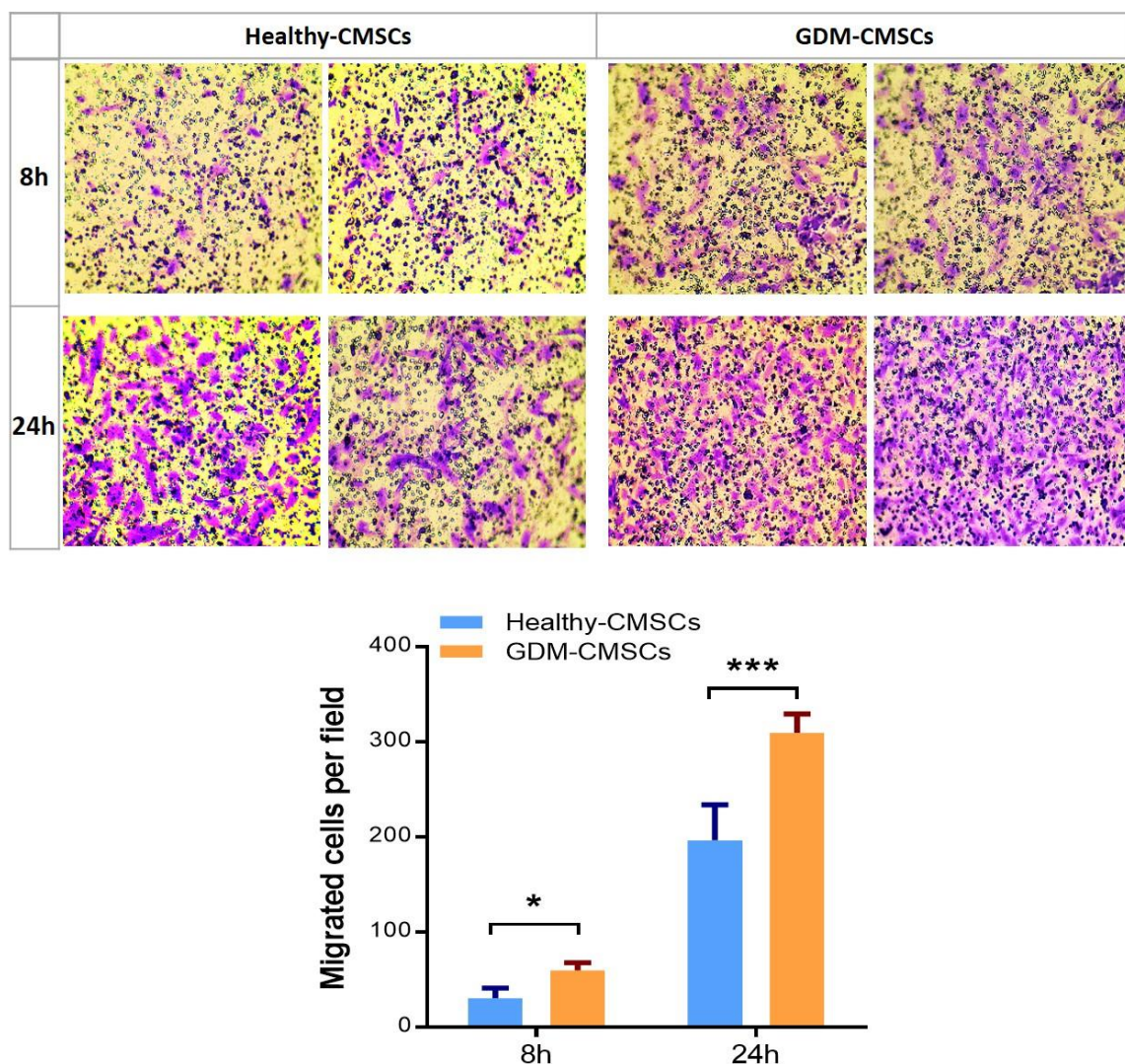


Figure 5-10. Transwell migration assay

Cell motility was evaluated by Transwell migration assay. Representative images are migrated H-CMSCs and GDM-CMSCs stained with crystal violet after 8 and 24 hours of migration period from 6 H-CMSCs (Healthy03-08) and 6 G-CMSCs (GDM04-09) samples in duplicate. Cell migration ability was calculated by counting migrated cells per field by image J. Results represent mean \pm SEM. Statistical significance was determined by Student's t-test, $*p < 0.05$, $***p < 0.001$.

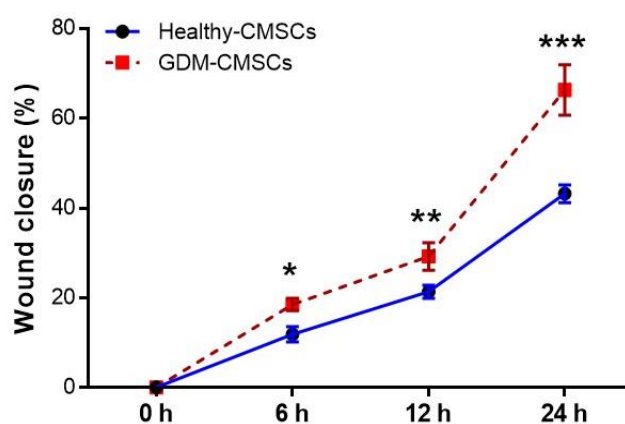
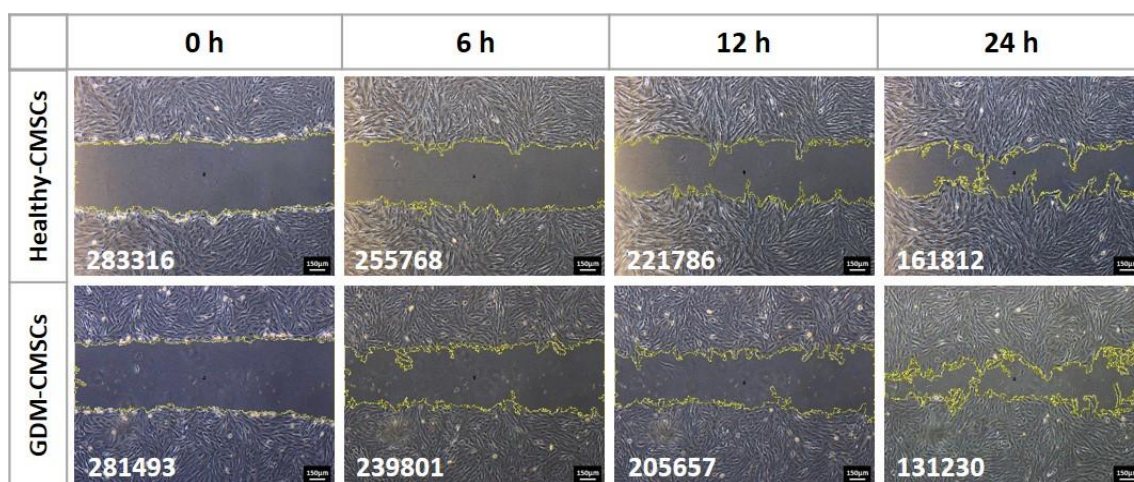


Figure 5-11. Wound healing assay

Representative images of wound healing assay from 6 H-CMSCs (Healthy03-08) and 6 G-CMSCs (GDM04-09) samples. Images were captured by light microarray after allowing H-CMSCs and GDM-CMSCs to migrate into the middle wound field after 0, 6, 12, 24 hours. Scale bar, 150 μ m. Percentage of wound closure was calculated by measuring the reduction in wound area after incubated for indicated time period. Images were modified (the yellow lines for edges of the wounds) and measured by image J. Numbers shown on the left corner represent the wound area. Statistical significance was determined by Student's t-test, * $p < 0.05$, ** $p < 0.01$, *** $p < 0.001$.

Cardiovascular development was identified as the most enriched biological function in GDM-CMSCs. The related DEGs showed altered expression, especially in cardiogenesis and vasculogenesis. Transcription factor NK2 homeobox 5 (*NKX2.5*) which has an important role in functioning heart development and formation showed increased in GDM06 and GDM08 microarrays, but a 1.6-fold decrease in GDM07. Validating *NKX2.5* expression by real-time PCR, most GDM-CMSCs had a 2-fold upregulation while a more significant increase in *NKX2.5* expression could be found in GDM03, GDM08 and GDM10 which showed more than 5-fold upregulated expression. Signalling transduction through platelet-derived growth factor (PDGF)-A and tyrosine kinase receptor mesenchymal epithelial transition factor (*MET*) is involved in early heart development^{439, 440}. *PDGFA* and *MET* expression was consistent with microarray data, showing an average of 2-fold upregulation in GDM-CMSCs vs H-CMSCs. The increased expression of noggin (*NOG*) was also confirmed by real-time PCR with significant increases from 3-12 fold in GDM-CMSCs compared to H-CMSCs (Figure 5-12A).

The opposite trend was found in vasculogenesis-associated genes, which showed a significantly reduced expression in GDM-CMSCs. R-spondin 3 (*RSPO3*) and chemokine *CXCL12* were two of the top 10 downregulated genes in GDM-CMSCs, both involved in vasculogenesis and angiogenesis. *CXCL12* showed 10-fold and greater reduced expression in GDM-CMSCs vs H-CMSCs. The reduction of *RSPO3* was not as significant as with microarray data, which had an average of 2-fold decrease in GDM-CMSCs as well as other vasculogenesis regulators; ras interacting protein 1 (*RASIP1*) and heme oxygenase 1 (*HMOX1*) (Figure 5-12B).

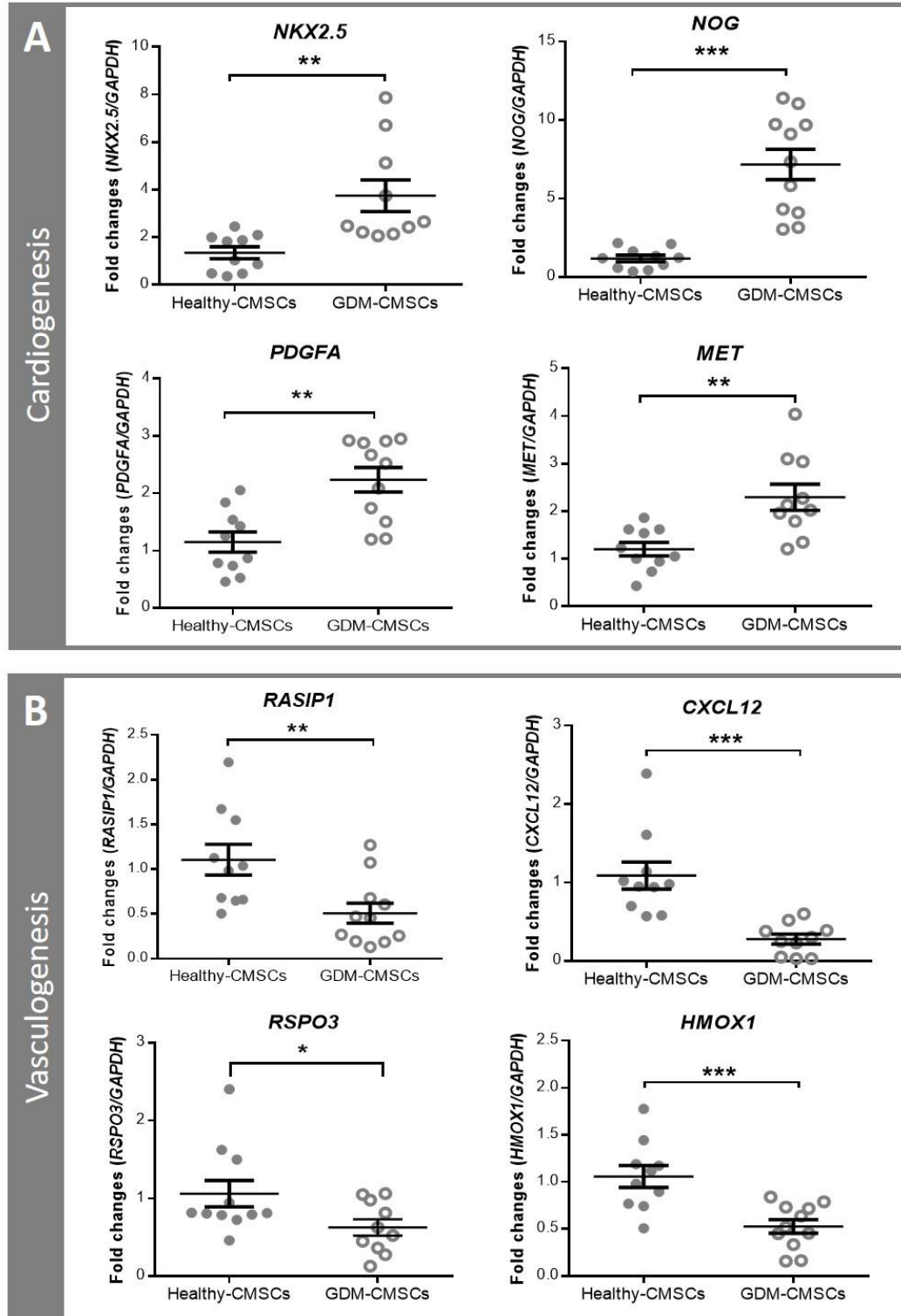


Figure 5-12 Real-time PCR validated the genes involved in cardiovascular development
Expression level of each gene was normalised to *GAPDH* expression. Results represent mean \pm SEM. Statistical significance was determined by Student's t-test, * $p < 0.05$, ** $p < 0.01$, *** $p < 0.001$.

5.4.4 Canonical pathway analysis

Pathways mediating cardiac development and cell movement are both upregulated in GDM-CMSCs while the majority of downregulated pathways are involved in metabolic processes

IPA canonical pathways analysis was used to evaluate pathways altered in GDM-CMSCs based on DEGs. The canonical pathways refer to the well-characterised cell signalling pathways that present common properties of a particular signalling module or pathway. Positively- and negatively- regulated pathways were identified by IPA with a p value indicating significance and the ratio of the number of DEGs that map to the all known genes in the pathway.

Positively-regulated pathways included growth factors pathways (bone morphogenetic protein (BMP), Wnt/ β -catenin, fibroblast growth factor (FGF), vascular endothelial growth factor (VEGF) signalling) and the transcription factor STAT3 pathway. These pathways are all involved in various growth and development processes. Moreover, Rac and Rho protein regulation signalling were also upregulated. Upregulated IL-1 mediated RXR function signalling was involved in the regulation of transport and metabolism of lipid, cholesterol, and bile acid (Figure 5-13A).

Among the down-regulated pathways identified by IPA, most of them were associated with degradation processes, including ethanol degradation, oxidative ethanol degradation, fatty acid α -oxidation as well as the degradation of neurotransmitters (histamine, dopamine, noradrenaline, serotonin) and other molecules (putrescine, tryptophan) (Figure 5-13B).

To elucidate the regulation of altered pathways and biological functions in GDM-CMSCs, we

built the gene regulatory networks of positively-/negatively- regulated pathways. DEGs were used as input nodes and the interaction network was generated according to literature findings and public database.

The enriched biological functions in GDM-CMSCs were associated with upregulated pathways revealed by IPA analysis. STAT3 pathway was most significantly upregulated signalling in GDM-CMSCs, which is imperative for development, cellular homeostasis, and regulating genes in cell growth, proliferation, differentiation in several tissues⁴⁴¹. The transcription factor STAT3 functions as a transducer of several cytokines and growth factors signalling. The upregulated growth factor pathways including BMP signalling, Wnt/ β -catenin signalling, and FGF signalling may also function through the activation of STAT3 signalling and regulate various development processes as well as enriched cellular functions in GDM-CMSCs such as cell growth and survival. Hierarchical clustering map illustrated that multiple upregulated DEGs were involved in BMP, Wnt/ β -catenin, FGF pathways and leading to increased activities (Figure 5-14A).

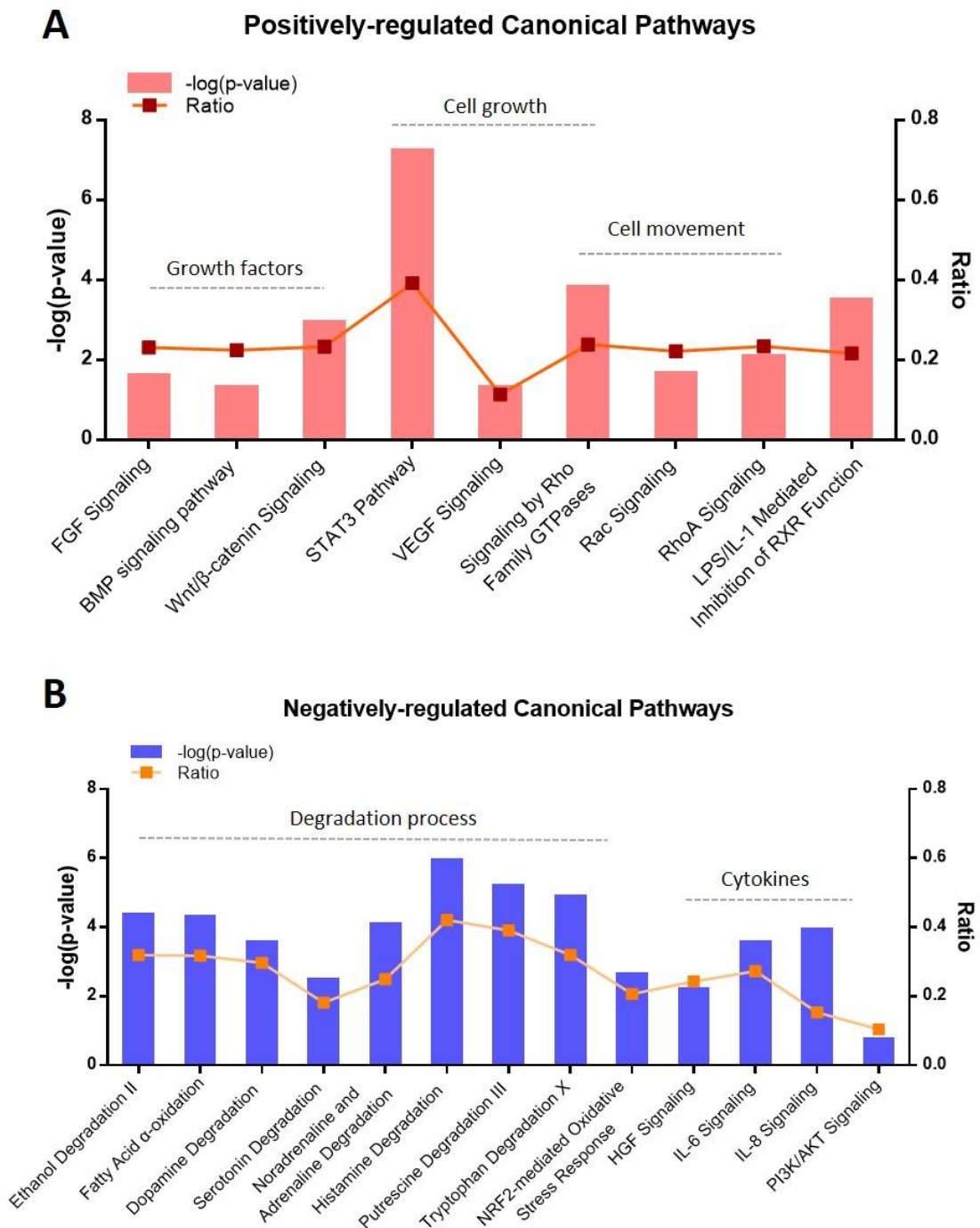


Figure 5-13. IPA canonical pathways analysis

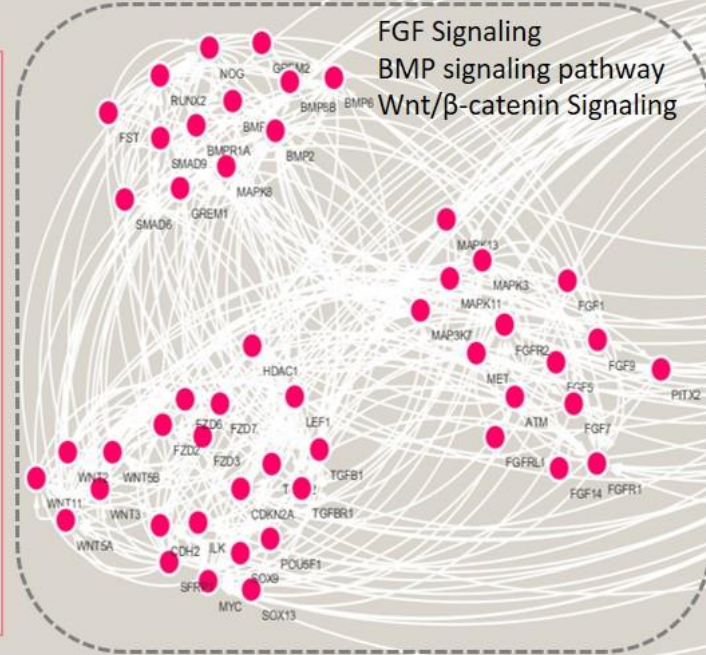
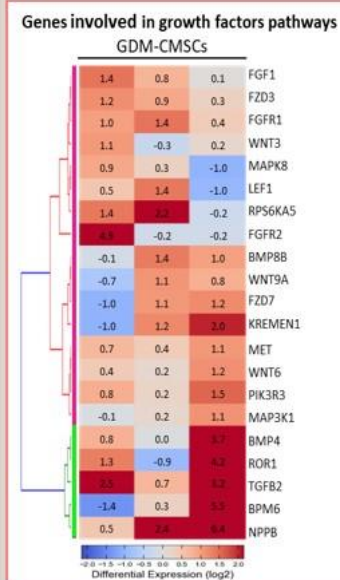
IPA canonical pathways analysis of positively- and negatively- regulated pathways in GDM-CMSCs. The x-axis indicates the altered canonical pathways. The left y-axis indicates the statistical significance p value, calculated using the Fisher exact test. The right y-axis represents the ratio of the numbers of genes in our dataset that map to the all known genes in the canonical pathway.

Notably, BMP, Wnt/ β -catenin, and FGF are key signalling pathways in heart development. As the cardiac-associated genes, *NKX2.5* and *NOG* are regulated downstream to BMP, Wnt/ β -catenin, and FGF pathways, the previously observed upregulation of *NKX2.5* and *NOG* in GDM-CMSCs (Figure 5-12A) may contribute to enhanced cardiogenesis potential via the modulation of BMP, Wnt/ β -catenin, and FGF pathways. Other important factors, such as *WNT3/11*, *LEF1*, *FZD* in the Wnt/ β -catenin signalling pathway, and *FGF1*, *MAPK*, *MET* in the FGF signalling pathway also displayed higher expression in GDM-CMSCs than H-CMSCs (Figure 5-14A).

Moreover, IPA pathway analysis identified increased activity of Rho family GTPase signalling in GDM-CMSCs, including Rac, RhoA, Cdc42 signalling. These GTP-binding proteins are activated by growth factors, cytokines and known to regulate cell migration, invasion, morphology, and cytoskeleton organisation⁴⁴² which are all critical for tissue repair process. The key component genes of Rho family signalling were upregulated in GDM-CMSCs. Hierarchical clustering map showed increased expression of genes involved in Rho/Rac signalling at a magnitude of \log_2 fold changes in all 3 GDM-CMSCs samples normalised to H-CMSCs expression levels (Figure 5-14B). In agreement with IPA biological function analysis and functional validation performed in Figure 5-9 and 5-10, enhanced cell movement capacity in GDM-CMSCs may be associated with the activation through Rho family signalling.

Positive-regulated Canonical pathways

A



Rac Signaling
Signaling by Rho Family GTPases

B

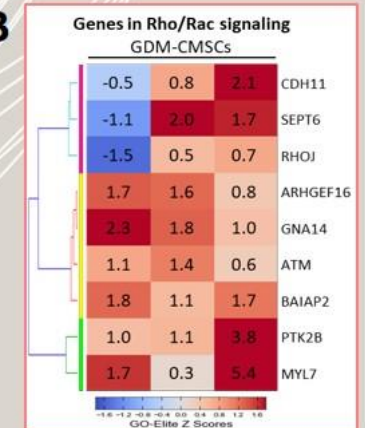


Figure 5-14. Interaction network of positively-regulated pathways

Interaction network was generated by Cytoscape visualization based on DEGs. Heat maps indicated the expression of genes involved in BMP, Wnt/ β -catenin, FGF Signaling and Rho family signaling. Each gene is normalised to a mean expression of 3 Healthy-CMSCs samples. Blue shows the genes with below mean expression while red is above mean expression. Numbers indicate the \log_2 fold change in each sample.

Significantly reduced expression in ALDH family genes results in negative association with metabolic pathways in GDM-CMSCs

Several pathways associated with degradation processes were significantly downregulated in GDM-CMSCs. Given the dysfunctional metabolic regulation in women with GDM, these pathways are of particular interest for investigating GDM-CMSCs behaviours. Figure 5-15 illustrates the genes associated with these enriched downregulated pathways and showed that the decreased activities of degradation pathways were highly connected to the significant reduction in aldehyde dehydrogenase family gene expression, *ALDH1*, *ALDH2*, *ALDH3* (Figure 5-15A). Aldehydes can be formed during the metabolism of amino acids, carbohydrates, lipids, vitamins as well as cytotoxic drugs and environmental chemicals. ALDH genes encode the key enzymes regulating cellular detoxification through oxidising endogenous and exogenous aldehydes, and play an important role in many degradation processes⁴⁴³.

Notably, *ALDH1A1* is one of the most downregulated genes in GDM-CMSCs (Table 5-1). Other genes including *ALDH1A2*, *ALDH2*, *ALDH3B1* were also significantly reduced in GDM microarray data comprising the core molecules in downregulated pathways network. The deficiency of ALDH family genes may lead to insufficient detoxification resulting in aldehydes accumulation and reactive oxygen species (ROS) imbalance. Additionally, a critical pathway for ROS regulation, the Nrf2-mediated oxidative stress response pathway, showed downregulated in GDM-CMSCs, owing to the low expression of important regulators, serine/threonine-protein kinase *PRKC* and antioxidant enzyme genes (*HMOX1*, *SOD2*, *AOX1*) (Figure 5-15B).

Other down-regulated pathways, such as “IL-6 signalling” and “HGF signalling” regulate multiple molecules involved in angiogenesis (Figure 5-13B). For instance, *CEBPB*, *FOS*, *ELK1*,

CXCL8, which are the important regulators in IL-6 and HGF signalling displayed low expression in GDM-CMSCs. Moreover, the downregulation of “PI3K/AKT signalling” may affect the potent angiogenic factors, IL-6, IL-8, HGF and VEGF signalling transduction through mediating the PI3K/AKT pathway to promote angiogenesis⁴⁴⁴⁻⁴⁴⁶. Biological function analysis identified the downregulated genes in angiogenesis and vasculogenesis that were the downstream components of IL-6, IL-8, HGF pathways, suggesting the regulatory network of reduced angiogenic potential in GDM-CMSCs. Apart from its important role in angiogenesis, PI3K/AKT signalling is also only involved in cell proliferation, growth, and metabolism⁴⁴⁷.

Negative-regulated Canonical pathways

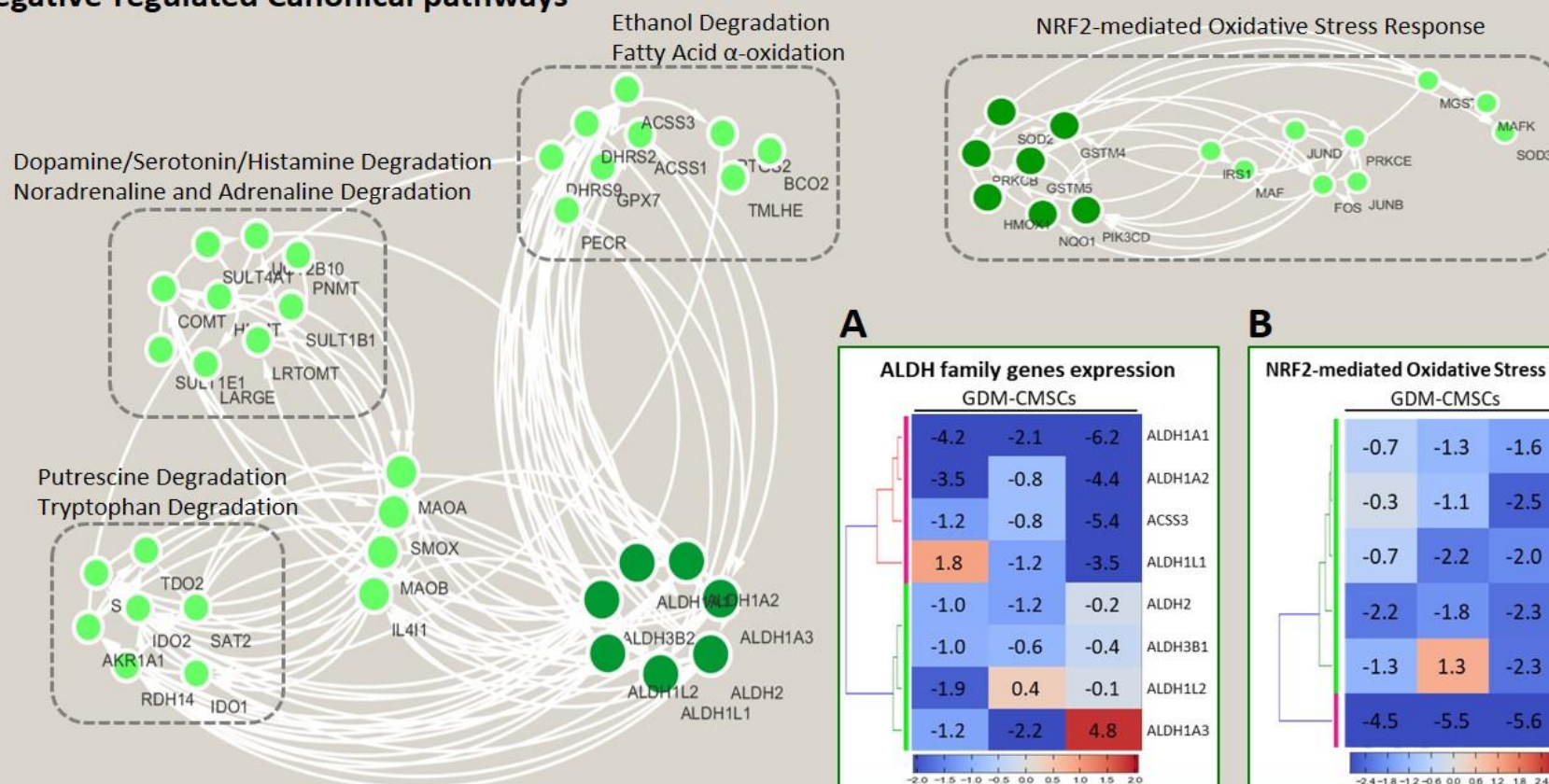


Figure 5-15. Interaction network of negatively-regulated pathways.

ALDH genes were the main molecules in the regulatory network. Networks were generated by Cytoscape visualization based on DEGs. Hierarchical clustering map showed significantly reduced in ALDH family genes expression in GDM-CMSCs and important regulators in Nrf2 pathway.

5.4.5 ALDH expression and function examination

Given that the decreased ALDH family genes expression affected several metabolic pathways and the negative activation of Nrf2-mediated oxidative stress regulation, GDM-CMSCs are likely to have imbalanced cellular ROS regulation. This may lead to increased oxidative stress, which are found in diabetic tissues⁴⁴⁸. The expression of *ALDH1A1*, *ALDH2*, *ALDH3B1* in GDM-CMSCs and H-CMSCs was validated with real-time PCR, and demonstrated significantly reduced expression levels in GDM-CMSCs (Figure 5-16). In accordance with microarray data, *ALDH1A1* was found to have a significantly decreased level of expression in GDM-CMSCs than in H-CMSCs (Figure 5-16A). Both *ALDH2* and *ALDH3B1* showed around 2-fold reduction in GDM-CMSCs with variation in individual samples (Figure 5-16B and C).

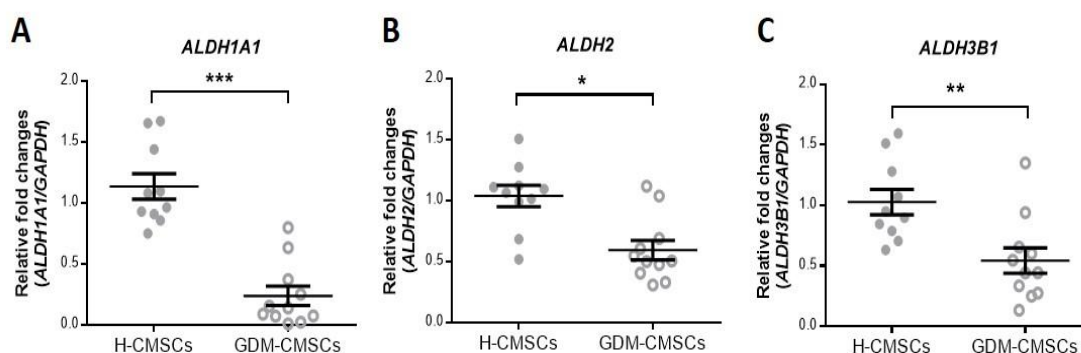


Figure 5-16. Real-time PCR validation of ALDHs expression

Validation of significantly decreased *ALDH1A1*, *ALDH2*, *ALDH3B1* expression in GDM-CMSCs. Expression level of each gene was normalised to *GAPDH* expression. Results represent mean \pm SEM. Statistical significance was determined by Student's t-test, * $p < 0.05$, ** $p < 0.01$, *** $p < 0.001$.

Low ALDH family genes expression in GDM-CMSCs may cause insufficient or impaired ALDH enzymatic function in detoxification of endogenous and exogenous aldehydes⁴⁴³. To evaluate ALDH enzymatic function, ALDH activity colorimetric assay was performed to measure the generation of nicotinamide adenine dinucleotide (NADH) during ALDH catalytic process for 30 minutes until the absorbance at 450 stop increasing. Acetaldehyde was used as a substrate to induce ALDH enzymatic activity.

In the initial 5 minutes, there was no statistical difference in ALDH activity between H-CMSCs and GDM-CMSCs. H-CMSCs and GDM-CMSCs increased ALDH activity from 0-15 minutes with continually increased catalytic efficiency but gradually declined thereafter in both groups. Of note, significantly lower levels of ALDH activity in GDM-CMSCs were observed at 10, 15, 20, and 25 minutes and the highest level of ALDH activity was seen at 15-min post-stimulation, showing significantly enhanced activity in H-CMSCs (Figure 5-17). The results confirmed that lower express of ALDH in GDM-CMSCs vs. H-CMSCs affected the enzymatic function of ALDH in detoxification.

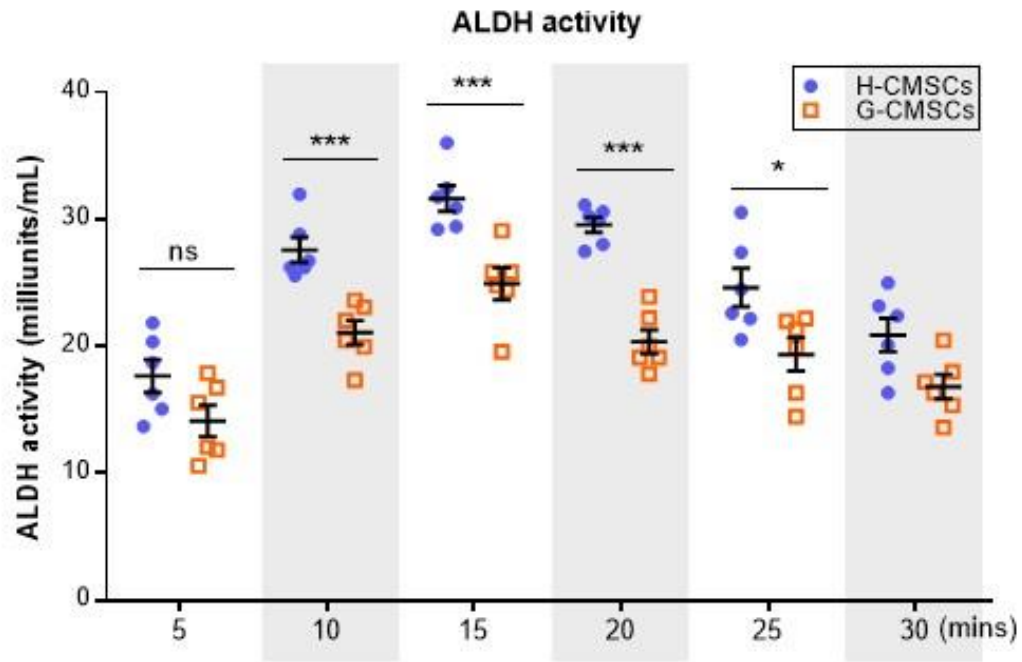


Figure 5-17. ALDH enzymatic activity

Reduced ALDH enzymatic function was detected in GDM-CMSCs by ALDH activity colorimetric assay measuring the absorbance at 450 nm. The results were obtained from 6 H-CMSCs (Healthy03-08) and 6 G-CMSCs (GDM04-09) samples in duplicate represented as mean \pm SEM. Statistical significance was determined by one-way ANOVA, * p < 0.05, ** p < 0.01, *** p < 0.001

5.4.6 ROS and oxidative stress

With impaired ALDH activity, accumulation of highly reactive and toxic aldehyde tends to induce ROS formation and increase oxidative stress. A significant reduction of antioxidative enzymes in GDM-CMSCs may lead to a deficiency in antioxidant defences. The detoxification enzymes NAD(P)H quinone dehydrogenase (*NQO1*) induced by Nrf2 signaling was significantly reduced in GDM-CMSCs (Figure 5-17). Likewise, the expression of superoxide dismutase (*SOD2*) located in mitochondria regulating antioxidant defences was also significantly downregulated in GDM-CMSCs (Figure 5-17). Owing to the reduction in antioxidative enzyme expression, GDM-CMSCs is therefore likely to have elevated cellular oxidative stress.

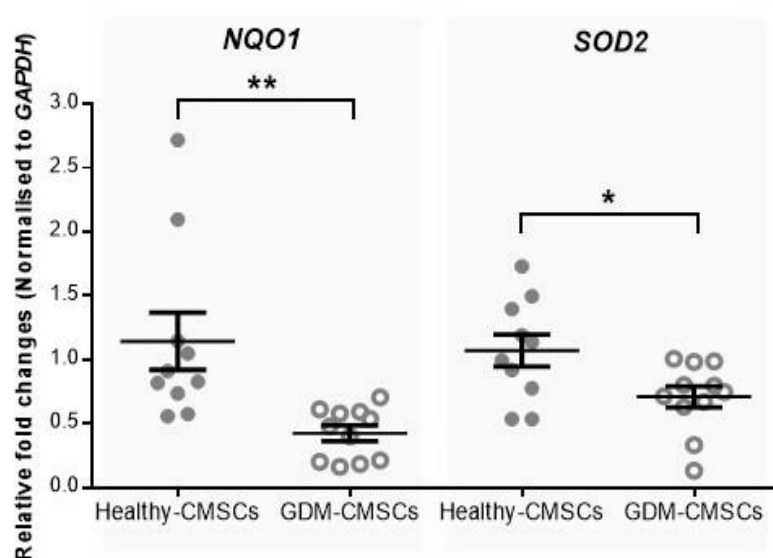


Figure 5-18. Real-time PCR validation of antioxidative enzyme expression

The expression of *NQO1* and *SOD2* involved in Nrf2-mediated oxidative stress pathway were significantly reduced in GDM-CMSCs. Expression level of each gene was normalised to *GAPDH* expression. Results represent mean \pm SEM. Statistical significance was determined by Student's t-test, * $p < 0.05$, ** $p < 0.01$

To examine the ROS production, H-CMSCs and GDM-CMSCs were treated with glucose to induce metabolic activity as hyperglycaemia is known to induce ROS levels in diabetes patients⁴⁴⁸. H₂O₂ treated-cells were used as positive control. ROS production was detected using the cell permeant reagent 2',7'- dichlorofluorescein diacetate (DCFDA) which showed green fluorescence once being oxidised by cellular ROS. After treating with 25 mM glucose for 30 minutes, both H-CMSCs and GDM-CMSCs had increased ROS production without significant difference between two groups. However, higher level of cellular ROS was observed in GDM-CMSCs after 2-hour glucose treatment which showed increased intensity of fluorescence compared to H-CMSCs (Figure 5-19A).

ROS production and changes over a period of time were quantified by measuring fluorescence via a plate reader. Observing the ROS production every 15 minutes, the ROS levels increased for first 45 minutes in both H-CMSCs and GDM-CMSCs following stimulating with glucose. The amount of ROS production was comparable in H-CMSCs and GDM-CMSCs. Between 45 to 90 minutes, ROS level showed significantly higher rates of increase in GDM-CMSCs than H-CMSCs. Notably, H-CMSCs did not produce increased amounts of ROS after 90 minutes and showed slightly reduced ROS generation whereas ROS level in GDM-CMSCs continued to increase and remained elevated from 90 minutes to the end of measured period (Figure 5-19B).

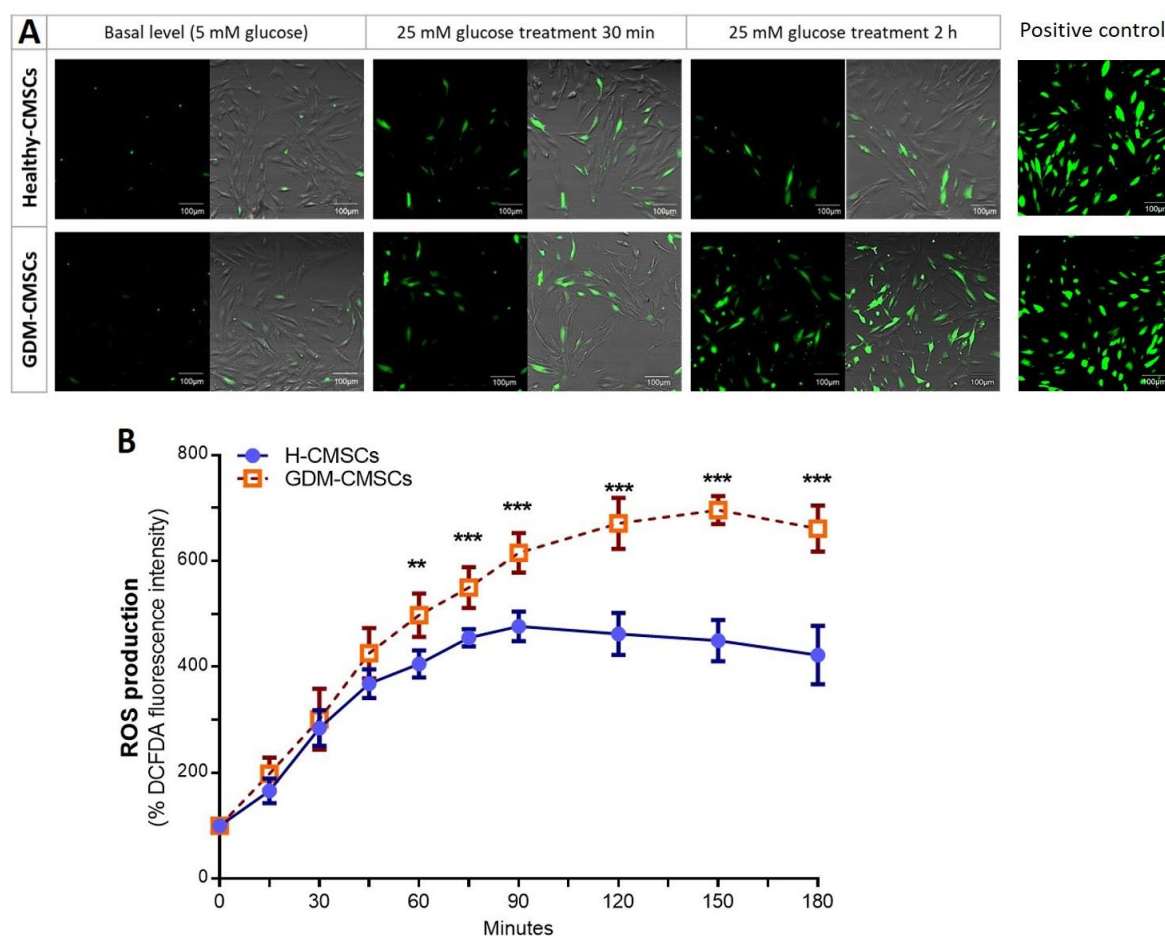


Figure 5-19. Detection of ROS production by DCFDA

(A) ROS production was detected by DCFDA staining (green). Representative fluorescent images were shown from 5 H-CMSCs (Healthy03-07) and 5 G-CMSCs (GDM04-08) samples at different time point and imaged by confocal microscopy. Scale bar, 100 μ m. H_2O_2 -treated H-/G- CMSCs were used as positive controls (B) Time-course measurement of ROS levels was determined by fluorescent intensity reading via a plate reader at the wavelengths of Ex/Em = 485/535 nm. The initial fluorescence intensity at 0 min was set at 100%. Data are given as mean \pm SEM from at least 6 samples in each group. Statistical significance was determined by one-way ANOVA, * p < 0.05, ** p < 0.01, *** p < 0.001

To further elucidate the role of ALDH activity and ROS regulation, the enzymatic function of ALDHs was suppressed by 100 μ M of N, N-diethylaminobenzaldehyde (DEAB), a commonly used selective inhibitor of ALDHs. H-CMSCs and GDM-CMSCs were incubated with DEAB for 48 hours and ALDH activity was examined. In the presence of DEAB (ALDH inhibitor) the ALDH activity was significantly suppressed in both H-CMSCs and GDM-CMSCs (Figure 5-20A). Moreover, when the ALDH function was suppressed, the ROS production was significantly increased during glucose-induced metabolic process (Figure 5-20B). DEAB pre-treated H-/GDM- CMSCs produced higher levels of ROS than un-treated H-/GDM- CMSCs. This finding suggested the strong association between the ALDH function and cellular ROS regulation.

Low levels of ROS are detectable in many metabolic processes; however, when ROS production is in excess of the cellular antioxidant capacity, it contributes to cellular damage. This can include DNA, protein, and lipid disruption. In GDM-CMSCs, downregulation of Nrf2-mediated oxidative stress regulation pathway and the impaired function of detoxifying enzymes ALDHs, suggests insufficient capacity to adapt to increased oxidative stress.

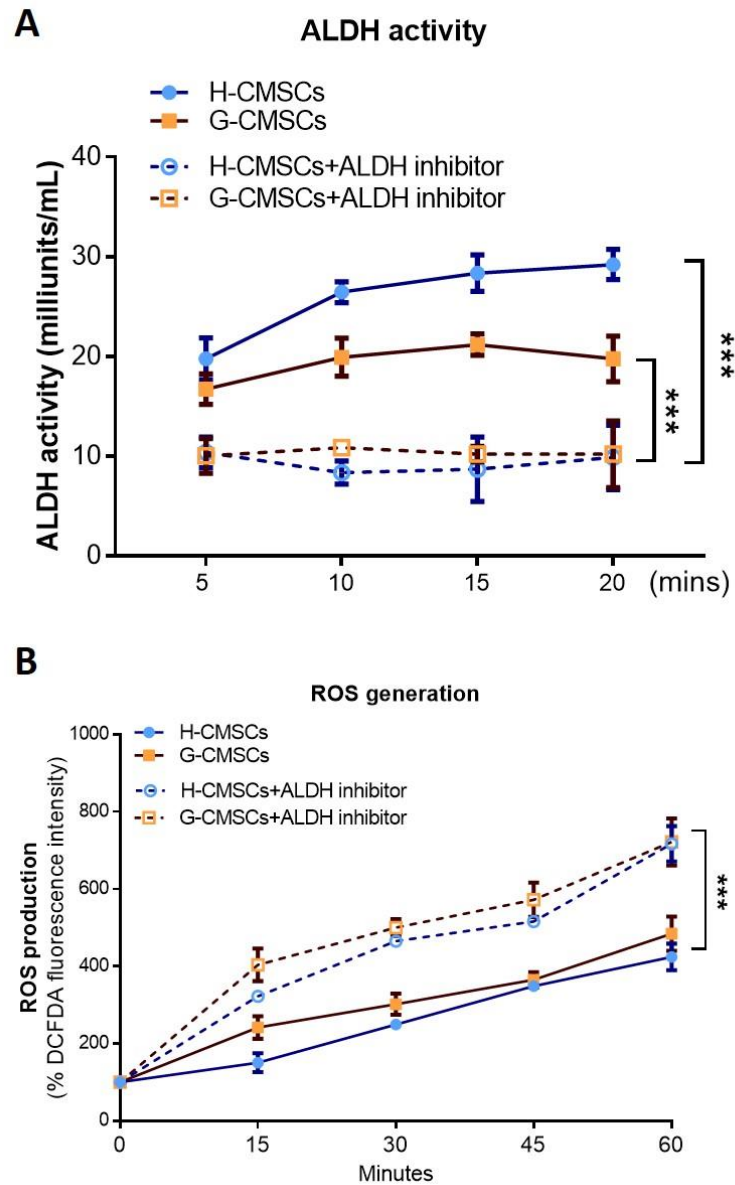


Figure 5-20. Inhibition of ALDH function by DEAB

5 H-CMSCs (Healthy03-07) and 5 G-CMSCs (GDM04-08) samples were pre-incubated with 100 mM DEAB for 48 hours. (A) ALDH enzymatic function was detected by ALDH activity colorimetric assay measuring the absorbance at 450 nm. (B) ROS generation was detected by DCFDA and the increasing level was determined by fluorescent intensity reading at the wavelengths of Ex/Em = 485/535 nm. The initial fluorescence intensity at 0 min was set at 100%. Data are given as mean \pm SEM. Statistical significance was determined by one-way ANOVA, *** $p < 0.001$

5.5 Discussion

Overrepresented and underrepresented biological functions in GDM-CMSCs

Microarray revealed that GDM had a number of upregulated genes involved in cell motility, cytoskeleton organization, survival, and together with epithelial development and skin formation. The ability of transplanted cells to mobilise and migrate to injury sites enables them to mediate tissue repair and regeneration⁴⁴⁹. According to IPA pathway analysis, the upregulation of Rho family GTPase signalling in GDM-CMSCs modulating actin cytoskeletal rearrangement is one of the fundamental migratory pathways⁴⁵⁰. Recently, a study showed that high glucose promoted human umbilical cord-derived MSCs migration ability and increased migration of transplanted MSCs into wound area in *in vivo* mouse models through the suppression of adhesion molecule, E-cadherin⁴⁵¹. Hyperglycaemia induced human induced pluripotent stem cells to express cytoskeleton remodelling regulators and enhanced their migration⁴⁵². Human umbilical endothelial cells isolated from GDM compared to healthy pregnancies showed increased migration ability although enhanced motility could be reflecting a proangiogenic state of GDM⁴⁵³.

By contrast, the opposite findings such as reduced wound closure ability in perivascular stem cells from GDM women⁴⁵⁴ and impaired migration in GDM umbilical cord-derived endothelial cells were also reported⁴⁵⁵. The controversial effects of GDM on cell motility may due to different cell sources; for instance, in chapter 3 we demonstrated opposite growth patterns of GDM-AMSCs and GDM-CMSCs compared to their healthy counterparts. Although CMSCs and AMSCs were grown in the same GDM condition, they could show different response to the same environmental factor and have different biological characteristics. Likewise, GDM environment may have different impacts on migration

ability in different placenta-associated cell types. Our results based on microarray analysis of CMSCs demonstrated that *AQP1*, *FLNB*, *CELSR1*, and *CD24* playing important roles in cell movement and cytoskeletal remodelling were significantly upregulated in GDM-CMSCs. The finding was further verified by migration assays to confirm the enhanced motility of GDM-CMSCs.

Despite of migration to the wound area, the ability of MSCs to differentiate and promote regeneration accelerates wound repair processes⁴⁵⁶. Several studies have indicated that the multi-lineage differentiation potential of perinatal tissue-derived MSCs enable them to develop into epithelium and promote skin regeneration⁴⁵⁷⁻⁴⁵⁹. Dehydrated placental membranes (amnion and chorion) have been used as skin substitute for burned and ulcerated surfaces for many years^{141, 460}. Nowadays, cryopreservation technology is able to maintain the structural and cellular integrity of placental membranes and retain endogenous amniotic and chorionic MSCs vitalisation. The presence of MSCs in cryopreserved placental membranes improved wound-healing therapies^{461, 462}. Microarray analysis identified increased skin regeneration potential in GDM-CMSCs characterised by the upregulation of epithelial development associated genes and regulators (*EDN1*, *KRT14*, *HBEGF*, *TGFB2*). The *in vitro* wound healing assays and activation of growth factors signalling (Wnt/ β -catenin, BMP) may also contribute to enhanced capacity of GDM-CMSCs in wound repair. In line with a microarray study of BM-MSCs, the expression of genes associated with wound healing was upregulated in BM-MSCs from type 1 diabetes patients although the enhanced wound closure was not observed in their *in vitro* results⁴⁶³.

In addition, activation of growth factors pathways, including Wnt/ β -catenin, BMP, FGF, and STAT3 was also positively associated with cardiogenesis in GDM-CMSCs and significant

upregulation of heart development-related genes (*NKX2.5*, *NOG*, *PDGFA*). However, the increased activation of Wnt/ β -catenin pathway may be associated with metformin treatment or the activation of insulin signal. One of Wnt pathway effectors is insulin/insulin-like growth factor receptor-dependent activation, which induces phosphorylation of various kinase protein in Wnt pathway⁴⁶⁴. Metformin were also reported to mediate Wnt/ β -catenin signalling in hepatic cells and intestinal cells^{465, 466}. FGF family proteins are involved in the regulation of energy metabolism and hyperglycaemic condition⁴⁶⁷. FGF-2 was significantly upregulated in diabetic nephropathy and high glucose environment increased FGF-2 mRNA as well as protein synthesis and secretion in human renal fibroblasts⁴⁶⁸. Thus, the enhanced activation of FGF pathway in G-CMSCs might also reflect the metabolic disorder condition in GDM women.

Cardiovascular development was the most enriched function in GDM-CMSCs; however, the downregulation of angiogenic factors (*RASIP1*, *CXCL12*, *RSPO3*) and angiogenesis inducing pathways (IL-6, IL-8) resulted in reduced vasculogenesis and angiogenesis potential in GDM-CMSCs. The reduced expression of angiogenesis-related genes in GDM-CMSCs might suggest that CMSCs did not contribute to frequently observed hypervascularisation in GDM placentas⁷⁷. The vasculogenesis and angiogenesis in placenta are regulated by placental endothelial cells which are derived from mesoderm during embryogenesis⁴⁶⁹ while CMSCs arise from extraembryonic tissues. Different origins of placental CMSCs and endothelial cells may result in different biological properties and responses under hyperglycaemic environment. High glucose environment induced endothelial cell dysfunctions leading to abnormal angiogenesis in diabetes patients^{470, 471}. However, enhanced angiogenesis was not found in CMSCs isolated from GDM women. In contrast, G-CMSCs showed reduced potential in angiogenesis. Our findings indicated that G-CMSCs were not directly involved in hyperglycaemia-induced angiogenesis. In line with

a recent study on placental chorionic villi-derived MSCs, the decreased tube formation ability and downregulation of VEGF were observed in GDM vs. healthy pregnancies⁴⁷².

ALDHs activity and ROS regulation

Pathways associated with several degradation processes were altered in GDM-CMSCs due to the significantly reduced ALDHs expression. As a critical detoxification enzyme, ALDH is highly expressed in various embryonic tissues, stem cells, progenitor cells^{473, 474} and protect them against oxidative damages by detoxifying exogenous and endogenous aldehyde⁴⁷⁵. ALDH was also used as an indicator for purifying proangiogenic BM-MSC subset with an enhanced secretory function for vascular regeneration⁴⁷⁶. However, the role of ALDHs in GDM placenta-derived MSCs has yet to be examined. Significantly reduced ALDH family genes in GDM-CMSCs revealed by our microarray data emphasises the impact of pregnancy complication on cellular detoxification. GDM-CMSCs showed significantly lower ALDHs enzymatic activity than H-CMSCs and insufficient capacity to manage increased oxidative stress induced by environmental stimulation with glucose.

The hyperglycaemic environment in GDM pregnancies tends to induce elevated ROS production and oxidative stress⁴⁷⁷. Although ROS can be induced by various molecules undergoing metabolic activities, glucose uptake is one of the major processes that stimulates instant ROS generation^{478, 479}. In diabetes patients, hyperglycaemic condition led to ROS imbalance and resulted in ROS-induced cellular damage and cell death⁴⁸⁰. We demonstrated that glucose induced instant ROS production in both H-CMSCs and G-CMSCs whereas the reduction of ROS levels in H-CMSCs after 1.5 hours was not seen in G-CMSCs. It suggested that G-CMSCs showed less capability of adapting to the instant increase in

ROS production than H-CMSCs.

In addition, impaired ALDH activity may exacerbate oxidative stress levels through causing ROS imbalance⁴⁸¹. Some studies have reported an association between impaired ALDH function and oxidative stress production. For instance, inhibition of *ALDH1A1* in human lens epithelial cells caused increased oxidative stress and induced mitochondrial damages⁴⁸². In an *in vivo* study, *ALDH2*-deficient mice showed increased ROS production and enhanced oxidative stress leading to cardiovascular complications⁴⁸³. We found higher levels of ROS was induced in GDM-CMSCs vs. H-CMSCs upon glucose stimulation and increased ROS levels in GDM-CMSCs showed no sign of reduction in our observation period. It is likely that improving ALDH function may enhance detoxification, reduce ROS formation, and therefore protect GDM-CMSCs from oxidative cell damage^{484, 485}. A recent study showed that treating decidual MSCs derived from preeclampsia women with *ALDH1A1* activator restored *ALDH1A1* activity and improved resistance to H₂O₂-induced oxidative stress in preeclampsia-derived MSCs⁴⁸⁶. Physiologically harmful environment of oxidative stress in GDM can be improved by antioxidants intake^{487, 488}; however, restoring ALDH function in GDM women might be another therapeutic option and fundamentally improve biological properties of GDM-CMSCs.

5.6 Summary

DNA microarray data provides an understanding of gene profile and biological functions altered in GDM-CMSCs which offers a valuable resource to the regenerative medicine development. To conclude from our findings, the uterine environment during pregnancy could impact on the stem cell biology derived from perinatal tissues. Enhanced migration ability of GDM-CMSCs may have clinical benefits for promoting systemically infused MSCs to migrate to the injured sites. However, detoxification enzyme ALDHs were significantly reduced in GDM-CMSCs leading to downregulation of several degradation pathways. Decreased ALDH activity in GDM-CMSCs was also associated with impaired ability to respond to oxidative stress with the evidence of elevated ROS production after glucose stimulation. The information based on microarray can be useful for exploring suitable clinical use of CMSCs from GDM and healthy pregnancies.

Advantages of G-CMSCs vs H-CMSCs	Disadvantages of G-CMSCs vs H-CMSCs
a) Enhanced migration ability with increased cytoskeleton organisation gene expression	a) Reduced proliferation and colony formation ability
b) Potential in promoting wound healing with skin formation and epithelium development	b) Low expression in vasculogenesis-associated genes
c) Increased cardiogenesis-associated gene expression	c) Impaired ALDH enzymatic function
d) Increased activity in growth factor pathway - BMP, Wnt/ β -catenin, and FGF pathways	d) Poor response to glucose-induced ROS

Chapter 6

Discussion, Conclusion and Future Work



6.1 Summative discussion and conclusion

6.1.1 Human placenta – an attractive source of MSCs

Regenerative medicine based on MSCs is aimed at enhancing tissue regeneration, restoring and maintaining the normal function of tissues or organs and also intended to assist in the treatment of many life-threatening or chronic, lifelong disease. Although bone marrow MSCs are the most popular and widely studied MSCs for many years, concerns about BM-MSCs^{489, 490} such as decreased numbers and stemness with donor's age, invasive isolation procedure, and allogeneic transplant rejection have encouraged researchers to explore new sources of MSCs. Nowadays, stem cells have been found in various adult tissues, neonatal-related tissues, and also induced pluripotent stem cells.

Placenta, developing during pregnancy and playing a pivotal role in embryogenesis, contains plentiful undifferentiated stem cells⁴⁹¹. As being a part of extra-embryonic tissues without the need for invasive procedures during cell extraction or ethical concerns, placenta has many advantages for MSCs therapy. The opportunity of storing perinatal stem cell in biobanks, including cord blood stem cells and placental stem cells, makes them rapidly available and become promising autologous sources for clinical applications^{492, 493}. There is no doubt that placental MSCs hold a great therapeutic potential; however, these MSCs emerge during pregnancies and only accessible postpartum whether biological properties of placental MSCs altered by pregnancy complications is unclear. Little is known about the effects of GDM on placenta-derived amniotic and chorionic MSCs.

In this study, cells were isolated from human placentas. To confirm their MSCs phenotype, firstly, cells derived from amniotic and chorionic membrane displayed attached fibroblast-

like morphology, which is normally observed in MSCs culture. Secondly, cells were examined for surface markers expression by flow cytometry to meet the minimal definition criteria for MSCs according to the International Society for Cellular Therapy¹⁰⁹. H-/G- CMSCs/AMSCs showed positive expression of CD73, CD90, CD105 and lacked the expression of CD14, CD19, CD34, CD45 and HLA-DR. Thirdly, these cells demonstrated differentiation ability towards mesenchymal lineage, such as osteogenesis, adipogenesis, and chondrogenesis.

Characterisation of CMSCs and AMSCs from GDM and healthy placentas demonstrated significantly fundamental differences between CMSCs and AMSCs and evidenced the altered proliferative, adipogenic, immunomodulatory potential in CMSCs/AMSCs derived from GDM placentas. CMSCs and AMSCs were isolated from different layers of placental membrane - chorion and amnion. Two layers are connected together acting as a protective barrier during fetal development and MSCs derived from both chorion and amnion are thought to have the same origin; however, they were found displaying distinct characteristics in our study. CMSCs showed enhanced proliferation and tri-lineage differentiation potential compared with AMSCs regardless of deriving from GDM or healthy placenta. Secretome of both CMSCs and AMSCs displayed immunomodulatory capacity in regulating T-cell proliferation and macrophage polarisation but more profound effects were found in CMSCs.

GDM is a temporary condition that usually disappears after pregnancy but it has long-term impacts on maternal health and fetal development. Embryonic stem cells and MSCs emerging during pregnancies are likely to be compromised by pregnancy complications. We found that GDM had distinct effect on CMSCs and AMSCs, for instance, altered proliferation ability was found in G-CMSCs and G-AMSCs vs. their healthy counterparts

while GDM affected CMSCs and AMSCs proliferation in an opposite manner. Likewise, adipogenic potential showed significantly enhanced in GDM-CMSC but not in GDM-AMSCs. Some studies have also demonstrated the influence of GDM on umbilical cord cell. Umbilical vein endothelial cells (HUVECs) and Wharton's jelly derived MSCs (WJ-MSCs) from GDM pregnancies showed decreased glucose uptake and mitochondrial oxygen consumption, increased generation of ROS, reflecting a metabolic disorder state in GDM women⁴⁹⁴. These alterations might be associated with endothelial dysfunction leading to adverse vascular functions in infants⁴⁹⁵. A study indicated that mitochondrial transcription and biogenesis gene expressions were altered in GDM-WJ-MSCs which contributed to impaired mitochondrial functions⁴⁹⁶ and may play a role in impaired insulin release and glucose sensitivity⁴⁹⁷.

Umbilical cord MSCs (UC-MSCs) isolated from obese pregnancies demonstrated greater adipogenesis tendency and less potential for myogenesis through the regulation of Wnt/glycogen synthase kinase (GSK)-3 β / β -catenin pathway⁴⁹⁸. In correspondence to the clinical finding that fetuses development in obese women have higher infant adiposity^{499, 500}. In chapter 3, we also found that CMSCs derived from GDM placenta showed enhanced adipogenic commitment with higher basal level of adipogenic-related gene expression and more responsive to the stimulation of adipogenesis differentiation media leading to enhanced adipocytes generation. Obese and GDM pregnancies have similar intrauterine environment - high levels of glucose and placental hormones, and this environment is usually found to have increased amount of adipocytes^{501, 502}. One of the hormones shows significantly increased in many obese and GDM pregnancies is insulin⁵⁰³, which is a common inducer for adipogenesis used in differentiation media⁵⁰⁴. High glucose condition was also reported to induce adipocyte-associated gene expression, such as proliferators activated receptor gamma (PPAR γ), lipoprotein lipase (LPL), and adiponectin⁵⁰⁵, and might

be a potent inducer for adipogenic commitment^{506, 507}.

Immunosuppressive capacity of MSCs contributes to significant therapeutic outcomes of cell therapy. Little is known about the effects of GDM environment on immunomodulatory ability in either placenta-derived MSCs or umbilical cord-derived MSCs. A study examining UC-MSCs from obese/diabetic women indicated that the expression of genes involved in MSCs immunomodulatory ability, such as HLA-G was detected at passaged 2 and reduced in subsequent passages while the reduction was not observed in healthy UC-MSCs. However, except for HLA-G gene examination by PCR, there was insufficient evidence of the altered immunomodulatory function in MSCs derived from obese/diabetic samples⁵⁰⁸. Therefore, our study investigated the immunomodulation in both H-MSCs and GDM-MSCs through secretome regulation on T-cell proliferation and activation as well as macrophage polarisation by co-culture system. The findings suggested that GDM- and H- CMSCs provided an equivalent immunoregulatory effect on T-cells while GDM-CMSCs had a reduced effect on macrophage regulation. However, both H- and GDM- CMSCs displayed a superior immunomodulatory capacity in regulation of both T-cells and macrophages than AMSCs.

Although some degrees of alterations were observed in GDM-CMSCs/AMSCs, the differentiation potential (osteogenesis, chondrogenesis), immunophenotype, and immunosuppressive ability were not significantly hampered by GDM environment. Most of the characteristics of GDM-CMSCs investigated in chapter 3 were comparable with H-CMSCs and same as GDM-AMSCs vs. H-AMSCs.

6.1.2 IPC generation – an application of autologous MSCs for diabetes therapy

Women with GDM during pregnancy carry a lifetime risk of developing type 2 diabetes of

up to 50-60%⁵⁰⁹. Infants born to GDM pregnancy are also at risk of type 2 diabetes in early adulthood. Exploring the regenerative potential of placental MSCs from GDM women provides a promising possibility of using autologous MSCs in future diabetes therapy. Differentiating autologous stem cells *in vitro* and then transplanting to the patients themselves eliminates the complications of graft rejection or requirements of immune suppression regimen in transplantation⁵¹⁰. A clinical study of diabetic patients on insulin injection receiving autologous bone-marrow stem cells transplantation showed an improvement of more than 50% reduction in insulin requirement⁵¹¹. However, in that study, the cell population used was a mixture of bone marrow HSCs and MSCs, and there was no complete follow-up study or the understanding of regulatory functions of transplanted cells in disease management. On the other hand, BM-MSCs from diabetic patients were generally thought to have been influenced under a prolonged diabetic environment. In diabetic mice models, a reduction in the numbers of endogenous BM-MSCs, impaired proliferation, survival, differentiation ability of BM-MSCs were reported^{512, 513}.

BM-MSCs from diabetic patients may be significantly influenced by prolonged exposure to hyperglycaemic and inflammatory environment for several years, while placental MSCs only emerge during pregnancy and could be more pluripotent than BM-MSCs. GDM environment affects some biological properties of CMSCs/AMSCs but does not entirely hamper their differentiation capacities. Through characterisation in chapter 3, we evidenced that GDM-CMSCs and AMSCs were able to demonstrate their stem cell functions via differentiation and immunomodulation; thus we sought to further investigate their therapeutic potential in diabetes cell therapy.

MSCs are known to have potential in pancreatic islets regeneration and insulin resistance

amelioration²⁰²; however, transplanted MSCs were not found to spontaneously convert to beta-cells or secrete insulin⁵¹⁴⁻⁵¹⁶. There are also some concerns regarding teratoma formation and the promotion of tumour growth by transplanting undifferentiated MSCs⁵¹⁷⁻⁵¹⁹. Therefore, generating insulin-producing cells (IPCs) or engineered islet-like clusters from MSCs, progenitor cells, or genetically modified cells have offered an alternative approach for diabetes therapy. In order to induce IPC generation from MSCs, several growth factors and small molecules were used to mimic beta-cell development environment, while cell responses to these stimulations varies in different tissue-derived MSCs.

We optimised a feasible approach for generating IPC from GDM-CMSCs and H-CMSCs with the ability to respond to glucose challenge and secrete insulin. GDM-CMSCs and H-CMSCs derived IPCs were functionally indistinguishable with similar morphology, comparable levels of beta-cell markers expression, and insulin secretion ability. However, IPCs differentiation method for GDM- and Healthy- AMSCs requires further optimisation. Although our study identified betacellulin as a potent inducer for insulin expression in AMSCs, insulin secretion function was not therefore improved. Insulin secretion is regulated by several internal or external factors, including insulin synthesis, insulin exocytosis, glucose sensing, functional structure formation, and environmental stimulation⁵²⁰⁻⁵²². The insufficient insulin secretion of AMSC-IPCs in our study requires further investigation. Overall, our findings conclude that for the efficiency of autologous therapies for GDM women, endogenous CMSCs is a potential therapeutic target which could be clinically applicable to diabetes treatment in the future.

While the advances of generating mature and glucose responsive IPCs from stem cells have brought a new strategy for diabetes treatment, the application in clinical practice

remains challenging. By stimulating with various compounds to induce IPC differentiation, the effective concentrations are inconsistent in different studies even though some studies used the same MSC source. Identifying specific cell surface markers for each stage of beta-cell regeneration may improve current IPC generation protocols⁵²³. Additionally, the intensively laboratory process of IPC production has reduced the willingness of investments in clinical research. Moreover, although research has showed that MSC-generated IPCs were able to secrete adequate amount of insulin in preclinical models, scientists are still struggling to find well-defined and reproducible condition of MSC-derived IPCs and mass production of mature beta-cells to meet clinical needs^{517, 523-525}. In present study, we evaluated the potential of using autologous CMSCs from GDM women for clinical application to diabetes treatment in the future. The IPC differentiation approach can be successfully applied to both H-CMSCs and GDM-CMSCs; however, differentiation method for AMSCs requires further optimisation and the long-term outcomes of using autologous MSC-derived IPCs needs to be investigated.

6.1.3 Microarray – insights of gene profile to functional molecular levels

Microarray technology allows scientists to study expression levels of a large number of genes at the same time. The large amount of data provided by microarrays requires computational analysis through bioinformatics approaches to explore biological meaningful hypothesis. We performed DNA microarray to further understand the characteristics of H-CMSCs and GDM-CMSCs. However, the limitation in present study was low sample sizes. In microarray data, gene profiles of 3 GDM-CMSCs samples showed variable expression with certain degrees of variability between each other while 3 H-CMSCs samples were relatively consistent. The scatter plot shown in Figure 6-1 demonstrated the relationship of expression patterns and variability in two experiments.

Gene with similar expression levels in two samples appeared a smooth linear curve while a non-linear indicates variation between two samples. An ideal experimental group with low variation should have a linear curve in the comparison of two independent samples within the same group. In Figure 6, three H-CMSCs samples showed high level of similarity while three G-CMSCs samples demonstrated some degrees of variation. Given that three G-CMSCs samples were collected from women received different treatments, it could have impact on their gene expression patterns and cause the variation. It is likely that increasing GDM sample sizes and analysing gene expression patterns based on different GDM treatments would provide more information regarding GDM-CMSCs transcriptional profile and reduce the variations.

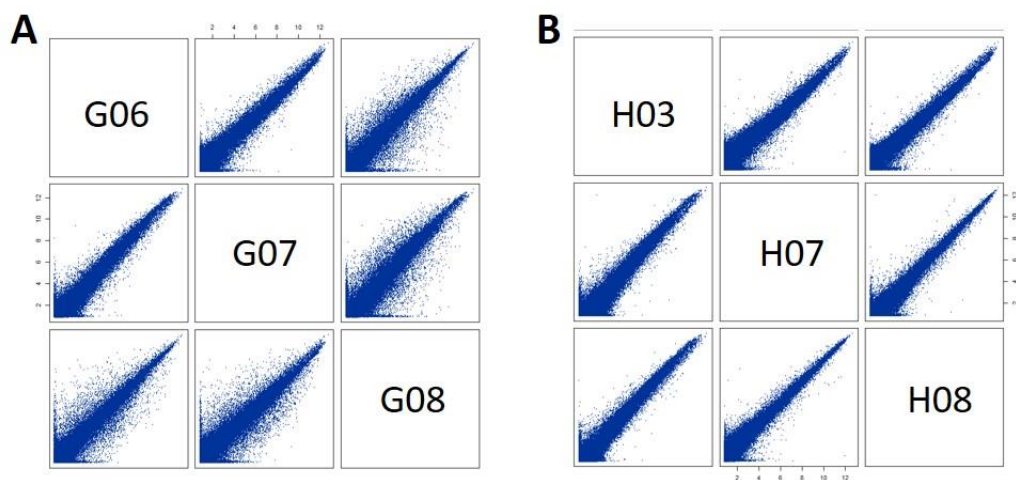


Figure 6-1. Scatter plot matrix of microarray data

(A) Three GDM-CMSCs (GDM06, 07, 08) and (B) three H-CMSCs (H03, 07, 08) used for microarray experiment. A scatter plot is used to examine each microarray chip that has unusual/similar expression patterns compared to other microarray chips during fluorescent intensity detection. It can be used to visualise variations in gene expression between two arrays. Gene with similar expression levels in two samples appeared a smooth linear curve. In contrast, a non-linear curve indicates variations between two samples. The X and Y axes are the normalised intensity for the samples (log2 scaled), normalised to RNA control (poly A⁺ RNA with Spike-IN, Figure 5-1) and experimental control (healthy group), respectively.

Importantly, we validated gene expression by real-time PCR with 10 healthy and 11 GDM samples in order to verify the microarray results. The PCR is commonly used for microarray validation but some non-agreeing results of microarray and real-time PCR has been discussed, such as the difference in expression fold changes^{526, 527}. In our study, although expression fold changes of some validated genes were found to have different expression levels between microarray and real-time PCR results, the up- or down- regulated states were all in agreement with microarray data.

To gain insight into the biological characteristics of GDM-CMSCs, co-upregulated and co-downregulated genes in all 3 GDM samples were identified and used for biological functions and pathways analysis. Furthermore, gene regulatory networks reveal the alterations in a set of genes and pathways that regulate biological processes instead of simple activation or inhibition of a single gene or signaling⁵²⁸. Following microarray analysis with IPA software, functional assays confirmed the overrepresented or underrepresented biological functions in GDM-CMSCs, including enhanced cell migration and spreading ability but an impairment in ALDHs enzymatic function and ROS regulation. The validation and investigation of the most represented biological functions in GDM-CMSCs was discussed in chapter 5 while the information obtained from microarray data may also be useful in many other aspects^{529, 530}. Microarray results, containing the expression of thousands of genes, can be used to study the drug target for GDM, association between GDM and the risk of type 2 diabetes, gene correlation with GDM progression, as well as transcriptional signature of GDM-CMSCs. For instance, *PTAFR* (platelet activating factor receptor), *CMYA5* (cardiomyopathy associated 5), and *CCR7* (C-C Motif chemokine receptor 7) were detected in H-CMSCs but absent in GDM-CMSCs while *PROM2* (prominin 2) and *GDF6* (growth differentiation factor 6) were only detectable in GDM-CMSCs. The presence or absence of these genes could be meaningful in some

biological properties of H-CMSCs and GDM-CMSCs. Undoubtedly, there is still a lot remained to be explored in our microarray data.

The main aim of this study is to determine the potential of GDM-MSCs in regenerative medicine. Through characterisation in chapter 3, we investigated stem cells properties and showed that both Healthy- and GDM- CMSCs/AMSCs were able to grow, proliferate, differentiate, and regulate immune cells *in vitro*. Moreover, GDM-CMSCs could be successfully differentiated into IPCs and display comparable functions with H-CMSCs derived IPCs, suggesting a promising potential for diabetes therapy in the future. Through microarray transcriptional profiling and bioinformatics, we were able to identify the enhanced and impaired biological functions in GDM-CMSCs based on their genome profile and this information would be valuable for developing potential application of GDM-MSCs in clinical practice.

The increasing incidence of metabolic diseases during pregnancy affects the physiology of several maternal and fetal organ developments⁵³¹. Maternal nutrients and metabolic activities significantly link to fetal programming and the later development of metabolic disorders in mothers and their children^{532, 533}. GDM environment affected the epigenetic signature of cord blood⁵³⁴ and newborns exposed to GDM were more likely to have epigenetic differences in metabolic pathways⁵³⁵. We demonstrated that biological properties of CMSCs/AMSCs were altered in GDM pregnancy, including the increased adipogenic potential, immature senescence under high glucose culture, decreased metabolic enzyme (ALDHs) activities, and down regulation in metabolic pathways activation. These findings reflect the influence of GDM on cell biological properties and the altered features in GDM-CMSCs/AMSCs might be associated with the long-term risk of type 2 diabetes development. For instance, increased adipocyte formation and

accumulation were found in many obese diabetes patients⁵³⁶; senescence-associated secretory phenotypes (SASP) that secreted proinflammatory cytokines and exacerbated insulin resistance were frequently seen in type 2 diabetes patients^{537, 538}. The study of GDM-CMSCs/AMSCs would provide further understanding of the fetal and maternal metabolic disorder development.

The findings in our study were obtained by using H-CMSCs, H-AMSCs, G-CMSCs, and G-AMSCs as a single experimental group. However, the individual differences within each group may cause variabilities in some results. For example, the severity of GDM and different treatment methods may have direct impact on biological characteristics in individual samples. At this stage, we were unable to collect more GDM placentas for further analysis, but in future study, treatment methods and blood glucose levels of each patient should be taken into account. Increasing sample size and experimental groups such as high-BMI GDM, low-BMI GDM, metformin-treated GDM, or insulin-treated GDM would reduce variabilities and provide further understating about GDM-MSCs.

6.2 Future work

Our study has raised a number of considerations for future work. First, as autologous cell transplant is aimed at personalised medicine, variation in individual donor condition correlating to the CMSCs/AMSCs differentiation and characterisation result should be taken into account. For future study of GDM-MSCs, considering the individual differences during analysis, including glycaemic control and medical condition in each patient would provide more detailed understanding of GDM-MSC biological properties.

In this study, all gene expressions were examined by SYBR-Green based real-time PCR, which is a highly specific, double-stranded DNA binding dye. However, genes with low expression levels are difficult to be detected by SYBR-Green dye and the small gene copy variations between samples are likely to be neglected. Thus, future study using TaqMan-based PCR via a fluorogenic probe will allow the detection of small gene copy variations and provide more accurate gene expression results than SYBR-Green based method.

To apply autologous MSC-generated IPCs in clinical practice the safety and efficacy of these IPCs for cell therapy need to be investigated. By using *in vivo* models, it would provide further understanding of the maturity, function, and survival of IPCs in a physically relevant situation. Although some functional features of IPCs were similar to beta-cells, the comprehensive comparison would require, such as the amount of insulin release and cell behaviours between lab-grown IPCs and mature beta-cells in human body. More importantly, whether islet-like clusters generated in our protocol are pure beta-cells or composed of heterogeneous population remains unknown.

Microarray data also raises some questions and opportunities for future study. The pathways analysis revealed the upregulation of several growth factors pathways (BMP,

Wnt, FGF). Although these pathways have critical roles in regulating cardiac regeneration, they are also involved in many cellular functions. The exact relationship of upregulated pathways and cardiogenesis potential in GDM-CMSCs requires further elucidation. The potential of GDM-CMSCs in wound healing was identified by IPA analysis and the expression of genes associated with healing process as well as migration ability were validated through *in vitro* assays. However, wound healing assay is a simple experiment but the wound repair process is complicated. *In vivo* models would provide more convincing evidence for wound healing studies. In addition, there are many freely available and commercial platforms for microarray data processing. In present study, IPA software (Qiagen) was used to perform biological functions and pathways analysis based on Ingenuity Knowledge Base (Qiagen), while with other bioinformatics software based on different database, it might provide some undiscovered findings in our microarray data. However, IPA is a powerful software for microarray analysis that can also be used to predict upstream regulators, biomarkers, comparison and interaction networks which have not yet been discovered with our GDM and healthy CMSCs microarray data.

Chapter 7

References



1. Scholl, TO, Sowers, M, Chen, X, and Lenders, C (2001). Maternal glucose concentration influences fetal growth, gestation, and pregnancy complications. *Am J Epidemiol* **154**: 514-520.
2. Ryan, EA, and Enns, L (1988). Role of gestational hormones in the induction of insulin resistance. *J Clin Endocrinol Metab* **67**: 341-347.
3. Kjos, SL, and Buchanan, TA (1999). Gestational diabetes mellitus. *N Engl J Med* **341**: 1749-1756.
4. Expert Committee on the, D, and Classification of Diabetes, M (2003). Report of the expert committee on the diagnosis and classification of diabetes mellitus. *Diabetes Care* **26 Suppl 1**: S5-20.
5. (2014). Diagnostic criteria and classification of hyperglycaemia first detected in pregnancy: a World Health Organization Guideline. *Diabetes Res Clin Pract* **103**: 341-363.
6. Webber, J, Charlton, M, and Johns, N (2015). Diabetes in pregnancy: management of diabetes and its complications from preconception to the postnatal period (NG3). *British Journal of Diabetes* **15**: 107-111.
7. Farrar, D, Simmonds, M, Bryant, M, Lawlor, DA, Dunne, F, Tuffnell, D, et al. (2017). Risk factor screening to identify women requiring oral glucose tolerance testing to diagnose gestational diabetes: A systematic review and meta-analysis and analysis of two pregnancy cohorts. *PLoS One* **12**: e0175288.
8. Hedderson, MM, Darbinian, JA, and Ferrara, A (2010). Disparities in the risk of gestational diabetes by race-ethnicity and country of birth. *Paediatr Perinat Epidemiol* **24**: 441-448.
9. Metzger, BE, Coustan, DR, and Comm, O (1998). Summary and recommendations of the fourth international workshop-conference on gestational diabetes mellitus. *Diabetes Care* **21**: B161-B167.
10. Guariguata, L, Linnenkamp, U, Beagley, J, Whiting, DR, and Cho, NH (2014). Global estimates of the prevalence of hyperglycaemia in pregnancy. *Diabetes Res Clin Pract* **103**: 176-185.
11. Zhu, Y, and Zhang, C (2016). Prevalence of Gestational Diabetes and Risk of Progression to Type 2 Diabetes: a Global Perspective. *Curr Diab Rep* **16**: 7.
12. (2015) *Diabetes in Pregnancy: Management of Diabetes and Its Complications from Preconception to the Postnatal Period*: London.
13. American Diabetes, A (2014). Diagnosis and classification of diabetes mellitus. *Diabetes Care* **37 Suppl 1**: S81-90.
14. Walker, JD (2008). NICE guidance on diabetes in pregnancy:

management of diabetes and its complications from preconception to the postnatal period. NICE clinical guideline 63. London, March 2008. *Diabet Med* **25**: 1025-1027.

15. Lauenborg, J, Hansen, T, Jensen, DM, Vestergaard, H, Molsted-Pedersen, L, Hornnes, P, *et al.* (2004). Increasing incidence of diabetes after gestational diabetes: a long-term follow-up in a Danish population. *Diabetes Care* **27**: 1194-1199.
16. Sacks, DA, Hadden, DR, Maresh, M, Deerochanawong, C, Dyer, AR, Metzger, BE, *et al.* (2012). Frequency of gestational diabetes mellitus at collaborating centers based on IADPSG consensus panel-recommended criteria: the Hyperglycemia and Adverse Pregnancy Outcome (HAPO) Study. *Diabetes Care* **35**: 526-528.
17. White, SL, Lawlor, DA, Briley, AL, Godfrey, KM, Nelson, SM, Oteng-Ntim, E, *et al.* (2016). Early Antenatal Prediction of Gestational Diabetes in Obese Women: Development of Prediction Tools for Targeted Intervention. *Plos One* **11**.
18. Torloni, MR, Betran, AP, Horta, BL, Nakamura, MU, Atallah, AN, Moron, AF, *et al.* (2009). Prepregnancy BMI and the risk of gestational diabetes: a systematic review of the literature with meta-analysis. *Obes Rev* **10**: 194-203.
19. Collaboration, NCDRF (2016). Trends in adult body-mass index in 200 countries from 1975 to 2014: a pooled analysis of 1698 population-based measurement studies with 19.2 million participants. *Lancet* **387**: 1377-1396.
20. (1998). Effect of intensive blood-glucose control with metformin on complications in overweight patients with type 2 diabetes (UKPDS 34). UK Prospective Diabetes Study (UKPDS) Group. *Lancet* **352**: 854-865.
21. Charles, B, Norris, R, Xiao, X, and Hague, W (2006). Population pharmacokinetics of metformin in late pregnancy. *Ther Drug Monit* **28**: 67-72.
22. Rowan, JA, Hague, WM, Gao, W, Battin, MR, Moore, MP, and Mi, GTI (2008). Metformin versus insulin for the treatment of gestational diabetes. *N Engl J Med* **358**: 2003-2015.
23. Scarlett, JA, Gray, RS, Griffin, J, Olefsky, JM, and Kolterman, OG (1982). Insulin treatment reverses the insulin resistance of type II diabetes mellitus. *Diabetes Care* **5**: 353-363.
24. Wulffele, MG, Kooy, A, Lehert, P, Bets, D, Ogterop, JC, Borger van der Burg, B, *et al.* (2002). Combination of insulin and metformin in the

- treatment of type 2 diabetes. *Diabetes Care* **25**: 2133-2140.
25. Bryson, CL, Ioannou, GN, Rulyak, SJ, and Critchlow, C (2003). Association between gestational diabetes and pregnancy-induced hypertension. *American Journal of Epidemiology* **158**: 1148-1153.
 26. Joffe, GM, Esterlitz, JR, Levine, RJ, Clemens, JD, Ewell, MG, Sibai, BM, *et al.* (1998). The relationship between abnormal glucose tolerance and hypertensive disorders of pregnancy in healthy nulliparous women. *Am J Obstet Gynecol* **179**: 1032-1037.
 27. Yu, Y, Jenkins, AJ, Nankervis, AJ, Hanssen, KF, Scholz, H, Henriksen, T, *et al.* (2009). Anti-angiogenic factors and pre-eclampsia in type 1 diabetic women. *Diabetologia* **52**: 160-168.
 28. Suwaki, N, Masuyama, H, Masumoto, A, Takamoto, N, and Hiramatsu, Y (2007). Expression and potential role of peroxisome proliferator-activated receptor gamma in the placenta of diabetic pregnancy. *Placenta* **28**: 315-323.
 29. Carpenter, MW (2007). Gestational diabetes, pregnancy hypertension, and late vascular disease. *Diabetes Care* **30 Suppl 2**: S246-250.
 30. Denney, JM, and Quinn, KH (2018). Gestational Diabetes: Underpinning Principles, Surveillance, and Management. *Obstet Gynecol Clin North Am* **45**: 299-314.
 31. Crowther, CA, Hiller, JE, Moss, JR, McPhee, AJ, Jeffries, WS, Robinson, JS, *et al.* (2005). Effect of treatment of gestational diabetes mellitus on pregnancy outcomes. *N Engl J Med* **352**: 2477-2486.
 32. Retnakaran, R, Qi, Y, Connelly, PW, Sermer, M, Zinman, B, and Hanley, AJ (2010). Glucose intolerance in pregnancy and postpartum risk of metabolic syndrome in young women. *J Clin Endocrinol Metab* **95**: 670-677.
 33. Boney, CM, Verma, A, Tucker, R, and Vohr, BR (2005). Metabolic syndrome in childhood: association with birth weight, maternal obesity, and gestational diabetes mellitus. *Pediatrics* **115**: e290-296.
 34. Bellamy, L, Casas, JP, Hingorani, AD, and Williams, D (2009). Type 2 diabetes mellitus after gestational diabetes: a systematic review and meta-analysis. *Lancet* **373**: 1773-1779.
 35. Baptiste-Roberts, K, Barone, BB, Gary, TL, Golden, SH, Wilson, LM, Bass, EB, *et al.* (2009). Risk factors for type 2 diabetes among women with gestational diabetes: a systematic review. *Am J Med* **122**: 207-214 e204.
 36. Daly, B, Toulis, KA, Thomas, N, Gokhale, K, Martin, J, Webber, J, *et al.* (2018). Increased risk of ischemic heart disease, hypertension, and

- type 2 diabetes in women with previous gestational diabetes mellitus, a target group in general practice for preventive interventions: A population-based cohort study. *PLoS Med* **15**: e1002488.
37. Kim, C, Newton, KM, and Knopp, RH (2002). Gestational diabetes and the incidence of type 2 diabetes: a systematic review. *Diabetes Care* **25**: 1862-1868.
 38. Malcolm, J (2012). Through the looking glass: gestational diabetes as a predictor of maternal and offspring long-term health. *Diabetes Metab Res Rev* **28**: 307-311.
 39. Yajnik, CS (2010). Fetal programming of diabetes: still so much to learn! *Diabetes Care* **33**: 1146-1148.
 40. Plagemann, A, Harder, T, Kohlhoff, R, Rohde, W, and Dorner, G (1997). Glucose tolerance and insulin secretion in children of mothers with pregestational IDDM or gestational diabetes. *Diabetologia* **40**: 1094-1100.
 41. Retnakaran, R, Qi, Y, Sermer, M, Connelly, PW, Hanley, AJ, and Zinman, B (2010). Beta-cell function declines within the first year postpartum in women with recent glucose intolerance in pregnancy. *Diabetes Care* **33**: 1798-1804.
 42. Friedman, JE, Ishizuka, T, Shao, J, Huston, L, Highman, T, and Catalano, P (1999). Impaired glucose transport and insulin receptor tyrosine phosphorylation in skeletal muscle from obese women with gestational diabetes. *Diabetes* **48**: 1807-1814.
 43. Garvey, WT, Maianu, L, Zhu, JH, Hancock, JA, and Golichowski, AM (1993). Multiple defects in the adipocyte glucose transport system cause cellular insulin resistance in gestational diabetes. Heterogeneity in the number and a novel abnormality in subcellular localization of GLUT4 glucose transporters. *Diabetes* **42**: 1773-1785.
 44. Retnakaran, R, Hanley, AJ, Raif, N, Connelly, PW, Sermer, M, and Zinman, B (2004). Reduced adiponectin concentration in women with gestational diabetes: a potential factor in progression to type 2 diabetes. *Diabetes Care* **27**: 799-800.
 45. Winkler, G, Cseh, K, Baranyi, E, Melczer, Z, Speer, G, Hajos, P, *et al.* (2002). Tumor necrosis factor system in insulin resistance in gestational diabetes. *Diabetes Res Clin Pract* **56**: 93-99.
 46. Kautzky-Willer, A, Pacini, G, Tura, A, Biegelmayer, C, Schneider, B, Ludvik, B, *et al.* (2001). Increased plasma leptin in gestational diabetes. *Diabetologia* **44**: 164-172.

47. Watanabe, RM (2011). Inherited destiny? Genetics and gestational diabetes mellitus. *Genome Med* **3**: 18.
48. Robitaille, J, and Grant, AM (2008). The genetics of gestational diabetes mellitus: evidence for relationship with type 2 diabetes mellitus. *Genet Med* **10**: 240-250.
49. Mao, H, Li, Q, and Gao, S (2012). Meta-analysis of the relationship between common type 2 diabetes risk gene variants with gestational diabetes mellitus. *PLoS One* **7**: e45882.
50. Moen, GH, Sommer, C, Prasad, RB, Sletner, L, Groop, L, Qvigstad, E, *et al.* (2017). MECHANISMS IN ENDOCRINOLOGY: Epigenetic modifications and gestational diabetes: a systematic review of published literature. *Eur J Endocrinol* **176**: R247-R267.
51. Aerts, L, Vercruysse, L, and Van Assche, FA (1997). The endocrine pancreas in virgin and pregnant offspring of diabetic pregnant rats. *Diabetes Res Clin Pract* **38**: 9-19.
52. Serradas, P, Gangnerau, MN, Giroix, MH, Saulnier, C, and Portha, B (1998). Impaired pancreatic beta cell function in the fetal GK rat. Impact of diabetic inheritance. *J Clin Invest* **101**: 899-904.
53. Buchanan, TA (2001). Pancreatic B-cell defects in gestational diabetes: implications for the pathogenesis and prevention of type 2 diabetes. *J Clin Endocrinol Metab* **86**: 989-993.
54. Ahokas, RA, and McKinney, ET (2008). Development and physiology of the placenta and membranes. *Global Library Women's Medicine*.
55. Huppertz, B (2008). The anatomy of the normal placenta. *J Clin Pathol* **61**: 1296-1302.
56. Moffett-King, A (2002). Natural killer cells and pregnancy. *Nat Rev Immunol* **2**: 656-663.
57. Handwerger, S (2010). New insights into the regulation of human cytotrophoblast cell differentiation. *Mol Cell Endocrinol* **323**: 94-104.
58. Wang, Y, and Zhao, S (2010) *Vascular Biology of the Placenta*: San Rafael (CA).
59. Griffiths, SK, and Campbell, JP (2015). Placental structure, function and drug transfer. *Bja Educ* **15**: 84-89.
60. Moore, KL, and Persaud, T (2004). Clinically oriented embryology. *The Developing Human* **10**.
61. Goplerud, JM, and Delivoriapapadopoulos, M (1985). Physiology of the Placenta - Gas-Exchange. *Ann Clin Lab Sci* **15**: 270-278.
62. Knipp, GT, Audus, KL, and Soares, MJ (1999). Nutrient transport across

- the placenta. *Adv Drug Deliv Rev* **38**: 41-58.
63. Cole, LA (2010). Biological functions of hCG and hCG-related molecules. *Reprod Biol Endocrin* **8**.
 64. Newbern, D, and Freemarm, M (2011). Placental hormones and the control of maternal metabolism and fetal growth. *Curr Opin Endocrinol Diabetes Obes* **18**: 409-416.
 65. Costa, MA (2016). The endocrine function of human placenta: an overview. *Reprod Biomed Online* **32**: 14-43.
 66. Kasuga, Y, Miyakoshi, K, Ikenoue, S, Kadohira, I, Matsumoto, T, Minegishi, K, *et al.* (2013). Complete chorion-amnion separation presenting as a stuck fetus. *Acta Obstet Gyn Scan* **92**: 990-991.
 67. Bourne, G (1962). The foetal membranes. A review of the anatomy of normal amnion and chorion and some aspects of their function. *Postgrad Med J* **38**: 193-201.
 68. Parolini, O, Alviano, F, Bagnara, GP, Bilic, G, Buhring, HJ, Evangelista, M, *et al.* (2008). Concise review: isolation and characterization of cells from human term placenta: outcome of the first international Workshop on Placenta Derived Stem Cells. *Stem Cells* **26**: 300-311.
 69. Niknejad, H, Peirovi, H, Jorjani, M, Ahmadiani, A, Ghanavi, J, and Seifalian, AM (2008). Properties of the amniotic membrane for potential use in tissue engineering. *Eur Cells Mater* **15**: 88-99.
 70. Parry, S, and Strauss, JF, 3rd (1998). Premature rupture of the fetal membranes. *N Engl J Med* **338**: 663-670.
 71. Trexler, JC (1998). Williams obstetrics. *J Nurse-Midwifery* **43**: 134-135.
 72. Baergen, RN (2005). *Manual of Benirschke and Kaufmann's pathology of the human placenta*, Springer Science & Business Media.
 73. Diamant, YZ, Metzger, BE, Freinkel, N, and Shafrir, E (1982). Placental Lipid and Glycogen-Content in Human and Experimental Diabetes-Mellitus. *Am J Obstet Gynecol* **144**: 5-11.
 74. Radaelli, T, Varastehpour, A, Catalano, P, and Haugeul-de Mouzon, S (2003). Gestational diabetes induces placental genes for chronic stress and inflammatory pathways. *Diabetes* **52**: 2951-2958.
 75. Taricco, E, Radaelli, T, de Santis, MSN, and Cetin, I (2003). Foetal and placental weights in relation to maternal characteristics in gestational diabetes. *Placenta* **24**: 343-347.
 76. Kim, C (2010). *Gestational diabetes during and after pregnancy*, Springer.
 77. Huynh, J, Dawson, D, Roberts, D, and Bentley-Lewis, R (2015). A

- systematic review of placental pathology in maternal diabetes mellitus. *Placenta* **36**: 101-114.
78. Mayhew, T, Charnock-Jones, D, and Kaufmann, P (2004). Aspects of human fetoplacental vasculogenesis and angiogenesis. III. Changes in complicated pregnancies. *Placenta* **25**: 127-139.
 79. Vambergue, A, and Fajardy, I (2011). Consequences of gestational and pregestational diabetes on placental function and birth weight. *World J Diabetes* **2**: 196-203.
 80. Visiedo, F, Bugatto, F, Quintero-Prado, R, Cozar-Castellano, I, Bartha, JL, and Perdomo, G (2015). Glucose and Fatty Acid Metabolism in Placental Explants From Pregnancies Complicated With Gestational Diabetes Mellitus. *Reprod Sci* **22**: 798-801.
 81. Stanirowski, PJ, Szukiewicz, D, Pyzlak, M, Abdalla, N, Sawicki, W, and Cendrowski, K (2017). Impact of pre-gestational and gestational diabetes mellitus on the expression of glucose transporters GLUT-1, GLUT-4 and GLUT-9 in human term placenta. *Endocrine* **55**: 799-808.
 82. Monteiro, LJ, Norman, JE, Rice, GE, and Illanes, SE (2016). Fetal programming and gestational diabetes mellitus. *Placenta* **48**: S54-S60.
 83. Osmond, DTD, King, RG, Brennecke, SP, and Gude, NM (2001). Placental glucose transport and utilisation is altered at term in insulin-treated, gestational-diabetic patients. *Diabetologia* **44**: 1133-1139.
 84. Desoye, G, and Nolan, CJ (2016). The fetal glucose steal: an underappreciated phenomenon in diabetic pregnancy. *Diabetologia* **59**: 1089-1094.
 85. Garvey, WT, and Birnbaum, MJ (1993). Cellular Insulin Action and Insulin-Resistance. *Bailliere Clin Endoc* **7**: 785-873.
 86. Garvey, WT, Maianu, L, Hancock, JA, Golichowski, AM, and Baron, A (1992). Gene expression of GLUT4 in skeletal muscle from insulin-resistant patients with obesity, IGT, GDM, and NIDDM. *Diabetes* **41**: 465-475.
 87. Gallo, LA, Barrett, HL, and Nitert, MD (2017). Review: Placental transport and metabolism of energy substrates in maternal obesity and diabetes. *Placenta* **54**: 59-67.
 88. Scholler, M, Wadsack, C, Lang, I, Etschmaier, K, Schweinzer, C, Marsche, G, *et al.* (2012). Phospholipid Transfer Protein in the Placental Endothelium Is Affected by Gestational Diabetes Mellitus. *J Clin Endocr Metab* **97**: 437-445.
 89. Gauster, M, Hiden, U, van Poppel, M, Frank, S, Wadsack, C, Hauguel-de

- Mouzon, S, *et al.* (2011). Dysregulation of Placental Endothelial Lipase in Obese Women With Gestational Diabetes Mellitus. *Diabetes* **60**: 2457-2464.
90. Briana, DD, and Malamitsi-Puchner, A (2009). Adipocytokines in Normal and Complicated Pregnancies. *Reprod Sci* **16**: 921-937.
 91. Pedersen, J (1952). Course of Diabetes during Pregnancy. *Acta Endocrinol-Cop* **9**: 342-364.
 92. Blau, HM, Brazelton, TR, and Weimann, JM (2001). The evolving concept of a stem cell: entity or function? *Cell* **105**: 829-841.
 93. Wagers, AJ, and Weissman, IL (2004). Plasticity of adult stem cells. *Cell* **116**: 639-648.
 94. Pipino, C, Shangaris, P, Resca, E, Zia, S, Deprest, J, Sebire, NJ, *et al.* (2013). Placenta as a reservoir of stem cells: an underutilized resource? *British medical bulletin* **105**.
 95. Gekas, C, Rhodes, KE, Van Handel, B, Chhabra, A, Ueno, M, and Mikkola, HKA (2010). Hematopoietic stem cell development in the placenta. *Int J Dev Biol* **54**: 1089-1098.
 96. Davies, JE, Walker, JT, and Keating, A (2017). Concise Review: Wharton's Jelly: The Rich, but Enigmatic, Source of Mesenchymal Stromal Cells. *Stem Cell Transl Med* **6**: 1620-1630.
 97. Subramanian, A, Fong, CY, Biswas, A, and Bongso, A (2015). Comparative Characterization of Cells from the Various Compartments of the Human Umbilical Cord Shows that the Wharton's Jelly Compartment Provides the Best Source of Clinically Utilizable Mesenchymal Stem Cells. *Plos One* **10**.
 98. Arutyunyan, I, Elchaninov, A, Makarov, A, and Fatkhudinov, T (2016). Umbilical Cord as Prospective Source for Mesenchymal Stem Cell-Based Therapy. *Stem Cells Int*.
 99. Hordyjewska, A, Popiolek, L, and Horecka, A (2015). Characteristics of hematopoietic stem cells of umbilical cord blood. *Cytotechnology* **67**: 387-396.
 100. Chen, JH, Lu, ZJ, Cheng, D, Peng, S, and Wang, HY (2011). Isolation and Characterization of Porcine Amniotic Fluid-Derived Multipotent Stem Cells. *Plos One* **6**.
 101. Kim, J, Lee, Y, Kim, H, Hwang, KJ, Kwon, HC, Kim, SK, *et al.* (2007). Human amniotic fluid-derived stem cells have characteristics of multipotent stem cells. *Cell Proliferat* **40**: 75-90.
 102. Prusa, AR, and Hengstschlager, M (2002). Amniotic fluid cells and

- human stem cell research: a new connection. *Med Sci Monit* **8**: RA253-257.
103. Robboy, SJ, and Hoda, RS (2000). Pathology of the Human Placenta. *International Journal of Gynecological Pathology* **19**: 401.
 104. Cross, JC (1998). Formation of the placenta and extraembryonic membranes. *Ann N Y Acad Sci* **857**: 23-32.
 105. Macias, MI, Grande, J, Moreno, A, Dominguez, I, Bornstein, R, and Flores, AI (2010). Isolation and characterization of true mesenchymal stem cells derived from human term decidua capable of multilineage differentiation into all 3 embryonic layers. *Am J Obstet Gynecol* **203**.
 106. Domnina, AP, Novikova, PV, Lyublinskaya, OG, Zenin, VV, Fridlyanskaya, II, Mikhailov, VM, *et al.* (2016). Mesenchymal stem cells with irreversibly arrested proliferation stimulate decidua development in rats. *Exp Ther Med* **12**: 2447-2454.
 107. Igura, K, Zhang, X, Takahashi, K, Mitsuru, A, Yamaguchi, S, and Takashi, TA (2004). Isolation and characterization of mesenchymal progenitor cells from chorionic villi of human placenta. *Cytotherapy* **6**: 543-553.
 108. Parolini, O, Alviano, F, Bagnara, GP, Bilic, G, Buhning, HJ, Evangelista, M, *et al.* (2008). Concise review: Isolation and characterization of cells from human term placenta: Outcome of the first international workshop on placenta derived stem cells. *Stem Cells* **26**: 300-311.
 109. Dominici, M, Le Blanc, K, Mueller, I, Slaper-Cortenbach, I, Marini, FC, Krause, DS, *et al.* (2006). Minimal criteria for defining multipotent mesenchymal stromal cells. The International Society for Cellular Therapy position statement. *Cytotherapy* **8**: 315-317.
 110. Wu, Z, Hui, G, Lu, Y, Liu, T, Huang, Q, and Guo, L (2012). Human amniotic epithelial cells express specific markers of nerve cells and migrate along the nerve fibers in the corpus callosum. *Neural Regen Res* **7**: 41-45.
 111. Insausti, CL, Blanquer, M, Garcia-Hernandez, AM, Castellanos, G, and Moraleda, JM (2014). Amniotic membrane-derived stem cells: immunomodulatory properties and potential clinical application. *Stem Cells Cloning* **7**: 53-63.
 112. Shaw, KA, Parada, SA, Gloystein, DM, and Devine, JG (2018). The Science and Clinical Applications of Placental Tissues in Spine Surgery. *Global Spine Journal*: 2192568217747573.
 113. Tamagawa, T, Ishiwata, I, and Saito, S (2004). Establishment and characterization of a pluripotent stem cell line derived from human

- amniotic membranes and initiation of germ layers in vitro. *Hum Cell* **17**: 125-130.
114. Miki, T, Lehmann, T, Cai, H, Stolz, DB, and Strom, SC (2005). Stem cell characteristics of amniotic epithelial cells. *Stem Cells* **23**: 1549-1559.
 115. Kim, EY, Lee, KB, and Kim, MK (2014). The potential of mesenchymal stem cells derived from amniotic membrane and amniotic fluid for neuronal regenerative therapy. *BMB Rep* **47**: 135-140.
 116. Tamagawa, T, Oi, S, Ishiwatai, I, Ishikawa, H, and Nakamura, Y (2007). Differentiation of mesenchymal cells derived from human amniotic membranes into hepatocyte-like cells in vitro. *Human Cell* **20**: 77-84.
 117. Alviano, F, Fossati, V, Marchionni, C, Arpinati, M, Bonsi, L, Franchina, M, *et al.* (2007). Term amniotic membrane is a high throughput source for multipotent mesenchymal stem cells with the ability to differentiate into endothelial cells in vitro. *Bmc Dev Biol* **7**.
 118. Pratama, G, Vaghjiani, V, Tee, JY, Liu, YH, Chan, J, Tan, C, *et al.* (2011). Changes in culture expanded human amniotic epithelial cells: implications for potential therapeutic applications. *PLoS One* **6**: e26136.
 119. Casey, ML, and MacDonald, PC (1996). Interstitial collagen synthesis and processing in human amnion: a property of the mesenchymal cells. *Biol Reprod* **55**: 1253-1260.
 120. Tabatabaei, M, Mosaffa, N, Nikoo, S, Bozorgmehr, M, Ghods, R, Kazemnejad, S, *et al.* (2014). Isolation and partial characterization of human amniotic epithelial cells: the effect of trypsin. *Avicenna J Med Biotechnol* **6**: 10-20.
 121. Abdulrazzak, H, Moschidou, D, Jones, G, and Guillot, PV (2010). Biological characteristics of stem cells from foetal, cord blood and extraembryonic tissues. *J R Soc Interface* **7**: S689-S706.
 122. Bailo, M, Soncini, M, Vertua, E, Signoroni, PB, Sanzone, S, Lombardi, G, *et al.* (2004). Engraftment potential of human amnion and chorion cells derived from term placenta. *Transplantation* **78**: 1439-1448.
 123. Portmann-Lanz, B, Schoeberlein, A, Sager, R, Mohr, S, Rollini, P, Huber, A, *et al.* (2007). Placenta stem cells as autologous grafts for peripartum neuroregeneration - The neural differentiation potential of human placental mesenchymal stem cells. *Am J Obstet Gynecol* **197**: S30-S30.
 124. Kmiecik, G, Niklinska, W, Kuc, P, Pancewicz-Wojtkiewicz, J, Fil, D, Karwowska, A, *et al.* (2013). Fetal membranes as a source of stem cells. *Adv Med Sci-Poland* **58**: 185-195.
 125. Jones, GN, Moschidou, D, Puga-Iglesias, TI, Kuleszewicz, K, Vanleene,

- M, Shefelbine, SJ, *et al.* (2012). Ontological differences in first compared to third trimester human fetal placental chorionic stem cells. *PLoS One* **7**: e43395.
126. Muench, MO, Kapidzic, M, Gormley, M, Gutierrez, AG, Ponder, KL, Fomin, ME, *et al.* (2017). The human chorion contains definitive hematopoietic stem cells from the fifteenth week of gestation. *Development* **144**: 1399-1411.
 127. Heazlewood, CF, Sherrell, H, Ryan, J, Atkinson, K, Wells, CA, and Fisk, NM (2014). High Incidence of Contaminating Maternal Cell Overgrowth in Human Placental Mesenchymal Stem/Stromal Cell Cultures: A Systematic Review. *Stem Cell Transl Med* **3**: 1305-1311.
 128. Ilancheran, S, Michalska, A, Peh, G, Wallace, EM, Pera, M, and Manuelpillai, U (2007). Stem cells derived from human fetal membranes display multilineage differentiation potential. *Biol Reprod* **77**: 577-588.
 129. Miki, T, and Strom, SC (2006). Amnion-derived pluripotent/multipotent stem cells. *Stem Cell Rev* **2**: 133-142.
 130. Li, CD, Zhang, WY, Jiang, XX, and Mao, N (2007). Human-placenta-derived mesenchymal stem cells inhibit proliferation and function of allogeneic immune cells. *Cell Tissue Res* **330**: 437-446.
 131. Wolbank, S, Peterbauer, A, Fahrner, M, Hennerbichler, S, van Griensven, M, Stadler, G, *et al.* (2007). Dose-dependent immunomodulatory effect of human stem cells from amniotic membrane: a comparison with human mesenchymal stem cells from adipose tissue. *Tissue Eng* **13**: 1173-1183.
 132. Sargent, IL (1993). Maternal and Fetal Immune-Responses during Pregnancy. *Exp Clin Immunogenet* **10**: 85-102.
 133. Ilancheran, S, Moodley, Y, and Manuelpillai, U (2009). Human fetal membranes: a source of stem cells for tissue regeneration and repair? *Placenta* **30**: 2-10.
 134. Rebmann, V, Nardi, FD, Wagner, B, and Horn, PA (2014). HLA-G as a Tolerogenic Molecule in Transplantation and Pregnancy. *J Immunol Res*.
 135. Wang, QS, Yang, QN, Wang, Z, Tong, HX, Ma, LY, Zhang, Y, *et al.* (2016). Comparative analysis of human mesenchymal stem cells from fetal-bone marrow, adipose tissue, and Warton's jelly as sources of cell immunomodulatory therapy. *Hum Vacc Immunother* **12**: 85-96.
 136. Fournel, S, Aguerre-Girr, M, Huc, X, Lenfant, F, Alam, A, Toubert, A, *et al.* (2000). Cutting edge: soluble HLA-G1 triggers CD95/CD95 ligand-

- mediated apoptosis in activated CD8⁺ cells by interacting with CD8. *J Immunol* **164**: 6100-6104.
137. Magatti, M, De Munari, S, Vertua, E, Nassauto, C, Albertini, A, Wengler, GS, *et al.* (2009). Amniotic mesenchymal tissue cells inhibit dendritic cell differentiation of peripheral blood and amnion resident monocytes. *Cell Transplant* **18**: 899-914.
 138. Bailo, M, Soncini, M, Vertua, E, Signoroni, PB, Sanzone, S, Lombardi, G, *et al.* (2004). Engraftment potential of human amnion and chorion cells derived from term placenta. *Transplantation* **78**: 1439-1448.
 139. Yamahara, K, Harada, K, Ohshima, M, Ishikane, S, Ohnishi, S, Tsuda, H, *et al.* (2014). Comparison of angiogenic, cytoprotective, and immunosuppressive properties of human amnion- and chorion-derived mesenchymal stem cells. *PLoS One* **9**: e88319.
 140. Davis, JS (1910). Skin transplantation. *Johns Hopkins Hospital Reports* **15**: 307-396.
 141. Stern, M (1913). The grafting of preserved amniotic membrane to burned and ulcerated surfaces, substituting skin grafts: a preliminary report. *Journal of the American Medical Association* **60**: 973-974.
 142. Burger, K (1937). Artificial vaginal reconstruction with the help of amnion. *Zentralbl Gynaekol* **61**: 2437.
 143. de Rotth, A (1940). Plastic repair of conjunctival defects with fetal membranes. *Arch Ophthalmol-Chic* **23**: 522-525.
 144. Kim, JC, and Tseng, SC (1995). Transplantation of preserved human amniotic membrane for surface reconstruction in severely damaged rabbit corneas. *Cornea* **14**: 473-484.
 145. Zelen, CM, Serena, TE, Gould, L, Le, L, Carter, MJ, Keller, J, *et al.* (2016). Treatment of chronic diabetic lower extremity ulcers with advanced therapies: a prospective, randomised, controlled, multi-centre comparative study examining clinical efficacy and cost. *Int Wound J* **13**: 272-282.
 146. Koob, TJ, Lim, JJ, Masee, M, Zabek, N, and Denozieri, G (2014). Properties of dehydrated human amnion/chorion composite grafts: Implications for wound repair and soft tissue regeneration. *J Biomed Mater Res B Appl Biomater* **102**: 1353-1362.
 147. Koob, TJ, Rennert, R, Zabek, N, Masee, M, Lim, JJ, Temenoff, JS, *et al.* (2013). Biological properties of dehydrated human amnion/chorion composite graft: implications for chronic wound healing. *Int Wound J* **10**: 493-500.

148. Zelen, CM, Snyder, RJ, Serena, TE, and Li, WW (2015). The Use of Human Amnion/Chorion Membrane in the Clinical Setting for Lower Extremity Repair: A Review. *Clin Podiatr Med Sur* **32**: 135-+.
149. Russo, A, Bonci, P, and Bonci, P (2012). The effects of different preservation processes on the total protein and growth factor content in a new biological product developed from human amniotic membrane. *Cell Tissue Bank* **13**: 353-361.
150. Iravani, K, Hashemi, SB, Tehrani, M, and Rashidi, M (2014). Amniotic membrane in reconstruction of larynx following chondrosarcoma resection: a case report. *Am J Otolaryngol* **35**: 520-523.
151. Muralidharan, S, Gu, J, Laub, GW, Cichon, R, Daloisio, C, and McGrath, LB (1991). A new biological membrane for pericardial closure. *J Biomed Mater Res* **25**: 1201-1209.
152. Wang, T, Liang, C, Xu, X, and Shi, W (2015). Total ocular surface amniotic membrane transplantation for paraquat-induced ocular surface injury. *Can J Ophthalmol* **50**: 461-465.
153. Alsina-Gibert, M, and Pedregosa-Fauste, S (2012). Amniotic membrane transplantation in the treatment of chronic lower limb ulcers. *Actas Dermosifiliogr* **103**: 608-613.
154. Mohammadi, AA, Johari, HG, and Eskandari, S (2013). Effect of amniotic membrane on graft take in extremity burns. *Burns* **39**: 1137-1141.
155. Lim, R (2017). Concise Review: Fetal Membranes in Regenerative Medicine: New Tricks from an Old Dog? *Stem Cell Transl Med* **6**: 1767-1776.
156. Jerman, UD, Veranic, P, and Kreft, ME (2014). Amniotic Membrane Scaffolds Enable the Development of Tissue-Engineered Urothelium with Molecular and Ultrastructural Properties Comparable to that of Native Urothelium. *Tissue Eng Part C-Me* **20**: 317-327.
157. Reboucas, JD, Santos-Magalhaes, NS, and Formiga, FR (2016). Cardiac Regeneration using Growth Factors: Advances and Challenges. *Arq Bras Cardiol* **107**: 271-275.
158. Zhao, P, Ise, H, Hongo, M, Ota, M, Konishi, I, and Nikaido, T (2005). Human amniotic mesenchymal cells have some characteristics of cardiomyocytes. *Transplantation* **79**: 528-535.
159. Fujimoto, KL, Miki, T, Liu, LJ, Hashizume, R, Strom, SC, Wagner, WR, *et al.* (2009). Naive Rat Amnion-Derived Cell Transplantation Improved Left Ventricular Function and Reduced Myocardial Scar of Postinfarcted

- Heart. *Cell Transplantation* **18**: 477-486.
160. Tsuji, H, Miyoshi, S, Ikegami, Y, Hida, N, Asada, H, Togashi, I, *et al.* (2010). Xenografted Human Amniotic Membrane-Derived Mesenchymal Stem Cells Are Immunologically Tolerated and Transdifferentiated Into Cardiomyocytes. *Circ Res* **106**: 1613-1623.
 161. Ventura, C, Cantoni, S, Bianchi, F, Lionetti, V, Cavallini, C, Scarlata, I, *et al.* (2007). Hyaluronan mixed esters of butyric and retinoic acid drive cardiac and endothelial fate in term placenta human mesenchymal stem cells and enhance cardiac repair in infarcted rat hearts. *J Biol Chem* **282**: 14243-14252.
 162. Chen, HJ, Chen, CH, Chang, MY, Tsai, DC, Baum, EZ, Hariri, R, *et al.* (2015). Human Placenta-Derived Adherent Cells Improve Cardiac Performance in Mice With Chronic Heart Failure. *Stem Cell Transl Med* **4**: 269-275.
 163. Liu, YH, Peng, KY, Chiu, YW, Ho, YL, Wang, YH, Shun, CT, *et al.* (2015). Human Placenta-Derived Multipotent Cells (hPDMCs) Modulate Cardiac Injury: From Bench to Small and Large Animal Myocardial Ischemia Studies. *Cell Transplantation* **24**: 2463-2478.
 164. Yamahara, K, Harada, K, Ohshima, M, Ishikane, S, Ohnishi, S, Tsuda, H, *et al.* (2014). Comparison of Angiogenic, Cytoprotective, and Immunosuppressive Properties of Human Amnion- and Chorion-Derived Mesenchymal Stem Cells. *Plos One* **9**.
 165. Du, WJ, Li, X, Chi, Y, Ma, FX, Li, ZJ, Yang, SG, *et al.* (2016). VCAM-1(+) placenta chorionic villi-derived mesenchymal stem cells display potent pro-angiogenic activity. *Stem Cell Res Ther* **7**.
 166. Uchida, S, Inanaga, Y, Kobayashi, M, Hurukawa, S, Araie, M, and Sakuragawa, N (2000). Neurotrophic function of conditioned medium from human amniotic epithelial cells. *J Neurosci Res* **62**: 585-590.
 167. Sankar, V, and Muthusamy, R (2003). Role of human amniotic epithelial cell transplantation in spinal cord injury repair research. *Neuroscience* **118**: 11-17.
 168. Yan, ZJ, Zhang, P, Hu, YQ, Zhang, HT, Hong, SQ, Zhou, HL, *et al.* (2013). Neural Stem-Like Cells Derived from Human Amnion Tissue are Effective in Treating Traumatic Brain Injury in Rat. *Neurochem Res* **38**: 1022-1033.
 169. Kong, XY, Cai, Z, Pan, L, Zhang, L, Shu, J, Dong, YL, *et al.* (2008). Transplantation of human amniotic cells exerts neuroprotection in MPTP-induced Parkinson disease mice. *Brain Res* **1205**: 108-115.

170. Park, S, Kim, E, Koh, SE, Maeng, S, Lee, WD, Lim, J, *et al.* (2012). Dopaminergic differentiation of neural progenitors derived from placental mesenchymal stem cells in the brains of Parkinson's disease model rats and alleviation of asymmetric rotational behavior. *Brain Res* **1466**: 158-166.
171. Jiang, H, Zhang, YY, Tian, KW, Wang, BB, and Han, S (2017). Amelioration of experimental autoimmune encephalomyelitis through transplantation of placental derived mesenchymal stem cells. *Sci Rep-Uk* **7**.
172. Fisher-Shoval, Y, Barhum, Y, Sadan, O, Yust-Katz, S, Ben-Zur, T, Lev, N, *et al.* (2012). Transplantation of Placenta-Derived Mesenchymal Stem Cells in the EAE Mouse Model of MS. *J Mol Neurosci* **48**: 176-184.
173. Pozzobon, M, Franzin, C, Piccoli, M, and De Coppi, P (2014). Fetal stem cells and skeletal muscle regeneration: a therapeutic approach. *Front Aging Neurosci* **6**.
174. Kawamichi, Y, Cui, CH, Toyoda, M, Makino, H, Horie, A, Takahashi, Y, *et al.* (2010). Cells of Extraembryonic Mesodermal Origin Confer Human Dystrophin in the Mdx Model of Duchenne Muscular Dystrophy. *J Cell Physiol* **223**: 695-702.
175. Jones, GN, Moschidou, D, Abdulrazzak, H, Kalirai, BS, Vanleene, M, Osatis, S, *et al.* (2014). Potential of Human Fetal Chorionic Stem Cells for the Treatment of Osteogenesis Imperfecta. *Stem Cells Dev* **23**: 262-276.
176. Jin, J, Wang, J, Huang, JA, Huang, F, Fu, JAH, Yang, XJ, *et al.* (2014). Transplantation of human placenta-derived mesenchymal stem cells in a silk fibroin/hydroxyapatite scaffold improves bone repair in rabbits. *J Biosci Bioeng* **118**: 593-598.
177. Maymo, JL, Riedel, R, Perez-Perez, A, Magatti, M, Maskin, B, Duenas, JL, *et al.* (2018). Proliferation and survival of human amniotic epithelial cells during their hepatic differentiation. *Plos One* **13**.
178. Takashima, S, Ise, H, Akaike, T, and Nikaido, T (2004). Human amniotic epithelial cells possess hepatocyte-like characteristics and functions. *Cell Struct Funct* **29**: 73-84.
179. Makarev, E, Izumchenko, E, Aihara, F, Wysocki, PT, Zhu, QS, Buzdin, A, *et al.* (2016). Common pathway signature in lung and liver fibrosis. *Cell Cycle* **15**: 1667-1673.
180. Manuelpillai, U, Tchongue, J, Lourensz, D, Vaghjiani, V, Samuel, CS, Liu, A, *et al.* (2010). Transplantation of Human Amnion Epithelial Cells

- Reduces Hepatic Fibrosis in Immunocompetent CCl₄-Treated Mice. *Cell Transplantation* **19**: 1157-1168.
181. Zhang, DG, Jiang, MY, and Miao, DS (2011). Transplanted Human Amniotic Membrane-Derived Mesenchymal Stem Cells Ameliorate Carbon Tetrachloride-Induced Liver Cirrhosis in Mouse. *Plos One* **6**.
 182. Ricci, E, Vanosi, G, Lindenmair, A, Hennerbichler, S, Peterbauer-Scherb, A, Wolbank, S, *et al.* (2013). Anti-fibrotic effects of fresh and cryopreserved human amniotic membrane in a rat liver fibrosis model. *Cell Tissue Bank* **14**: 475-488.
 183. Lin, JS, Zhou, L, Sagayaraj, A, Jumat, NH, Choolani, M, Chan, JK, *et al.* (2015). Hepatic differentiation of human amniotic epithelial cells and in vivo therapeutic effect on animal model of cirrhosis. *J Gastroenterol Hepatol* **30**: 1673-1682.
 184. Cargnoni, A, Gibelli, L, Tosini, A, Signoroni, PB, Nassuato, C, Arienti, D, *et al.* (2009). Transplantation of allogeneic and xenogeneic placenta-derived cells reduces bleomycin-induced lung fibrosis. *Cell Transplant* **18**: 405-422.
 185. Cui, P, Xin, H, Yao, Y, Xiao, S, Zhu, F, Gong, Z, *et al.* (2018). Human amnion-derived mesenchymal stem cells alleviate lung injury induced by white smoke inhalation in rats. *Stem Cell Res Ther* **9**: 101.
 186. Ballen, KK, Verter, F, and Kurtzberg, J (2015). Umbilical cord blood donation: public or private? *Bone Marrow Transpl* **50**: 1271-1278.
 187. Couto, PS, Bersenev, A, and Verter, F (2017). The first decade of advanced cell therapy clinical trials using perinatal cells (2005-2015). *Regen Med* **12**: 953-968.
 188. Bharucha, C, Elliott, S, Campbell, D, Hunter, R, and McComb, L (1997). The Belfast Cord Blood Bank. *Ulster Med J* **66**: 9-12.
 189. Biunno, I, and DeBlasio, P (2014). Fundamental principles of a Stem cell biobank. *Stem Cells in Animal Species: From Pre-clinic to Biodiversity*. Springer. pp 151-166.
 190. Antoniadou, E, and David, AL (2016). Placental stem cells. *Best Pract Res Cl Ob* **31**: 13-29.
 191. Vaught, J, Kelly, A, and Hewitt, R (2009). A Review of International Biobanks and Networks: Success Factors and Key Benchmarks. *Biopreserv Biobank* **7**: 143-150.
 192. Huppertz, B, Kivity, V, Sammar, M, Grimpel, Y, Leepaz, N, Orendi, K, *et al.* (2011). Cryogenic and low temperature preservation of human placental villous explants - a new way to explore drugs in pregnancy

- disorders. *Placenta* **32 Suppl**: S65-76.
193. Bild, DE, Selby, JV, Sinnock, P, Browner, WS, Braveman, P, and Showstack, JA (1989). Lower-Extremity Amputation in People with Diabetes - Epidemiology and Prevention. *Diabetes Care* **12**: 24-31.
 194. Inzucchi, SE (2002). Oral antihyperglycemic therapy for type 2 diabetes - Scientific review. *Jama-J Am Med Assoc* **287**: 360-372.
 195. Kelly, WD, Lillehei, RC, Merkel, FK, Idezuki, Y, and Goetz, FC (1967). Allotransplantation of the pancreas and duodenum along with the kidney in diabetic nephropathy. *Surgery* **61**: 827-837.
 196. Hampson, FA, Freeman, SJ, Ertner, J, Drage, M, Butler, A, Watson, CJ, *et al.* (2010). Pancreatic transplantation: surgical technique, normal radiological appearances and complications. *Insights Imaging* **1**: 339-347.
 197. Shapiro, AMJ, Lakey, JRT, Ryan, EA, Korbitt, GS, Toth, E, Warnock, GL, *et al.* (2000). Islet transplantation in seven patients with type 1 diabetes mellitus using a glucocorticoid-free immunosuppressive regimen. *New Engl J Med* **343**: 230-238.
 198. Samstein, B, and Platt, JL (2001). Physiologic and immunologic hurdles to xenotransplantation. *J Am Soc Nephrol* **12**: 182-193.
 199. Reske, AP, Reske, AW, and Metze, M (2015). Complications of immunosuppressive agents therapy in transplant patients. *Minerva Anesthesiol* **81**: 1244-1261.
 200. Lee, RH, Seo, MJ, Reger, RL, Spees, JL, Pulin, AA, Olson, SD, *et al.* (2006). Multipotent stromal cells from human marrow home to and promote repair of pancreatic islets and renal glomeruli in diabetic NOD/scid mice. *P Natl Acad Sci USA* **103**: 17438-17443.
 201. Sordi, V, Malosio, ML, Marchesi, F, Mercalli, A, Melzi, R, Giordano, T, *et al.* (2005). Bone marrow mesenchymal stem cells express a restricted set of functionally active chemokine receptors capable of promoting migration to pancreatic islets. *Blood* **106**: 419-427.
 202. Zang, L, Hao, HJ, Liu, JJ, Li, YJ, Han, WD, and Mu, YM (2017). Mesenchymal stem cell therapy in type 2 diabetes mellitus. *Diabetol Metab Syndr* **9**.
 203. Ezquer, F, Ezquer, M, Contador, D, Ricca, M, Simon, V, and Conget, P (2012). The Antidiabetic Effect of Mesenchymal Stem Cells Is Unrelated to Their Transdifferentiation Potential But to Their Capability to Restore Th1/Th2 Balance and to Modify the Pancreatic Microenvironment. *Stem Cells* **30**: 1664-1674.

204. Bell, GI, Meschino, MT, Hughes-Large, JM, Broughton, HC, Xenocostas, A, and Hess, DA (2012). Combinatorial Human Progenitor Cell Transplantation Optimizes Islet Regeneration Through Secretion of Paracrine Factors. *Stem Cells Dev* **21**: 1863-1876.
205. Chandravanshi, B, and Bhonde, RR (2017). Shielding Engineered Islets With Mesenchymal Stem Cells Enhance Survival Under Hypoxia. *J Cell Biochem* **118**: 2672-2683.
206. Devaraj, S, Dasu, MR, and Jialal, I (2010). Diabetes is a proinflammatory state: a translational perspective. *Expert Rev Endocrinol Metab* **5**: 19-28.
207. Yeung, TY, Seeberger, KL, Kin, T, Adesida, A, Jomha, N, Shapiro, AMJ, *et al.* (2012). Human Mesenchymal Stem Cells Protect Human Islets from Pro-Inflammatory Cytokines. *Plos One* **7**.
208. Guney, MA, and Gannon, M (2009). Pancreas Cell Fate. *Birth Defects Res C* **87**: 232-248.
209. Pokrywczynska, M, Krzyzanowska, S, Jundzill, A, Adamowicz, J, and Drewa, T (2013). Differentiation of Stem Cells into Insulin-Producing Cells: Current Status and Challenges. *Arch Immunol Ther Ex* **61**: 149-158.
210. Timper, K, Seboek, D, Eberhardt, M, Linscheid, P, Christ-Crain, M, Keller, U, *et al.* (2006). Human adipose tissue-derived mesenchymal stem cells differentiate into insulin, somatostatin, and glucagon expressing cells. *Biochem Bioph Res Co* **341**: 1135-1140.
211. Xin, Y, Jiang, X, Wang, YS, Su, XJ, Sun, MY, Zhang, LH, *et al.* (2016). Insulin-Producing Cells Differentiated from Human Bone Marrow Mesenchymal Stem Cells In Vitro Ameliorate Streptozotocin-Induced Diabetic Hyperglycemia. *Plos One* **11**.
212. Santamaria, X, Massasa, EE, Feng, Y, Wolff, E, and Taylor, HS (2011). Derivation of insulin producing cells from human endometrial stromal stem cells and use in the treatment of murine diabetes. *Mol Ther* **19**: 2065-2071.
213. Si, YL, Zhao, YL, Hao, HJ, Liu, JJ, Guo, YL, Mu, YM, *et al.* (2012). Infusion of Mesenchymal Stem Cells Ameliorates Hyperglycemia in Type 2 Diabetic Rats. *Diabetes* **61**: 1616-1625.
214. Xie, Z, Hao, H, Tong, C, Cheng, Y, Liu, J, Pang, Y, *et al.* (2016). Human umbilical cord-derived mesenchymal stem cells elicit macrophages into an anti-inflammatory phenotype to alleviate insulin resistance in type 2 diabetic rats. *Stem Cells* **34**: 627-639.

215. Deloukas, P, Schuler, GD, Gyapay, G, Beasley, EM, Soderlund, C, Rodriguez-Tome, P, *et al.* (1998). A physical map of 30,000 human genes. *Science* **282**: 744-746.
216. Brown, PO, and Botstein, D (1999). Exploring the new world of the genome with DNA microarrays. *Nat Genet* **21**: 33-37.
217. (2006). Making the most of microarrays. *Nat Biotechnol* **24**: 1039-1039.
218. Schulze, A, and Downward, J (2001). Navigating gene expression using microarrays - a technology review. *Nat Cell Biol* **3**: E190-E195.
219. Bumgarner, R (2013). Overview of DNA microarrays: types, applications, and their future. *Current protocols in molecular biology* **101**: 22.21. 21-22.21. 11.
220. Quackenbush, J (2006). Microarray analysis and tumor classification. *New Engl J Med* **355**: 960-960.
221. Overbeek, R, Fonstein, M, D'Souza, M, Pusch, GD, and Maltsev, N (1999). The use of gene clusters to infer functional coupling. *P Natl Acad Sci USA* **96**: 2896-2901.
222. Mao, XY, Young, BD, and Lu, YJ (2007). The application of single nucleotide polymorphism microarrays in cancer research. *Curr Genomics* **8**: 219-228.
223. Govindarajan, R, Duraiyan, J, Kaliyappan, K, and Palanisamy, M (2012). Microarray and its applications. *J Pharm Bioallied Sci* **4**: S310-312.
224. Marongiu, F, Gramignoli, R, Sun, Q, Tahan, V, Miki, T, Dorko, K, *et al.* (2010). Isolation of amniotic mesenchymal stem cells. *Curr Protoc Stem Cell Biol* **Chapter 1**: Unit 1E 5.
225. Koo, BK, Park, IY, Kim, J, Kim, JH, Kwon, A, Kim, M, *et al.* (2012). Isolation and Characterization of Chorionic Mesenchymal Stromal Cells from Human Full Term Placenta. *Journal of Korean medical science* **27**: 857-863.
226. Mosmann, T (1983). Rapid colorimetric assay for cellular growth and survival: application to proliferation and cytotoxicity assays. *J Immunol Methods* **65**: 55-63.
227. Stone, V, Johnston, H, and Schins, RPF (2009). Development of in vitro systems for nanotoxicology: methodological considerations. *Crit Rev Toxicol* **39**: 613-626.
228. Wang, P, Henning, SM, and Heber, D (2010). Limitations of MTT and MTS-based assays for measurement of antiproliferative activity of green tea polyphenols. *PLoS One* **5**: e10202.
229. Riss, TL, Moravec, RA, Niles, AL, Duellman, S, Benink, HA, Worzella, TJ,

- et al.* (2004). Cell Viability Assays. In: Sittampalam, GS, *et al.* (eds). *Assay Guidance Manual*: Bethesda (MD).
230. Menon, V, Thomas, R, Ghale, AR, Reinhard, C, and Pruszk, J (2014). Flow cytometry protocols for surface and intracellular antigen analyses of neural cell types. *J Vis Exp*.
 231. Birmingham, E, Niebur, GL, McHugh, PE, Shaw, G, Barry, FP, and McNamara, LM (2012). Osteogenic differentiation of mesenchymal stem cells is regulated by osteocyte and osteoblast cells in a simplified bone niche. *Eur Cell Mater* **23**: 13-27.
 232. Strutt, B, Khalil, W, and Killinger, D (1996). Growth and differentiation of human adipose stromal cells in culture. *Methods Mol Med* **2**: 41-51.
 233. Pittenger, MF, Mackay, AM, Beck, SC, Jaiswal, RK, Douglas, R, Mosca, JD, *et al.* (1999). Multilineage potential of adult human mesenchymal stem cells. *Science* **284**: 143-147.
 234. Marion, NW, and Mao, JJ (2006). Mesenchymal stem cells and tissue engineering. *Methods Enzymol* **420**: 339-361.
 235. Dexheimer, V, Frank, S, and Richter, W (2012). Proliferation as a requirement for in vitro chondrogenesis of human mesenchymal stem cells. *Stem Cells Dev* **21**: 2160-2169.
 236. Ye, J, Coulouris, G, Zaretskaya, I, Cutcutache, I, Rozen, S, and Madden, TL (2012). Primer-BLAST: a tool to design target-specific primers for polymerase chain reaction. *BMC Bioinformatics* **13**: 134.
 237. Ruiz-Villalba, A, van Pelt-Verkuil, E, Gunst, QD, Ruijter, JM, and van den Hoff, MJ (2017). Amplification of nonspecific products in quantitative polymerase chain reactions (qPCR). *Biomol Detect Quantif* **14**: 7-18.
 238. Keer, JT (2008). Quantitative real-time PCR Analysis. *Essentials of Nucleic Acid Analysis: A Robust Approach*: 132.
 239. Chen, L, and Flies, DB (2013). Molecular mechanisms of T cell co-stimulation and co-inhibition. *Nat Rev Immunol* **13**: 227-242.
 240. Deans, RJ, and Moseley, AB (2000). Mesenchymal stem cells: biology and potential clinical uses. *Experimental hematology* **28**: 875-884.
 241. Mimeault, M, and Batra, SK (2006). Concise review: recent advances on the significance of stem cells in tissue regeneration and cancer therapies. *Stem Cells* **24**: 2319-2345.
 242. Pipino, C, Shangaris, P, Resca, E, Zia, S, Deprest, J, Sebire, NJ, *et al.* (2013). Placenta as a reservoir of stem cells: an underutilized resource? *Br Med Bull* **105**: 43-68.
 243. Brooke, G, Tong, H, Levesque, JP, and Atkinson, K (2008). Molecular

- trafficking mechanisms of multipotent mesenchymal stem cells derived from human bone marrow and placenta. *Stem Cells Dev* **17**: 929-940.
244. Hass, R, Kasper, C, Bohm, S, and Jacobs, R (2011). Different populations and sources of human mesenchymal stem cells (MSC): A comparison of adult and neonatal tissue-derived MSC. *Cell communication and signaling : CCS* **9**: 12.
 245. Tsagias, N, Koliakos, I, Lappa, M, Karagiannis, V, and Koliakos, GG (2011). Placenta perfusion has hematopoietic and mesenchymal progenitor stem cell potential. *Transfusion* **51**: 976-985.
 246. Hsiao, EY, and Patterson, PH (2012). Placental regulation of maternal-fetal interactions and brain development. *Developmental neurobiology* **72**: 1317-1326.
 247. Kim, HS, Cho, SH, Kwon, HS, Sohn, IS, and Hwang, HS (2014). The significance of placental ratios in pregnancies complicated by small for gestational age, preeclampsia, and gestational diabetes mellitus. *Obstetrics & gynecology science* **57**: 358-366.
 248. Hadarits, O, Zoka, A, Barna, G, Al-Aissa, Z, Rosta, K, Rigo, J, *et al.* (2016). Increased Proportion of Hematopoietic Stem and Progenitor Cell Population in Cord Blood of Neonates Born to Mothers with Gestational Diabetes Mellitus. *Stem Cells Dev* **25**: 13-17.
 249. An, B, Kim, E, Song, H, Ha, KS, Han, ET, Park, WS, *et al.* (2017). Gestational Diabetes Affects the Growth and Functions of Perivascular Stem Cells. *Mol Cells* **40**: 434-439.
 250. Hess, D, Li, L, Martin, M, Sakano, S, Hill, D, Strutt, B, *et al.* (2003). Bone marrow-derived stem cells initiate pancreatic regeneration. *Nat Biotechnol* **21**: 763-770.
 251. Gao, X, Song, L, Shen, K, Wang, H, Qian, M, Niu, W, *et al.* (2014). Bone marrow mesenchymal stem cells promote the repair of islets from diabetic mice through paracrine actions. *Mol Cell Endocrinol* **388**: 41-50.
 252. Hao, H, Liu, J, Shen, J, Zhao, Y, Liu, H, Hou, Q, *et al.* (2013). Multiple intravenous infusions of bone marrow mesenchymal stem cells reverse hyperglycemia in experimental type 2 diabetes rats. *Biochem Biophys Res Commun* **436**: 418-423.
 253. Reichert, D, Friedrichs, J, Ritter, S, Kaubler, T, Werner, C, Bornhauser, M, *et al.* (2015). Phenotypic, Morphological and Adhesive Differences of Human Hematopoietic Progenitor Cells Cultured on Murine versus

- Human Mesenchymal Stromal Cells. *Sci Rep* **5**: 15680.
254. Lefterova, MI, Haakonsson, AK, Lazar, MA, and Mandrup, S (2014). PPARgamma and the global map of adipogenesis and beyond. *Trends Endocrinol Metab* **25**: 293-302.
 255. Fu, Y, Luo, N, Klein, RL, and Garvey, WT (2005). Adiponectin promotes adipocyte differentiation, insulin sensitivity, and lipid accumulation. *J Lipid Res* **46**: 1369-1379.
 256. Mantovani, A, Sica, A, Sozzani, S, Allavena, P, Vecchi, A, and Locati, M (2004). The chemokine system in diverse forms of macrophage activation and polarization. *Trends Immunol* **25**: 677-686.
 257. Tsuchiya, S, Yamabe, M, Yamaguchi, Y, Kobayashi, Y, Konno, T, and Tada, K (1980). Establishment and Characterization of a Human Acute Monocytic Leukemia-Cell Line (Thp-1). *Int J Cancer* **26**: 171-176.
 258. Nemeth, K, Leelahavanichkul, A, Yuen, PST, Mayer, B, Parmelee, A, Doi, K, *et al.* (2009). Bone marrow stromal cells attenuate sepsis via prostaglandin E-2-dependent reprogramming of host macrophages to increase their interleukin-10 production. *Nat Med* **15**: 42-49.
 259. Chiossone, L, Conte, R, Spaggiari, GM, Serra, M, Romei, C, Bellora, F, *et al.* (2016). Mesenchymal Stromal Cells Induce Peculiar Alternatively Activated Macrophages Capable of Dampening Both Innate and Adaptive Immune Responses. *Stem Cells* **34**: 1909-1921.
 260. Genin, M, Clement, F, Fattaccioli, A, Raes, M, and Michiels, C (2015). M1 and M2 macrophages derived from THP-1 cells differentially modulate the response of cancer cells to etoposide. *Bmc Cancer* **15**.
 261. Oliveira, MS, and Barreto-Filho, JB (2015). Placental-derived stem cells: Culture, differentiation and challenges. *World journal of stem cells* **7**: 769-775.
 262. Antoniadou, E, and David, AL (2016). Placental stem cells. *Best Pract Res Clin Obstet Gynaecol* **31**: 13-29.
 263. Trounson, A, and McDonald, C (2015). Stem Cell Therapies in Clinical Trials: Progress and Challenges. *Cell stem cell* **17**: 11-22.
 264. Jaramillo-Ferrada, PA, Wolvetang, EJ, and Cooper-White, JJ (2012). Differential mesengenic potential and expression of stem cell-fate modulators in mesenchymal stromal cells from human-term placenta and bone marrow. *J Cell Physiol* **227**: 3234-3242.
 265. Araujo, AB, Salton, GD, Furlan, JM, Schneider, N, Angeli, MH, Laureano, AM, *et al.* (2017). Comparison of human mesenchymal stromal cells from four neonatal tissues: Amniotic membrane, chorionic membrane,

- placental decidua and umbilical cord. *Cytotherapy* **19**: 577-585.
266. Kim, J, Piao, Y, Pak, YK, Chung, D, Han, YM, Hong, JS, *et al.* (2015). Umbilical cord mesenchymal stromal cells affected by gestational diabetes mellitus display premature aging and mitochondrial dysfunction. *Stem Cells Dev* **24**: 575-586.
 267. Pierdomenico, L, Lanuti, P, Lachmann, R, Grifone, G, Ciani, E, Gialò, L, *et al.* (2011). Diabetes mellitus during pregnancy interferes with the biological characteristics of Wharton's jelly mesenchymal stem cells. *The Open Tissue Engineering and Regenerative Medicine Journal* **4**.
 268. Hermiston, ML, Xu, Z, and Weiss, A (2003). CD45: A critical regulator of signaling thresholds in immune cells. *Annu Rev Immunol* **21**: 107-137.
 269. Shvitiel, S, Kollet, O, Lapid, K, Schajnovitz, A, Goichberg, P, Kalinkovich, A, *et al.* (2008). CD45 regulates retention, motility, and numbers of hematopoietic progenitors, and affects osteoclast remodeling of metaphyseal trabecules. *J Exp Med* **205**: 2381-2395.
 270. Mareschi, K, Ferrero, I, Rustichelli, D, Aschero, S, Gammaitoni, L, Aglietta, M, *et al.* (2006). Expansion of mesenchymal stem cell isolated from pediatric and adult donor bone marrow. *Journal of Cellular Biochemistry* **97**: 744-754.
 271. Kanematsu, D, Shofuda, T, Yamamoto, A, Ban, C, Ueda, T, Yamasaki, M, *et al.* (2011). Isolation and cellular properties of mesenchymal cells derived from the decidua of human term placenta. *Differentiation* **82**: 77-88.
 272. Koike, C, Zhou, KX, Takeda, Y, Fathy, M, Okabe, M, Yoshida, T, *et al.* (2014). Characterization of Amniotic Stem Cells. *Cell Reprogram* **16**: 298-305.
 273. Gaillard, R (2015). Maternal obesity during pregnancy and cardiovascular development and disease in the offspring. *European journal of epidemiology* **30**: 1141-1152.
 274. Tamashiro, KL, and Moran, TH (2010). Perinatal environment and its influences on metabolic programming of offspring. *Physiology & behavior* **100**: 560-566.
 275. Lehnen, H, Zechner, U, and Haaf, T (2013). Epigenetics of gestational diabetes mellitus and offspring health: the time for action is in early stages of life. *Molecular human reproduction* **19**: 415-422.
 276. West, NA, Kechris, K, and Dabelea, D (2013). Exposure to Maternal Diabetes in Utero and DNA Methylation Patterns in the Offspring. *Immunometabolism* **1**: 1-9.

277. Uebel, K, Pusch, K, Gedrich, K, Schneider, KT, Hauner, H, and Bader, BL (2014). Effect of maternal obesity with and without gestational diabetes on offspring subcutaneous and preperitoneal adipose tissue development from birth up to year-1. *BMC pregnancy and childbirth* **14**: 138.
278. Moseti, D, Regassa, A, and Kim, WK (2016). Molecular Regulation of Adipogenesis and Potential Anti-Adipogenic Bioactive Molecules. *Int J Mol Sci* **17**.
279. Ma, X, Wang, D, Zhao, W, and Xu, L (2018). Deciphering the Roles of PPARgamma in Adipocytes via Dynamic Change of Transcription Complex. *Front Endocrinol (Lausanne)* **9**: 473.
280. Jones, JR, Barrick, C, Kim, KA, Lindner, J, Blondeau, B, Fujimoto, Y, *et al.* (2005). Deletion of PPARgamma in adipose tissues of mice protects against high fat diet-induced obesity and insulin resistance. *Proc Natl Acad Sci U S A* **102**: 6207-6212.
281. Sekiya, I, Larson, BL, Vuoristo, JT, Cui, JG, and Prockop, DJ (2004). Adipogenic differentiation of human adult stem cells from bone marrow stroma (MSCs). *J Bone Miner Res* **19**: 256-264.
282. Bae, YK, Kwon, JH, Kim, M, Kim, GH, Choi, SJ, Oh, W, *et al.* (2018). Intracellular Calcium Determines the Adipogenic Differentiation Potential of Human Umbilical Cord Blood-Derived Mesenchymal Stem Cells via the Wnt5a/beta-Catenin Signaling Pathway. *Stem Cells Int*.
283. Hu, C, Cao, H, Pan, X, Li, J, He, J, Pan, Q, *et al.* (2016). Adipogenic placenta-derived mesenchymal stem cells are not lineage restricted by withdrawing extrinsic factors: developing a novel visual angle in stem cell biology. *Cell Death Dis* **7**.
284. Ingulli, E (2010). Mechanism of cellular rejection in transplantation. *Pediatric nephrology* **25**: 61-74.
285. Kyurkchiev, D, Bochev, I, Ivanova-Todorova, E, Mourdjeva, M, Oreshkova, T, Belemezova, K, *et al.* (2014). Secretion of immunoregulatory cytokines by mesenchymal stem cells. *World journal of stem cells* **6**: 552-570.
286. Caruso, M, Evangelista, M, and Parolini, O (2012). Human term placental cells: phenotype, properties and new avenues in regenerative medicine. *International journal of molecular and cellular medicine* **1**: 64-74.
287. Glennie, S, Soeiro, I, Dyson, PJ, Lam, EWF, and Dazzi, F (2005). Bone marrow mesenchymal stem cells induce division arrest anergy of

- activated T cells. *Blood* **105**: 2821-2827.
288. Akiyama, K, Chen, C, Wang, DD, Xu, XT, Qu, CY, Yamaza, T, *et al.* (2012). Mesenchymal-Stem-Cell-Induced Immunoregulation Involves FAS-Ligand-/FAS-Mediated T Cell Apoptosis. *Cell stem cell* **10**: 544-555.
 289. Chinnadurai, R, Copland, IB, Patel, SR, and Galipeau, J (2014). IDO-Independent Suppression of T Cell Effector Function by IFN-gamma-Licensed Human Mesenchymal Stromal Cells. *Journal of Immunology* **192**: 1491-1501.
 290. Bachmann, MF, and Oxenius, A (2007). Interleukin 2: from immunostimulation to immunoregulation and back again. *Embo Rep* **8**: 1142-1148.
 291. Haddad, R, and Saldanha-Araujo, F (2014). Mechanisms of T-Cell Immunosuppression by Mesenchymal Stromal Cells: What Do We Know So Far? *Biomed Res Int*.
 292. Spaggiari, GM, and Moretta, L (2013). Cellular and molecular interactions of mesenchymal stem cells in innate immunity. *Immunology and cell biology* **91**: 27-31.
 293. Glenn, JD, and Whartenby, KA (2014). Mesenchymal stem cells: Emerging mechanisms of immunomodulation and therapy. *World journal of stem cells* **6**: 526-539.
 294. Parsa, R, Andresen, P, Gillett, A, Mia, S, Zhang, XM, Mayans, S, *et al.* (2012). Adoptive Transfer of Immunomodulatory M2 Macrophages Prevents Type 1 Diabetes in NOD Mice. *Diabetes* **61**: 2881-2892.
 295. Cao, XC, Han, ZB, Zhao, H, and Liu, Q (2014). Transplantation of mesenchymal stem cells recruits trophic macrophages to induce pancreatic beta cell regeneration in diabetic mice. *Int J Biochem Cell B* **53**: 372-379.
 296. Cho, DI, Kim, MR, Jeong, HY, Jeong, HC, Jeong, MH, Yoon, SH, *et al.* (2014). Mesenchymal stem cells reciprocally regulate the M1/M2 balance in mouse bone marrow-derived macrophages. *Exp Mol Med* **46**.
 297. Selleri, S, Bifsha, P, Civini, S, Pacelli, C, Dieng, MM, Lemieux, W, *et al.* (2016). Human mesenchymal stromal cell-secreted lactate induces M2-macrophage differentiation by metabolic reprogramming. *Oncotarget* **7**: 30193-30210.
 298. Spaggiari, GM, Abdelrazik, H, Becchetti, F, and Moretta, L (2009). MSCs inhibit monocyte-derived DC maturation and function by selectively interfering with the generation of immature DCs: central role of MSC-

- derived prostaglandin E(2). *Blood* **113**: 6576-6583.
299. Vasandan, AB, Jahnavi, S, Shashank, C, Prasad, P, Kumar, A, and Prasanna, J (2016). Human Mesenchymal stem cells program macrophage plasticity by altering their metabolic status via a PGE(2)-dependent mechanism. *Sci Rep-Uk* **6**.
 300. Nawaz, A, Aminuddin, A, Kado, T, Takikawa, A, Yamamoto, S, Tsuneyama, K, *et al.* (2017). CD206(+) M2-like macrophages regulate systemic glucose metabolism by inhibiting proliferation of adipocyte progenitors. *Nat Commun* **8**.
 301. Roszer, T (2015). Understanding the Mysterious M2 Macrophage through Activation Markers and Effector Mechanisms. *Mediat Inflamm*.
 302. Katakura, T, Miyazaki, M, Kobayashi, M, Herndon, DN, and Suzuki, F (2004). CCL17 and IL-10 as effectors that enable alternatively activated macrophages to inhibit the generation of classically activated macrophages. *Journal of Immunology* **172**: 1407-1413.
 303. Mueller, SM, and Glowacki, J (2001). Age-related decline in the osteogenic potential of human bone marrow cells cultured in three-dimensional collagen sponges. *Journal of cellular biochemistry* **82**: 583-590.
 304. Cianfarani, F, Toietta, G, Di Rocco, G, Cesareo, E, Zambruno, G, and Odorisio, T (2013). Diabetes impairs adipose tissue-derived stem cell function and efficiency in promoting wound healing. *Wound repair and regeneration : official publication of the Wound Healing Society [and] the European Tissue Repair Society* **21**: 545-553.
 305. Sun, Y, Deng, W, Geng, L, Zhang, L, Liu, R, Chen, W, *et al.* (2015). Mesenchymal stem cells from patients with rheumatoid arthritis display impaired function in inhibiting Th17 cells. *Journal of immunology research* **2015**: 284215.
 306. Hales, CN, and Barker, DJ (1992). Type 2 (non-insulin-dependent) diabetes mellitus: the thrifty phenotype hypothesis. *Diabetologia* **35**: 595-601.
 307. Monteiro, LJ, Norman, JE, Rice, GE, and Illanes, SE (2016). Fetal programming and gestational diabetes mellitus. *Placenta* **48 Suppl 1**: S54-S60.
 308. Kasher-Meron, M, and Grajower, MM (2017). Preventing progression from gestational diabetes mellitus to diabetes: A thought-filled review. *Diabetes Metab Res Rev* **33**.
 309. Brawerman, GM, and Dolinsky, VW (2018). Therapies for gestational

- diabetes and their implications for maternal and offspring health: Evidence from human and animal studies. *Pharmacol Res*.
310. Ashcroft, FM, and Rorsman, P (2012). Diabetes mellitus and the beta cell: the last ten years. *Cell* **148**: 1160-1171.
 311. Inzucchi, SE (2002). Oral antihyperglycemic therapy for type 2 diabetes: scientific review. *JAMA* **287**: 360-372.
 312. Shapiro, AM, Lakey, JR, Ryan, EA, Korbitt, GS, Toth, E, Warnock, GL, *et al.* (2000). Islet transplantation in seven patients with type 1 diabetes mellitus using a glucocorticoid-free immunosuppressive regimen. *N Engl J Med* **343**: 230-238.
 313. Volarevic, V, Arsenijevic, N, Lukic, ML, and Stojkovic, M (2011). Concise review: Mesenchymal stem cell treatment of the complications of diabetes mellitus. *Stem Cells* **29**: 5-10.
 314. Xie, QP, Huang, H, Xu, B, Dong, X, Gao, SL, Zhang, B, *et al.* (2009). Human bone marrow mesenchymal stem cells differentiate into insulin-producing cells upon microenvironmental manipulation in vitro. *Differentiation* **77**: 483-491.
 315. Gabr, MM, Sobh, MM, Zakaria, MM, Refaie, AF, and Ghoneim, MA (2008). Transplantation of Insulin-Producing Clusters Derived From Adult Bone Marrow Stem Cells to Treat Diabetes in Rats. *Exp Clin Transplant* **6**: 236-243.
 316. Yang, LJ, Li, SW, Hatch, H, Ahrens, K, Cornelius, JG, Petersen, BE, *et al.* (2002). In vitro trans-differentiation of adult hepatic stem cells into pancreatic endocrine hormone-producing cells. *P Natl Acad Sci USA* **99**: 8078-8083.
 317. Wong, RSY (2011). Extrinsic Factors Involved in the Differentiation of Stem Cells into Insulin-Producing Cells: An Overview. *Exp Diabetes Res*.
 318. Lumelsky, N, Blondel, O, Laeng, P, Velasco, I, Ravin, R, and McKay, R (2001). Differentiation of embryonic stem cells to insulin-secreting structures similar to pancreatic islets. *Science* **292**: 1389-1394.
 319. Van Hoof, D, D'Amour, KA, and German, MS (2009). Derivation of insulin-producing cells from human embryonic stem cells. *Stem Cell Res* **3**: 73-87.
 320. Taneera, J, Rosengren, A, Renstrom, E, Nygren, JM, Serup, P, Rorsman, P, *et al.* (2006). Failure of transplanted bone marrow cells to adopt a pancreatic beta-cell fate. *Diabetes* **55**: 290-296.
 321. McLean, AB, D'Amour, KA, Jones, KL, Krishnamoorthy, M, Kulik, MJ, Reynolds, DM, *et al.* (2007). Activin a efficiently specifies definitive

- endoderm from human embryonic stem cells only when phosphatidylinositol 3-kinase signaling is suppressed. *Stem Cells* **25**: 29-38.
322. Hashemian, SJ, Kouhnavard, M, and Nasli-Esfahani, E (2015). Mesenchymal Stem Cells: Rising Concerns over Their Application in Treatment of Type One Diabetes Mellitus. *J Diabetes Res*.
 323. Evans-Molina, C, Vestermarck, GL, and Mirmira, RG (2009). Development of insulin-producing cells from primitive biologic precursors. *Curr Opin Organ Tran* **14**: 56-63.
 324. Lesage, F, Zia, S, Jimenez, J, Deprest, J, and Toelen, J (2017). The amniotic fluid as a source of mesenchymal stem cells with lung-specific characteristics. *Prenat Diagn* **37**: 1093-1099.
 325. Fukuchi, Y, Nakajima, H, Sugiyama, D, Hirose, I, Kitamura, T, and Tsuji, K (2004). Human placenta-derived cells have mesenchymal stem/progenitor cell potential. *Stem Cells* **22**: 649-658.
 326. Tsai, PJ, Wang, HS, Lin, CH, Weng, ZC, Chen, TH, and Shyu, JF (2014). Intraportal injection of insulin-producing cells generated from human bone marrow mesenchymal stem cells decreases blood glucose level in diabetic rats. *Endocr Res* **39**: 26-33.
 327. Tang, DQ, Cao, LZ, Burkhardt, BR, Xia, CQ, Litherland, SA, Atkinson, MA, *et al.* (2004). In vivo and in vitro characterization of insulin-producing cells obtained from murine bone marrow. *Diabetes* **53**: 1721-1732.
 328. Rutter, GA (2001). Nutrient-secretion coupling in the pancreatic islet beta-cell: recent advances. *Mol Aspects Med* **22**: 247-284.
 329. Assmann, A, Ueki, K, Winnay, JN, Kadowaki, T, and Kulkarni, RN (2009). Glucose Effects on Beta-Cell Growth and Survival Require Activation of Insulin Receptors and Insulin Receptor Substrate 2. *Mol Cell Biol* **29**: 3219-3228.
 330. Garcia-Ocaña, A, and Alonso, LC (2010). Glucose mediated regulation of beta cell proliferation. *Open Endocrinol J* **4**: 55-65.
 331. Bonnerweir, S, Deery, D, Leahy, JL, and Weir, GC (1989). Compensatory Growth of Pancreatic Beta-Cells in Adult-Rats after Short-Term Glucose-Infusion. *Diabetes* **38**: 49-53.
 332. Xin, Y, Jiang, X, Wang, Y, Su, X, Sun, M, Zhang, L, *et al.* (2016). Insulin-Producing Cells Differentiated from Human Bone Marrow Mesenchymal Stem Cells In Vitro Ameliorate Streptozotocin-Induced Diabetic Hyperglycemia. *PLoS One* **11**: e0145838.
 333. Kieffer, TJ (2016). Closing in on Mass Production of Mature Human Beta

- Cells. *Cell stem cell* **18**: 699-702.
334. Rukstalis, JM, and Habener, JF (2009). Neurogenin3 A master regulator of pancreatic islet differentiation and regeneration. *Islets* **1**: 177-184.
 335. Villaseñor, A, Chong, DC, and Cleaver, O (2008). Biphasic Ngn3 Expression in the Developing Pancreas. *Dev Dynam* **237**: 3270-3279.
 336. Du, AP, Hunter, CS, Murray, J, Noble, D, Cai, CL, Evans, SM, *et al.* (2009). Islet-1 is Required for the Maturation, Proliferation, and Survival of the Endocrine Pancreas. *Diabetes* **58**: 2059-2069.
 337. Guo, T, Wang, WP, Zhang, H, Liu, YA, Chen, P, Ma, KT, *et al.* (2011). ISL1 Promotes Pancreatic Islet Cell Proliferation. *Plos One* **6**.
 338. Fujimoto, K, and Polonsky, KS (2009). Pdx1 and other factors that regulate pancreatic beta-cell survival. *Diabetes Obes Metab* **11**: 30-37.
 339. Swisa, A, Avrahami, D, Eden, N, Zhang, J, Feleke, E, Dahan, T, *et al.* (2017). PAX6 maintains beta cell identity by repressing genes of alternative islet cell types. *Journal of Clinical Investigation* **127**: 230-243.
 340. Sander, M, Neubuser, A, Kalamaras, J, Ee, HC, Martin, GR, and German, MS (1997). Genetic analysis reveals that PAX6 is required for normal transcription of pancreatic hormone genes and islet development. *Gene Dev* **11**: 1662-1673.
 341. Nakajima-Nagata, N, Sugai, M, Sakurai, T, Miyazaki, J, Tabata, YH, and Shimizu, A (2004). Pdx-1 enables insulin secretion by regulating synaptotagmin 1 gene expression. *Biochem Bioph Res Co* **318**: 631-635.
 342. Klemen, MS, Dolensek, J, Rupnik, MS, and Stozer, A (2017). The triggering pathway to insulin secretion: Functional similarities and differences between the human and the mouse cells and their translational relevance. *Islets* **9**: 109-139.
 343. Thorens, B (2015). GLUT2, glucose sensing and glucose homeostasis. *Diabetologia* **58**: 221-232.
 344. Han, SM, Han, SH, Coh, YR, Jang, G, Ra, JC, Kang, SK, *et al.* (2014). Enhanced proliferation and differentiation of Oct4-and Sox2-overexpressing human adipose tissue mesenchymal stem cells. *Exp Mol Med* **46**.
 345. Dimri, GP, Lee, X, Basile, G, Acosta, M, Scott, G, Roskelley, C, *et al.* (1995). A biomarker that identifies senescent human cells in culture and in aging skin in vivo. *Proc Natl Acad Sci U S A* **92**: 9363-9367.
 346. Tang, DQ, Cao, LZ, Burkhardt, BR, Xia, CQ, Litherland, SA, Atkinson, MA, *et al.* (2004). In vivo and in vitro characterization of insulin-producing

- cells obtained from murine bone marrow. *Diabetes* **53**: 1721-1732.
347. D'Amour, KA, Agulnick, AD, Eliazer, S, Kelly, OG, Kroon, E, and Baetge, EE (2005). Efficient differentiation of human embryonic stem cells to definitive endoderm. *Nat Biotechnol* **23**: 1534-1541.
 348. Micallef, SJ, Janes, ME, Knezevic, K, Davis, RP, Elefanty, AG, and Stanley, EG (2005). Retinoic acid induces Pdx1-positive endoderm in differentiating mouse embryonic stem cells. *Diabetes* **54**: 301-305.
 349. Goicoa, S, Alvarez, S, Ricordi, C, Inverardi, L, and Dominguez-Bendala, J (2006). Sodium butyrate activates genes of early pancreatic development in embryonic stem cells. *Cloning Stem Cells* **8**: 140-149.
 350. Chandra, V, G, S, Phadnis, S, Nair, PD, and Bhonde, RR (2009). Generation of pancreatic hormone-expressing islet-like cell aggregates from murine adipose tissue-derived stem cells. *Stem Cells* **27**: 1941-1953.
 351. L'Amoreaux, WJ, Cuttitta, C, Santora, A, Blaize, JF, Tachjadi, J, and El Idrissi, A (2010). Taurine regulates insulin release from pancreatic beta cell lines. *J Biomed Sci* **17 Suppl 1**: S11.
 352. Ito, T, Schaffer, SW, and Azuma, J (2012). The potential usefulness of taurine on diabetes mellitus and its complications. *Amino Acids* **42**: 1529-1539.
 353. Chandra, V, Swetha, G, Phadnis, S, Nair, PD, and Bhonde, RR (2009). Generation of Pancreatic Hormone-Expressing Islet-Like Cell Aggregates from Murine Adipose Tissue-Derived Stem Cells. *Stem Cells* **27**: 1941-1953.
 354. Boujendar, S, Arany, E, Hill, D, Remacle, C, and Reusens, B (2003). Taurine supplementation of a low protein diet fed to rat dams normalizes the vascularization of the fetal endocrine pancreas. *J Nutr* **133**: 2820-2825.
 355. Bai, L, Meredith, G, and Tuch, BE (2005). Glucagon-like peptide-1 enhances production of insulin in insulin-producing cells derived from mouse embryonic stem cells. *J Endocrinol* **186**: 343-352.
 356. Abraham, EJ, Leech, CA, Lin, JC, Zulewski, H, and Habener, JF (2002). Insulinotropic hormone glucagon-like peptide-1 differentiation of human pancreatic islet-derived progenitor cells into insulin-producing cells. *Endocrinology* **143**: 3152-3161.
 357. Donnelly, D (2012). The structure and function of the glucagon-like peptide-1 receptor and its ligands. *Brit J Pharmacol* **166**: 27-41.
 358. Yue, FM, Cui, L, Johkura, K, Ogiwara, N, and Sasaki, K (2006). Glucagon-

- like peptide-1 differentiation of primate embryonic stem cells into insulin-producing cells. *Tissue Engineering* **12**: 2105-2116.
359. Gabr, MM, Zakaria, MM, Refaie, AF, Abdel-Rahman, EA, Reda, AM, Ali, SS, *et al.* (2017). From Human Mesenchymal Stem Cells to Insulin-Producing Cells: Comparison between Bone Marrow- and Adipose Tissue-Derived Cells. *Biomed Res Int*.
 360. Li, H, Lam, A, Xu, AM, Lam, KSL, and Chung, SK (2010). High dosage of Exendin-4 increased early insulin secretion in differentiated beta cells from mouse embryonic stem cells. *Acta Pharmacol Sin* **31**: 570-577.
 361. Kumar, SS, Alarfaj, AA, Munusamy, MA, Singh, AJAR, Peng, IC, Priya, SP, *et al.* (2014). Recent Developments in beta-Cell Differentiation of Pluripotent Stem Cells Induced by Small and Large Molecules. *Int J Mol Sci* **15**: 23418-23447.
 362. Kassem, DH, Kamal, MM, El-Kholy, AG, and El-Mesallamy, HO (2016). Exendin-4 enhances the differentiation of Wharton's jelly mesenchymal stem cells into insulin-producing cells through activation of various beta-cell markers. *Stem Cell Res Ther* **7**.
 363. Rattananinsruang, P, Dechsukhum, C, and Leeanansaksiri, W (2018). Establishment of Insulin-Producing Cells From Human Embryonic Stem Cells Underhypoxic Condition for Cell Based Therapy. *Front Cell Dev Biol* **6**.
 364. Van Pham, P, Nguyen, PTM, Nguyen, ATQ, Pham, VM, Bui, ANT, Dang, LTT, *et al.* (2014). Improved differentiation of umbilical cord blood-derived mesenchymal stem cells into insulin-producing cells by PDX-1 mRNA transfection. *Differentiation* **87**: 200-208.
 365. Demeterco, C, Beattie, GM, Dib, SA, Lopez, AD, and Hayek, A (2000). A role for activin A and betacellulin in human fetal pancreatic cell differentiation and growth. *J Clin Endocr Metab* **85**: 3892-3897.
 366. Nagaoka, T, Fukuda, T, Hlashizume, T, Nishiyama, T, Tada, H, Yamada, H, *et al.* (2008). A betacellulin mutant promotes differentiation of pancreatic acinar AR42J cells into insulin-producing cells with low affinity of binding to ErbB1. *J Mol Biol* **380**: 83-94.
 367. Gabr, MM, Zakaria, MM, Refaie, AF, Khater, SM, Ashamallah, SA, Ismail, AM, *et al.* (2014). Generation of Insulin-Producing Cells from Human Bone Marrow-Derived Mesenchymal Stem Cells: Comparison of Three Differentiation Protocols. *Biomed Res Int*.
 368. Komatsu, M, Sato, Y, Yamada, S, Yamauchi, K, Hashizume, K, and Aizawa, T (2002). Triggering of insulin release by a combination of cAMP signal

- and nutrients: an ATP-sensitive K⁺ channel-independent phenomenon. *Diabetes* **51 Suppl 1**: S29-32.
369. Nazarov, I, Lee, JW, Soupene, E, Etemad, S, Knapik, D, Green, W, *et al.* (2012). Multipotent Stromal Stem Cells from Human Placenta Demonstrate High Therapeutic Potential. *Stem Cell Transl Med* **1**: 359-372.
 370. Romer, AI, and Sussel, L (2015). Pancreatic islet cell development and regeneration. *Curr Opin Endocrinol* **22**: 255-264.
 371. Guillemain, G, Filhoulaud, G, Da Silva-Xavier, G, Rutter, GA, and Scharfmann, R (2007). Glucose is necessary for embryonic pancreatic endocrine cell differentiation. *J Biol Chem* **282**: 15228-15237.
 372. Fowden, AL, and Hill, DJ (2001). Intra-uterine programming of the endocrine pancreas. *British Medical Bulletin* **60**: 123-142.
 373. Ford, SP, Zhang, L, Zhu, M, Miller, MM, Smith, DT, Hess, BW, *et al.* (2009). Maternal obesity accelerates fetal pancreatic β -cell but not α -cell development in sheep: prenatal consequences. *American Journal of Physiology-Regulatory, Integrative and Comparative Physiology* **297**: R835-R843.
 374. Chavey, A, Movassat, J, and Portha, B (2011). Impact and Mechanisms of Pancreatic Beta-Cell Mass Programming by Maternal Diabetes-Insight from Animal Model Studies. *Gestational Diabetes*. InTech.
 375. Assmann, A, Ueki, K, Winnay, JN, Kadowaki, T, and Kulkarni, RN (2009). Glucose effects on beta-cell growth and survival require activation of insulin receptors and insulin receptor substrate 2. *Mol Cell Biol* **29**: 3219-3228.
 376. Assmann, A, Hinault, C, and Kulkarni, RN (2009). Growth factor control of pancreatic islet regeneration and function. *Pediatr Diabetes* **10**: 14-32.
 377. Soria, B (2001). In-vitro differentiation of pancreatic beta-cells. *Differentiation* **68**: 205-219.
 378. Bush, NC, Chandler-Laney, PC, Rouse, DJ, Granger, WM, Oster, RA, and Gower, BA (2011). Higher Maternal Gestational Glucose Concentration Is Associated with Lower Offspring Insulin Sensitivity and Altered beta-Cell Function. *J Clin Endocr Metab* **96**: E803-E809.
 379. Cao, LZ, Tang, DQ, Horb, ME, Li, SW, and Yang, LJ (2004). High glucose is necessary for complete maturation of Pdx1-VP16-expressing hepatic cells into functional insulin-producing cells. *Diabetes* **53**: 3168-3178.
 380. Oh, SH, Muzzonigro, TM, Bae, SH, LaPlante, JM, Hatch, HM, and

- Petersen, BE (2004). Adult bone marrow-derived cells trans-differentiating into insulin-producing cells for the treatment of type I diabetes. *Lab Invest* **84**: 607-617.
381. Zhu, Y, Liu, Q, Zhou, Z, and Ikeda, Y (2017). PDX1, Neurogenin-3, and MAFA: critical transcription regulators for beta cell development and regeneration. *Stem Cell Res Ther* **8**: 240.
 382. Gradwohl, G, Dierich, A, LeMeur, M, and Guillemot, F (2000). neurogenin3 is required for the development of the four endocrine cell lineages of the pancreas. *P Natl Acad Sci USA* **97**: 1607-1611.
 383. Sharma, A, and Rani, R (2017). Do we really need to differentiate mesenchymal stem cells into insulin-producing cells for attenuation of the autoimmune responses in type 1 diabetes: immunoprophylactic effects of precursors to insulin-producing cells. *Stem Cell Res Ther* **8**: 167.
 384. Wang, H, Ren, Y, Hu, X, Ma, M, Wang, X, Liang, H, *et al.* (2017). Effect of Wnt Signaling on the Differentiation of Islet beta-Cells from Adipose-Derived Stem Cells. *Biomed Res Int* **2017**: 2501578.
 385. Yu, TZ, Sheu, SS, Robotham, JL, and Yoon, YS (2008). Mitochondrial fission mediates high glucose-induced cell death through elevated production of reactive oxygen species. *Cardiovasc Res* **79**: 341-351.
 386. Li, YM, Schilling, T, Benisch, P, Zeck, S, Meissner-Weigl, J, Schneider, D, *et al.* (2007). Effects of high glucose on mesenchymal stem cell proliferation and differentiation. *Biochem Bioph Res Co* **363**: 209-215.
 387. Cramer, C, Freisinger, E, Jones, RK, Slakey, DP, Dupin, CL, Newsome, ER, *et al.* (2010). Persistent high glucose concentrations alter the regenerative potential of mesenchymal stem cells. *Stem Cells Dev* **19**: 1875-1884.
 388. Turinetto, V, Vitale, E, and Giachino, C (2016). Senescence in Human Mesenchymal Stem Cells: Functional Changes and Implications in Stem Cell-Based Therapy. *Int J Mol Sci* **17**.
 389. Chang, TC, Hsu, MF, and Wu, KK (2015). High glucose induces bone marrow-derived mesenchymal stem cell senescence by upregulating autophagy. *PLoS One* **10**: e0126537.
 390. Rekittke, NE, Ang, M, Rawat, D, Khatri, R, and Linn, T (2016). Regenerative Therapy of Type 1 Diabetes Mellitus: From Pancreatic Islet Transplantation to Mesenchymal Stem Cells. *Stem Cells Int*.
 391. Chang, CM, Kao, CL, Chang, YL, Yang, MJ, Chen, YC, Sung, BL, *et al.* (2007). Placenta-derived multipotent stem cells induced to

- differentiate into insulin-positive cells. *Biochem Bioph Res Co* **357**: 414-420.
392. Sone, H, and Kagawa, Y (2005). Pancreatic beta cell senescence contributes to the pathogenesis of type 2 diabetes in high-fat diet-induced diabetic mice. *Diabetologia* **48**: 58-67.
 393. Tersey, SA, Levasseur, EM, Syed, F, Farb, TB, Orr, KS, Nelson, JB, *et al.* (2018). Episodic beta-cell death and dedifferentiation during diet-induced obesity and dysglycemia in male mice. *FASEB J*: fj201800150RR.
 394. Wang, HS, Shyu, JF, Shen, WS, Hsu, HC, Chi, TC, Chen, CP, *et al.* (2011). Transplantation of Insulin-Producing Cells Derived From Umbilical Cord Stromal Mesenchymal Stem Cells to Treat NOD Mice. *Cell Transplantation* **20**: 455-466.
 395. Shi, Y, Hou, LL, Tang, FC, Jiang, W, Wang, PG, Ding, MX, *et al.* (2005). Inducing embryonic stem cells to differentiate into pancreatic beta cells by a novel three-step approach with activin A and all-trans retinoic acid. *Stem Cells* **23**: 656-662.
 396. Ostrom, M, Loffler, KA, Edfalk, S, Selander, L, Dahl, U, Ricordi, C, *et al.* (2008). Retinoic Acid Promotes the Generation of Pancreatic Endocrine Progenitor Cells and Their Further Differentiation into beta-Cells. *Plos One* **3**.
 397. Zarrouki, B, Benterki, I, Fontés, G, Peyot, M-L, Seda, O, Prentki, M, *et al.* (2014). Epidermal growth factor receptor signaling promotes pancreatic β -cell proliferation in response to nutrient excess in rats through mTOR and FOXM1. *Diabetes* **63**: 982-993.
 398. Otonkoski, T, Beattie, GM, Mally, MI, Ricordi, C, and Hayek, A (1993). Nicotinamide Is a Potent Inducer of Endocrine Differentiation in Cultured Human Fetal Pancreatic-Cells. *Journal of Clinical Investigation* **92**: 1459-1466.
 399. Yue, F, Cui, L, Johkura, K, Ogiwara, N, and Sasaki, K (2006). Glucagon-like peptide-1 differentiation of primate embryonic stem cells into insulin-producing cells. *Tissue Eng* **12**: 2105-2116.
 400. Hui, H, Yu, R, Bousquet, C, and Perfetti, R (2002). Transfection of pancreatic-derived beta-cells with a minigene encoding for human glucagon-like peptide-1 regulates glucose-dependent insulin synthesis and secretion. *Endocrinology* **143**: 3529-3539.
 401. Oliver-Krasinski, JM, Kasner, MT, Yang, J, Crutchlow, MF, Rustgi, AK, Kaestner, KH, *et al.* (2009). The diabetes gene Pdx1 regulates the

- transcriptional network of pancreatic endocrine progenitor cells in mice. *J Clin Invest* **119**: 1888-1898.
402. Papaetis, GS, Papakyriakou, P, and Panagiotou, TN (2015). Central obesity, type 2 diabetes and insulin: exploring a pathway full of thorns. *Arch Med Sci* **11**: 463-482.
 403. Kolterman, OG, Kim, DD, Shen, L, Ruggles, JA, Nielsen, LL, Fineman, MS, *et al.* (2005). Pharmacokinetics, pharmacodynamics, and safety of exenatide in patients with type 2 diabetes mellitus. *Am J Health Syst Pharm* **62**: 173-181.
 404. Zhao, Q, Yang, Y, Hu, J, Shan, Z, Wu, Y, and Lei, L (2016). Exendin-4 enhances expression of Neurod1 and Glut2 in insulin-producing cells derived from mouse embryonic stem cells. *Arch Med Sci* **12**: 199-207.
 405. Oh, YS, Shin, S, Lee, YJ, Kim, EH, and Jun, HS (2011). Betacellulin-induced beta cell proliferation and regeneration is mediated by activation of ErbB-1 and ErbB-2 receptors. *PLoS One* **6**: e23894.
 406. Cho, YM, Lim, JM, Yoo, DH, Kim, JH, Chung, SS, Park, SG, *et al.* (2008). Betacellulin and nicotinamide sustain PDX1 expression and induce pancreatic beta-cell differentiation in human embryonic stem cells. *Biochem Biophys Res Commun* **366**: 129-134.
 407. Voisin, L, Foisy, S, Giasson, E, Lambert, C, Moreau, P, and Meloche, S (2002). EGF receptor transactivation is obligatory for protein synthesis stimulation by G protein-coupled receptors. *Am J Physiol Cell Physiol* **283**: C446-455.
 408. Buteau, J, Foisy, S, Joly, E, and Prentki, M (2003). Glucagon-like peptide 1 induces pancreatic beta-cell proliferation via transactivation of the epidermal growth factor receptor. *Diabetes* **52**: 124-132.
 409. Lee, KW, and Pausova, Z (2013). Cigarette smoking and DNA methylation. *Front Genet* **4**: 132.
 410. Bajaj, M (2012). Nicotine and insulin resistance: when the smoke clears. *Diabetes* **61**: 3078-3080.
 411. Morimoto, A, Tatsumi, Y, Deura, K, Mizuno, S, Ohno, Y, and Watanabe, S (2013). Impact of cigarette smoking on impaired insulin secretion and insulin resistance in Japanese men: The Saku Study. *J Diabetes Investig* **4**: 274-280.
 412. Thorens, B (2015). GLUT2, glucose sensing and glucose homeostasis. *Diabetologia* **58**: 221-232.
 413. Parnaud, G, Lavallard, V, Bedat, B, Matthey-Doret, D, Morel, P, Berney, T, *et al.* (2015). Cadherin engagement improves insulin secretion of

- single human beta-cells. *Diabetes* **64**: 887-896.
414. Maes, E, and Pipeleers, D (1984). Effects of glucose and 3',5'-cyclic adenosine monophosphate upon reaggregation of single pancreatic B-cells. *Endocrinology* **114**: 2205-2209.
 415. Piscaglia, AC, Shupe, T, Gasbarrini, A, and Petersen, BE (2007). Microarray RNA/DNA in different stem cell lines. *Curr Pharm Biotechnol* **8**: 167-175.
 416. Perez-Iratxeta, C, Palidwor, G, Porter, CJ, Sanche, NA, Huska, MR, Suomela, BP, *et al.* (2005). Study of stem cell function using microarray experiments. *Febs Lett* **579**: 1795-1801.
 417. Synnergren, J, and Sartipy, P (2011). Microarray analysis of undifferentiated and differentiated human pluripotent stem cells. *Methodological Advances in the Culture, Manipulation and Utilization of Embryonic Stem Cells for Basic and Practical Applications*. InTech.
 418. Draghici, S, Khatri, P, Eklund, AC, and Szallasi, Z (2006). Reliability and reproducibility issues in DNA microarray measurements. *Trends Genet* **22**: 101-109.
 419. Rosenwald, A, Wright, G, Chan, WC, Connors, JM, Campo, E, Fisher, RI, *et al.* (2002). The use of molecular profiling to predict survival after chemotherapy for diffuse large-B-cell lymphoma. *New Engl J Med* **346**: 1937-1947.
 420. Shipp, MA, Ross, KN, Tamayo, P, Weng, AP, Kutok, JL, Aguiar, RCT, *et al.* (2002). Diffuse large B-cell lymphoma outcome prediction by gene-expression profiling and supervised machine learning. *Nat Med* **8**: 68-74.
 421. Ramalho-Santos, M, Yoon, S, Matsuzaki, Y, Mulligan, RC, and Melton, DA (2002). "Stemness": Transcriptional profiling of embryonic and adult stem cells. *Science* **298**: 597-600.
 422. Evsikov, AV, and Solter, D (2003). Comment on " 'Stemness': Transcriptional profiling of embryonic and adult stem cells" and "A stem cell molecular signature" (II). *Science* **302**.
 423. Ivanova, NB, Dimos, JT, Schaniel, C, Hackney, JA, Moore, KA, and Lemischka, IR (2002). A stem cell molecular signature. *Science* **298**: 601-604.
 424. Shi, LM, Reid, LH, Jones, WD, Shippy, R, Warrington, JA, Baker, SC, *et al.* (2006). The MicroArray Quality Control (MAQC) project shows inter- and intraplatform reproducibility of gene expression measurements. *Nat Biotechnol* **24**: 1151-1161.

425. Chuaqui, RF, Bonner, RF, Best, CJ, Gillespie, JW, Flaig, MJ, Hewitt, SM, *et al.* (2002). Post-analysis follow-up and validation of microarray experiments. *Nat Genet* **32 Suppl**: 509-514.
426. Tan, P (2004). Experimental Validation of Microarray Data.
427. Taniguchi, M, Miura, K, Iwao, H, and Yamanaka, S (2001). Quantitative assessment of DNA microarrays - Comparison with Northern blot analyses. *Genomics* **71**: 34-39.
428. Ambra, R, Manca, S, Palumbo, MC, Leoni, G, Natarelli, L, De Marco, A, *et al.* (2014). Transcriptome analysis of human primary endothelial cells (HUVEC) from umbilical cords of gestational diabetic mothers reveals candidate sites for an epigenetic modulation of specific gene expression. *Genomics* **103**: 337-348.
429. Koskinen, A, Lehtoranta, L, Laiho, A, Laine, J, Kaapa, P, and Soukka, H (2015). Maternal diabetes induces changes in the umbilical cord gene expression. *Placenta* **36**: 767-774.
430. Yang, IV (2006). Use of external controls in microarray experiments. *Method Enzymol* **411**: 50-+.
431. Kim, HY (2017). Statistical notes for clinical researchers: Chi-squared test and Fisher's exact test. *Restor Dent Endod* **42**: 152-155.
432. Tarca, AL, Romero, R, and Draghici, S (2006). Analysis of microarray experiments of gene expression profiling. *Am J Obstet Gynecol* **195**: 373-388.
433. Singh, A, Singh, A, and Sen, D (2016). Mesenchymal stem cells in cardiac regeneration: a detailed progress report of the last 6 years (2010-2015). *Stem Cell Res Ther* **7**.
434. Garbern, JC, and Lee, RT (2013). Cardiac Stem Cell Therapy and the Promise of Heart Regeneration. *Cell stem cell* **12**: 689-698.
435. Guan, XM, Ma, X, Zhang, L, Feng, HY, and Ma, Z (2014). Evaluation of CD24 as a marker to rapidly define the mesenchymal stem cell phenotype and its differentiation in human nucleus pulposus. *Chinese Med J-Peking* **127**: 1474-1481.
436. Schabath, H, Runz, S, Joumaa, S, and Altevogt, P (2006). CD24 affects CXCR4 function in pre-B lymphocytes and breast carcinoma cells. *J Cell Sci* **119**: 314-325.
437. Schack, LM, Buettner, M, Wirth, A, Neunaber, C, Krettek, C, Hoffmann, A, *et al.* (2016). Expression of CD24 in Human Bone Marrow-Derived Mesenchymal Stromal Cells Is Regulated by TGF beta 3 and Induces a Myofibroblast-Like Genotype. *Stem Cells Int.*

438. Lagares, D, Garcia-Fernandez, RA, Jimenez, CL, Magan-Marchal, N, Busnadiego, O, Lamas, S, *et al.* (2010). Endothelin 1 contributes to the effect of transforming growth factor beta1 on wound repair and skin fibrosis. *Arthritis Rheum* **62**: 878-889.
439. Kang, J, Gu, Y, Li, P, Johnson, BL, Sucov, HM, and Thomas, PS (2008). PDGF-A as an epicardial mitogen during heart development. *Dev Dynam* **237**: 692-701.
440. Madonna, R, Rokosh, G, De Caterina, R, and Bolli, R (2010). Hepatocyte growth factor/Met gene transfer in cardiac stem cells-potential for cardiac repair. *Basic Res Cardiol* **105**: 443-452.
441. Levy, DE, and Darnell, JE, Jr. (2002). Stats: transcriptional control and biological impact. *Nat Rev Mol Cell Biol* **3**: 651-662.
442. Schmitz, AA, Govek, EE, Bottner, B, and Van Aelst, L (2000). Rho GTPases: signaling, migration, and invasion. *Exp Cell Res* **261**: 1-12.
443. Vasiliou, V, and Nebert, DW (2005). Analysis and update of the human aldehyde dehydrogenase (ALDH) gene family. *Hum Genomics* **2**: 138-143.
444. Hou, Y, Ryu, CH, Jun, JA, Kim, SM, Jeong, CH, and Jeun, SS (2014). IL-8 enhances the angiogenic potential of human bone marrow mesenchymal stem cells by increasing vascular endothelial growth factor. *Cell Biol Int* **38**: 1050-1059.
445. Jee, SH, Chu, CY, Chiu, HC, Huang, YL, Tsai, WL, Liao, YH, *et al.* (2004). Interleukin-6 induced basic fibroblast growth factor-dependent angiogenesis in basal cell carcinoma cell line via JAK/STAT3 and PI3-kinase/Akt pathways. *J Invest Dermatol* **123**: 1169-1175.
446. Karar, J, and Maity, A (2011). PI3K/AKT/mTOR Pathway in Angiogenesis. *Front Mol Neurosci* **4**: 51.
447. Yu, JS, and Cui, W (2016). Proliferation, survival and metabolism: the role of PI3K/AKT/mTOR signalling in pluripotency and cell fate determination. *Development* **143**: 3050-3060.
448. Giacco, F, and Brownlee, M (2010). Oxidative stress and diabetic complications. *Circ Res* **107**: 1058-1070.
449. De Becker, A, and Riet, IV (2016). Homing and migration of mesenchymal stromal cells: How to improve the efficacy of cell therapy? *World J Stem Cells* **8**: 73-87.
450. Etienne-Manneville, S, and Hall, A (2002). Rho GTPases in cell biology. *Nature* **420**: 629-635.
451. Oh, JY, Choi, GE, Lee, HJ, Jung, YH, Ko, SH, Chae, CW, *et al.* (2018). High

- Glucose-Induced Reactive Oxygen Species Stimulates Human Mesenchymal Stem Cell Migration Through Snail and EZH2-Dependent E-Cadherin Repression. *Cell Physiol Biochem* **46**: 1749-1767.
452. Madonna, R, Geng, YJ, Shelat, H, Ferdinandy, P, and De Caterina, R (2014). High glucose-induced hyperosmolarity impacts proliferation, cytoskeleton remodeling and migration of human induced pluripotent stem cells via aquaporin-1. *Biochim Biophys Acta* **1842**: 2266-2275.
 453. Troncoso, F, Acurio, J, Herlitz, K, Aguayo, C, Bertoglia, P, Guzman-Gutierrez, E, *et al.* (2017). Gestational diabetes mellitus is associated with increased pro-migratory activation of vascular endothelial growth factor receptor 2 and reduced expression of vascular endothelial growth factor receptor 1. *PLoS One* **12**: e0182509.
 454. An, B, Kim, E, Song, H, Ha, KS, Han, ET, Park, WS, *et al.* (2017). Gestational Diabetes Affects the Growth and Functions of Perivascular Stem Cells. *Mol Cells* **40**: 434-439.
 455. Gui, J, Rohrbach, A, Borns, K, Hillemanns, P, Feng, L, Hubel, CA, *et al.* (2015). Vitamin D rescues dysfunction of fetal endothelial colony forming cells from individuals with gestational diabetes. *Placenta* **36**: 410-418.
 456. Lee, DE, Ayoub, N, and Agrawal, DK (2016). Mesenchymal stem cells and cutaneous wound healing: novel methods to increase cell delivery and therapeutic efficacy. *Stem Cell Res Ther* **7**: 37.
 457. Skardal, A, Mack, D, Kapetanovic, E, Atala, A, Jackson, JD, Yoo, J, *et al.* (2012). Bioprinted amniotic fluid-derived stem cells accelerate healing of large skin wounds. *Stem Cells Transl Med* **1**: 792-802.
 458. Zebardast, N, Lickorish, D, and Davies, JE (2010). Human umbilical cord perivascular cells (HUCPVC): A mesenchymal cell source for dermal wound healing. *Organogenesis* **6**: 197-203.
 459. Luo, G, Cheng, W, He, W, Wang, X, Tan, J, Fitzgerald, M, *et al.* (2010). Promotion of cutaneous wound healing by local application of mesenchymal stem cells derived from human umbilical cord blood. *Wound Repair Regen* **18**: 506-513.
 460. Brantley, JN, and Verla, TD (2015). Use of Placental Membranes for the Treatment of Chronic Diabetic Foot Ulcers. *Adv Wound Care (New Rochelle)* **4**: 545-559.
 461. Nichols, F, and Overly, A (2016). Novel Approach for Enterocutaneous Fistula Treatment with the Use of Viable Cryopreserved Placental Membrane. *Case Rep Surg* **2016**: 8797691.

462. Duan-Arnold, Y, Gyurdieva, A, Johnson, A, Uveges, TE, Jacobstein, DA, and Danilkovitch, A (2015). Retention of Endogenous Viable Cells Enhances the Anti-Inflammatory Activity of Cryopreserved Amnion. *Adv Wound Care (New Rochelle)* **4**: 523-533.
463. Davies, LC, Alm, JJ, Heldring, N, Moll, G, Gavin, C, Batsis, I, *et al.* (2016). Type 1 Diabetes Mellitus Donor Mesenchymal Stromal Cells Exhibit Comparable Potency to Healthy Controls In Vitro. *Stem Cells Transl Med* **5**: 1485-1495.
464. Palsgaard, J, Emanuelli, B, Winnay, JN, Sumara, G, Karsenty, G, and Kahn, CR (2012). Cross-talk between Insulin and Wnt Signaling in Preadipocytes ROLE OF WNT CO-RECEPTOR LOW DENSITY LIPOPROTEIN RECEPTOR-RELATED PROTEIN-5 (LRP5). *J Biol Chem* **287**: 12016-12026.
465. Kim, MH, Jee, JH, Park, S, Lee, MS, Kim, KW, and Lee, MK (2014). Metformin enhances glucagon-like peptide 1 via cooperation between insulin and Wnt signaling. *J Endocrinol* **220**: 117-128.
466. Subramaniam, N, Sherman, MH, Rao, R, Wilson, C, Coulter, S, Atkins, AR, *et al.* (2012). Metformin-Mediated Bambi Expression in Hepatic Stellate Cells Induces Prosurvival Wnt/beta-Catenin Signaling. *Cancer Prev Res* **5**: 553-561.
467. Nies, VJM, Sancar, G, Liu, WL, van Zutphen, T, Struik, D, Yu, RT, *et al.* (2016). Fibroblast Growth Factor Signaling in Metabolic Regulation. *Front Endocrinol* **6**.
468. Vasko, R, Koziolk, M, Ikehata, M, Rastaldi, MP, Jung, K, Schmid, H, *et al.* (2009). Role of basic fibroblast growth factor (FGF-2) in diabetic nephropathy and mechanisms of its induction by hyperglycemia in human renal fibroblasts. *Am J Physiol-Renal* **296**: F1452-F1463.
469. Ferguson, JE, 3rd, Kelley, RW, and Patterson, C (2005). Mechanisms of endothelial differentiation in embryonic vasculogenesis. *Arterioscler Thromb Vasc Biol* **25**: 2246-2254.
470. Kolluru, GK, Bir, SC, and Kevil, CG (2012). Endothelial dysfunction and diabetes: effects on angiogenesis, vascular remodeling, and wound healing. *Int J Vasc Med* **2012**: 918267.
471. Tahergorabi, Z, and Khazaei, M (2012). Imbalance of angiogenesis in diabetic complications: the mechanisms. *Int J Prev Med* **3**: 827-838.
472. Mathew, SA, and Bhonde, R (2017). Mesenchymal stromal cells isolated from gestationally diabetic human placenta exhibit insulin resistance, decreased clonogenicity and angiogenesis. *Placenta* **59**: 1-

8.

473. Moreb, JS (2008). Aldehyde dehydrogenase as a marker for stem cells. *Curr Stem Cell Res Ther* **3**: 237-246.
474. Storms, RW, Trujillo, AP, Springer, JB, Shah, L, Colvin, OM, Ludeman, SM, *et al.* (1999). Isolation of primitive human hematopoietic progenitors on the basis of aldehyde dehydrogenase activity. *Proc Natl Acad Sci U S A* **96**: 9118-9123.
475. Singh, S, Brocker, C, Koppaka, V, Chen, Y, Jackson, BC, Matsumoto, A, *et al.* (2013). Aldehyde dehydrogenases in cellular responses to oxidative/electrophilic stress. *Free Radic Biol Med* **56**: 89-101.
476. Sherman, SE, Kuljanin, M, Cooper, TT, Putman, DM, Lajoie, GA, and Hess, DA (2017). High Aldehyde Dehydrogenase Activity Identifies a Subset of Human Mesenchymal Stromal Cells with Vascular Regenerative Potential. *Stem Cells* **35**: 1542-1553.
477. Coughlan, MT, Vervaart, PP, Permezel, M, Georgiou, HM, and Rice, GE (2004). Altered placental oxidative stress status in gestational diabetes mellitus. *Placenta* **25**: 78-84.
478. Forrester, SJ, Kikuchi, DS, Hernandez, MS, Xu, Q, and Griendling, KK (2018). Reactive Oxygen Species in Metabolic and Inflammatory Signaling. *Circ Res* **122**: 877-+.
479. Liemburg-Apers, DC, Willems, PHGM, Koopman, WJH, and Grefte, S (2015). Interactions between mitochondrial reactive oxygen species and cellular glucose metabolism. *Arch Toxicol* **89**: 1209-1226.
480. Volpe, CMO, Villar-Delfino, PH, dos Anjos, PMF, and Nogueira-Machado, JA (2018). Cellular death, reactive oxygen species (ROS) and diabetic complications. *Cell Death Dis* **9**.
481. Singh, S, Brocker, C, Koppaka, V, Chen, Y, Jackson, BC, Matsumoto, A, *et al.* (2013). Aldehyde dehydrogenases in cellular responses to oxidative/electrophilic stress. *Free Radical Bio Med* **56**: 89-101.
482. Choudhary, S, Xiao, T, Vergara, LA, Srivastava, S, Nees, D, Piatigorsky, J, *et al.* (2005). Role of aldehyde dehydrogenase isozymes in the defense of rat lens and human lens epithelial cells against oxidative stress. *Invest Ophthalmol Vis Sci* **46**: 259-267.
483. Wenzel, P, Muller, J, Zurmeyer, S, Schuhmacher, S, Schulz, E, Oelze, M, *et al.* (2008). ALDH-2 deficiency increases cardiovascular oxidative stress--evidence for indirect antioxidative properties. *Biochem Biophys Res Commun* **367**: 137-143.
484. Lappas, M, Hiden, U, Desoye, G, Froehlich, J, Hauguel-de Mouzon, S,

- and Jawerbaum, A (2011). The role of oxidative stress in the pathophysiology of gestational diabetes mellitus. *Antioxid Redox Signal* **15**: 3061-3100.
485. Li, H, Yin, Q, Li, N, Ouyang, Z, and Zhong, M (2016). Plasma Markers of Oxidative Stress in Patients with Gestational Diabetes Mellitus in the Second and Third Trimester. *Obstet Gynecol Int* **2016**: 3865454.
 486. Kusuma, GD, Abumaree, MH, Perkins, AV, Brennecke, SP, and Kalionis, B (2017). Reduced aldehyde dehydrogenase expression in preeclamptic decidual mesenchymal stem/stromal cells is restored by aldehyde dehydrogenase agonists. *Sci Rep* **7**: 42397.
 487. Bo, S, Lezo, A, Menato, G, Gallo, ML, Bardelli, C, Signorile, A, *et al.* (2005). Gestational hyperglycemia, zinc, selenium, and antioxidant vitamins. *Nutrition* **21**: 186-191.
 488. Jamilian, M, Hashemi Dizaji, S, Bahmani, F, Taghizadeh, M, Memarzadeh, MR, Karamali, M, *et al.* (2017). A Randomized Controlled Clinical Trial Investigating the Effects of Omega-3 Fatty Acids and Vitamin E Co-Supplementation on Biomarkers of Oxidative Stress, Inflammation and Pregnancy Outcomes in Gestational Diabetes. *Can J Diabetes* **41**: 143-149.
 489. Isern, J, and Mendez-Ferrer, S (2011). Stem cell interactions in a bone marrow niche. *Curr Osteoporos Rep* **9**: 210-218.
 490. Wood, KJ, and Goto, R (2012). Mechanisms of rejection: current perspectives. *Transplantation* **93**: 1-10.
 491. Delo, DM, De Coppi, P, Bartsch, G, Jr., and Atala, A (2006). Amniotic fluid and placental stem cells. *Methods Enzymol* **419**: 426-438.
 492. Teofili, L, Silini, AR, Bianchi, M, Valentini, CG, and Parolini, O (2018). Incorporating placental tissue in cord blood banking for stem cell transplantation. *Expert Rev Hematol*: 1-13.
 493. Badowski, MS, and Harris, DT (2012). Collection, processing, and banking of umbilical cord blood stem cells for transplantation and regenerative medicine. *Methods Mol Biol* **879**: 279-290.
 494. Amrithraj, AI, Kodali, A, Nguyen, L, Teo, AKK, Chang, CW, Karnani, N, *et al.* (2017). Gestational Diabetes Alters Functions in Offspring's Umbilical Cord Cells With Implications for Cardiovascular Health. *Endocrinology* **158**: 2102-2112.
 495. Hou, Q, Lei, MX, Hu, K, and Wang, M (2015). The Effects of High Glucose Levels on Reactive Oxygen Species-Induced Apoptosis and Involved Signaling in Human Vascular Endothelial Cells. *Cardiovasc*

- Toxicol* **15**: 140-146.
496. Kim, J, Piao, Y, Pak, YK, Chung, D, Han, YM, Hong, JS, *et al.* (2015). Umbilical Cord Mesenchymal Stromal Cells Affected by Gestational Diabetes Mellitus Display Premature Aging and Mitochondrial Dysfunction. *Stem Cells Dev* **24**: 575-586.
 497. Sivitz, WI, and Yorek, MA (2010). Mitochondrial dysfunction in diabetes: from molecular mechanisms to functional significance and therapeutic opportunities. *Antioxid Redox Signal* **12**: 537-577.
 498. Boyle, KE, Patinkin, ZW, Shapiro, ALB, Baker, PR, Dabelea, D, and Friedman, JE (2016). Mesenchymal Stem Cells From Infants Born to Obese Mothers Exhibit Greater Potential for Adipogenesis: The Healthy Start BabyBUMP Project. *Diabetes* **65**: 647-659.
 499. Neri, C, and Edlow, AG (2016). Effects of Maternal Obesity on Fetal Programming: Molecular Approaches. *Csh Perspect Med* **6**.
 500. Tong, JF, Yan, X, Zhu, MJ, Ford, SP, Nathanielsz, PW, and Du, M (2009). Maternal obesity downregulates myogenesis and beta-catenin signaling in fetal skeletal muscle. *Am J Physiol-Endoc M* **296**: E917-E924.
 501. Miao, M, Dai, M, Zhang, Y, Sun, F, Guo, XR, and Sun, GJ (2017). Influence of maternal overweight, obesity and gestational weight gain on the perinatal outcomes in women with gestational diabetes mellitus. *Sci Rep-Uk* **7**.
 502. Chu, SY, Callaghan, WM, Kim, SY, Schmid, CH, Lau, J, England, LJ, *et al.* (2007). Maternal obesity and risk of gestational diabetes mellitus. *Diabetes Care* **30**: 2070-2076.
 503. Herring, SJ, and Oken, E (2011). Obesity and diabetes in mothers and their children: can we stop the intergenerational cycle? *Curr Diab Rep* **11**: 20-27.
 504. Klemm, DJ, Leitner, JW, Watson, P, Nesterova, A, Reusch, JE, Goalstone, ML, *et al.* (2001). Insulin-induced adipocyte differentiation. Activation of CREB rescues adipogenesis from the arrest caused by inhibition of prenylation. *J Biol Chem* **276**: 28430-28435.
 505. Aguiari, P, Leo, S, Zavan, B, Vindigni, V, Rimessi, A, Bianchi, K, *et al.* (2008). High glucose induces adipogenic differentiation of muscle-derived stem cells. *Proc Natl Acad Sci U S A* **105**: 1226-1231.
 506. Zhang, X, Meng, K, Pu, Y, Wang, C, Chen, Y, and Wang, L (2018). Hyperglycemia Altered the Fate of Cardiac Stem Cells to Adipogenesis through Inhibiting the β -Catenin/TCF-4 Pathway. *Cellular Physiology and Biochemistry* **49**: 2254-2263.


507. Chuang, CC, Yang, RS, Tsai, KS, Ho, FM, and Liu, SH (2007). Hyperglycemia enhances adipogenic induction of lipid accumulation: Involvement of extracellular signal-regulated protein kinase 1/2, phosphoinositide 3-kinase/Akt, and peroxisome proliferator-activated receptor gamma signaling. *Endocrinology* **148**: 4267-4275.
508. Montanucci, P, Pescara, T, Pennoni, I, Alunno, A, Bistoni, O, Torlone, E, *et al.* (2016). Functional Profiles of Human Umbilical Cord-Derived Adult Mesenchymal Stem Cells in Obese/Diabetic Versus Healthy Women. *Curr Diabetes Rev.*
509. Noctor, E, and Dunne, FP (2015). Type 2 diabetes after gestational diabetes: The influence of changing diagnostic criteria. *World Journal of Diabetes* **6**: 234-244.
510. El-Badri, N, and Ghoneim, MA (2013). Mesenchymal stem cell therapy in diabetes mellitus: progress and challenges. *J Nucleic Acids* **2013**: 194858.
511. Bhansali, A, Upreti, V, Khandelwal, N, Marwaha, N, Gupta, V, Sachdeva, N, *et al.* (2009). Efficacy of Autologous Bone Marrow-Derived Stem Cell Transplantation in Patients With Type 2 Diabetes Mellitus. *Stem Cells Dev* **18**: 1407-1415.
512. Shin, L, and Peterson, DA (2012). Impaired Therapeutic Capacity of Autologous Stem Cells in a Model of Type 2 Diabetes. *Stem Cell Transl Med* **1**: 125-135.
513. Madhira, SL, Challa, SS, Chalasani, M, Nappanveethl, G, Bhonde, RR, Ajumeera, R, *et al.* (2012). Promise(s) of Mesenchymal Stem Cells as an In Vitro Model System to Depict Pre-Diabetic/Diabetic Milieu in WNIN/GR-Ob Mutant Rats. *Plos One* **7**.
514. Wu, H, and Mahato, RI (2014). Mesenchymal Stem Cell-based Therapy for Type 1 Diabetes. *Discov Med* **17**: 139-143.
515. Dor, Y, Brown, J, Martinez, OI, and Melton, DA (2004). Adult pancreatic beta-cells are formed by self-duplication rather than stem-cell differentiation. *Nature* **429**: 41-46.
516. Lechner, A, Yang, YG, Blacken, RA, Wang, L, Nolan, AL, and Habener, JF (2004). No evidence for significant transdifferentiation of bone marrow into pancreatic beta-cells in vivo. *Diabetes* **53**: 616-623.
517. Ezquer, M, Arango Rodriguez, M, Giraud Billoud, MG, and Ezquer, F (2014). Mesenchymal stem cell therapy in type 1 diabetes mellitus and its main complications: from experimental findings to clinical practice.
518. Qi, H, Yang, YL, Xie, HB, Zhou, HX, Deng, CY, and Li, FR (2011). Teratoma

- Derived From Bone Marrow Mesenchymal Stem Cells in a Diabetic Microenvironment. *Pancreas* **40**: 981-983.
519. Cuiffo, BG, and Karnoub, AE (2012). Mesenchymal stem cells in tumor development Emerging roles and concepts. *Cell Adhes Migr* **6**: 220-230.
 520. Kelly, C, McClenaghan, NH, and Flatt, PR (2011). Role of islet structure and cellular interactions in the control of insulin secretion. *Islets* **3**: 41-47.
 521. Fu, Z, Gilbert, ER, and Liu, D (2013). Regulation of insulin synthesis and secretion and pancreatic Beta-cell dysfunction in diabetes. *Curr Diabetes Rev* **9**: 25-53.
 522. Tokarz, VL, MacDonald, PE, and Klip, A (2018). The cell biology of systemic insulin function. *J Cell Biol* **217**: 2273-2289.
 523. Naujok, O, Burns, C, Jones, PM, and Lenzen, S (2011). Insulin-producing Surrogate beta-cells From Embryonic Stem Cells: Are We There Yet? *Molecular Therapy* **19**: 1759-1768.
 524. Dayan, N (2014). Making insulin producing beta cells from stem cells-how close are we?
 525. Raikwar, SP, and Zavazava, N (2009). Insulin producing cells derived from embryonic stem cells: are we there yet? *J Cell Physiol* **218**: 256-263.
 526. Larkin, JE, Frank, BC, Gavras, H, Sultana, R, and Quackenbush, J (2005). Independence and reproducibility across microarray platforms. *Nat Methods* **2**: 337-344.
 527. Morey, JS, Ryan, JC, and Van Dolah, FM (2006). Microarray validation: factors influencing correlation between oligonucleotide microarrays and real-time PCR. *Biol Proced Online* **8**: 175-193.
 528. Maudsley, S, Chadwick, W, Wang, L, Zhou, Y, Martin, B, and Park, SS (2011). Bioinformatic approaches to metabolic pathways analysis. *Methods Mol Biol* **756**: 99-130.
 529. Butte, A (2002). The use and analysis of microarray data. *Nat Rev Drug Discov* **1**: 951-960.
 530. Chengalvala, MV, Chennathukuzhi, VM, Johnston, DS, Stevis, PE, and Kopf, GS (2007). Gene expression profiling and its practice in drug development. *Curr Genomics* **8**: 262-270.
 531. Malek, A (2014). The impact of metabolic disease associated with metabolic syndrome on human pregnancy. *Curr Pharm Biotechnol* **15**: 3-12.
 532. Godfrey, KM (2002). The role of the placenta in fetal programming-a

- review. *Placenta* **23 Suppl A**: S20-27.
533. Brenseke, B, Prater, MR, Bahamonde, J, and Gutierrez, JC (2013). Current thoughts on maternal nutrition and fetal programming of the metabolic syndrome. *J Pregnancy* **2013**: 368461.
 534. Haertle, L, El Hajj, N, Dittrich, M, Muller, T, Nanda, I, Lehnen, H, *et al.* (2017). Epigenetic signatures of gestational diabetes mellitus on cord blood methylation. *Clin Epigenetics* **9**: 28.
 535. Ruchat, SM, Houde, AA, Voisin, G, St-Pierre, J, Perron, P, Baillargeon, JP, *et al.* (2013). Gestational diabetes mellitus epigenetically affects genes predominantly involved in metabolic diseases. *Epigenetics* **8**: 935-943.
 536. Camp, HS, Ren, D, and Leff, T (2002). Adipogenesis and fat-cell function in obesity and diabetes. *Trends Mol Med* **8**: 442-447.
 537. Burton, DGA, and Faragher, RGA (2018). Obesity and type-2 diabetes as inducers of premature cellular senescence and ageing. *Biogerontology* **19**: 447-459.
 538. Palmer, AK, Tchkonja, T, LeBrasseur, NK, Chini, EN, Xu, M, and Kirkland, JL (2015). Cellular Senescence in Type 2 Diabetes: A Therapeutic Opportunity. *Diabetes* **64**: 2289-2298.

Appendix – Ethical approval



University Hospitals of North Midlands 
NHS Trust

RESEARCH AND DEVELOPMENT DEPARTMENT

Academic Research Unit
Courtyard Annexe – C Block
Newcastle Road
Stoke-on-Trent
ST4 6QG

Telephone: 01782 675387

Fax: 01782 675399

Email: Darren.Clement@uhns.nhs.uk
research.governance@uhns.nhs.uk

Ref: DC/CR

28th June 2016

Dr Pensee Wu
Consultant in Maternal Foetal Medicine
University Hospitals of North Midlands NHS Trust
Maternity Department
The Royal Stoke University Hospital
Newcastle Road
Stoke-on-Trent
ST4 6QG

Dear Dr Wu

Re: PERSONALISED approach to FETal stem Cell bank Use – do pregnancy complications affect stem cell behaviour for autologous use? – PERFEC-U

Chief Investigator: Dr Pensee Wu

Sponsor/Co-Sponsor: University Hospitals of North Midlands NHS Trust

SSI Submission Date: 17/03/2016

I can confirm that the above project has been given NHS Permission for Research by the Research & Development Department for the University Hospitals of North Midlands NHS Trust and the details entered on to the R&D database.

I note that this research project has been approved by **West Midlands – Solihull Research Ethics Committee reference: 15/WM/0342**

NHS permission for the above research has been granted on the basis described in the application form, protocol and supporting documentation. The documents reviewed were:

Document	Version Number	Date
Protocol	2.1	03/03/16
PIS (C)	1.1	15/12/15
PIS (G)	1.1	15/12/15
PIS (P)	1.1	15/12/15
Consent Form (C)	1.1	15/12/15
Consent Form (G)	1.1	15/12/15

R&D ID: 1125 UKCRN ID: n/a CSP ID: n/a REC REF: 15/WM/0342

Consent Form (P)	1.1	15/12/15
------------------	-----	----------

The research sponsor or the Chief Investigator, or the local Principal Investigator at a research site, may take appropriate urgent safety measures in order to protect research participants against any immediate hazard to their health or safety. The R&D office should be notified that such measures have been taken. The notification should also include the reasons why the measures were taken and the plan for further action. The R&D office should be notified within the same time frame of notifying the REC and any other regulatory bodies.

Approval by the R&D Dept therefore assumes that you have read, understand and agree to comply with the:

- ❖ Research Governance Framework (www.gov.uk/government/publications/research-governance-framework-for-health-and-social-care-second-edition)
- ❖ Data Protection Act
- ❖ Health and Safety Act
- ❖ ICH Guidelines on good clinical practice
- ❖ All applicable Trust policies & procedures

In line with these requirements may I draw your attention to the need for you to provide the following documentation/notifications to the R&D Department throughout the course of the study and that all amendments (including changes to the local research team) need to be submitted to R&D in accordance with guidance in IRAS:-

- ❖ Annual Progress Report Form (sent to you by this department)
- ❖ End of Study Declaration Form (available on IRAS website)
- ❖ Changes to study start and end dates
- ❖ Changes in study personnel

Please note that the NHS organisation is required to monitor research to ensure compliance with the Research Governance Framework and other legal and regulatory requirements. This will be achieved by random audit by our department.

I would like to take this opportunity to wish you well with your research. If you need any further advice or guidance please do not hesitate to contact us.

Yours sincerely



Dr Darren Clement

R&D Manager – University Hospitals of North Midlands NHS Trust

Cc Fidelma O'Mahony – Clinical Director Maternity, UHNM
Darren Clement – Guy Hilton Research Centre, UHNM
Li-Yun Chen – Student Researcher, Keele University
Zara Richards – Postgraduate Research Administrator, Keele University
Jill Stacey – Professional Head for Research Nursing, UHNM
Helen Grocott – Information Governance Manager, UHNM
Laura Longshaw – R&D Auditor & Monitor, UHNM
Dawn Sirdefield – R&D Auditor & Monitor, UHNM

R&D ID: 1125 UKCRN ID: n/a CSP ID: n/a REC REF: 15/WM/0342